MONASH University

Identification of Novel Targets of SOX9 in Mammalian Testis Development

Aleisha Jane Symon

Bachelor of Science, Graduate Diploma of Reproductive Sciences

A thesis submitted for the degree of Doctor of Philosophy at
Monash University in 2019

Department of Anatomy and Developmental Biology,
Faculty of Medicine, Nursing and Health Sciences
and
Hudson Institute of Medical Research,
Melbourne, Australia

Copyright notice

Table of Contents

Abstract

SOX9 is indispensable for development and function of the mammalian testis. In humans, deleterious mutation to *SOX9* can result in Disorders of Sex Development (DSD) in chromosomally XY individuals, resulting in a wide spectrum of phenotypes ranging from complete XY sex reversal to compromised fertility. In mice, *Sox9* is both necessary and sufficient for testis formation since complete loss in XY gonads leads to ovarian development, while ectopic *Sox9* expression in XX gonads leads to testis development. In the XY gonad *SOX9* drives the Sertoli cell differentiation which in turn directs the differentiation and function of other testicular cell types. High-throughput sequencing of XY *Sox9* mutant gonads together with Sox9 chromatin binding analyses indicate that Sox9 regulates thousands of genes in the developing testis. To date, only a handful of target genes have been characterised with functions pertaining to a limited number of Sertoli cell characteristics, suggesting that there are many more targets of SOX9 to be discovered. Identification of these factors will improve our understanding of the genes involved orchestrating sex determination and development. As such, discovery of SOX9 target genes will also reveal candidate genes possibly mutated in unsolved XY DSD. Therefore, this thesis aimed to identify and investigate the role of novel target genes of SOX9 during testis development.

The exclusive use of mice as a model of testis development has limitations which are addressed in Chapters 2 and 3. Ablation of *Sox9* immediately after sex determination (E13.5) in XY mice does not cause sex reversal, allowing testis development to continue. In Chapter 2, this approach has provided a model whereby transcriptomic analysis is able to identify alterations to *Sox9* target gene expression in an intact Sertoli cell environment. When combined with mouse Sox9 chromatin immunoprecipitation, 37 direct target genes with a wide variety of putative functions have been identified. Chapter 3 describes an approach to evaluate Sertoli cell functions regulated by SOX9 using the human Sertoli-like cell line, NT2/D1. Through a combination of cell culture methods, Xcelligence and transepithelial assays it is demonstrated that SOX9 controls cell proliferation, adhesion and polarity.

Analysis of genes dysregulated in *Sox9* knockout mouse testes identified a cytoskeletal scaffolding protein, *Nedd9.* Therefore, chapter 4 focussed on characterising the function of Nedd9 in the testis. Chromatin immunoprecipitation identified SOX9 binding to the proximal promoter of *NEDD9* in NT2/D1 cells. Using the analytical approach developed in Chapter 3, *NEDD9* was revealed to partly control Sertoli cell proliferation, a function also observed in mouse testes as *Nedd9* knockout mice showed a 15% decrease in embryonic testis size.

In summary, this thesis has identified a number of potential novel SOX9 target genes, from which *NEDD9* was selected and functionally validated with the use of a human cell line. More broadly,

these approaches will allow multiple SOX9 target genes to be characterised and provide a stronger molecular basis to understand the mechanisms governing human testis development. Additionally, this information is essential to gain insights into the involvement of these genes in XY DSD.

Declaration

This thesis is an original work of my research and contains no material which has been accepted for the award of any other degree or diploma at any university or equivalent institution and that, to the best of my knowledge and belief, this thesis contains no material previously published or written by another person, except where due reference is made in the text of the thesis.

Signature:

Print Name: Aleisha Jane Symon

Date: 18/08/2019

Publications during enrolment

Symon A, Harley V. SOX9: A genomic view of tissue specific expression and action. *The international journal of biochemistry & cell biology*. 2017;87:18-22.

Rahmoun M, Lavery R, Laurent-Chaballier S, Bellora N, Philip GK, Rossitto M, Symon A, Pailhoux E, Cammas F, Chung J, Bagheri-Fam S, Murphy M, Bardwell V, Zarkower D, Boizet-Bonhoure B, Clair P, Harley V, Poulat F. In mammalian foetal testes, SOX9 regulates expression of its target genes by binding to genomic regions with conserved signatures. *Nucleic acids research*. 2017;45(12):7191-211.

Barseghyan H, Symon A, Zadikyan M, Almalvez M, Segura EE, Eskin A, Bramble MS, Arboleda VA, Baxter R, Nelson SF, Délot EC, Harley V, Vilain E. Identification of novel candidate genes for 46, XY disorders of sex development (DSD) using a C57BL/6J-Y POS mouse model. *Biology of sex differences*. 2018;9(1):8

Conference Proceedings and Presentations

Oral Presentations

2018

8th International Vertebrate Sex Determination Conference, Hawaii, USA

Abstract title: Unravelling the role of SOX9 target genes in Mammalian Sex Determination using NT2/D1 cells

2017

ComBio, Adelaide, Australia

Abstract title: Elucidating the role of SOX9 target genes in embryonic testis development.

Monash University Developmental Biology Workshop, Clayton, Australia

Abstract title: Identifying Novel Targets of SOX9 in Mammalian Sex Determination

2016

Monash Anatomy and Developmental Biology Student Symposium, Clayton, Australia

Abstract title: Identifying novel genes from integrated SOX9 knockout RNAseq and SOX9 ChIPseq datasets

5th Australian Sex Summit, Victoria, Australia

Abstract title: Identifying novel genes from integrated SOX9 knockout RNAseq and SOX9 ChIPseq datasets

2015

Monash Anatomy and Developmental Biology Student Symposium, Clayton, Australia

Abstract title: Identifying targets of SOX9 in Mammalian Sex Determination

Poster Presentations

2018

39th Annual Lorne Genome Conference, Lorne, Australia

Abstract title: Identifying Novel Testis-Determining Genes from Integrated RNAseq and ChIPseq Data

2017

38th Annual Lorne Genome Conference, Lorne, Australia

Abstract title: Identifying novel genes from integrated SOX9 knockout RNAseq and SOX9 ChIPseq datasets

Monash Anatomy and Developmental Biology Student Symposium, Clayton, Australia
Abstract title: Identifying novel genes from integrated SOX9 knockout RNAseq and SOX9 ChIPseq datasets

2016
37th Annual Lorne Genome Conference, Lorne, Australia
Abstract title: Identifying novel genes from integrated SOX9 knockout RNAseq and SOX9 ChIPseq datasets

49th Annual Society for the Study of Reproduction (SSR) meeting, San Diego, USA
Abstract title: Sex determination: Identifying novel genes from integrated SOX9 knockout RNAseq and SOX9 ChIPseq datasets

2015
36th Annual Lorne Genome Conference, Lorne, Australia
Abstract title: Characterisation of three potential SOX9 target genes in the developing testis

Seventh International Symposium on Vertebrate Sex Determination, Hawaii, USA
Abstract title: *Nedd9,* a Sox9 responsive gene in the Mammalian Testis

6th Annual ASMR Victorian Student Research Symposium, Melbourne, Victoria
Abstract title: *Dhh, Etv5 and Nedd9 -* novel targets of Sox9 in mammalian sex determination

Awards and Prizes arising from this thesis

2017

Keith Dixon Prize for best developmental biology student poster, Combio Conference

Australia New Zealand Society for Developmental Biology (ANZSCDB) Travel Award, ComBio Conference

Best Oral Presentation, Monash University Developmental Biology Workshop

1st Prize, Centre for Endocrinology and Metabolism, Hudson Institute of Medical Research 3 Minute Thesis Competition

2016

C. Lalor Burdick Scholarship and Burroughs Wellcome Fund Scholarship Embryology Course in support of attending the MBL Embryology course at Woods Hole

Best Oral Presentation (2nd year student), Monash Anatomy and Developmental Biology Student Symposium

2015

Monash University MBio Postgraduate Discovery Award for PhD

1st Prize, Centre for Reproductive Health, Hudson Institute of Medical Research 3 Minute Thesis Competition

Acknowledgements

This thesis is the product of a long journey which I have so many people to thank for. To quote Isaac Newton, I truly feel like I am standing on the shoulders of Giants.

Firstly, I would like to thank Professor Vincent Harley for giving me the opportunity to do this research in his lab. Vince's guidance and mentorship has been invaluable, teaching me more than I could ever have imagined and has enabled me to develop into an independent scientist. I would also like express my gratitude to my co-supervisor, Dr Peter Stanton, who never failed to support me and help keep me grounded. Without your support I'm not sure how I would have made it to the end Peter.

I would like to extend my thanks to members of the Harley lab, both past and present for your support and making the lab a brilliant place to work in. Dr Dimi Alankarage, Dr Stefan Bagheri-fam and Dr Rowena Lavery, thank you for laying the foundations and for your guidance in planning this project. To Dr Dan Bird, Brittany Croft, Dr Hannah Loke, Allara Zylberberg and Maisie Hands, thank you for all your technical support, emotional support and friendship. I would like to make a special mention to Janelle Browne, who I wish could have been listed as an official supervisor. Janelle, I really couldn't be here without you. You have been the best (graduate diploma) supervisor, turned mentor, turned friend that I ever could have imagined. Thank you for celebrating even the smallest of wins with me and holding my hand through the hardest of days. I can't wait to see what amazing things Ryan and Callie are able to achieve with your support.

I am grateful to the Hudson Institute of Medical Research for providing a motivating workplace, for introducing me to some amazing people and for supporting my development as a researcher. A special thanks to Dr Jemma Evans, Dr Simon Chu, Prof. Lois Salamonsen, Prof. Peter Fuller and A/Prof. Peter Temple-Smith for your continual guidance and advice. To Dr Amy Winship and Dr Harriet Fitzgerald, thank you for making the Hudson Institute a place I wanted be every day and for your continued friendship. You are both inspiring women and I am so grateful to call you my friends. To the Histology and Micro Imaging platforms, thank you for all your technical support. To my fellow Woods' Hole Embryologists, I cannot believe that three years after meeting you we still talk every day. I am so grateful for all the technical advice, for every giggle and for every pep talk. To all my collaborators, but particularly to Dr Francis Poulat, Dr Hayk Barseghyan, Prof. Eric Vilain, Dr Anna Nikonova, Prof. Peter Koopman and Prof. Andrew Sinclair, thank you for the many stimulating discussions we have engaged in and valuable comments on my research. I would also like to thank the Department of Anatomy and Developmental Biology at Monash University for awarding me the MBio Postgraduate Discovery Scholarship which allowed me the opportunity to complete this PhD research.

Abbreviations

°C	Degrees Celsius
µg	Microgram
µl	Microlitre
AMH	Anti Müllerian Hormone
ATCC	American Type Tissue Culture
bp	Base pair
BPES	Blepharophimosis/ptosis/epicanthus inversus syndrome
CBLN4	Cerebellin 4
CBX2	Chromobox homolog 2
CD	Campomelic Dysplasia
cDNA	Complementary DNA
ChIP	Chromatin Immunoprecipitation
ChIPseq	Chromatin Immunoprecipitation with sequencing
Ck19	Cytokeratin
COL2A1	Collagen, type II, alpha 1
CRE	Cre recombinase
CRISPR	Clustered regularly interspaced short palindromic repeats
CYP26B1	Cytochrome P450, family 26, subfamily b, polypeptide 1
DAPI	4′,6-diamidino-2-phenylindole
DAX1	Dosage-sensitive sex reversal, adrenal hypoplasia critical region, on chromosome X, gene 1
DHH	Desert hedgehog
DMRT1	Double sex and mab-3 related transcription factor 1
DNA	Deoxyribonucleic acid
DSD	Disorder of sex development
E	Embryonic day
eALDI	Alternate long distance initiator
Enh	Enhancer
ESR	Estrogen Receptor
eSR-A	Sex reversal enhancer-A
eSR-B	Sex reversal enhancer-B
ETV5	E-twenty-six variant 5
FACS	Fluorescence activated cell sorting
FBS	Fetal bovine serum
FGF9	Fibroblast growth factor 9
FGFR2	Fibroblast growth factor receptor 2
FOG2	Zinc finger protein, FOG gamily member 2
FOXL2	Forkhead box L2
GADD45γ	Growth arrest and DNA-damage-inducible, gamma
GATA4	GATA binding protein 4
GDNF	Glial cell derived neurotrophic factor
GFP	Green fluorescent protein
GSTM6	Glutathione S-transferase, mu 6
H3K27Ac	Histone 3, lysine 27, acetylation
HMG	High mobility group
IGFR1	Insulin like growth factor 1 receptor
IgG	Immunoglobulin G
INSR	Insulin receptor
INSRR	Insulin receptor-related receptor
kb	Kilobase
KO	Knockout
LHX9	Lim homeobox 9
MAPK	Mitogen activated protein kinase
mRNA	Messenger RNA

NCBI	National centre for biotechnology information
NEDD9	Neural precursor cell expressed, developmentally downregulated 9
NR5A1	Nuclear receptor subfamily 5, group A, member 1
NT2/D1	Ntera 2, clone D1
NT3	Neurotrophin 3
OMIM	Online Mendelian Inheritance of Man
P38	P38 Mitogen activated protein kinase
PADI2	Peptidyl arginine deiminase 2
PDGF	Platelet derived growth factpr
PGD2	Prostaglandin D2
PGDS	Prostaglandin D2 synthase
PH3	Phospho-histone H3
PMC	Peritubular myoid cells
PQA	Proline, glutamine alanine rich
PQS	Proline, serine and glutamine rich
PTCH1	Patched 1
qRT-PCR	Quantitative RT-PCR
RIPA	Radioimmunoprecipitation buffer
RNA	Ribonucleic acid
RNAseq	Ribonucleic acid sequencing
RSPO1	R-spondin 1
SDHA	Succinate dehydrogenase complex, subunit A, flavoprotein
SDS	Sodium dodecyl sulfate
SEM	Standard error of the mean
SF1	Steroidogenic factor 1
SOX	SRY-box
SOX10	SRY-box 10
SOX5	SRY-box 5
SOX6	SRY-box 6
SOX8	SRY-box 8
SOX9	SRY-box 9
SRA	Autosomal Sex Reversal
SRY	Sex determining region Y
STRA8	Stimulated By Retinoic Acid 8
TBP	TATA-binding protein
TES	Testis-specific Enhancer of *Sox9*
TESCO	TES core
TGFβ	Transforming growth factor β
TMEM117	Transmembrane protein 117
TMEM185b	Transmembrane protein 185b
TSS	Transcription start site
VNN1	Vanin 1
WNT4	Wingless-type MMTV integration site family, member 4
WT	Wildtype
WT1	Wilms tumour 1
WT1-KTS	Wilms tumour 1-lysine-threonine-serine
XYSR	XY sex reversal region

Chapter 1:
Literature Review

1.1   Introduction

The gonads have the unique ability to differentiate into two distinct organs during embryonic development, either the ovaries in females or the testis in males. Male and female gonads arise from the same tissue known as the bipotential gonad or urogenital ridge and both organs produce gametes and sex hormones but otherwise are vastly different in both function and morphology (Brennan & Capel, 2004). Genetic mutations in pathways essential to the development of the gonad can severely perturb both formation and function of the gonad and can also result in sex reversal i.e. XY females and XX males (Ono & Harley, 2013).

Sex determination refers to the mechanisms which determine if the gonads will develop as testes or ovaries and as a consequence, if the organism will develop as a male or female. It is an intricate process dictated by the genetic makeup of an individual, where many signalling molecules and pathways interlace to decide the sex of the gonads. The cascades of gene networks initiated at sex determination lead to the differentiation of sexually dimorphic cells which form the gonads and then the give rise to secondary sex characteristics which we associate with 'maleness' and 'femaleness' (Brennan & Capel, 2004).

Despite the testis and ovary arising from the same structure, they are remarkably different as a consequence of their dramatically disparate development (Brennan & Capel, 2004). This review will focus on male of sex determination, and the role which the transcription factor SOX9 plays in regulating the development of the mammalian testis.

1.2   Development of the Mammalian Testis

The bipotential gonad or genital ridge, is the tissue which the testes and ovaries differentiate from. The genital ridge begins as narrow bands of proliferating cells; in mice this first appears around embryonic day 10 (E10) and in humans around gestational week 4 (Nef, Stevant, & Greenfield, 2019). Soon after this (E10.3) the primordial germ cells colonise the thickening genital ridge (Hu, Okumura, & Page, 2013; Molyneaux & Wylie, 2004; Richardson & Lehmann, 2010). Primordial germ cells migrate to the gonads and intermix with the undifferentiated somatic cells, joining the cells in a tissue with otherwise no distinct structure (Ungewitter & Yao, 2013). Following their arrival, sex determination occurs, committing the bipotential gonad to the testicular or ovarian pathway (Ginsburg, Snow, & McLaren, 1990; McLaren, 2003). The cells commit to either the male fate or the female fate; the supporting cell precursors can develop as either Sertoli cells or granulosa cells, the steroidogenic cells can form either Leydig cells or Theca cells and the germ cells can proceed to develop in a fashion which will later equip them for spermatogenesis or oogenesis (**Figure 1.1**).
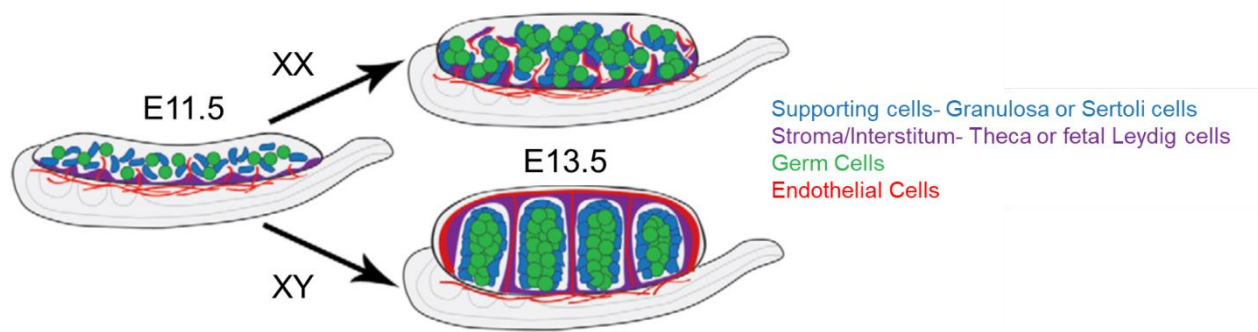
Figure 1.1 Illustration of the developing XX and XY gonad

Cells of the testis and ovary share common lineage with the supporting cells (blue) differentiating into either granulosa or Sertoli cells and Steroidogenic cells (Theca or fetal Leydig cells) making up the Stroma/Interstitium. From E11.5 to E13.5 there is a dramatic change in the organisation of the gonad, dependent on the sex chromosomes present (XX or XY). Figure adapted from (Jameson, Natarajan, et al., 2012)

Sertoli Cell differentiation

The differentiation of the supporting cell lineage or Sertoli cells in the male is the first event to occur in sex determination, initiated by the presence of the Y chromosome, and more specifically the presence of the sex determining gene *SRY* (Sex Determining Region of Y chromosome) *(Koopman, Munsterberg, Capel, Vivian, & Lovell-Badge, 1990; Sinclair et al., 1990)*. The role of *SRY* will be furthered explored in Section 1.4.

The earliest known morphological event in the formation of the testis is a wave of Sertoli cell proliferation from E11.25-E13.5 in mice, a feature unique to the male gonad (Ungewitter & Yao, 2013). In this time the width of the XY gonad doubles every 24 hours. Without this proliferation, the Sertoli cells do not aggregate to form cords (Schmahl & Capel, 2003). In mice this proliferation begins in a critical window (E10.8-11.2), with the administration of proliferation inhibitors to XY gonads resulting in no cord formation and reduced expression of male markers (Schmahl & Capel, 2003). Administration of proliferation inhibitors after this critical window still leads to smaller gonads but does not inhibit testis formation (Schmahl & Capel, 2003). This critical window coincides with the onset of *SRY* expression and thus the initial sex determination event, emphasising the importance proliferation plays in the choice between the male and female fate in gonadal development.

The Sertoli cells are responsible for coordinating testis morphogenesis. Following their differentiation they direct the partitioning of the gonad into two compartments; the testis cords and interstitial space (**Figure 1.2**) (Ungewitter & Yao, 2013)

Compartmentalisation of the testis

Testis cords are required to protect the spermatagonial stem cells, and to provide an immune privileged compartment for gametes to be generated in. The interstitial space houses Leydig cells which are required for producing testosterone, the steroid crucial to the virilisation of the internal and external male genitalia as well as the male specific vasculature which is essential for transporting testosterone around the organism (**Figure1. 2**).

The compartmentalisation of the testis occurs in 3 distinct phases. Firstly, the interstitial cell population is established which will lie outside the testis cords. Secondly, the testis-specific vasculature is formed and lastly, a basal membrane forms to encapsulate the cords in an environment where spermatogenesis can later occur (Ungewitter & Yao, 2013). The interstitial cell population consists of Leydig cells, non-Leydig progenitors and blood endothelial cells. Two progenitor populations in the fetal testis give rise to these cells; the coelomic epithelium and cells in the gonad-mesonephoric boarder (DeFalco, Takahashi, & Capel, 2011). In mouse gonadogenesis, beginning at E10.5, the interstitial cells migrate into the developing testis. This

migration is critical to the formation of cords. When gonads are cultured without the mesonephros, or have a physical barrier separating the structures, cord formation does not proceed (Tilmann & Capel, 1999). Furthermore, XX gonads can be induced to organise into testis cords and express male-specific genes by culturing them with an XY gonad at their surface (Tilmann & Capel, 1999). This migration is facilitated in part by chemotactic signals produced by Sertoli cells, such as Neurotrophin 3 (NT3) and Platlet-Derived Growth Factors (PDGFs) (Brennan, Tilmann, & Capel, 2003; Cupp, Tessarollo, & Skinner, 2002; Cupp, Uzumcu, & Skinner, 2003; Gnessi et al., 1995).
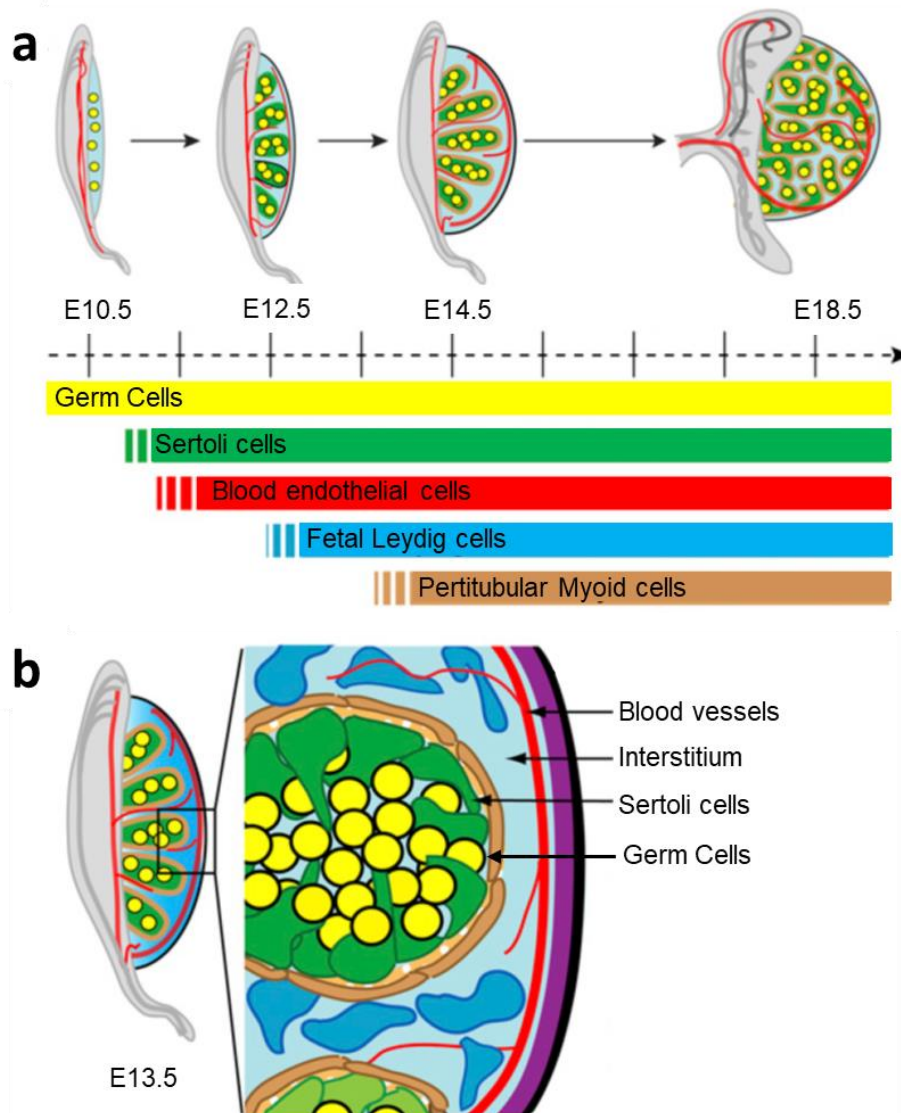
Figure 1.2. Schematic of the Anatomy of the Developing Testis. **(a)**The bipotential gonad is colonised with germ cells (yellow) prior to sex determination. The Sertoli cells are the first somatic cells to differentiate, followed closely by the migration of blood endothelial cells (red) into the gonad to lay down the primitive vasculature. This leads to the differentiation of the fetal Leydig cells (blue) and peritubular myoid cells (brown). **(b)** Following sex determination, the testis is compartmentalised into testis cords surrounded by interstital space. The testis cords are comprised of Sertoli cells (green) encapsulating mitotically arrested germ cells (yellow) with an outer layer of peritubular myoid cells (brown) and extra cellular matrix for support. The interstitium consists of the steroidogenic fetal Leydig cells (blue), surrounded by mesenchyme and the blood vascular network (red). Figure adapted from (Svingen & Koopman, 2013)

The testis-specific vasculature is formed by endothelial cells migrating into the developing gonad from E12.0-E12.5 (**Figure 1.3**). Prior to E12.0, the gonads of both sexes contain a primitive vasculature structure, known as the mesonephric vascular plexus, within the mesonephros. The XY testis adopts a unique mechanism to establish vasculature where the mesonephric vascular plexus is disassembled, allowing the individual endothelial cells to migrate through the gonad before reassembling in the coelomic domain (Coveney, Cool, Oliver, & Capel, 2008). This migratory event gives rise to the main testicular artery, the coelomic vessel, as well as a microvascular network throughout the testis. This process is required for the formation of the testis cords (Combes et al., 2009; Cool, DeFalco, & Capel, 2011).

Even though testis cord formation is dependent on endothelial cell formation it is also an inherent property of Sertoli cells, as cell culture studies show that in the absence of other cell types Sertoli cells can aggregate to form cord-like structures(Hadley, Byers, Suarez-Quian, Kleinman, & Dym, 1985). However, Sertoli cells alone cannot form functional testis cords which protect and nourish the germ cells (**Figure 1.2**). In the wild type gonad, these cords encapsulate germ cells and are surrounded by peritubular myoid cells (PMC) which work with the Sertoli cells to deposit a basal lamina. The basal lamina deposition is critical to isolate the inner wall of the cord, later providing the right environment for the formation of sperm. The PMC's are distinguishable by E13.5 and are in direct contact with Sertoli cells (Clark, Garland, & Russell, 2000). The differentiation of PMC's is likely directed by Sertoli cells. Desert Hedgehog (DHH) is a factor secreted by Sertoli cells which binds to the Patched-1 (PTCH1) receptor on the surface of PMC's (see section 1.4.2). XY mice with *Dhh* knocked out have abnormal PMC's and lack the basal lamina, thereby exposing the germ cells to factors in the interstium and disrupting spermatogenesis (Clark et al., 2000; Pierucci-Alves, Clark, & Russell, 2001; Yao, Whoriskey, & Capel, 2002). However, XX mice overexpressing *Dhh* do not develop PMC's indicating that while it is required for their function and the laying down of the basal lamina, it is not the driving factor behind their differentiation (Barsoum, Bingham, Parker, Jorgensen, & Yao, 2009).
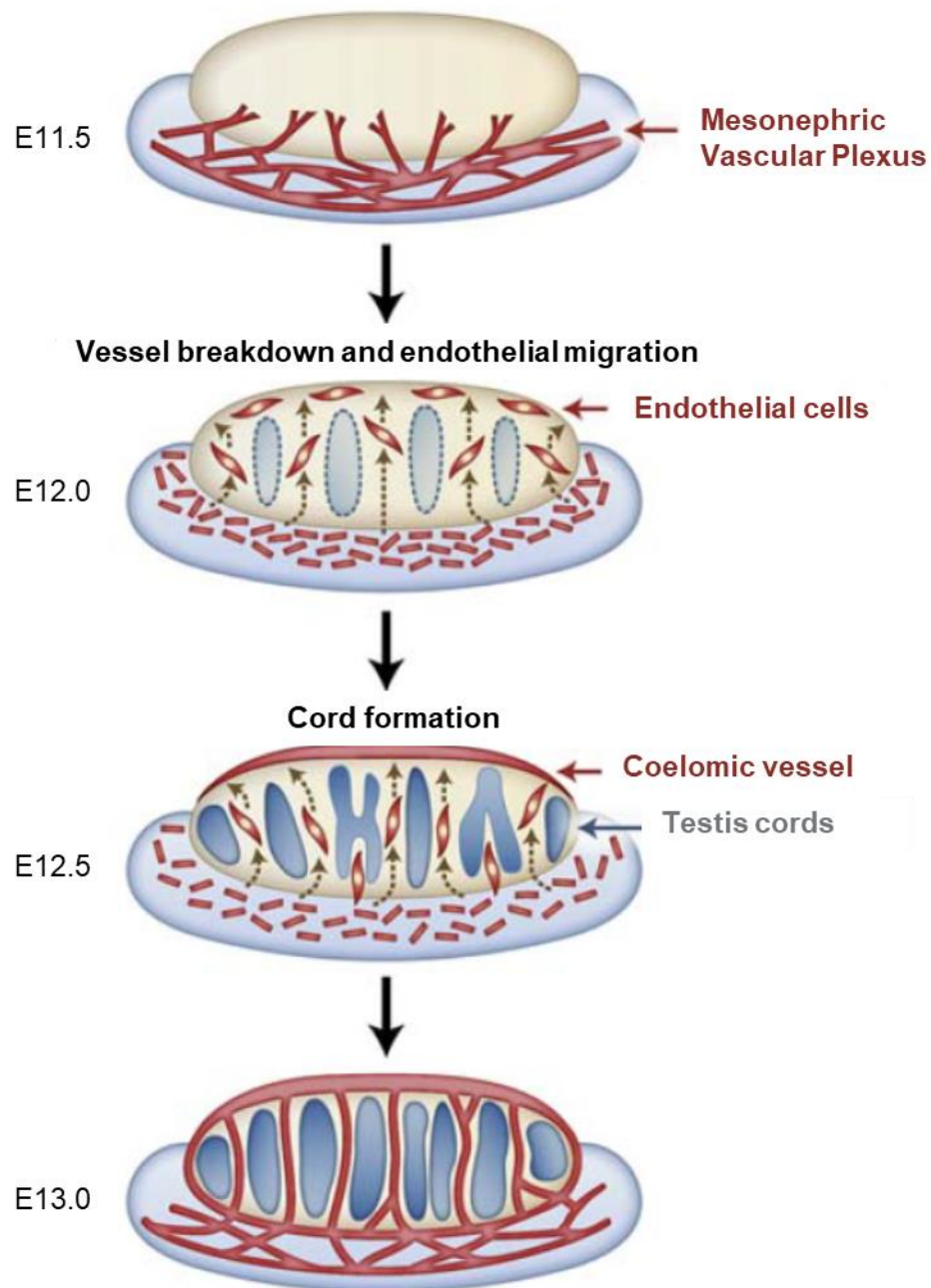
Figure 1.3. Schematic of endothelial cell migration and testis cord formation. At E11.5 there is minimal vascularisation of the gonad, but prominent vessel structure in mesonephros of both XY and XX gonads, the mesonephric vascular plexus. At E12.0 in XY gonads the mesonephric vascular plexus breaks down and endothelial cells migrate into the testis towards the opposite side, the coelomic domain. By E12.5 the coelomic vessel is clearly visible and the testis cords have formed between the tracks of the endothelial cells. Figure adapted from (Ungewitter & Yao, 2013)

Germ cells in testis development

Germ cells are the precursor of sperm and oocytes, and therefore are crucial to fertility. They have the potential to differentiate to either gamete precursor, regardless of genetic sex (spermatagonia in the testis and oogonia in the ovary). Germ cells migrate to the gonads during the biopotential phase, and unlike the rest of the gonad, do not have their fate decided until E12.5, after the other cells of the gonad have begun to differentiate (Y. T. Lin & Capel, 2015). The presence of germ cells in the gonad is not required for the development of the testis, as the gonad and the male phenotype develop normally in agametic conditions (Merchant-Larios & Centeno, 1981). This is in contrast to ovarian development, which requires germ cells within the gonad for development (Merchant-Larios & Centeno, 1981) . In the testis, germ cell development is arrested in the mitotic phase, as opposed to the ovary where the germ cells enter meiosis. Retinoic acid is a key factor controlling this process. Retinoic acid is produced in the mesonephros (XX and XY) which activates the expression of *Stra8*, a gene required to promote entry of germ cells into meiosis (Bowles et al., 2006; Koubova et al., 2006). In the XY gonad, a Cytochrome P450 family member, Cyp26b1 is produced early by Sertoli cells to ensure the breakdown of retinoic acid and thus mitotic arrest (see Section 4.3.2) (H. Li, MacLean, Cameron, Clagett-Dame, & Petkovich, 2009). Other genetic mechanisms ensure that testicular germ cells will not enter spermatogenesis until puberty are now coming to light, as reviewed by Spiller and Bowles (2015) (Spiller & Bowles, 2015).

1.3 Human Disorders of Sex Development

Defects in sex determination and development cause Disorders of Sex Development (DSD). These are a broad spectrum of disorders that arise when chromosomal, gonadal or anatomical sex is atypical (Hughes, Houk, Ahmed, Lee, & Lawson Wilkins Pediatric Endocrine Society/European Society for Paediatric Endocrinology Consensus, 2006).Considering all congenital genital anomalies, the rate of these disorders is estimated to be as high as 1:200 (Nordenvall, Frisen, Nordenstrom, Lichtenstein, & Nordenskjold, 2014). DSD can be classified according to karyotype: 46, XX DSD, 46, XY DSD and sex chromosomal DSD (aneuploidies). The most common of these aneuploidies is XXY-XXXXY causing Klinefelter syndrome and XO causing Turner syndrome(Matzuk & Lamb, 2008).

46, XY DSDs are characterised by ambiguous or female external genitalia with a XY karyotype (Mendonca, Domenice, Arnhold, & Costa, 2009). The most common cause of 46, XY DSD is partial androgen insensitivity syndrome where the differences in sex development are a result of perturbation to androgen synthesis (Michala & Creighton, 2010). 46, XY testicular DSD refers to cases where patients have complete or partial gonadal dysgenesis, with a much rarer incidence of 1:10,000 births (Skakkebaek, Rajpert-De Meyts, & Main, 2001). Mutations to *SRY*

account for about 15% of 46, XY testicular DSD, and while many other genes (outlined in **table 1**) are known to be causal of these conditions, genetic diagnosis remains elusive in 50% of cases (Eggers et al., 2016). Since many 46, XY DSD cases are due to errors in testis development, it is no surprise that many of the genes being discovered as causal are responsible for critical processes in the formation of the gonads (Barseghyan et al., 2018; Eggers et al., 2016).

Table 1. 46, XY DSD causative genes and associated phenotypes.

Gene	Class of Protein	Human Phenotype-Sex Organs	Human Phenotype-Other Organs	Mouse Phenotype
ARX	Transcription Factor	Dysgenic testis No Mullerian structures Ambiguous external genitalia	Lissencephaly Epilepsy Temperature Instability	Arx-: Arrest of Leydig cell differentiation, abnormal neuronal migration
ATRX	Chromatin Remodelling Protein	Dysgenic testis No Mullerian structures Varied external genitalia	α-Thalassemia Mental Retardation Dysmorphic face	Atrx-: embryonic lethal Sertoli cell specific Atrx-: small testes, discontinuous tubules (fetal period), delayed onset of spermatogenesis
CBX2	Polycomb Protein	Normal ovaries Mullerian structures present Female external genitalia	Normal	Cbx2-/-: sex reversal
DHH	Signalling	Dysgenic testis Mullerian structures present Female external genitalia	Minifascicular neuropathy	Dhh-/-: abnormal peritubular tissue, severely restricted spermatogenesis and thin perineurial sheaths
DMRT1	Transcription Factor	Dysgenic testis or ovotestis Some have Mullerian structures present Varied external genitalia	Facial abnormality Mental Retardation Microcephaly	Dmrt1-/-: severely impaired testis development (postnatal)
FGFR2	Transmembrane Catalytic Receptor	Dysgenic testis with dysgerminoma Female external genitalia	Craniofacial abnormalities Craniosynostosis Bracycephaly Elbow and Knee contractures	Fgfr2$^{C342Y/C342Y}$: Sex reversal of supporting cells, reduced number of Leydig cells
FOG2	Transcription Factor	Dysgenic testis or ovotestis Mullerian structures present Ambiguous genitalia	Mutation without 46, XY DSD have cardio myopathy	Fog2-/-: embryonic lethal but analysis before death indicated severe abnormalities of testis development
GATA4	Transcription Factor	Dysgenic testis No Mullerian Structures Ambigous/Male external genitalia	Congenital heart disease	Gata4-/-: embryonic lethal Gata4^{ki}: severe abnormalities of testis development
MAMLD1	Transcriptional Co-activator?	Normal Function No Mullerian Structres Hypospadias	Normal	Normal
MAP3K1	Kinase	Dysgenic testis Some have Mullerian structures present Varied external genitalia	Normal	No gonadal phenotype
NROB1 (DAX1)	Nuclear Receptor/ Transcription Factor	Dysgenic testis or ovary Some have Mullerian structures present Varied external genitalia	Cleft palate Mental retardation	Transgenic model: delayed testicular development
NR5A1 (SF1)	Nuclear Receptor/ Transcription Factor	Dysgenic testis Some have Mullerian structures present Varied external genitalia	Adrenal insufficiency	NR5A1-/-: no gonads or adrenal glands NR5A1+/-: impaired adrenal response, small gonads
SOX9	Transcription Factor	Dysgenic testis or ovotestis Some have Mullerian structures present Female or ambiguous external genitalia	Campomelic Dysplasia	Sox9-/-: no urogenital tract or gonads
SRY	Transcription Factor	Dysgenic testis or ovotestis Some have Mullerian structures present Female or ambiguous external genitalia	Normal	Sry-: Dysgenic testes, Mullerian ducts present
WNT4	Signalling Molecule	Dysgenic testis Mullerian structures present Ambiguous external genitalia	Cleft lips and palate Tetralogy of Fallot Intrauterine growth retardation Microcephaly Mental Retardation	Transgenic model: disruption of normal testicular vasculature and function but no sex reversal
WT1	Transcription Factor	Dysgenic testis or ovotestis Some have Mullerian structures present Female or ambiguous external genitalia	Wilms tumour Renal abnormalities Gonadal tumours	Wt1-/-: no urogenital tract or gonads
WWOX	Oxodoreductase	Dysgenic testis or ovotestis No Mullerian structures Female external genitalia	Normal	Wwox-/-: Leydig cell hypoplasia, postnatal lethality, bone growth defects

Table adapted from (Ono & Harley, 2013) with additional information from (Bashamboo & McElreavey, 2015) and (Bagheri-Fam et al., 2015)

Patients with DSD are often misdiagnosed and mismanaged due to the lack of genetic information associated with the development of the testis. The challenges faced by mismanaged patients include increased risk of gonadoblastoma, fertility issues, gender dysphoria and risks to psychosexual and psychosocial wellbeing (Bashamboo & McElreavey, 2015; Lee et al., 2016). Even with proper diagnosis, they often require surgery and lifelong endocrine care (Michala & Creighton, 2010). Investigating the pathways that function during sex determination and gonadal development will allow better understanding of the mechanisms involved in normal reproductive development as well as how any defects may cause disorders of sex development, thereby improving outcomes for patients.

1.4   The Genetic Control of Mammalian Sex Determination

The genetic control of mammalian sex determination and gonadal cell differentiation is a tussle between pro-testis and pro-ovarian genes, where the presence of the Y chromosome tips the balance in favour of male cell fate (Berta et al., 1990). The induction of testis formation is initiated by a transcription factor encoded on the Y chromosome, *SRY*, without which, ovarian cell differentiation commences (Brennan & Capel, 2004). The expression of *SRY* triggers the activation of the *SRY*-related HMG box 9 (*SOX9*), another transcription factor, thereby initiating a genetic cascade that leads to the formation of the testis (Brennan & Capel, 2004).

Genetic regulation in the bipotential gonad

The first step in the development of the gonad is the establishment of the primordial structure, the bipotential gonad, which has the potential to develop into either testes or ovaries. The proper establishment and genetic patterning of the bipotential gonad is indispensable for future development. Thus, to investigate the processes involved in the development of the testis, first it is important to understand how the biopotential gonad regulated and what genes are essential to its patterning. Many genes have been identified as key players in the development of the bipotential gonad, including *GATA4*, *NR5A1*, *WT1*, *LHX9* and *EMX2* (**Figure 1.4**) (Birk et al., 2000; Fujimoto et al., 2013; Hammes et al., 2001; Hu et al., 2013; Kreidberg et al., 1993; Luo, Ikeda, & Parker, 1994; N. Miyamoto, Yoshida, Kuratani, Matsuo, & Aizawa, 1997; Sadovsky et al., 1995). These genes are all critical for gonadal development, and without which gonads are not present in both sexes. What follows is a brief description of how these genes contributes to the formation of the bipotential gonad

GATA4

GATA4 is a member of the highly conserved GATA family, which is characterised by its 2 zinc finger domains. These domains are crucial for binding DNA and activating gene expression as well as for binding to other transcription cofactors. *Gata4* is the earliest known transcription

factor to define the bipotential gonad, with expression present by E10 in the coelomic epithelial cells of mice (Hu et al., 2013). Subsequently, *Gata4* marks the developing somatic cell lineages of the gonad (Sertoli cells in testes and granulosa cells in ovaries) (Viger, Mertineit, Trasler, & Nemer, 1998). Mice with *Gata4* knocked out completely die before genital ridge formation due to its essential role in the development of multiple organ systems thus, to investigate its role in the bipotential gonad *Gata4* had to be conditionally deleted after E8.75 (Hu et al., 2013). These mice die by E11.5, the time of sex determination, however they exhibit no signs of initiation of gonad formation showing that Gata4 plays a very early role in gonadogenesis (Hu et al., 2013). This study demonstrated that Gata4 also controls the expression of two other genes critical the formation of the gonad which are expressed in gonadal progenitors, *Nr5a1* and *Lhx9,* whose role will be discussed later in this section (Hu et al., 2013). After sex determination, *Gata4* expression persists in the testes but is markedly reduced in the ovaries indicative of a later role in testicular development and function (Viger et al., 1998).

In humans, mutation to *GATA4* is commonly associated with congenital heart defects (OMIM:600576). While over 120 variants have been described in association with cardiac defects, only a small handful of studies report mutations which lead to 46, XY Disorders of Sex Development (DSD) (Eggers et al., 2016; Harrison et al., 2014; Lourenco et al., 2011; Martinez de LaPiscina et al., 2018; White et al., 2011). The phenotype of these patients ranges from micro penis through to complete gonadal dysgenesis. Interestingly, many of the mutations leading to DSD are located in the N-terminal zinc finger domain which is responsible for DNA binding and cofactor interaction (Martinez de LaPiscina et al., 2018). Further mutations have been found in the regulatory regions, both upstream and downstream of *GATA4* indicating the likely disruption of gonadal regulatory elements (Harrison et al., 2014; White et al., 2011). The role of GATA4 beyond the bipotential gonad will be further discussed later in this review.

WT1

WT1 encodes a zinc finger DNA-binding protein, also WT1, which is inactivated in some Wilms' tumours and has important roles in gonad development. It is required for the formation of the bipotential gonad in both males and females (Kreidberg et al., 1993). Human mutation to *WT1* cause a range of conditions including Frasier syndrome (OMIM:136680), WAGR (Wilms tumour, aniridia, genitourinary abnormalities, mental retardation) (OMIM:194072) and Denys-Drash Syndrome (DDS) (OMIM:194080) where the defining phenotypes include urogenital abnormalities. These range from cryptorchidism and hypospadias in WAGR to sex reversal and gonadal dysgenesis, eventually leading to gonadoblastoma in DDS and Frasier

syndromes (Frasier, Bashore, & Mosier, 1964; Haning, Chesney, Moorthy, & Gilbert, 1985; Kinberg, Angle, & Wilson, 1987; Klamt et al., 1998; Pelletier et al., 1991; Riccardi, Sujansky, Smith, & Francke, 1978). Complete ablation of *WT1* results in embryonic lethality and the failure of kidney and gonad development due to apoptosis of the primordial mesonephric structure (Kreidberg et al., 1993).

While there are 24 isoforms of WT1, the two major isoforms are the result of variable splicing at exon 9, coding for the insertion of a lysine, threonine and serine (KTS) between the third and fourth zinc finger resulting in the variants WT1+KTS and WT1-KTS. While partly redundant, each of these isoforms performs distinct roles in the development of the embryonic gonad. Disruption of the balance between these isoforms perturbs the development of the male gonad (Hammes et al., 2001; Wilhelm & Englert, 2002). Ablation studies have identified *WT1-KTS* as the variant responsible for the survival of the primordial gonad, as knockout mice have increased apoptosis. Importantly, this variant is also responsible for activating the expression of *NR5A1,* the gene encoding SF1 (the role of which is discussed later in this section) (Wilhelm & Englert, 2002).
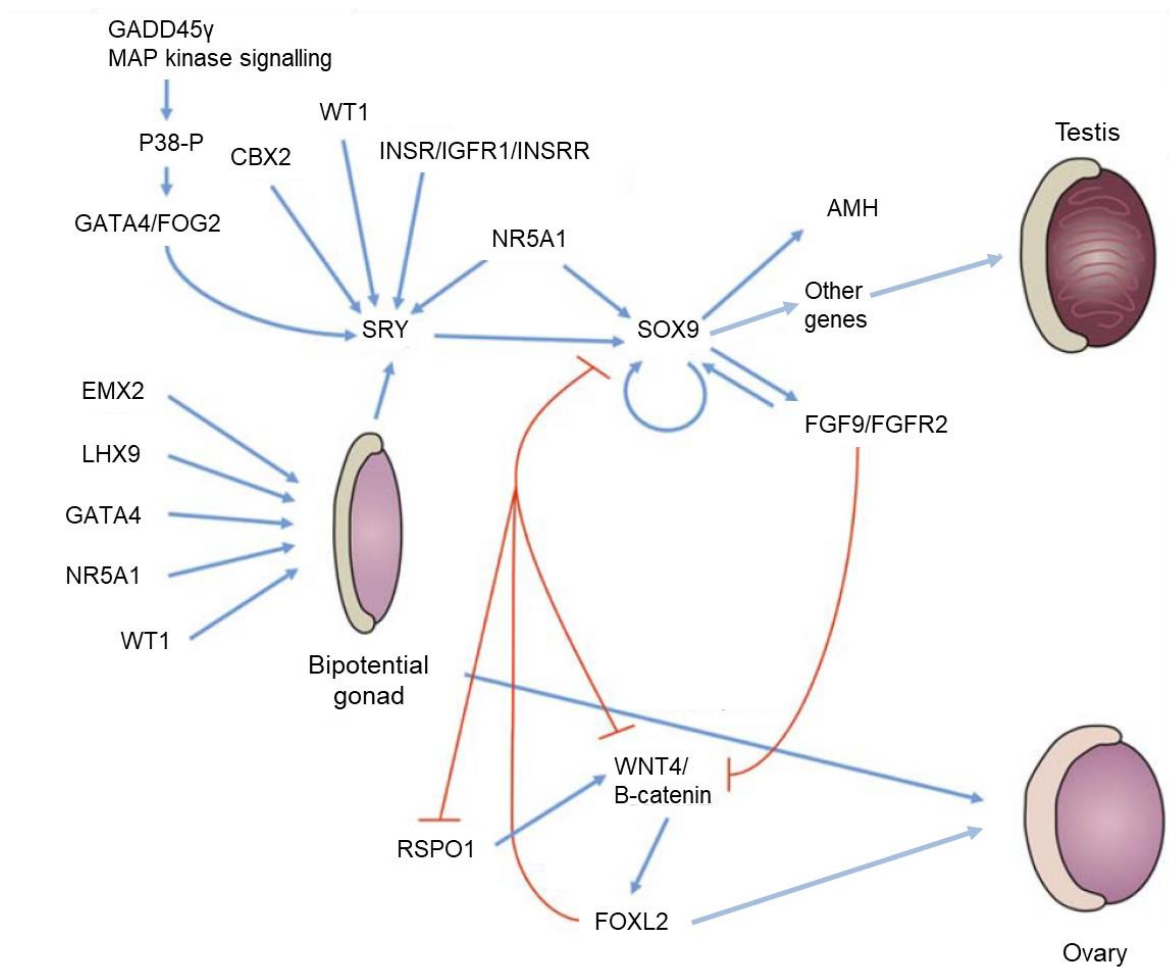
Figure 1.4. Gene regulatory networks which drive the development of the testis and ovary. Genes that have been shown to play a role in gonad development, sex determination and differentiation. Arrows do not necessarily imply direct regulation. The testis and ovary develop from the bipotential gonad, depending on the presence of *SRY* and activation of sex specific gene cascades. Genes from one pathway can repress gene expression in the other as indicated in red. Other genes refers to direct target genes of *SOX9* both characterised and yet to be discovered which have a role in gonad development. Figure adapted from (Croft, Ayers, Sinclair, & Ohnesorg, 2016)

NR5A1

The gene *NR5A1* encodes an orphan nuclear receptor, Steroidogenic factor 1, or SF1. SF1 is essential for the regulation of the development and function of the endocrine system, including the urogenital ridge and the adrenal glands. It is critical for the survival of the bipotential gonad, male sex determination and for the maintenance of the male factors in the gonad after sex determination (Wilhelm & Englert, 2002). In the biopotential gonad, *Nr5a1* is expressed from E9.5, under the regulation of Wt1 and Lhx9 (Wilhelm & Englert, 2002). Mice lacking *Nr5a1* develop biopotential gonads which subsequently completely deteriorate through apoptosis, leaving the mice to be born without gonads or adrenal glands (Luo et al., 1994). In humans, heterozygous mutation to *NR5A1* presents through a wide variety of clinical symptoms including adrenal failure, primary ovarian insufficiency and 46,XY Disorders of Sex Development (DSD) ranging from hypospadias to complete gonadal dysgenesis (OMIM:184757) (Achermann, Ito, Ito, Hindmarsh, & Jameson, 1999; Allali et al., 2011; Kohler et al., 2008; L. Lin et al., 2007). In contrast, haploinsufficiency in mice leads to delayed expression of steroidogenic genes which recovers by birth, suggesting the possible action of compensatory pathways or less dependence on *SF1* than in humans (Park et al., 2005).

LHX9

Lim homeobox 9 (*LHX9*) encodes a transcription factor which is expressed in the early genital ridge, under the control of GATA4 (Birk et al., 2000; Hu et al., 2013). LHX9 is responsible for proliferation of the bipotential gonad, as well as activating the expression of *Nr5a1* (Birk et al., 2000) (Wilhelm & Englert, 2002). In mutant mice the gonad ceases growth at E11.5 resulting in a complete gonadal regression by E13.5 (Birk et al., 2000). As a result, all *Lhx9* mutant mice are born with female genitalia and with no gonads, regardless of the presence or absence of a Y chromosome (Birk et al., 2000). To date, mutations causing have not been found in human patients despite its high level of conservation with mouse *Lhx9 (Ottolenghi et al., 2001)*. The role of human *LHX9*, and potential redundant genes needs to be further investigated to draw conclusions about the importance of its role.

EMX2

Empty spiracles homeobox 2, or *EMX2*, encodes another transcription factor which is essential for the developing neural system in vertebrates (Kastury et al., 1994; Matsuo et al., 1997). *Emx2* is expressed in the coelomic epithelium and the mesonephros of both sexes from E10. Strong expression is maintained in the female gonad, but it fades in the male at E13.5, indicative of an early role in gonad development. Supporting this, mutant *Emx2* mice completely fail to develop kidneys, ureters, gonads and genital tracts (N. Miyamoto et al., 1997). Similar to *Lhx9*, *Wt1*, and *Nr5a1* mutants the *Emx2* mutant mice have an impaired

thickening of the coelomic epithelium before E12, suggesting a critical role In early cell proliferation or differentiation of the coelomic epithelium (N. Miyamoto et al., 1997; Svingen & Koopman, 2007). Mutation to *EMX2* in humans has not yet been identified as causative of DSD yet. As homeobox transcription factors are abundant throughout development, it is possible that there are redundant genes in the human, able to compensate for any loss of function.

SRY in the developing testis

SRY was discovered as the testis determining factor in both humans and mice in 1990 and is the founding member of the SOX (SRY-related HMG box) family of transcription factors (Gubbay et al., 1990; Sinclair et al., 1990). In fact, *SRY* is the sex determining gene in most mammals, with the exception of monotremes (Wallis et al., 2007). SRY is defined by its high mobility group (HMG)-box which binds DNA at (A/T)ACAA(T/A) sequences. This binding introduces a 60-85° bend to the DNA, allowing SRY to modify the chromatin and regulate the transcription of its target genes (Harley & Goodfellow, 1994).

The majority of our understanding of SRY and its role in sex determination has come from studies in mice. In the embryonic mouse, *Sry* expression begins at day 10.5 (E10.5) in the somatic cells, peaking at E11.5 (Koopman et al., 1990). *Sry* is sufficient for the differentiation of the male somatic lineage, Sertoli cells, and thus the differentiation of the testis. This was highlighted in 1991 where Koopman et al., introduced *Sry* to XX embryos, resulting in testicular development despite the absence of a Y chromosome(Koopman, Gubbay, Vivian, Goodfellow, & Lovell-Badge, 1991). Chimeric mouse studies have demonstrated a threshold for Sry expression where gonads containing 35-40% of XY somatic cells directed the formation of a testis whereas gonads with fewer than 10% of XY somatic cells developed as ovaries(Burgoyne, Buehr, & McLaren, 1988).

The timing of initiation of *Sry* expression is crucial to proper testis development. In naturally occurring sex reversed mouse strains, delays in the onset and the peak level of *Sry* expression of 6-10 hours is enough to cause the XY gonad to develop as an ovary(Bullejos & Koopman, 2005). Transgenic mouse studies confirm this naturally occurring phenomenon. In mice where *Sry* expression is under the control of a heat shock promoter and thus can be induced at a range of experimental time points, delays of 6-hours also resulted in ovarian development dominating(Hiramatsu et al., 2009). Given the critical window for the induction of *Sry* expression, it is not surprising that *Sry* knockout mice develop ovaries and subsequently as females(Kato et al., 2013). The critical boundary of this window to ensure male development ensues is likely defined by the need to prevent female pathways activating.

Unlike the timing of initiation of *Sry* expression, the duration seems to have less importance as it varies among species. In mice, *Sry* expression peaks at E11.5 and declines to undetectable levels after E12.5 (Hacker, Capel, Goodfellow, & Lovell-Badge, 1995; Koopman et al., 1990). Similarly, in human the pattern of *SRY* expression also declines after reaching a peak at the time of sex determination (Carnegie Stage 17-23) however unlike in the mouse it does not completely disappear (Del Valle et al., 2017; Hanley et al., 2000). *Sry* expression is also maintained in the goat (Montazer-Torbati et al., 2010).

SRY targets *SOX9*, upregulating its expression to ensure the male fate (Sekido & Lovell-Badge, 2008). SOX9 is arguably the key player in male sex development. *Sox9* expression is upregulated immediately after *Sry* however unlike *Sry, Sox9* expression persists in the mouse gonad beyond E12.5 (Kent, Wheatley, Andrews, Sinclair, & Koopman, 1996; Morais da Silva et al., 1996). The role and regulation of *SOX9* in the developing testis will be further explored later in this review. While other genes, such as *Cbln4*, have been defined as targets of Sry their role in testis development requires further clarification (Bradford, Hiramatsu, et al., 2009).

The spatio-temporal expression of *Sry* in mice is somewhat unusual. Expression begins at the centre of the developing gonad and extends to the poles over several hours(Bullejos & Koopman, 2001). This dynamic wave of expression has a significant impact on testis development, as *Sox9* subsequently follows the same pattern leaving the poles more vulnerable to XY sex reversal (Bagheri-Fam et al., 2008; Bullejos & Koopman, 2001; Wilhelm et al., 2007). Thus, when ovotestes are formed it is likely that the ovarian cells will be seen at the poles while the testicular tissues are in the centre. Multiple testicular factors critically ensure the proper spatio-temporal expression and action of *SRY*, these include SF1, CBX2, WT1, Insulin-like growth factor signalling, GATA4/FOG2, MAP kinase signalling and GADD45γ (**Figure 1.4**). By understanding how these genes influence *SRY* expression we can begin to piece together the complex puzzle that is the sex determination of the male gonad.

SF1

SF1 can bind to the promoter of *SRY* and partly increase its expression (de Santa Barbara et al., 2001). Mutation to a putative binding site in the proximal *SRY* promoter abolished this activity (de Santa Barbara et al., 2001).. Studies on the porcine proximal promoter of *SRY* have also identified SF1 as an important regulator of *SRY* activity (Pilon et al., 2003). Aside from its role in the regulation of *SRY*, SF1 plays a crucial role in cooperating with SRY to upregulate the expression of its key target gene, SOX9 (Croft et al., 2018; Gonen et al., 2018; Sekido & Lovell-Badge, 2008). This role will be explored later in this review.

CBX2

CBX2 encodes a polycomb group transcription factor which regulates gene expression by modifying histones to mediate gene silencing. Mutation to *CBX2* in both humans and mice leads to 46, XY sex reversal accompanied by a dramatic decrease in *Sry* transcripts (OMIM:602770) (Biason-Lauber, Konrad, Meyer, DeBeaufort, & Schoenle, 2009; Katoh-Fukui et al., 2012; Katoh-Fukui et al., 1998). Even when the male phenotype is restored by forcing *Sry* expression in the absence of *Cbx2* the testes are still hypoplastic, indicative of a role in proliferation too (Katoh-Fukui et al., 2012). A recent study addressed the changes to histone marks in *Cbx2* knockout mice and revealed that many of the genes with a loss of repression were part of the (pro-female) Wnt4 pathway. Unsurprisingly, the male phenotype was restored when *Wnt4* was simultaneously knocked out with *Cbx2* suggesting that the stabilisation of the male fate requires repression of the female pathway to ensure there is no block to *Sry* expression (Garcia-Moreno et al., 2019).

WT1

Aside from its critical role in the establishment of the bipotential gonad, WT1 also plays a critical role in the regulation of *SRY* expression. The WT1 +KTS variant is primarily involved in the male sex determination pathway by activating the expression of *Sry*. The absence or mutation of this variant leads to reduced *Sry* levels and consequently, reduced *Sox9* (Bradford, Wilhelm, et al., 2009; Hammes et al., 2001).

WT1 and GATA4 transcriptionally cooperate to activate *SRY* expression in the mouse, human and pig *SRY* proximal promoter (Y. Miyamoto, Taniguchi, Hamel, Silversides, & Viger, 2008). Unsurprisingly, the WT1 +KTS variant had almost double the synergistic action compared to the -KTS variant (Y. Miyamoto et al., 2008).

Insulin-like growth factor signalling

The insulin-like growth factors are critical for sex determination and testicular function as loss of all three insulin receptor genes (*Insulin receptor (Insr), Insulin like growth factor 1 receptor (Igfr1)* and *Insulin receptor-related receptor (Insrr)*) causes male to female sex reversal in mice (Nef et al., 2003). XY gonads with all three receptors missing had dramatically reduced *Sry* and *Sox9* levels and consequentially expressed female markers, indicating a critical role for insulin signalling in male sex determination (Nef et al., 2003). Furthermore, *GADD45γ* expression was also reduced in these mutant mice, the role of which will be discussed later in this review (Nef et al., 2003; Pitetti et al., 2013). Interestingly, both the XY and XX gonads displayed a reduction in size also indicating that insulin signalling contributes to proliferation in the gonad (Nef et al., 2003). This reduction in size stems from both a reduction in Sertoli cell proliferation as well as a reduction in Leydig cell proliferation (Neirijnck et al., 2018). Specific ablation of *Insr* and *Igfr1* from Sertoli cells only displayed a reduced testis weight of

72% in adult mice, and similarly when both genes were ablated specifically from Leydig cells a reduction of 85% was observed (Neirijnck et al., 2018). Interestingly though, the fetal Leydig cell population was unaffected by the loss of Leydig *Insr* and *Igfr1* thus signifying that Sertoli cell insulin signalling which drive male differentiation (Neirijnck et al., 2018).

GATA4/FOG2

In addition to its role in the establishment of the bipotential gonad, GATA4 is also required for testis differentiation. Mutation to the domain which interacts with a binding partner, FOG2, or complete loss of FOG2 results in significantly reduced *SRY* levels and subsequently failure of Sertoli cell differentiation leading to sex reversal (Bouma, Washburn, Albrecht, & Eicher, 2007; Tevosian et al., 2002). Mutation to *FOG2* in humans can also lead to 46, XY sex reversal and similar to *GATA4* mutation (explored earlier in this review), is also associated with cardiac anomalies (OMIM:603693) (Bashamboo et al., 2014).

Many GATA binding sites can be identified in the *SRY* proximal promoter. Phosphorylation of GATA4 via the Map kinase signalling cascade enhances its DNA binding ability and increases expression of transcripts which it regulates (**Figure 1.5**) (Warr et al., 2012). The Map kinase signalling pathway is further discussed below. As mentioned above, GATA4 also synergises with WT1 at the *SRY* proximal promoter to activate *SRY* expression thus deeming it a critical component of the *SRY* regulatory pathway (Y. Miyamoto et al., 2008). Interestingly, when GATA4 is transfected into cells without WT1, it does not activate the human promoter, only the mouse and pig (Y. Miyamoto et al., 2008). Furthermore, mutation to the WT1 binding site but not the GATA sites abolishes *SRY* activation on the mouse promoter suggesting it is the direct interaction of WT1 with the promoter which is needed to initiate *SRY* expression (Y. Miyamoto et al., 2008).
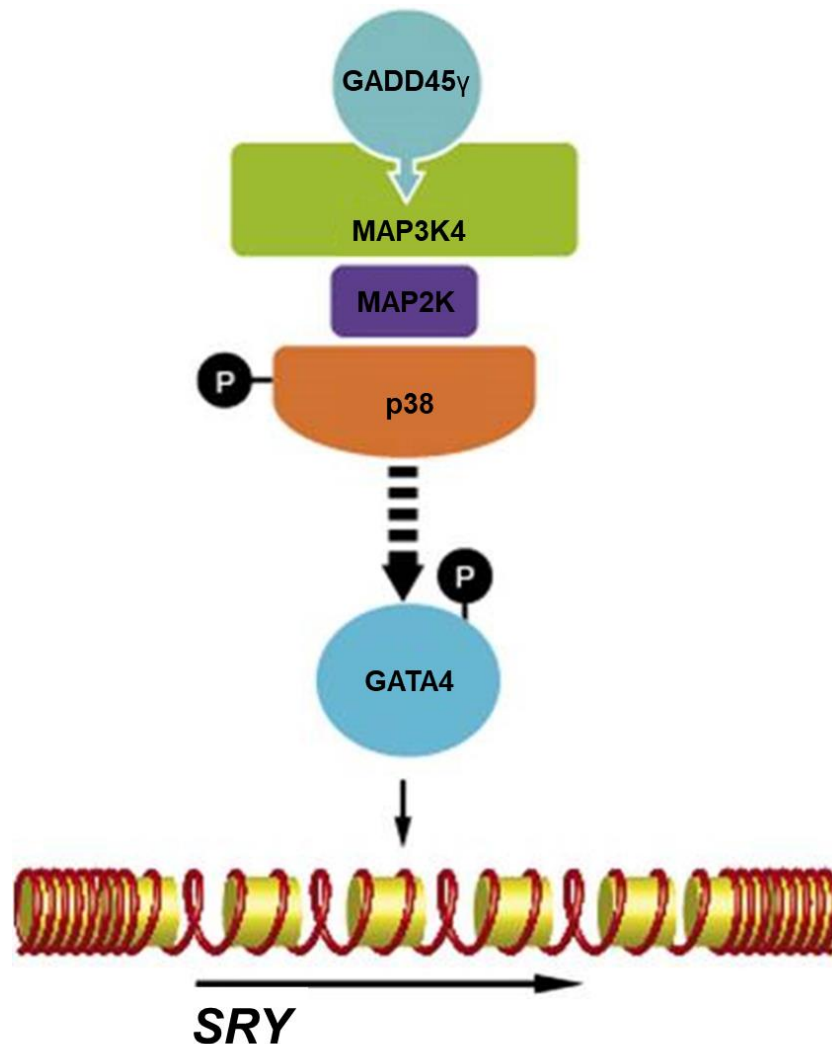
Figure 1.5. MAP kinase signalling cascade in the developing testis*. GADD45γ activates MAP3K4 in pre-Sertoli cells, in mice around E10.5. Through a MAP2K, MAP3K4 phosphorylates p38, thus activating it (indicated by a circled P). Either directly or indirectly, p38 activates GATA4 by phosphorylation which in turn acts upon the *SRY* promoter to induce expression. Figure adapted from (Warr et al., 2012).

MAP kinase signalling

The mitogen-activated protein (MAP) kinase signalling pathway is required for *Sry* regulation and testis development in both mice and in humans. Targeted mutation to kinases at all levels of the canonical three-tier Map kinase signalling cascade (Map3k, Map2k, Mapk) lead to male to female sex reversal (Bogani et al., 2009; Warr et al., 2012; Warr, Siggers, Carre, Wells, & Greenfield, 2016). Mutation to *Map3k4* and *p38 Mapk* in mice results in reduced phosphorylation of Gata4, which directly regulates *Sry* expression, therefore leading to a reduction in *Sry* levels and disrupted testis development (**Figure 1.5**).

In humans, mutation to *MAP3K1* has been associated with a 46, XY sex reversal in a number of patients (OMIM: 600982) where the mutations directly affect the ability of MAP3K1 to phosphorylate its downstream targets p38, MAPK1 and MAPK3 (Granados et al., 2017; Pearlman et al., 2010). Surprisingly though, mutation to *Map3k1* in mice elicits only minor abnormalities in gonadal development such as an increase in gonadal length, highlighting the limitations of relying on mouse models to investigate sex determination (Warr et al., 2016).

GADD45γ

GADD45γ is a member of the G̲rowth A̲rrest and D̲NA D̲amage response proteins which are implicated in DNA repair and active DNA demethylation, as well the activation of MAP kinase signalling (**Figure 1.5**). Mutation to *Gadd45γ* in XY mice causes a range of gonadal phenotypes from infertility, to gonadal dysgenesis, to complete sex reversal depending on genetic background (Johnen et al., 2013). These phenotypes have been attributed to a delay and failure of *Sry* expression to reach threshold levels necessary to initiate male differentiation (Johnen et al., 2013). In these mutants p38 MAP kinase signalling is impaired, presumably resulting in a reduction of GATA4 phosphorylation which causes the reduction of *Sry* expression (Gierl, Gruhn, von Seggern, Maltry, & Niehrs, 2012; Johnen et al., 2013). Transgenic overexpression of *Map3k4* in *Gadd45γ* deficient embryos rescues the sex reversal phenotype reiterating the importance of this signal transduction pathway to regulating *Sry* levels. *Gadd45γ* possibly provides the link between insulin signalling and *Sry* expression as knocking out all three insulin receptors in mice also reduces *Gadd45γ* (Larney, Bailey, & Koopman, 2014; Nef et al., 2003; Pitetti et al., 2013). Human mutations to *GADD45γ* leading to sex reversal are yet to be reported however as with the MAP kinase genes, it is possible that a related protein plays a more prominent role in human testis development.

SOX9 in the developing testis

SOX9 is arguably the most critical gene in male sex determination. As the only key target of SRY, it stands atop of the male sex determining pathway. It initiates and regulates a wide

variety of processes in Sertoli cells essential to the differentiation of the male gonad. It was discovered as the gene mutated in Campomelic Dysplasia (CD) and Autosomal Sex Reversal (SRA), a semi-lethal, skeletal malformation syndrome affecting multiple organ systems including the gonads, as two thirds of XY patients are sex reversed (OMIM:114290) (Wagner et al., 1994).

Similar to SRY, SOX9 is a member of the SOX family and thus contains the signature HMG box but unlike SRY is a member of the SOXE family, along with *SOX8* and *SOX10* (Bowles, Schepers, & Koopman, 2000). Three exons encode the 509 amino acid protein which contains 4 domains; the highly conserved HMG box, a dimerization domain and two transactivation domains (**Figure 1.6**). While the HMG box of all SOX proteins recognises and binds the consensus sequence, AACAAT, SOX9 optimally binds AGAACAATGG-the core sequence flanked by 5'AG and 3'GG nucleotides (Mertin, McDowall, & Harley, 1999). SRY and the other SOX proteins do not have affinity for these flanking nucleotides, suggesting a mechanism for how the SOX proteins achieve specificity (Mertin et al., 1999).

Another feature unique to the SOXE proteins in the 40 amino acid dimerization domain (**Figure 1.6**). This domain mediates dimerization by binding to the HMG box of other SOXE proteins in a co-operative manner to form both homo- and hetero- dimers (Huang, Jankowski, Cheah, Prabhakar, & Jauch, 2015). This dimerization exclusively occurs between SOXE transcription factors (Huang et al., 2015). Dimerization of SOX9 is required for chondrogenesis, but not for Sertoli cell function so it is unsurprising that human mutations in the dimer domain of *SOX9* result in CD without SRA as the Sertoli cell function of SOX9 is retained (Bernard et al., 2003). This points to a mechanism whereby *SOX9* is able to act in a tissue specific manner, regulating different target genes. Two transactivation domains are needed for maximal transcriptional activation activity of SOX9 (McDowall et al., 1999) (**Figure 1.6**). These are a proline, serine and glutamine (PQS) rich region at the C-terminus and a proline, glutamine alanine (PQA) rich region (McDowall et al., 1999). Mutations in these regions result in CD and SRA (McDowall et al., 1999; Sudbeck, Schmitz, Baeuerle, & Scherer, 1996).
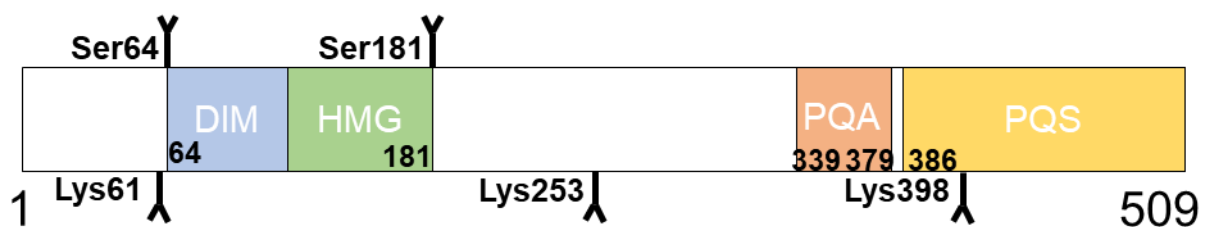
Figure 1.6. SOX9 protein structure. SOX9 consists of a single chain of 509 amino acids. The Dimerisation domain (DIM, blue) immediately precedes the HMG box (green). Further towards the C-terminus of the protein protein are the proline, glutamine, alanine rich region (PQA, orange) and the proline, glutamine serine rich region (PQS, yellow) which are required for transactivation. Post-translational modifications are made at the highlighted residues which target SOX9 protein for either sumoylation or ubiquitination. Figure adapted from (Symon & Harley, 2017).

In humans, loss of one functional allele of *SOX9*, comparable to a 50% reduction in *SOX9* levels, results in a loss of Sertoli cell function and thus sex reversal (G. J. Kim et al., 2015; Wagner et al., 1994). This differs in mice where gonadal development proceeds normally with 50% of wild type levels (Barrionuevo et al., 2006). It is not until the mRNA levels decrease to 23% that phenotypic indications of sex reversal are first seen (Gonen, Quinn, O'Neill, Koopman, & Lovell-Badge, 2017). As complete ablation of *Sox9* is embryonic lethal at E11.5, before testis development has proceeded, conditional knockouts have been used to investigate its role in testicular development (Barrionuevo et al., 2006; Gonen et al., 2017). When *Sox9* is removed before sex determination in the primordial gonad, such as with *Cytokeratin-Cre* (*Ck19-Cre*), XY mice develop ovaries and show complete sex reversal thus reiterating its central role in sex determination and testis development (Barrionuevo et al., 2006). Sox9 has also been ablated in Sertoli cells after sex determination using Amh-*Cre,* where Sox9 protein is detected at E12.5 but is mostly lost by E13.5 (**Figure 1.7, a**) (Barrionuevo et al., 2009). Normal testis development proceeds and the male mice are fertile until 5 months of age indicating that Sox9 also plays a crucial role in the maintenance of testis function (**Figure 1.7, b**) (Barrionuevo et al., 2009). When these mice are crossed to a *Sox8* null background, ovary-specific markers are detected in embryonic testes and Sertoli cell junction integrity is lost in embryonic testes which results in complete primary infertility (Barrionuevo et al., 2009; Georg, Barrionuevo, Wiech, & Scherer, 2012).
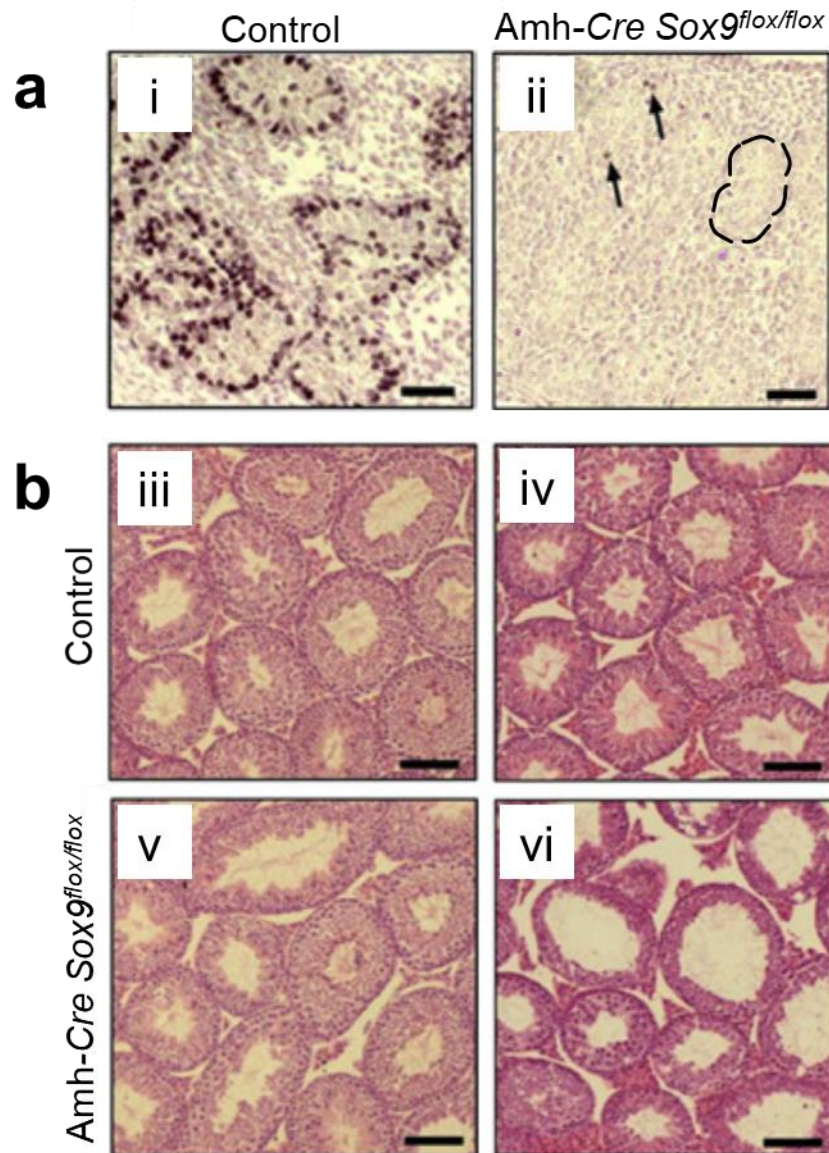
Figure 1.7. Amh-*Cre Sox9^flox/flox* testes (a) Immunoistochemistry of wildtype (i) and *Sox9* knockout (ii) testes at E13.5 showing that Sox9 (brown staining) is almost completely lost from the testes by E13.5, with only a few cells expressing Sox9 (ii, black arrows). A cord devoid of Sox9 positive cells has been outlined with a black dotted line. Scale bars represent 10µm **(b)** Hematoxylin and eosin stain of control (v and vi) and *Sox9* knockout (vii and viii) gonads at 3 months and 5 months after birth. In the *Sox9* knockout testes the tubules are normal and contain sperm at 3 months (vii) but by 5 months are devoid of sperm. Scale bars represent 50µm. Figures adapted from (Barrionuevo et al., 2009)

Gain of function models have also reinforced the indispensable role of Sox9 in testis development. Driving *Sox9* over expression in the gonads of XX mice induces testis formation, as does the chance insertion of a transgene (*Odd sex*) in the regulatory region of *Sox9* which induces inappropriate expression in the gonad (Bishop et al., 2000; Qin et al., 2004; Vidal, Chaboissier, de Rooij, & Schedl, 2001). Crossing these *Odd sex* mice to XY mice with ablated *Sry* resulted in completely normal testis development and normal fertility, reiterating that Sox9 is both necessary and sufficient for testis development (Qin & Bishop, 2005). Conversely, ovarian development requires the repression of *Sox9*, by factors such as *Wnt4, Rspo1* and *Foxl2 (Y. Kim et al., 2006; Maatouk et al., 2008; Schmidt et al., 2004).* Repression of *Sox9* must be maintained throughout life to prevent the trans-differentiation of granulosa cells into Sertoli cells, which will eventually lead to the rest of the gonad developing a male phenotype (Lindeman et al., 2015; Schmidt et al., 2004; Uhlenhaut et al., 2009; Zhao, Svingen, Ng, & Koopman, 2015).

To better understand the critical role that *SOX9* plays in the development of the testis, it is vital to explore both its regulation and action in a testis-specific context.

1.4.1   Regulation of *SOX9* in the developing testis

In humans, *SOX9* is located on chromosome 17 and in mice is located on chromosome 11. In both species, *SOX9* expression increases in the male gonad following the onset of *SRY* transcription, reaching a maximum by Carnegie stage 18-21 in humans and E11.5 in mice (Hanley et al., 2000; Jameson, Natarajan, et al., 2012). *SOX9* is located in a vast region lacking other protein coding genes, 2.5Mb in humans and 2.2Mb in mice (Symon & Harley, 2017). This gene 'desert' contains numerous regulatory elements, allowing expression to be tightly controlled in many different tissues at various times throughout development and adulthood (Symon & Harley, 2017).

Mutations in the regulatory region of *SOX9* cause CD, or isolated aspects of the CD syndrome such as craniofacial malformations called Pierre Robin Syndrome (Gordon et al., 2009). The position of the breakpoint on the chromosome can dictate the phenotype associated with the disease. For example, Pierre Robin Syndrome is a feature of CD but can also occur in isolation when chromosomal breakpoints are greater than 1Mb upstream of the *SOX9* transcription start site (Benko et al., 2009; Gordon et al., 2014). Transgenic reporter studies have also demonstrated how distinct enhancers control tissue-specific expression of *SOX9* however the search for testis-specific enhancers has been difficult as the human counterparts of mouse enhancers are not always conserved (Symon & Harley, 2017).

In 2008, the first testis-specific enhancer of *Sox9* was reported by Sekido and Lovell-Badge (Sekido & Lovell-Badge, 2008). This was discovered using a bacterial artificial chromosome

carrying a 120kb fragment which encompassed *Sox9* and some of its regulatory region, both up and downstream of the transcription start site along with a *lacZ* reporter gene. Mice expressing this construct mimicked features of *Sox9* expression in the testis including onset of gonadal expression at E10.5, increasing at E11.5 and then becoming restricted to the testis by E12.5 (Sekido & Lovell-Badge, 2008). Fragmentation of the construct narrowed down the regulatory region to a 3.2kb element, located -13 to -10kb upstream of the *Sox9* transcription start site, termed TES (Testis-specific Enhancer of *Sox9*). Within TES, a 1.4kb element was defined which recapitulates Sertoli cell *Sox9* activity and named TESCO (TES Core) (Sekido & Lovell-Badge, 2008). Furthermore, Chromatin Immunoprecipitation (ChIP) experiments demonstrated that both Sry and Sf1 bind to TES *in vivo* at E11.5 in the testis and *Sox9* binds to TES at E12.5 (Y. Li, Zheng, & Lau, 2014; Sekido & Lovell-Badge, 2008). This suggests a feed-forward regulatory loop whereby Sf1 initiates transcription in both gonads, Sry upregulates transcription in the male gonad and when a critical threshold is reached, Sox9 acts to maintain its own expression (Sekido & Lovell-Badge, 2008).

TES has also been implicated in the repression of *Sox9* in the ovary through multiple mechanisms. Firstly, the WNT4 signalling pathway, specifically β-catenin, disrupts Sf1 binding to TES thereby inhibiting *Sox9* expression and the differentiation of Sertoli cells (Bernard et al., 2012). Similarly, overexpression of *Dax1*, an orphan nuclear receptor, also inhibits *Sox9* expression by competing with Sf1 to bind to TES (Ludbrook et al., 2012). In humans, duplications of *DAX1* causes male to female sex reversal in XY patients (OMIM:300473). ChIP on ovaries has also demonstrated that both pro-female factors, Esr1 (Estrogen Receptor 1) and Foxl2 (a forkhead domain transcription factor) bind to TES *in vivo* suggesting repression to allow the differentiation of granulosa cells (Jakob & Lovell-Badge, 2011; Uhlenhaut et al., 2009). Conditional knockout of *Foxl2* from adult ovaries leads to reprogramming of the somatic cell lineage to Sertoli cells following the onset of *Sox9* expression (Uhlenhaut et al., 2009). Interestingly though, complete ablation of *Foxl2* from mice ovaries does not result in XX sex reversal suggesting that its key role at TES is to maintain *Sox9* repression (Schmidt et al., 2004; Uda et al., 2004). In support of this later role, in humans mutation to *FOXL2* results in BPES (Blepharophimosis/ptosis/epicanthus inversus syndrome) which is associated with premature ovarian failure caused by an absence of functional granulosa cells leading to oocyte atresia (OMIM:110100) (Schmidt et al., 2004; Uda et al., 2004).

Despite these properties supporting TES as an important regulator of *SOX9* in the developing testis, ablation of TES/TESCO does not cause XY sex reversal or even disrupted testis development (Gonen et al., 2017). However deletion of TES/TESCO did reduce *Sox9* mRNA to 44% of wildtype, indicating that while it makes a major contribution to *Sox9* expression it does not act alone (Gonen et al., 2017). Furthermore, in transgenic mice, the human *TES*

sequence has no testis-specific enhancer activity and despite a large number of idiopathic human XY gonadal dysgenesis cases being investigated mutations to TES have not been identified, indicating that there must be additional enhancers controlling *SOX9* in testis development (Sekido & Lovell-Badge, 2013).

It was over ten years before more enhancers governing *SOX9* expression in the developing testis were discovered. Published in 2018, Gonen et al., utilised assays which marked open chromatin in Sertoli cells at E13.5, combined with ChIPseq for a marker of active enhancers (H3K27Ac) to identify 33 potential sites in mice (Gonen et al., 2018; Maatouk et al., 2017). Using transgenic mice to identify enhancer activity, this was narrowed down to 4 enhancers termed Enh13, Enh14, Enh32 and Enh8 (**Figure 1.8**) (Gonen et al., 2018). The strongest expression was observed in Enh13, and unexpectedly Enh8 was strongly expressed in the ovary but not testis at E13.5. Intriguingly, Enh8 displays much more 'open' chromatin in granulosa cells than in Sertoli cells warranting further investigation of the role of the enhancer.

Homozygous deletion of Enh13 revealed that it is critical for sex determination, as XY mice developed ovaries (Gonen et al., 2018). *Sox9* transcript levels were depleted to that of XX control gonads (Gonen et al., 2018). ChIP assays revealed that Sry strongly binds to Enh13 at E11.5, as does Sox9 at E13.5, signifying that Enh13 is involved and critical for both the initiation and maintenance of *Sox9* expression in the developing testis (Gonen et al., 2018).

Unlike TES, Enh13 is highly conserved between humans and mice and actually maps to the distal 5' end of a 32.5kb region termed XYSR, located upstream of *SOX9* in humans which has been found deleted in multiple cases of XY DSD (**Figure 1.8**) (Gonen et al., 2018; G. J. Kim et al., 2015). Strongly supporting this, a simultaneous study found that deleting the mouse equivalent of XYSR results in male-to-female sex reversal (Ogawa et al., 2018). Using CRISPR/Cas9 and analysing sequence conservation, this 32.5kb was refined to 783bp which fully contains the 557bp Enh13 (Ogawa et al., 2018).
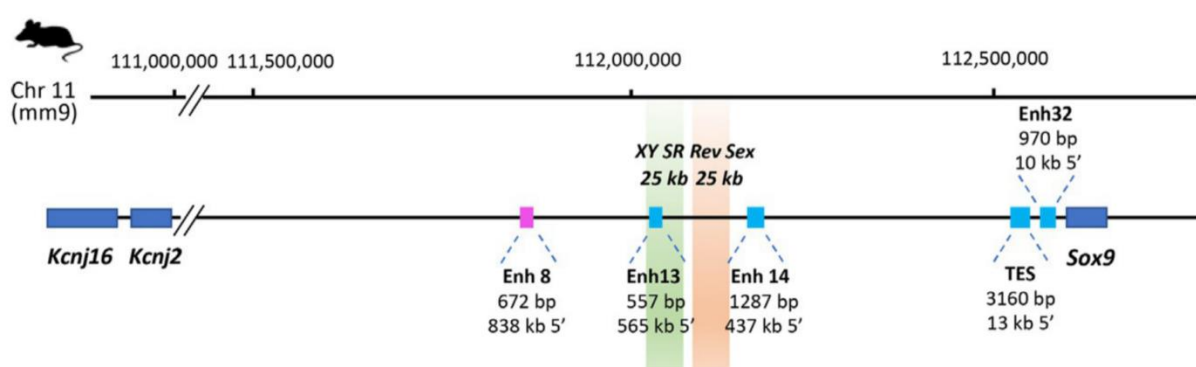
Figure 1.8. Enhancers involved in regulating *Sox9* in the developing mouse testis. Several gonadal enhancers have been identified so far. TES was the first enhancer discovered and is located 13kb upstream of *Sox9*. Three other enhancers; Enh13, Enh14 and Enh32 have recently been characterised. Enh13 is located within the human XY SR region (green shading). No mouse enhancers have been detected within the human *Rev Sex* region (orange shading). Enh8 has ovarian expression and may serve as a repressor. The sizes and locations of the enhancers are indicated above or below each enhancer. Figure adapted from (Gonen & Lovell-Badge, 2019)

Due to the high sequence conservation at Enh13, and DSD patients with deletions encompassing the homologous region (XY SR) it was assumed highly likely to play similar active role in human *SOX9* regulation (Gonen et al., 2018). This evidence soon followed, with Croft and colleagues identifying the homologous enhancer to Enh13 in humans by analysing XX testicular patients with micro duplications in the regulatory region of *SOX9* (Croft et al., 2018). This analysis led them to a 1514bp enhancer they termed Sex Reversal Enhancer-A (eSR-A), which fully encompasses the homologous region of Enh13. Interestingly, luciferase assay showed that eSR-A is activated by SOX9+SF1, but not SRY+SF1 suggesting that unlike Enh13 in the mouse it is required for maintenance but not for initiation of *SOX9* expression (Croft et al., 2018). However, as duplication of the region containing eSR-A in XX causes female-to-male sex reversal it is probable that it does play an early role in the development of the testis (Croft et al., 2018).

Croft et al., identified two more novel human enhancers of testicular *SOX9* activity termed enhancer Alternate Long-Distance Initiator (eALDI) and Sex Reversal Enhancer-B (eSR-B) (Croft et al., 2018). Luciferase assays demonstrated that it is likely that eALDI acts in the initiation of *SOX9* expression in human as it is significantly activated by SRY+SF1 and the addition of FOXL2 markedly reduced this expression (Croft et al., 2018). Furthermore, deletion of the orthologous region in the mouse did reduce *Sox9* levels by over 50% very early in testis development, but not enough to cause sex reversal suggesting that at least in the mouse, this enhancer is not the sole initiator (Croft et al., 2018). Sex Reversal Enhancer-B is likely involved in upregulation and maintenance, similar to eSR-A, as it is responsive to SOX9+SF1 in luciferase assay. Mouse mutation studies however showed no change in *Sox9* transcription, indicating that eSR-B is a human-specific enhancer (Croft et al., 2018). Interestingly, luciferase assay also demonstrated that eSR-A, eSR-B and eALDI synergise to double their relative activities when activated with SOX9+SF1, suggesting that the enhancers have a combined role in the autoregulation of *SOX9* expression (Croft et al., 2018). Understanding the higher-order chromatin structure of the gene desert encompassing *SOX9* will provide much more information regarding its complex regulation in the developing testis.

1.4.2   SOX9 role in the developing testis

SOX9 is a versatile regulator of cell fate commitment. It acts in a tissue-specific manner to modulate key cellular processes through the regulation of the expression of target genes. In hair follicle stem cells SOX9 is required for the maintenance of stem-ness, whereas in bone SOX9 is required for the differentiation of chondrocytes (Adam et al., 2015; Kadaja et al., 2014; Ohba, He, Hojo, & McMahon, 2015). Expression and chromatin immunoprecipitation analyses in bone have shown that SOX9 upregulates thousands of genes coding for extra-cellular

specific proteins in the chondrocytes, essential to their bone-specific function (Ohba et al., 2015). Likewise, in the atrioventricular canal cells of the heart, SOX9 modulates the expression of key transcription factors required for the development of the heart valves (Garside et al., 2015). Thus, it is likely that in the developing testis, SOX9 is activating the transcription of many genes required for the differentiation and function of Sertoli cells.

Key to the versatility of SOX9, and its ability to modulate the transcription of different genes in different tissues are its interactions with binding partners (Symon & Harley, 2017). The SOX9 DNA binding sequence is not specific enough to discriminate between target genes and non-target genes, meaning that co-factors are extremely important for varying its tissue-specific action (Lefebvre, Dumitriu, Penzo-Mendez, Han, & Pallavi, 2007). It is these binding partners that allow one set of genes to be regulated in the testis, while another is regulated in the bone and another in hair follicle stem cells (Adam et al., 2015). For example, in the bone *SOX9* binding to the promoter of a key extra cellular matrix protein, *COL2A1*, is critically stabilised by the adjacent binding of SOX5 and SOX6 (Kamachi, Uchikawa, & Kondoh, 2000). However, in neurogenesis SOX5 and SOX6 compete with SOX9 for binding sites, thus interfering with its function and act as repressors (Stolt et al., 2006). In the developing testis, SOX9 binding has a signature known as the "Sertoli Cell Signature" (SCS) where SOX9 binds in organised clusters with GATA4 and DMRT1, two other transcription factors required for Sertoli cell differentiation (Rahmoun et al., 2017).

In the mouse testis Sox9 acts primarily as a transcriptional activator, binding to the promoters of pro-testis genes among others with roles yet to be discerned (Rahmoun et al., 2017). Interestingly, evidence is emerging that Sox9 may also be able to directly repress pro-female genes in the developing testis such as *Wnt4* and *Foxl2,* further cementing its role as a highly versatile transcription factor (Rahmoun et al., 2017). Chromatin immunoprecipitation in embryonic mouse and bovine testes at E13.5 uncovered 4293 regions bound in the developing mammalian testis, 3849 of which were annotated in close proximity to genes (Rahmoun et al., 2017). Gene ontology term enrichment analysis showed that the male sex determination pathway, along with other genetic pathways which contribute to gonadal development and function (FGF, Hedgehog and WNT signalling) were significantly enriched in these bound genes (Rahmoun et al., 2017). Furthermore, most genes already implicated in sex determination and gonad differentiation were bound by SOX9 in both mouse and bovine testes including Amh, Dhh, Fgf9 and Foxl2. Many of these binding regions were orthologous, hinting to a highly conserved sex determination and differentiation mechanism across mammalian species (Rahmoun et al., 2017).

A major challenge in investigating *Sox9* action in the testis has been the limitations of available mouse models. As discussed earlier in this review, the development of *Sox9* knockout models has only recently begun to provide clues regarding the intricate role of testicular target gene regulation. The first *Sox9* heterozygous mutant mice were reported in 2001 where the mice displayed skeletal malformations, similar to CD, but lacked any gonadal phenotypes which later would be explained by *Sox9* not being depleted below threshold levels (Bi et al., 2001; Gonen et al., 2017). This highlighted a major difference between humans and mice in sex determination where in humans, loss of one *SOX9* allele is enough to cause gonadal dysgenesis. These mice died shortly after birth, preventing the establishment of a founder population (Bi et al., 2001). In 2006 lethality of *Sox9* ablation was circumvented by using the Cre/loxP to conditionally inactivate both *Sox9* alleles in the primordial gonad where the Cre recombinase was under the control of the *Ck19* promoter (Barrionuevo et al., 2006). This showed for the first time that XY sex reversal can be achieved with complete loss of *Sox9* in mouse gonads (Barrionuevo et al., 2006). These results also provided evidence that Sox9, not Sry, is repressing the female pathway, as the initiation of ovarian markers occurred even in the presence of Sry. A major drawback of these gonads however was that they did not specifically highlight *Sox9* action as the transcriptional profiles of the gonads resembled that of a wild type ovary. In 2009 *Sox9* was knocked out in intact testes using Amh-*Cre* which removes *Sox9* after sex determination meaning that morphologically the gonads are still testes with intact Sertoli cells (Barrionuevo et al., 2009). This suggests that *Sox9* has critical roles at both sex determination and later in maintenance of testis function. With the advent of next generation sequencing combined with these models we can now analyse *Sox9* action at a genome-wide and cellular level.

Transcriptional profiling of Amh-*Cre Sox9^{flox/flox}* mice at E13.5, the point where *Sox9* is lost in Sertoli cells (**Figure 1.7**), revealed that 240 genes were downregulated compared to wild type testes, and thus would normally be positively regulated by *Sox9* in the developing testis (Rahmoun et al., 2017). Of these 240 genes, 40% were bound by Sox9 in ChIPseq analysis showing that Sox9 positively, and directly regulates the transcription of many target genes in the developing testis. It is possible that some of these genes are crucial to testis development. Thirty-seven of these bound and positively regulated genes had expression levels in XY mutant testes which were an intermediate level between XY and XX wildtype testes. This suggests that *Sox9* is not the sole regulator of these genes as they are still partially active. Among these genes are *Amh, Sox10* and *Dhh*, each of which have known roles in sexual differentiation. Given that Sox9 binds with Dmrt1 and Gata4 in the developing testis, it is likely that they too are contributing to the regulation of expression of key sex determining genes. Interestingly, 107 genes were upregulated in the knockout suggesting a repressive action by

Sox9, however only 22% of these were bound by Sox9 suggesting that in the testis Sox9 is more likely to directly activate than repress genes (Rahmoun et al., 2017).

Regulation of RNA splicing is also emerging as a role of Sox9 in the developing testis. In chondrocytes SOX9 directly regulates splicing of *COL2A1*, an extra-cellular matrix protein, via a direct interaction with the splicing protein p54^{nrb} (Hata et al., 2008). Sex-specific splicing is a critical sex determination mechanism in *Drosophila* but until recently had not yet been implicated in mammalian sex determination (Salz, 2011). Transcriptional profiling of Amh-*Cre Sox9$^{flox/flox}$* mice also revealed that Sox9 is involved in sex-specific RNA splicing in the developing testis (Rahmoun et al., 2017). In XY mutant testes, RNA processing was significantly affected in 154 genes. Along with influencing the production of sex-specific protein isoforms, intron retention may be a powerful mechanism to regulate protein activity without altering transcription. For example, in XY mutant testes and XX wildtype ovaries, *Gadd45γ* retains its second intron which disrupts the open reading frame and leads to a truncated 52 amino acid protein, as opposed to the 159 amino acid protein found in XY wildtype testes (Rahmoun et al., 2017). Furthermore, there is no difference in *Gadd45γ* expression between XX and XY wildtype testes suggesting that Sox9 is regulating its sex-specific activity by other mechanisms. Given that Sox9 protein does not seem to splice RNA itself, this poses the question as to how Sox9 regulates splicing. The simplest description would be that Sox9 regulates the transcription of a known splicing factor. However, given that Sox9 binds 70/154 differentially spliced genes and 28% of these are bound at the exon/intron boundaries involved in the splicing events, it is possible that Sox9 recruits or regulates binding of the splicing machinery to the target genes (Rahmoun et al., 2017). The possibility that Sox9 can bind to pre-mRNA can also not yet be ruled out.

High throughput analysis of the transcriptome and Sox9 protein binding in the developing testis has identified many genes as Sox9 targets, some with essential testicular roles but most with testicular function yet to be discerned. A wide variety of testicular development and function is regulated by *SOX9* via its handful of target genes identified so far. The most crucial of these include *AMH, FGF9/FGFR2, PGDS/PGD2, CYP26B1, ETV5, SOX8/SOX10, GDNF* and *PADI2*.

AMH

Anti Müllerian hormone (AMH, also known as Müllerian inhibiting substance, Mis) was the first target of testicular SOX9 characterised, and the only target to be proven both *in vitro* and *in vivo* (Arango, Lovell-Badge, & Behringer, 1999). *Amh* is first expressed in mouse gonads at E12.0, immediately following the onset of *Sox9* expression and is excreted exclusively by Sertoli cells in the testis. It is responsible for the degeneration of the internal female genitalia

(Müllerian ducts), but not gonadal development (Brennan & Capel, 2004). Mutation to *AMH* in humans causes Persistent Müllerian duct syndrome, a condition resulting in bilateral cryptorchidism in otherwise normal virilized males as well as the development of an infantile uterus and fallopian tubes (OMIM:600957) (Knebelmann et al., 1991). Sox9 and Sf1 cooperate to appropriately increase *Amh* levels in the testis, but it is Sox9 alone that is required for the initiation of expression (Arango et al., 1999). Mutagenesis of the Sox9 binding site in the *Amh* promoter completely abolishes transcription, leading to pseudohermaphrodism, similar to the phenotype observed in humans (Arango et al., 1999). Furthermore, Sox9 ChIP assays have shown that binding to this site is enriched (Y. Li et al., 2014; Rahmoun et al., 2017; Sekido & Lovell-Badge, 2008). While *Amh* mutation in mice causes no gonadal perturbations, it has long been suspected to have a redundant function in inducing mesonephric cell migration as it is able to induce cell migration *in vitro* and testis cord formation in XX gonads (Ross, Tilman, Yao, MacLaughlin, & Capel, 2003).

FGF9/FGFR2

Fibroblast Growth Factor (FGF) signalling is ubiquitous throughout mammalian embryonic development, regulating cell differentiation and migration as well as organ morphogenesis (Cool & Capel, 2009). *Fgf9* is the key Fgf in mouse gonad development which is secreted by Sertoli cells. It is expressed in both the XY and XX gonad prior to sex determination and after the onset of *Sox9* expression is upregulated in the XY gonad and lost in the XX gonad (Y. Kim et al., 2006).

In mice, *Fgf9* ablation from testes results in predominantly female gonadal development, with variable gonadal phenotypes ranging from testicular hypoplasia through to completely sex reversed (Colvin, Green, Schmahl, Capel, & Ornitz, 2001). In these *Fgf9* knockout gonads, *Sox9* expression is lost without affecting *Sry* expression indicating that Fgf9 is able to regulate *Sox9* independently of its classic *Sry* regulation (Colvin et al., 2001). Furthermore, ectopic application of *Fgf9* in XX mice induces *Sox9* expression demonstrating that *Sox9* and *Fgf9* positively regulate each other in a feedforward loop (Y. Kim et al., 2006).

A critical component of Fgf9 action in the testis is its antagonism of the female pathway through *Wnt4*. In *Fgf9* knockout gonads, *Wnt4* is upregulated and similarly when *Wnt4* is ablated from the female gonad, *Fgf9* and *Sox9* are upregulated (Colvin et al., 2001; Y. Kim et al., 2006). *Wnt4* is also upregulated when *Sox9* is deleted from the gonad during sex determination, probably due to a loss of *Fgf9 (Barrionuevo et al., 2006). As Wnt4* can repress *Sox9* activation, it is unsurprising that deletion of *Wnt4* can rescue the male to female sex reversal seen in *Fgf9* knockout gonads (Jameson, Lin, & Capel, 2012). Interestingly though, *Sox9* ablation after sex determination does not affect *Fgf9* indicating that whilst Sox9 is required for the upregulation

of *Fgf9* expression, it is not the sole regulator afterwards. Aside from its cell-autonomous role in promoting the male pathway, Fgf9 also plays a crucial role in regulating the fate of germ cells, by directly acting on germ cells to inhibit meiosis (Bowles et al., 2010). In humans mutation to *FGF9* causes skeletal malformations, namely craniosynostosis and multiple synostoses (OMIM: 600921) (Rodriguez-Zabala et al., 2017). Despite significant research into *Fgf9* action in the developing testis leading to a well-established mechanism of action in the mouse, human variants leading to DSD are yet to be discovered, highlighting the possibility of stronger redundant pathways acting in human gonadal development.

FGFR2 is the receptor for FGF9 signalling in the testis. It is first expressed in coelomic epithelial cells of the primordial gonad of both sexes but localises to the nuclei of pre-Sertoli cells in the XY gonad at E11.0 (Schmahl, Kim, Colvin, Ornitz, & Capel, 2004). FGFR2 has important roles in proliferation and differentiation of Sertoli cells (Bagheri-Fam et al., 2008; Y. Kim et al., 2007). As the key receptor for Fgf9, it is unsurprising that XY *Fgfr2* mutant mice are also partially to completely sex reversed similar to the *Fgf9* mutant mice (Bagheri-Fam et al., 2008). Similarly, when crossed to *Wnt4* knockout mice, the sex reversal phenotype caused *Fgfr2* deletion is also rescued (Jameson, Lin, et al., 2012). Fgfr2 has 2 isoforms prevalent in mice gonads, Fgfr2b and Fgfr2b each with distinct ligand binding affinities and expression patterns and therefore distinct functions. It is Fgfr2c that is the dominant isoform in Sertoli cells and thus unsurprising that mutation can cause gonadal dysgenesis in both mice and humans (Bagheri-Fam et al., 2017; Bagheri-Fam et al., 2015; Y. Kim et al., 2007). Interestingly, *Fgfr2c* is required to repress another pro-female pathway, via *Foxl2* and simultaneous deletion of *Foxl2* partially rescues the sex reversal phenotype caused by *Fgfr2c* deletion (Bagheri-Fam et al., 2017). Evidence is now emerging that Sox9 may directly regulate the switch between these two isoforms in the testis by regulating splicing (Rahmoun et al., 2017).

PGD2/PGDS

Like FGF signalling, prostaglandin signalling is also regulated by SOX9 and is involved in a positive feedforward loop whereby it amplifies *SOX9* expression (Moniot et al., 2009). prostaglandin H2 is converted to prostaglandin D2 (PGD2) by Prostaglandin D2 synthase (PGDS) in Sertoli cells. PGD2 acts as an autocrine factor, promoting the nuclear translocation of *SOX9* by enhancing its ability to bind to the nuclear transport protein Importin β (Malki et al., 2005). Sox9 binds to the *Pgds* promoter in mice to promote the production of Pgd2, thus increasing the nuclear transport of Sox9 which directly maintains its own expression (Moniot et al., 2009; Wilhelm et al., 2007). Testis development proceeds normally, after a delay in Sertoli cell differentiation in *Pgds* knockout gonads however they present with cryptorchidism after the testes fail to descend in both heterozygous and homozygous mutants (Philibert et al.,

2013). To date, human cryptorchid patients have not been identified with PGD2/PGDS mutations, possibly explained by the existence of multiple mechanisms acting to reinforce *SOX9* expression and ensure thresholds are met to repress the female pathway and promote testis development (Philibert et al., 2013).

CYP26B1

Cytochrome P450 26b1 (CYP26B1) is an enzyme which acts to degrade retinoic acid (RA), originally produced in the mesonephros adjacent to the gonad in both sexes (Bowles et al., 2006). *Cyp26b1* is present in the bipotential gonad in both sexes but after sex determination becomes specific to the male somatic gonad cells (Bowles et al., 2006; Kashimada et al., 2011). In the developing ovary RA acts on germ cells, causing them to initiate meiosis and enter oogenesis. As meiosis is halted in the developing testis, so that germ cells can later enter spermatogenesis, CYP26B1 is required to break down any RA present during embryonic development (Bowles et al., 2006). In mice with *Cyp26b1* knocked out, the germ cells of the testis prematurely enter meiosis leading to mild ovotestis development and more importantly, impaired steroidogenesis leading to feminisation of the reproductive tract (Bowles et al., 2018). Sox9 and Sf1 act upstream of Cyp26b1, demonstrated by *in vitro* models and through a decrease of *Cyp26b1* when *Sox9* is ablated in mice models (Kashimada et al., 2011). Furthermore, high throughput studies have identified Sox9 binding to the Cyp26b1 promoter thus validating it as a direct target gene (Y. Li et al., 2014; Rahmoun et al., 2017). In *Foxl2* knockout ovaries, *Cyp26b1* expression increases by 20-fold suggesting that in the ovary *Foxl2* may also work to ensure the repression of *Cyp26b1* so that germ cells enter oogenesis (Kashimada et al., 2011). To date, human mutations to *CYP26B1* have not been found to lead to gonadal dysgenesis although it is intriguing to note that they are associated with skeletal and craniofacial anomalies, as can be seen in CD (OMIM: 605207) (Laue et al., 2011).

ETV5

Ets variant factor 5 (*ETV5*) is a transcription factor which is strongly expressed in the cords of the developing testis, namely the Sertoli cells and germ cells as well as the Leydig cells outside the testis cords (Alankarage et al., 2016). *Etv5* knockout mice lose the ability to self-renew and maintain spermatoagonial stem cells, which leads to unblocked spermatogenic differentiation and therefore a gradual depletion of germ cells and a Sertoli-cell only syndrome (C. Chen et al., 2005). *Etv5* maintains the spermatoagonial stem cell niche by regulating the expression of genes essential to the blood-testis barrier (Morrow et al., 2009). It also regulates chemokine signalling between Sertoli cells and germ cells, and Gdnf/Ret signalling which activates pathways essential for spermatoagonial self-renewal (Simon et al., 2010; Tyagi et al., 2009). In humans, a variant in *ETV5* (+48845G>T) is associated with a higher risk of non-

obstructive azoospermia and Sertoli cell only phenotype (O'Bryan et al., 2012). ETV5 is undoubtedly an important factor in mammalian reproduction.

Loss of *Sox9* from the developing XY gonad results in a loss of *Etv5* by 71%, to levels similar to the ovary (Alankarage et al., 2016). In cell culture using the human Sertoli-like line, NT2/D1 cells, loss of *SOX9* transcripts also results in a decrease in *ETV5*. Similarly, an increase of *SOX9* expression also results in an increase in *ETV5.* In this Sertoli-like cell line, SOX9 bound to both the proximal promoter and intron 1 of *ETV5* (Alankarage et al., 2016). ChIP experiments in mice at E12.5 and E13.5 however have not detected Sox9 binding to the *Etv5* promoter or intron 1 suggesting that it may not directly regulate *Etv5* until later in development (Y. Li et al., 2014; Rahmoun et al., 2017).

SOX8/SOX10

The SOXE family of transcription factors has 3 members with near identical DNA binding HMG domains; SOX9, SOX8 and SOX10 (Barrionuevo & Scherer, 2010). Following the onset of *Sox9* expression, *Sox8* and *Sox10* are expressed in Sertoli cells, although at lower levels than *Sox9* itself (Polanco, Wilhelm, Davidson, Knight, & Koopman, 2010; Schepers, Wilson, Wilhelm, & Koopman, 2003). Loss of *Sox9* in mice leads to the downregulation of both *Sox8* and *Sox10* in the embryonic testis, suggesting that they are both downstream of *Sox9* (Chaboissier et al., 2004; Rahmoun et al., 2017). It is worth noting however that neither *Sox8* or *Sox10* expression is completely abolished with the loss of *Sox9*, therefore suggesting that they are regulated by other factors in the testis too (Rahmoun et al., 2017).

In the absence of *Sox8* in mice the testes develop normally but progressively develop infertility at 5 months due to spermatogenic failure (O'Bryan et al., 2008; Sock, Schmidt, Hermanns-Borgmeyer, Bosl, & Wegner, 2001). Additionally, as previously discussed, perturbation to embryonic testis development is not seen until both *Sox8* and *Sox9* are deleted after sex determination suggesting that the key function of *Sox8* is to compensate for *Sox9* loss (Barrionuevo et al., 2009; Barrionuevo & Scherer, 2010). Indeed, Sox8 is able to synergistically bind with Sf1 to activate the *Amh* promoter, and with the loss of *Sox8*, *Amh* expression is reduced (Barrionuevo et al., 2009; Schepers et al., 2003). This points to a redundant relationship between SOX9 and SOX8, where SOX9 is functionally dominant but in its absence, SOX8 can compensate for many of its roles. Human mutations to *SOX8* leading to DSD have not been detected so far, suggesting that this compensatory mechanism may be intact in humans. However, as loss of only one copy of *SOX9* in humans is enough to cause XY sex reversal, the compensatory ability of SOX8 may not be as robust.

Due to the high conservation between the SOXE proteins, it was hypothesised that SOX10 is also part of a compensatory mechanism in the developing testis. Presumably due to the

functional redundancy with Sox9 and Sox8, deletion of *Sox10* in mice is unable to perturb testis development (Britsch et al., 2001; Peirano & Wegner, 2000). However, ectopic expression of *Sox10* in the developing XX gonad can cause sex reversal, indicating that it is capable of inducing the male pathway in the absence of *Sry, Sox9* and *Sox8* (Polanco et al., 2010). Furthermore, in humans duplication of the chromosomal region containing *SOX10* (22q13) has been found in 46, XX DSD suggesting that *SOX10* overexpression may also be capable of directing male development in humans too (Seeherunvong et al., 2004).

DHH

Desert Hedgehog (DHH) belongs to the Hedgehog family of morphogens which play important roles in the patterning and growth of organs (Cool & Capel, 2009). *Dhh* is expressed only in Sertoli cells of the developing testis and can first be detected at E11.5. In the embryonic testis, *Dhh* signalling is transduced by the Patched 1 (Ptch1) receptor, found on the surface of Leydig cells and peritubular myoid cells. In *Dhh* knockout mice, the Leydig cells and peritubular myoid cells fail to properly differentiate resulting in compromised testis cord structure and steroidogenesis, leading to male infertility (Clark et al., 2000; Yao et al., 2002). Similarly, ectopic expression of *Dhh* in ovaries can induce Leydig cell differentiation virilization of the female reproductive system (Barsoum et al., 2009). Furthermore, humans with mutations to *DHH* have similar defects to the knockout mice, causing phenotypes ranging from partial gonadal dysgenesis to complete sex reversal (OMIM: 605423) (Canto, Soderlund, Reyes, & Mendez, 2004; Das, Sanghavi, Gawde, Idicula-Thomas, & Vasudevan, 2011; Umehara et al., 2000). Thus, *DHH* is indisputably important to the development of the male gonad and virilization of the reproductive system.

In Amh-*Cre Sox9$^{flox/flox}$* gonads, *Dhh* expression is decreased by 2.5-fold, although not to levels as low as the female suggesting that other factors may also regulate its expression (Rahmoun et al., 2017). Indeed, in *Wt1* knockout mice *Dhh* is downregulated suggesting a possible regulatory connection however as *Sox9* expression is also controlled by Wt1 this connection may be indirect and through Sox9 (M. Chen et al., 2014; Gao et al., 2006). ChIP experiments have detected Sox9 binding to the promoter of *Dhh* at both E12.5 and E13.5 further verifying it as a key regulator of *Dhh* in the developing testis (Y. Li et al., 2014; Rahmoun et al., 2017)

GDNF

Glial cell-line derived neurotrophic factor (GDNF) is a growth factor produced by Sertoli cells which regulates the cell fate decision of spermatogonia, most importantly the decision to maintain self-renewal (Meng et al., 2000). Even the loss of one allele results in the depletion of the germ cells and overexpression of *Gdnf* causes an accumulation of undifferentiated spermatoagonia in the testis (Meng et al., 2000). When *Sox9* is knocked out after sex

determination using the Amh-*Cre Sox9^{flox/flox}*, *Gdnf* expression is significantly reduced (Barrionuevo et al., 2009) Furthermore, in the *Sox8/Sox9* double knockout *Gdnf* expression loss is further exacerbated (Barrionuevo et al., 2009). This may contribute to the progressive infertility phenotype seen in both *Sox9* knockout models. High throughput ChIP screens have identified both Sry and Sox9 as binding to the promoter of *Gdnf* indicating that it may also have a role early in sex determination and gonadal development (Y. Li et al., 2014; Rahmoun et al., 2017). Further studies are needed to discern what this role could be. To date, no mutations causing DSD in humans have been discovered in *GDNF*.

PADI2

Peptidyl arginine deiminase 2 (PADI2) is an enzyme which can change the charge of its target proteins by converting the amino acid arginine to citrulline (Ishigami et al., 2002). One such target protein is histone H3, suggesting that PADI2 can mediate gene regulation through epigenetic mechanisms (Zhang et al., 2012). *Padi2* is expressed soon after *Sox9* in the Sertoli cells and is barely expressed in the ovary throughout embryonic development. Sox9 positively controls *Padi2* expression by binding through intron 1 and in Amh-*Cre Sox9^{flox/flox}* mice, *Padi2* expression is markedly decreased (Rahmoun et al., 2017; Tsuji-Hosokawa et al., 2018). *In vitro* data also suggests that the female factor Foxl2 is able to repress *Padi2* transcription (Tsuji-Hosokawa et al., 2018). However, *Padi2* deficient mice have no disruptions to gonadal development and no alteration to histone H3 citrullination thus its gonadal role remains to be discerned (Tsuji-Hosokawa et al., 2018).

Others

Other genes have been placed downstream of *Sox9* in the developing testis including *Vnn1, Gstm6* and *Cbln4* due to their Sertoli cell expression patterns or *in vitro* data however direct connections are yet to be made (Beverdam et al., 2009; Bradford, Hiramatsu, et al., 2009; Wilson, Jeyasuria, Parker, & Koopman, 2005). Furthermore, testicular functions are yet to be elucidated. This may prove difficult due to redundant mechanisms being active *in vivo* warranting the need for a model where Sertoli cell function can be investigated.

Does SOX9 regulate undiscovered target genes during testis development?

This review aimed to contextualise the function of SOX9 in the developing testis. SOX9 is indispensable to the development of the testis in mammals, where loss or mutation can result in gonadal phenotypes ranging from complete sex reversal to fertility defects. Moreover, ectopic expression of *SOX9* in the XX gonad leads to initiation of the male pathway, even in the absence of the male sex determining factor, SRY. Therefore, SOX9 is both necessary and sufficient for the development and function of the testis.

High-throughput chromatin and transcriptomic studies have revealed that it is possible SOX9 is regulating the expression of thousands of genes in the developing testis, and importantly is modulating pathways vital to the development and function of the male gonad. Of the target genes investigated so far, many remain dispensable to testis development suggesting that SOX9 divides the labour between its target genes and may regulate multiple redundant pathways.

This suggests that SOX9 regulates a number of undiscovered target genes which have a role in testis development. As such these SOX9 transcriptional targets also represent candidate genes which may be mutated in cases of unsolved XY DSD.

1.5 Thesis outline

I hypothesise that SOX9 regulates a number of undiscovered target genes which play an important role in testis development. Therefore, the aim of the studies conducted in this thesis was to investigate novel target genes of SOX9 during testis development.

Modelling SOX9 function in Sertoli cells has been challenging until now. Complete ablation of *Sox9* before sex determination in mice causes complete XY sex reversal, where the gonad develops as an ovary, thereby precluding an investigation of Sox9 targets in a Sertoli cell environment (Barrionuevo et al., 2006; Lavery et al., 2011). Similarly, in humans a heterozygous loss of function is associated with XY sex reversal. While this highlights the necessity of Sox9 for testis development, it does not provide insight into which pathways and genes are directly controlled by Sox9. In contrast, ablation of *Sox9* immediately after the developmental stage of sex determination in XY mice does not switch fate of the gonad, allowing Sertoli cell development to continue (Barrionuevo et al., 2009). As such, this approach has provided an elegant model whereby transcriptomic analysis in appropriately-staged fetal testicular tissue is able to identify subtle alterations to SOX9 target genes expression (Barrionuevo et al., 2009; Rahmoun et al., 2017). When combined with Sox9 chromatin immunoprecipitation, direct target genes under the control of Sox9 can be identified. **Chapter 2** uses this mouse model to identify candidate SOX9 target genes.

Another challenge emerging in gonad development research is the limitation of using mice exclusively as a model. Firstly, functional redundancies within gene family members and via alternative pathways can mean that genetic ablation often results in no obvious phenotypic consequence (Barbaric, Miller, & Dear, 2007). Secondly, differences in the gene thresholds and genetic robustness between humans and mice are becoming more obvious. For example, testicular SOX9 function only needs to decrease by 50% in humans for XY sex reversal to occur, whereas in mice this threshold is 77% (Gonen et al., 2017). Therefore, investigation of the testicular function of many genes warrants a sensitive human model. **Chapter 3** describes

a model and analytical approach for investigating Sertoli cell SOX9 function using the human cell line, N-Tera2cl.D1.

By E11.5 in mice, at the onset of sex determination, previously published transcriptomic analysis in fetal mouse gonads has identified 580 genes with higher expression in Sertoli cells relative to the female equivalent granulosa cells (Jameson, Natarajan, et al., 2012). By E13.5 this number has increased to 1494. However, the testicular function of many of these genes has not been elucidated. A preliminary analysis of genes dysregulated in Amh-*Cre Sox9^{flox/flox}* gonads identified a cytoskeletal scaffolding protein-coding gene, *Nedd9,* as being regulated by *Sox9* in E13.5 Sertoli cells. **Chapter 4** investigates a SOX9 target gene, *NEDD9*, using the analytical approach developed in Chapter 3 to define its testicular and Sertoli cell functions.

Chapter 2:

Identification of Sox9 targets in the developing testis using RNAseq and ChIPseq

2.1 Introduction

Sex determination is a defining biological event in mammals where the gonads will differentiate into either testes or ovaries. The fate of the gonad will dictate which hormones are secreted and thus the secondary sex characteristics which develop. For example, androgens and insulin-like hormone 3 are required for testicular descent (Nation, Balic, Southwell, Newgreen, & Hutson, 2009). In mammals sex determination is governed by the presence of the Y chromosome, and thus the male sex determining gene, *SRY* (Sinclair et al., 1990). While it is clear that the gonads alone are not responsible for all sex differences, given their dominant influence over the key sex defining traits, the focus of the field has been understanding the factors that initiate and influence the differentiation of the gonad as a testis or ovary (Capel, 2017). Despite this effort, the mechanisms of sex determination and gonad development remain poorly defined. As up to 50% of Disorder of Sex Development (DSD) cases are without a clinical molecular diagnosis, it is clear that this process employs multiple pathways and requires intricate co-operation of many genes (Eggers et al., 2016; Leon, Reyes, & Harley, 2019). DSD encompasses a broad spectrum of conditions with overlapping phenotypes which creates complexities for clinical management including assessing the risk of tumour development, fertility prediction, and psychosocial aspects. By improving our understanding of the genes and pathways involved in sex determination and differentiation, it is hoped that the diagnosis rate will improve, enabling better clinical understanding and management.

Expression array technology (e.g. microarray, ChIP-on-Chip) and Next-generation sequencing (e.g. RNAseq, ChIPseq) has allowed the generation of large quantities of data that explore the intricacies and differences between testicular and ovarian cells during early gonadogenesis. By analysing the differences between the transcript profiles of male and female cells, differentially expressed genes have emerged as potential directors of gonad development. For example, a microarray in 2006 which compared Sertoli cell gene expression at E10.5 (shortly after *Sry* transcription begins) and at E11.5 (shortly after *Sox9* transcription begins) identified 266 genes which were upregulated after *Sox9* initiation (Beverdam & Koopman, 2006). Among these was *Gstm6* (Glutathione S-transferase, mu6) which was upregulated nearly 40-fold at E11.5. *Gstm6* was further investigated and later shown to be a target gene of Sox9 in testis development that likely functions in modulating the exposure of testicular tissue to toxicants (Beverdam et al., 2009). Many other transcriptome analyses on wild type gonads have been published that serve as valuable resources to understanding the genes and pathways required for sex determination (Cory, Boyer, Pilon, Lussier, & Silversides, 2007; Del Valle et al., 2017; Jameson et al., 2012; Nef et al., 2005; Small, Shima, Uzumcu, Skinner, & Griswold, 2005; Stevant & Nef, 2018).

SOX9 is arguably the most important gene in the development of the testis as it is both necessary and sufficient for male gonadogenesis (see Chapter 1, section 4.3 for an in-depth review). It's required both during sex determination and in regulating the development and function of the testis (F. Barrionuevo et al., 2009; Jakob & Lovell-Badge, 2011). Transcriptomic analyses have identified hundreds of genes as being both positively and negatively regulated after the onset of *Sox9* expression and ChIP studies have identified thousands of potential direct targets (Beverdam & Koopman, 2006; Jameson et al., 2012; Li, Zheng, & Lau, 2014). Thus, SOX9 is likely to divide its labour among many genes and pathways in the developing testis. Better understanding the target genes of SOX9 in the mammalian testis will improve understanding of the genes involved in the development of the testis.

In humans, heterozygous mutation to *SOX9* affects the development of the skeletal system, causing a condition called Campomelic Dysplasia (CD) (Foster et al., 1994; Wagner et al., 1994). The most prominent feature of CD is bowing of the long bones, along with other defects in cartilage formation and is associated with male-to-female sex reversal in two thirds of cases. Generation of *Sox9* mutant mice, and thus investigating its role in the testis, has been problematic. Homozygous *Sox9* mutant embryos die at E11.5, before the development of the testis. In 2001 the first *Sox9* heterozygous mutant mouse was reported which phenocopies most of the skeletal CD malformations but without the sex reversal, highlighting that the gonads in humans are more sensitive to *SOX9* gene dosage in humans than in mice (Bi et al., 2001; Gonen, Quinn, O'Neill, Koopman, & Lovell-Badge, 2017). These mice died perinatally, preventing the establishment of a founder population. The lethality of *Sox9* ablation was circumvented in 2006 using Cre/loxP under the control of the *Ck19* promoter to inactivate both copies of *Sox9* in the primordial gonad (F. Barrionuevo et al., 2006). This confirmed for the first time that XY sex reversal is caused by a loss of *Sox9* function in the testis. A major limitation of these mice however was that the gonads were completely sex reversed and resembled a wild-type ovary. It consequentially did not specifically highlight the action of *Sox9* in Sertoli cells (F. Barrionuevo et al., 2006).

In 2009 *Sox9* was knocked out in intact testes after sex determination using Cre under the control of the *Amh* promoter (Amh-*Cre Sox9*$^{flox/flox}$). This removes *Sox9* after sex determination and by E13.5 these mice express no Sox9 protein (F. Barrionuevo et al., 2009; Barseghyan et al., 2018). Morphologically, the gonads of these male mice are still testes with intact Sertoli cells, despite the loss of *Sox9*. Gonad development continues as normal until the mice reach 5 months of age where they progressively become infertile (F. Barrionuevo et al., 2009). This provides a system whereby *Sox9* action can be investigated at a genetic and cellular level in the developing testis.

This chapter details a bioinformatic approach used to discover novel targets of Sox9 in mammalian sex determination. The Amh-*Cre Sox9*^{*flox/flox*} model is a powerful model to identify Sox9 target genes. High throughput sequencing of the transcripts (RNAseq) in XY wild type (XY WT) vs XY knockout (XY KO) gonads has revealed genes which are responsive to the loss of *Sox9*. In addition, Sox9 ChIPseq in the mouse testis at E13.5, combined with the Sox9 ChIPseq in the bovine testis at the equivalent developmental stage (E90), has revealed genes which are bound by Sox9. This data is now published in (Rahmoun et al., 2017). By combining these datasets 37 genes, both bound and positively regulated by Sox9 in the developing testis, have been identified. Four of these genes are already validated sex determination genes, leaving 33 putative target genes.

2.2 Methods

Amh-Cre Sox9^{*flox/flox*} *mice-* Experiments on mice were carried out in strict adherence with the recommendations in the Australian code of practice for the care and use of animals for scientific purposes from the National Health and Medical Research Council. All procedures involving mice were approved by the MMCB animal ethics committee, Monash Medical Centre, Australia. Embryos from timed matings were firstly anaesthetised in ice-cold PBS before being euthanised by decapitation. Embryos were then fixed overnight in 4% PFA at 4°C, then washed in 1x PBS. Embryos were processed and embedded into paraffin by the Monash University Histology Platform. Sections were cut by microtome at 5µm and mounted onto slides

Immunofluorescence, gonads- Paraffin slides were baked at 60°C (30 minutes), deparaffinized in xylene, hydrated in 100% ethanol, and distilled in H_2O and PBS. Antigen retrieval was performed by microwaving slides on high in 10 mM sodium citrate (pH = 6.0) for 20 min. Slides were then washed in 1x PBS. Sections were then blocked for 30 minutes with either 5% normal donkey serum and incubated overnight at 4°C with the following primary antibodies: anti-Sox9 (1:200), and anti-Laminin antibody (1:100) (for details see Appendix 1). Sections were then washed three times in 1x PBS with 0.1% Tween 20 and incubated with the fluorescent-conjugated secondary antibodies; donkey anti-rabbit Alexa Fluor 488 (1:1000), for 30 minutes at room temperature. Sections were washed in 1x PBS with 0.1% Tween 20, then incubated in 0.1% Sudan Black in 70% EtOH for 5 minutes to quench background autofluorescence. Sections were washed again 1x PBS with 0.1% Tween 20, counterstained using DAPI, and then washed again in 1x PBS before being mounted using Dako Fluorescent Mounting Medium. Sections were imaged using fluorescence microscopy (Olympus Corp). This procedure and data has been published in (Barseghyan et al., 2018).

Bioinformatic analysis:

Amh-Cre;Sox9^{flox/flox} embryonic gonad RNA-seq- RNAseq was performed by Dr Rowena Lavery at the Hudson Institute of Medical Research as described in (Rahmoun et al., 2017). In brief, E13.5 gonads were separated from the mesonephros and total RNA was isolated using the RNeasy Kit (QIAGEN GmbH, D-40725 Germany). Embryos were genotyped and the RNA from six gonads were pooled into either XY wildtype (XY WT), XX wildtype (XX WT) and XY Amh-*Cre Sox9^{floxflox}* (XY KO). This was repeated in three biological replicates. To analyse the RNA gonads libraries were generated using the NuGEN Mondrian Technology and SPIA amplification methodology, and data was processed and aligned to the mouse genome (Ensembl version 38.77). To eliminate composition biases, the Trimmed Mean of M-values (TMM) method was used for normalization between the samples (Robinson & Oshlack, 2010). The adjusted p-value of 0.05 was used to assess which genes were differentially expressed between XY and XY KO. Graphs of gene expression were made and statistical tests carried out using GraphPad Prism.

SOX9 mouse and bovine embryonic testis ChIP-seq- SOX9 ChIP-seq was performed by Dr. Francis Poulat from the Institute of Human Genetics in Montpellier, France on XY E13.5 mouse and E90 bovine testes, as described in (Rahmoun et al., 2017). The tissue was fixed in PBS/1% formaldehyde before rabbit polyclonal anti-SOX9 IgG antibody bound to Dynamagnetic beads (Life technologies) were used for immunoprecipitation (IP) of sonicated chromatin (Gasca et al., 2002). Six independent IPs were pooled into 2 samples (3 IPs/sample) and were used for the construction of libraries. ChIPseq reads were aligned to mm9 or Bostau6. Peaks were called using the MACS software and peaks with an FDR<0.05 were kept for analysis (Y. Zhang et al., 2008). Peaks were assigned to the neighbouring genes using the PAVIS annotation tool (http://manticore.niehs.nih.gov/pavis2/) All bostau6 coordinates were converted to mm9 using UCSC Liftover (https://genome.ucsc.edu/cgi-bin/hgLiftOver) before analysis. Further details of these methods are described in (Rahmoun et al., 2017). For each species, nearest transcription start sites to peaks has been detailed along with the chromosomal location of the peak mapped to the mouse genome (Ensembl version 38.77) and the distance of the peak to the nearest transcription start site. The location of Sox9-bound peaks was converted and mapped to the human using UCSC Liftover and subsequently viewed using the Encyclopedia of DNA Elements (ENCODE) Ensembl Genome Browser. Pathway analysis was performed using the MetaCore™ GeneGo software to map genes to a global database of known networks (https://portal.genego.com/). The top 50 enriched (p<0.05) pathway networks were analysed from genes associated to the mouse and bovine SOX9 ChIP-seq peaks.

Analysis of datasets and selection of candidate SOX9 target genes- Intersection of datasets was performed using Venny (https://bioinfogp.cnb.csic.es/tools/venny/) and compared to the

published dataset detailing gene expression profiles in key cell types of the gonad using microarray (Jameson et al., 2012). This microarray dataset is also available at the GenitoUrinary Development Molecular Anatomy Project (GUDMAP). Gene ontology for statistical over representation of biological processes was performed using PANTHER (Mi, Muruganujan, & Thomas, 2013). ChIPseq peaks were converted from the mouse assembly (NCBI37/mm9) to the human (GRCh37/hg19) using UCSC Liftover (https://genome.ucsc.edu/cgi-bin/hgLiftOver) and files were created which contain the human peak co-ordinates (bed files). These files were uploaded to Ensembl and UCSC for visualisation and analysis. Statistical analysis of ChIPseq data was completed using GraphPad Prism.

2.3 Results

Sox9 RNA and protein expression in XY KO gonads at E13.5

In the XY KO (Amh-*Cre Sox9$^{flox/flox}$*) gonads, Cre is under the control of the *Amh* promoter. Amh is a well-characterised, direct target of Sox9 in the developing testis which reaches its peak expression by E12.5 (Jameson et al., 2012). Activation of Cre results in excision of the *Sox9* in Sertoli cells only, which results in 85% loss of *Sox9* RNA, to levels comparable to XX WT (**Figure 2.1 a**). There is also a loss of protein by E13.5 as seen by immunofluorescence (**Figure 2.1 b**), thus validating these mice as an appropriate model (F. Barrionuevo et al., 2009).
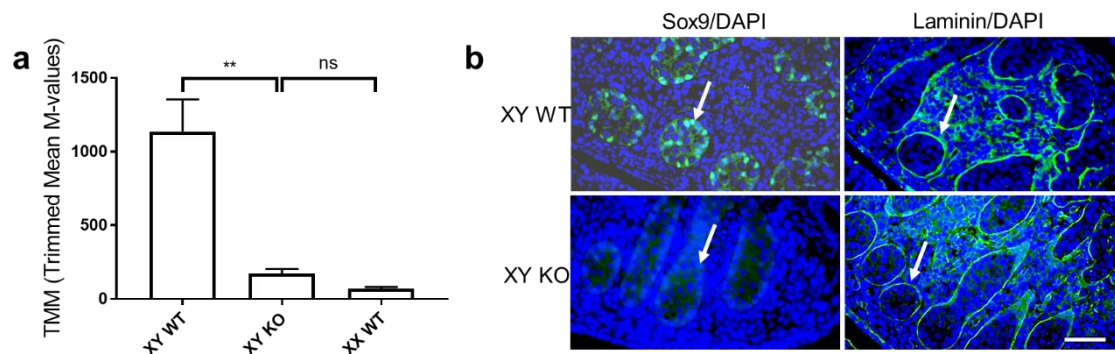
Figure 2.1. Sox9 RNA and protein in XY KO gonads at E13.5. (a) RNAseq data for *Sox9* in XY WT versus XY KO and XX WT gonads. *Sox9* RNA is significantly reduced to levels similar to XX WT in the XY KO. RNAseq data is expressed as TMM (Trimmed Mean of *M* values) and is representative of n=3 with six pooled E13.5 gonads per sample. Error bars represent SEM. **P<0.01 (one-way ANOVA followed by Tukey's multiple comparisons test). Ns, not significant. **(b)** Immunofluorescence of the wild-type and Sox9 knockout gonad at E13.5. Sox9 protein is lost from the testicular cords (white arrows) in the Amh-*Cre Sox9^{floxflox}* mice yet the testicular cords remain intact, as shown by the laminin stain. Sox9/Laminin is shown in green, and nuclei stained with DAPI are shown in blue (adapted from (Barseghyan et al., 2018))

Pathway Analysis of Sox9 knockout gonads

At E13.5, the removal of *Sox9* from mouse Sertoli cells results in the significant dysregulation of the expression of 269 genes between XY KO and XY WT (dysregulation ≥ 1.5 fold, adjusted P value <0.05). Of these genes, 186 (69%) were downregulated in the XY KO compared to XY WT. This suggests that SOX9 acts predominantly as a transcriptional activator in the embryonic testis (**Figure 2.2**). Hence forth these genes will now be referred to as 'Sox9 activated' genes, giving reference to their regulation in XY WT testes. Conversely, the 83 genes upregulated in the XY KO compared to XY WT will be referred to as 'Sox9 repressed' genes. Analysis of biological pathways in 'Sox9 activated' genes shows that genes involved in tube morphogenesis, epithelial cell differentiation, single-organism transport and organ development were significantly over-represented (**Figure 2.2**). In contrast, biological pathways over-represented in the 'Sox9 repressed' group were related to cardiac function, inviting future analyses to determine whether or not gene repression is a critical function by Sox9 in the developing testis.

Process	Fold Enrichment	P-value
Cell-cell signalling in cardiac conduction	>100	0.0125
Cardiac muscle cell action potential	75.15	0.048

Process	Fold Enrichment	P-value
Tube Morphogenesis	4.33	0.0138
Epithelial Cell differentiation	4.32	0.0143
Single-organism transport	2.67	0.0201
Organ Development	2.14	0.0016
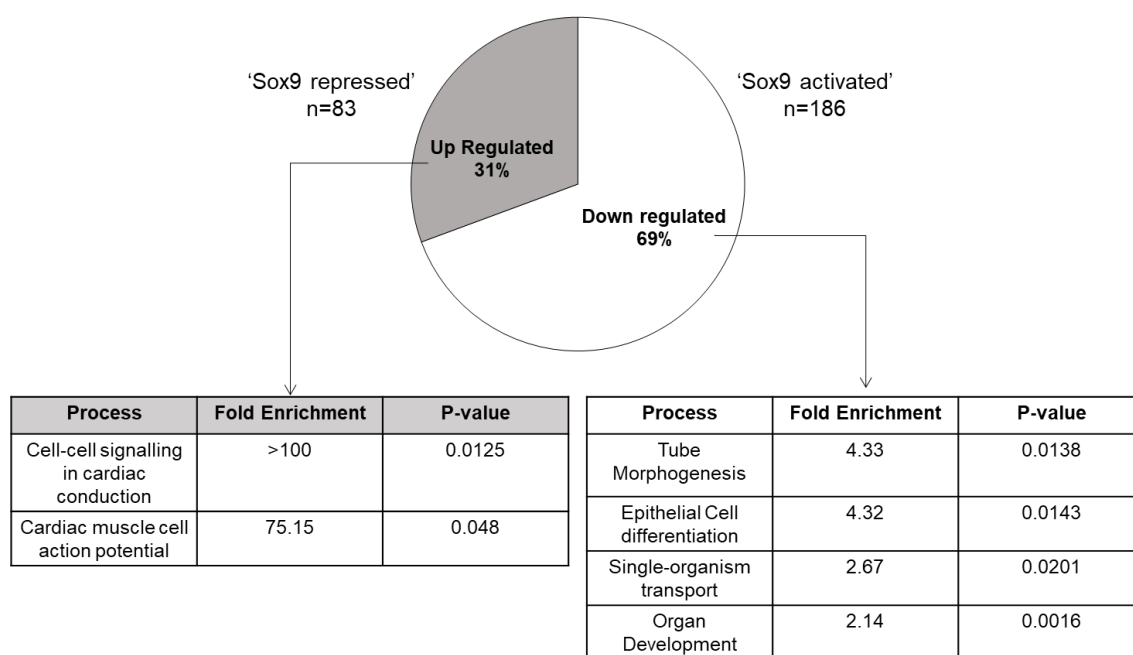
Figure 2.2. Pathway analysis of the differentially expressed genes between XY KO and XY WT. Pathway analysis was completed using PANTHER where gene lists were probed for over-expressed pathways and arranged by biological function with experimental evidence.(Mi et al., 2013).

Analysis of differentially regulated genes and cell type specific transcriptomes

As Sertoli cells direct the differentiation of the male gonad, it is likely that Sox9 is also indirectly regulating the expression of genes in other cell types via its direct target genes. The only cell type in the developing gonad to express *Sox9* is the Sertoli cells so therefore direct transcriptional targets must also be expressed in Sertoli cells. RNAseq has been carried out on the whole gonad meaning that genes in the other cell types of the testis which are indirectly responsive to the loss of *Sox9* will also be captured in this analysis.

To examine the effect that Sox9 is having on each of the cell types in the gonad, the 269 dysregulated genes were compared to a gene expression microarray dataset on sorted cells from the XX and XY gonad (Jameson et al., 2012). This analysis profiled gene expression in each of the key cell types in the male and female gonad. Subsequently, genes have been separated into groups based on 'enriched' expression in a gonadal cell type and sex. This provides a powerful model to identify genes with cell-type specific roles in gonad development. A limitation of this data is that the profiling has been completed using microarray (Affymetrix Mouse Genome 430 2.0 arrays), which provides a targeted expression analysis of over 39,000 genes (Jameson et al., 2012). However, as microarray has a relatively narrow dynamic range, genes with low expression are filtered out with background noise signal. In this microarray, the elimination of genes for which no expression information available in multiple cell types meant that over 25,000 genes were excluded and therefore only has data for 12,015 genes (Jameson et al., 2012). Of the 269 genes dysregulated in the RNAseq, information about the expression of 191 (71%) is captured in this dataset. This accounts for 148 of the 'Sox9 activated' genes and 43 of the 'Sox9 repressed' genes. For the purpose of this project, the analysis has been carried out excluding the genes not in the microarray. Therefore, the remainder of this chapter has further analysed 148 'Sox9 activated' genes and 43 'Sox9 repressed' genes.

An unbiased statistical approach was taken to ascertain if these Sox9 regulated genes were enriched in any cell types of the male or female gonads by Chi-square test. As Sox9 is a transcription factor it was unsurprising to find that 97 genes activated by Sox9 were enriched in the XY Sertoli cells (p<0.0001) (**Figure 2.3**). Furthermore, 10 'Sox9 repressed' genes are enriched in granulosa cells (p<0.0001). As granulosa and Sertoli cells differentiate from the same progenitor population this is unsurprising but invites the question of what their function may be in the female gonad (Chen et al., 2017). Four genes activated by Sox9 were enriched in XY Leydig cells, and three in germ cells demonstrating a potential paracrine action of Sox9,

yet these populations were not over-represented (ns). Detailed gene lists are provided in Appendix 2.
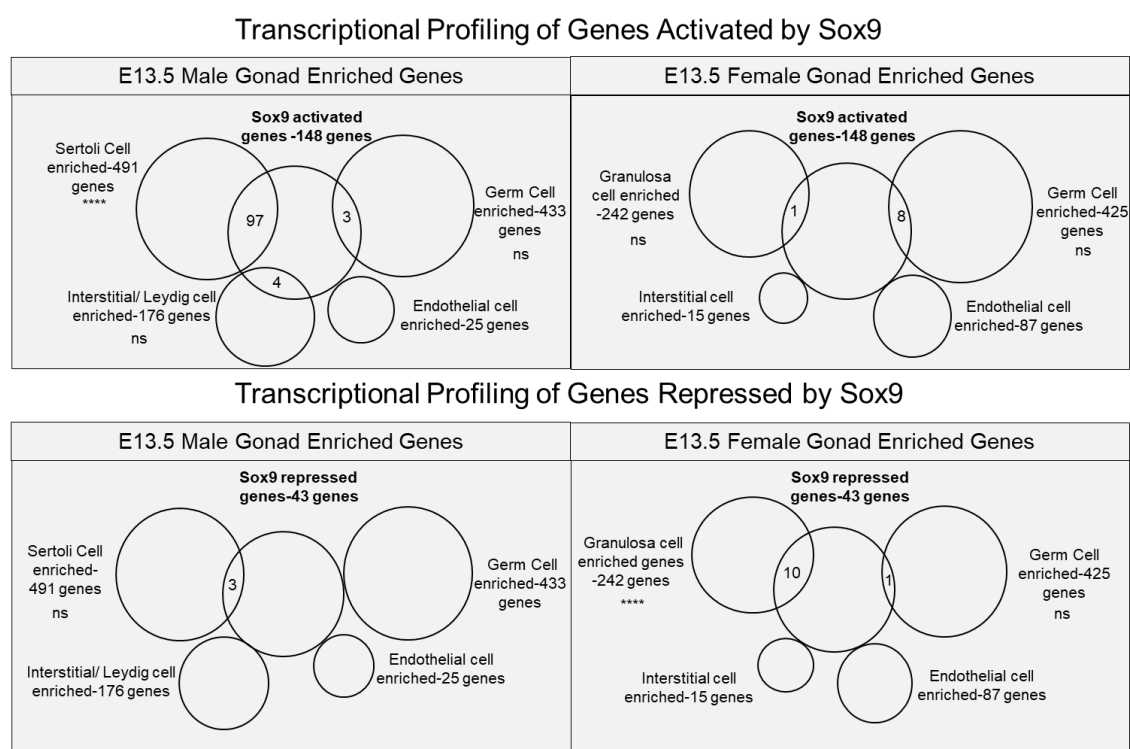
Figure 2.3. Transcriptional profiling of microarray-informative genes differentially expressed between the XY KO vs XY WT at E13.5. The top panel (left and right) shows genes activated by SOX9 in the male and female gonadal cells. The bottom panel (left and right) shows genes repressed by SOX9 in the male and female gonadal cells. Significance in gene overlap was tested with Chi-square, ****$P<0.0001$

Sox9 ChIPseq analysis

To identify direct transcriptional targets of Sox9 in the gonad, ChIP-seq on chromatin isolated from embryonic mouse and bovine gonads was performed by Dr Francis Poulat (now published in (Rahmoun et al., 2017)). 6430 peaks were identified in the mouse and 10604 in the bovine gonad. In both species Sox9 binding was most concentrated near the transcription start site (TSS) of genes (**Figure 2.4,** top panel left and right). In fact, very few peaks are found more than 200,000bp from transcription start sites. It is worth noting however, that Sox9 binding was identified as far away as 2,241,493bp 5'of a TSS in the mouse genome and 2,242,319bp of a TSS in the bovine genome. In the mouse genome, the median of the peaks was 183bp 3' of the transcription start site (+183) and in the bovine this was 143bp 3' (+143). In both species 50% of the peaks were located within a region which represents less than 0.001% of the genome (-500 to 500bp of TSS) (McLean et al., 2010) (**Figure 2.4**, bottom panel left and right). In the mouse 50% of the peaks are found -85bp to 377bp of TSS and in the bovine this was between -139bp to 406bp of TSS.

The genes bound in the mouse and bovine were intersected to identify genes which have conserved roles in mammalian sex determination and improve the signal to noise ratio. There were 4082 genes in common to both species (47% of bovine and 71% of mouse). Among these common genes were *Sox9, Amh* and *Fgf9,* all of which are known targets of Sox9 protein, thus validating this ChIPseq as an approach to identify Sox9 target genes with roles in sex determination and testis development.

Pathway analysis of the genes bound by Sox9 in the mouse and bovine testes revealed that the male sex differentiation pathway was enriched ($p=3.811 \times 10^{-6}$), as expected (**Table 2.1**). Other pathways enriched are also known to be involved in male sex determination and gonad function such as Fgf signalling, Hedgehog signalling and Wnt signalling. This analysis may also point to Sertoli cell functions which Sox9 controls, including cell cycle regulation and adhesion.
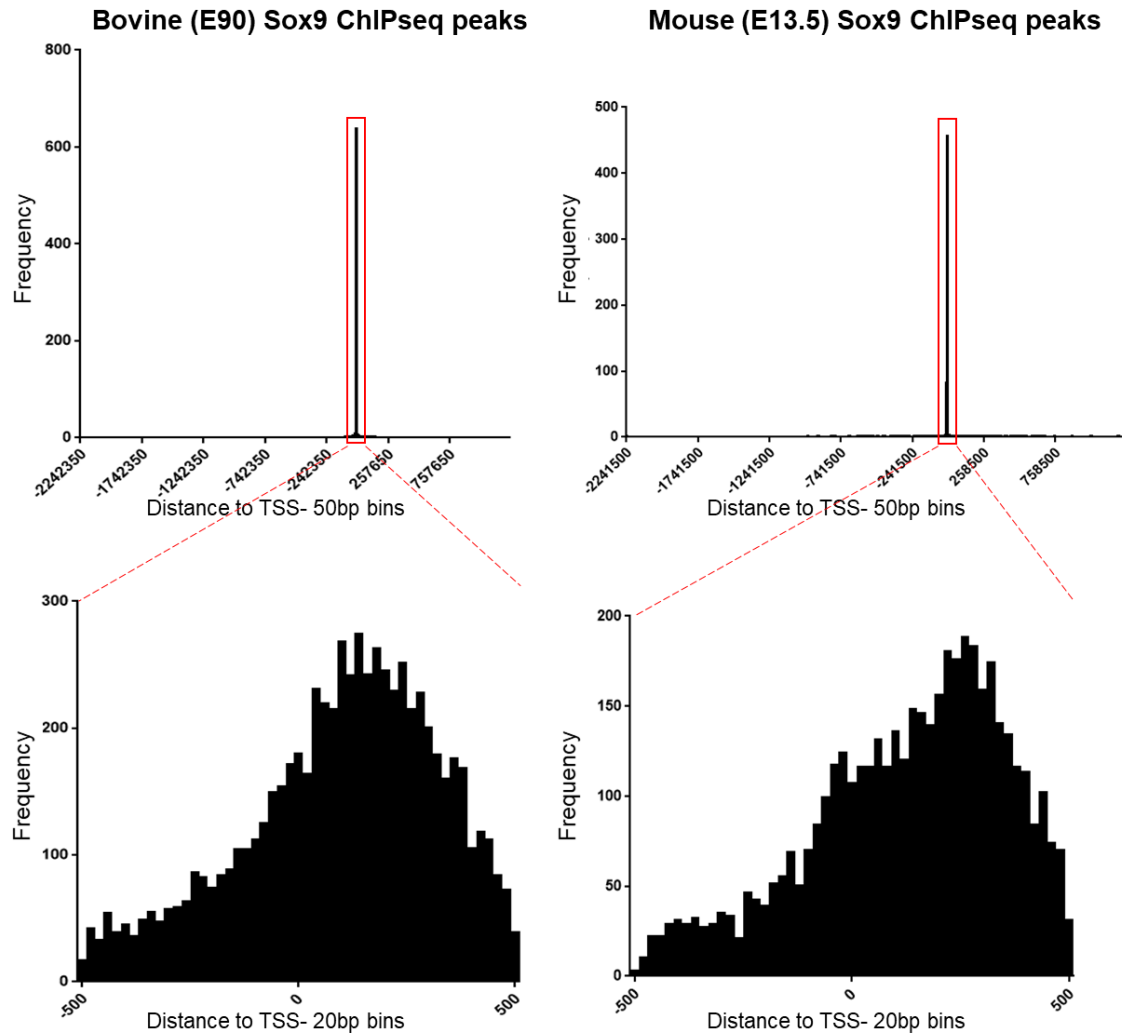
Figure 2.4. Histogram demonstrating frequency of ChIPpeaks relative to the transcription start site (TSS). Histograms represent the entire data set separated into 50bp bins (top panel, left and right). The Y axis represents the number of peaks (frequency) at each distance from TSS. The bottom panel, left and right, details the frequency of peaks found within 500bp of the TSS, separated in 20bp bins. This represents less than 0.001% of the genome

Table 2.1. Top 25 pathways enriched in Mouse and Bovine Sox9 ChIPseq peak associated genes.

	Mouse and Bovine combined Sox9 ChIPseq enriched processes	
	Pathway	**P-value**
1	Reproduction_FSH-beta signaling pathway	1.550E-14
2	Cell cycle_G1-S Growth factor regulation	6.286E-14
3	Signal transduction_NOTCH signaling	1.090E-13
4	Development_EMT_Regulation of epithelial-to-mesenchymal transition	5.176E-12
5	Development_Hedgehog signaling	9.256E-09
6	Signal transduction_WNT signaling	8.010E-08
7	Signal Transduction_TGF-beta, GDF and Activin signaling	1.171E-07
8	Signal Transduction_BMP and GDF signaling	1.232E-07
9	Cardiac development_FGF_ErbB signaling	1.414E-07
10	Development_Neurogenesis_Synaptogenesis	1.691E-07
11	Cell cycle_G1-S Interleukin regulation	1.717E-07
12	Development_Hemopoiesis, Erythropoietin pathway	2.440E-07
13	Development_Neurogenesis_Axonal guidance	3.139E-07
14	Cell cycle_G2-M	4.574E-07
15	Cell adhesion_Attractive and repulsive receptors	6.640E-07
16	Cell cycle_G0-G1	2.945E-06
17	Signal transduction_ESR1-nuclear pathway	3.503E-06
18	Reproduction_Male sex differentiation	3.811E-06
19	Reproduction_Progesterone signaling	9.899E-06
20	Development_Blood vessel morphogenesis	1.546E-05
21	Cytoskeleton_Regulation of cytoskeleton rearrangement	1.737E-05
22	Development_Ossification and bone remodeling	1.749E-05
23	Transcription_Nuclear receptors transcriptional regulation	1.976E-05
24	Cell adhesion_Cadherins	2.009E-05
25	Proliferation_Negative regulation of cell proliferation	2.103E-05

Identification and characterisation of candidate novel Sox9 target genes

To create a list of candidate target genes for analysis, the 148 Sox9 activated (RNAseq) and 4082 Sox9 bound (ChIP-seq) datasets were intersected to give a list of 59 genes that are bound and activated by Sox9 (see Appendix 2). As Sox9 carries out predominantly cell autonomous effects in the testis (**Figure 2.3**), this list of 59 genes was then intersected with the 491 Sertoli cell enriched genes defined in the microarray study (Jameson et al., 2012) This approach left 37 genes, 4 of which have already been confirmed as Sox9 target genes known to be involved in testis development (*Sox10, Sox9, Amh, Dhh*) thus validating the robustness of this filtering pipeline. A graphical summary of this workflow is presented in **Figure 2.5.** As demonstrated in **Figure 2.6**, these genes all represent a cohort which are most highly expressed in Sertoli cells relative to the other cell types of the testis and compared to granulosa cells. Majority of these genes increase in expression after peak *Sox9* expression is reached and follow a similar expression pattern to the known Sox9 target genes, *Sox10, Amh* and *Dhh*. The exception to this is *Nudt19* and *Gpr37*, both of which maintain a high expression from E11.5 to E12.5, indicating Sox9 may be maintaining their expression rather than initiating it. Both of these genes are targets of Sry at E11.5 according to ChIP-on-ChIP data (Li et al., 2014).
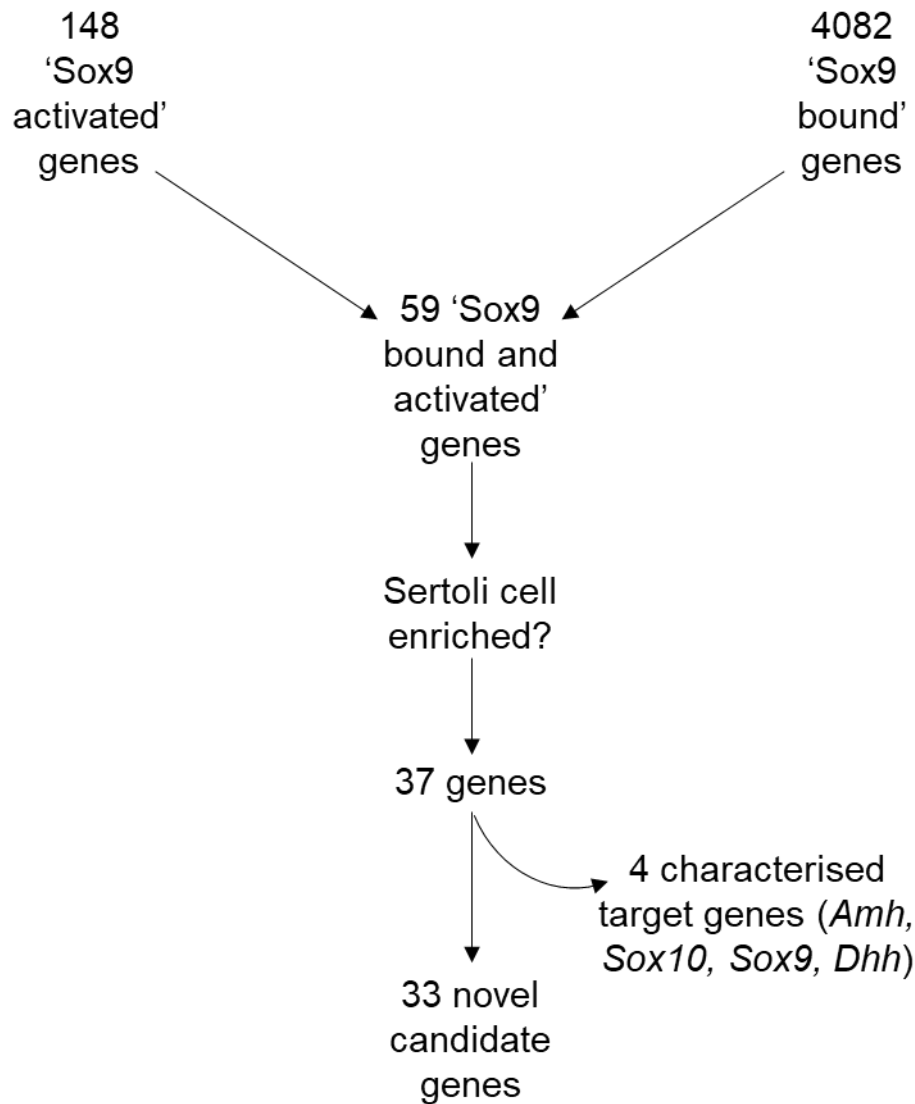
Figure 2.5. **Graphical representation of the workflow leading to the identification of novel candidate target genes**. '**Sox9 activated' genes refers to the 148 genes downregulated in the XY KO RNAseq. 'Sox9 bound' genes refers to the 4082 genes identified in both bovine and mouse Sox9 ChIPseq. The 59 genes in common were then filtered through a dataset identifying 491 genes as enriched in Sertoli cells at E13.5 (Jameson et al., 2012). This led to the identification of 37 Sox9 target genes, 4 of which have already been characterised leaving 33 novel candidate genes.
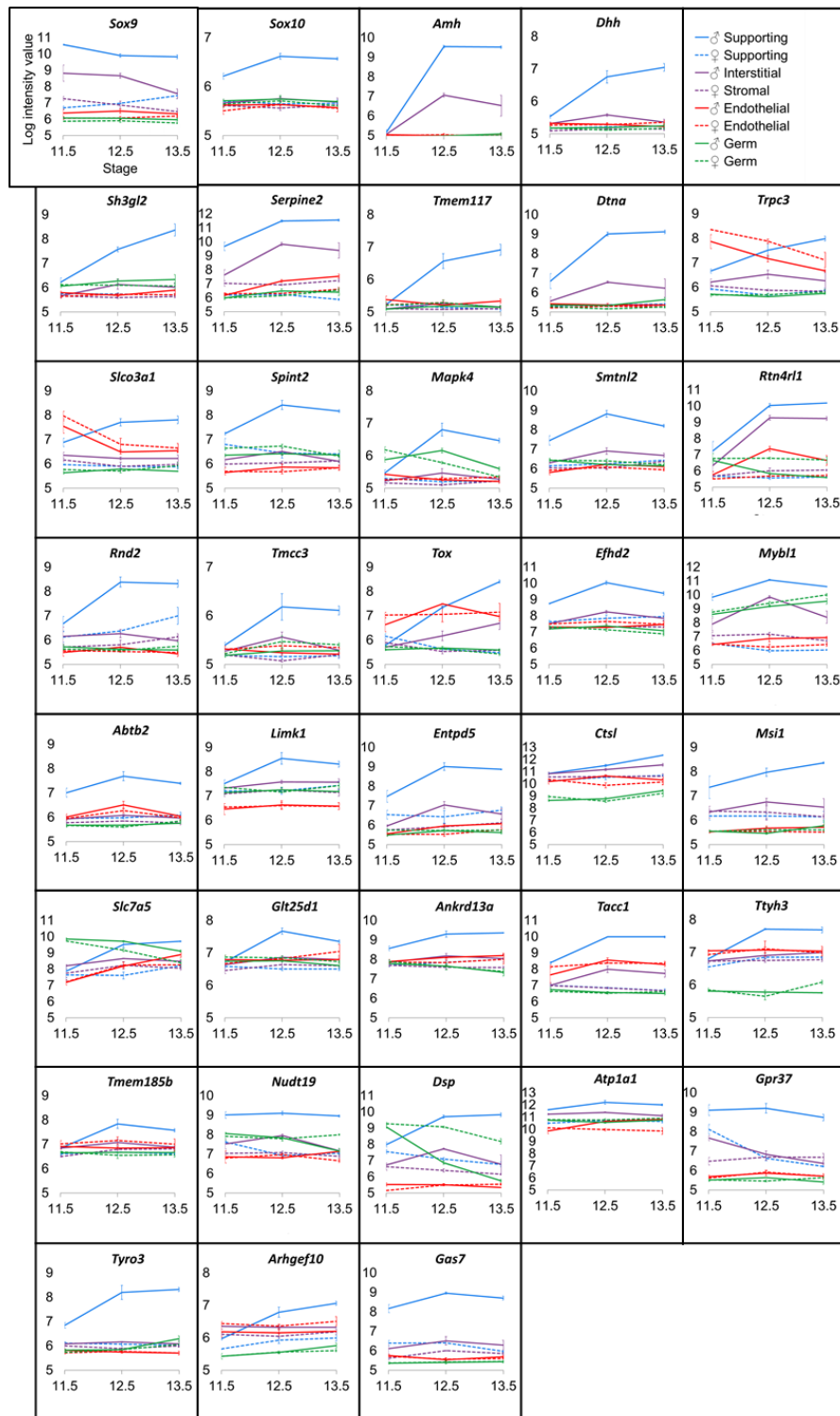
Figure 2.6. Expression profiles in cell types of the developing gonad of the 37 putative target genes. Profiles have been made using data from (Jameson et al., 2012), where expression profiles of cells of the developing gonad have been profiled at E11.5, E12.5 and E13.5. Solid lines represent male gonadal cells while dotted represent female gonadal cells. Blue represents supporting cells of the gonad, as detailed in the key in the top right panel. In males these are the Sertoli cells and in female, granulosa cells. The top row of graphs represents the targets of Sox9 which have already been characterised.

Further probing of each of the candidate target genes with the XY KO RNAseq revealed that 21/37 (57%) of the candidate genes were downregulated to levels similar to in XX WT gonads (**Table 2.2**, grey shading). These genes included *Sox10, Msi1* and *Mybl1* (**Figure 2.7, a**). The remaining 16 genes (43%) had expression levels intermediate of XY WT and XX WT gonads, indicative of other factors being involved in their regulation in the testis (**Table 2.2**, no shading). These included *Amh, Dhh* and *Serpine2* (**Figure 2.7, b**). Each of the genes were further evaluated using published literature to characterise their known function and roles in heritable disease phenotypes. This is summarised in **Table 2.2.** Of the 33 uncharacterised Sox9 target genes, 7 have characterised mutants/knockdown models with fertility defects (*Serpine2, Mybl1, Entpd5, Msi1, Atp1a1, Gpr37* and *Tyro3*). For 16 of these genes, fertility has not been reported on due to a variety of reasons including knockout mutants/models not existing and embryonic lethality.

Table 2.2. Summary of gene function and associated phentoypes of 37 candidate Sox9 target genes. Grey shading represents target genes with XY KO expression reduced to levels similar to XX. OMIM ID refers to the identification number on the Online Mendelian Inheritance in Man database. N/A refers to not analysed or reported. No refers to a negative result.

Gene	Protein Name	Protein Function	OMIM ID	Genitourinary/ Fertility defects- human	Other phenotypes- human	Genitourinary/ Fertility defects- mouse	Other phenotypes- mouse
Sox10	SRY-Box 10	Transcription factor- various tissue development	602229	Mutation can be associated with hypogonadotropic hypogonadism and cryptorchidism	Waardenburg syndrome, PCWH syndrome, Hirschsprung Disease- multiple organ systems affected due to disturbed neural crest development	Transgenic expression in XX results in male development	Knockout phenocopies human- multiple organ systems affected due to disturbed neural crest development
Sox9	SRY-Box 9	Transcription factor- various tissue development and function	608160	Haploinsufficiency causes XY sex reversal, duplication causes XX sex reversal	Campomelic Dysplasia, Acampomelic Campomelic Dysplasia- multiple organ systems, mainly skeletal affects	XY sex reversal only if transcripts are reduced below 23% of wildtype, transgenic expression in XX results in male development	Skeletal elements of Campomelic Dysplasia phenocopied in heterozygous mutant, plus perinatal death
Amh	Anti-Müllerian Hormone	TGFβ family member, hormone	600957	Persistent Müllerian ducts in males	No	Persistent Müllerian ducts in males	No
Dhh	Desert Hedgehog	Signalling molecule, morphogenesis	605423	XY partial gonadal dysgenesis and XY sex reversal	Minifascicular neuropathy- 1 patient	Infertile due to impaired Leydig cell function	Abnormal peripheral nerves
Serpine2	Serine Protease Inhibitor E2	Serine Protease Inhibitor	177010	Abnormal SERPINE2 protein found in semen of infertile men with abnormal seminal vesicle secretory activity	Allelic variants associated with risk of chronic obstructive pulmonary disease and emphysema	Male homozygous mutants have severely impaired fertility due to abnormal seminal vesicle No obvious developmental defects in testis, no impairment to sperm count or phenotype	Mild neurological defects
Sh3gl2	Endophilin-A1	Endophilin- cellular trafficking	604465	N/A	N/A	No	None due to functional redundancy with Sh3gl1 and Sh3gl3. Double and triple KO causes neurological defects and perinatal death
Tmem117	Transmembrane Protein 117	Transmembrane protein- mediates cell death	-	N/A	N/A	N/A	N/A
Dtna	Dystrobrevin Alpha	Membrane-associated cytoskeletal protein	601239	N/A	Left ventricular noncompaction 1, with or without congenital heart defects	No	Mildly dystrophic and mild defects at neuromuscular junction
Trpc3	Transient Receptor Potential Cation Channel Subfamily C Member 3	Ca²⁺ transport	602345	N/A	Spinocerebellar Ataxia 41- 1 patient	N/A	Paralysis and atrophy starting from 4 weeks of age, death at 12 weeks
Spint2	Serine Peptidase Inhibitor Kunitz, Type 2	Serine Peptidase Inhibitor	605124	N/A	Syndromic Congenital Sodium Diarrhea	N/A	Embryonic lethal by E7.5
Mapk4	Mitogen-Activated Protein Kinase 4	Protein kinase- signal transduction	176949	N/A	N/A	No	No
Smtnl2	Smoothelin Like 2	Cytoskeletal component- binds MAPKs	-	N/A	N/A	N/A	N/A
Slco3a1	Solute Carrier Organic Anion Transporter Family Member 3A1	Mediates organic anion transport, including Prostaglandin E2	612435	N/A	Crohn's disease	N/A	No
Rtn4rl1	Reticulon 4 Receptor Like 1	Cell surface receptor	610461	N/A	N/A	N/A	No
Rnd2	Rho Family GTPase 2	Small GTPase, signal transduction	601555	N/A	N/A	N/A	N/A
Efhd2	EF-Hand Domain Family Member D2	Ca²⁺ binding adapter protein	616450	N/A	N/A	No	Impaired immunity
Tmcc3	Transmembrane And Coiled-Coil Domain Family 3	Uncharacterised- found in Endoplasmic Reticulum	617459	N/A	N/A	N/A	N/A
Tox	Thymocyte selection-associated HMG box factor	Transcription factor –immune system regulation	606863	N/A	N/A	N/A	N/A
Mybl1	MYB Proto-Oncogene Like 1	Transcription factor- regulator of meiosis	159405	N/A	N/A	Male infertility due to meiotic arrest in germ cells	Abnormal mammary gland development, decreased fitness
Abtb2	Ankyrin Repeat And BTB Domain Containing 2	Scaffold protein- key role is to interact with E3 ubiquitin ligase	-	N/A	N/A	N/A	N/A
Limk1	LIM domain kinase 1	Serine/Threonine kinase which regulates actin polymerisation	601329	N/A	Possible association with Williams-beuren Syndrome	No	Abnormal spine morphology and synaptic function
Entpd5	Ectonucleoside Triphosphate Diphosphohydrolase 5	Drives protein glycosylation in Endoplasmic Reticulum	603162	N/A	N/A	Male infertility due to late spermatogenic arrest	Stunted growth, impaired liver function
Ctsl	Cathepsin L	Cysteine Protease, involved in intracellular protein metabolism, including collagens and elastins	116880	N/A	N/A	No fertility defects identified in knockout mice- can be used as a post-natal Sertoli cell marker	Impaired cardiac development and function, immune system defects

Table 2.2. continued

Gene	Protein Name	Protein Function	OMIM ID	Genitourinary/ Fertility defects- human	Other phenotypes- human	Genitourinary/ Fertility defects- mouse	Other phenotypes- human
Msi1	Musashi RNA Binding Protein 1	Post-transcriptional gene editing	603328	May be responsible for sexual transmission of Zika virus as Msi1 amplifies the viral replication	Congenital Microcephaly	No fertility defects reported in knockout mice but mice die at 1-2 months old. *In vivo* siRNA knockdown causes highly disrupted blood-testis-barrier and thus spermatogenesis as well as disrupted heat-stress response	Improper neural development embryonically and develop hydrocephaplus at 1-2 weeks after birth, eventually causing death at 1-2 months old
Slc7a5	Solute Carrier Family 7 Member 5	Mediates uptake or large, neutral amino acids	600182	N/A	Mutations linked to Autism Spectrum Disorder and motor delay	N/A	Embryonic lethal at E11.5 due to neural defects
Glt25d1	Collagen Beta(1-O)Galactosyltransferase 1	Post-translational galatosylation of collagen	617531	N/A	Brain small vessel disease	N/A	Complete ablation is embryonic lethal by E13.5, homozygous mutants are lethal by postnantal day 10 due to severe muscular and skeletal defects
Ankrd13a	Ankyrin Repeat Domain 13A	Regulates internalisation of cell-surface proteins such as EGFR	615123	N/A	Mutation linked to early-onset Parkinson's disease	N/A	N/A
Tacc1	Transforming Acidic Coiled-Coil Containing Protein 1	Scaffold protein which interacts with unliganded nuclear receptors including ERα and GR	605301	N/A	N/A	N/A	N/A
Ttyh3	Tweety Family Member 3	Ca^{2+}-activated Cl$^-$ channel	608919	N/A	N/A	N/A	N/A
Tmem185b	Transmembrane Protein 185B	Transmembrane protein- uncharacterised function, suspected GPCR activity	-	N/A	N/A	N/A	N/A
Nudt19	Nudix Hydrolase 19	Mediates hydrolysis of CoA esters	-	N/A	N/A	Elevated kidney coenzyme A. No fertility defects	N/A
Dsp	Desmoplakin	Critical component of desmosomes	125647	N/A	Dilated cardiomyopathy, woolly hair, skin fragility, keratoderma, tooth agenesis	No	Abnormal hair and coat, ventricular cardiomyopathy
Atp1a1	ATPase Na+/K+ Transporting Subunit Alpha 1	Transport of Na$^+$ and K$^+$ to maintain electrochemical gradient	182310	N/A	Charcot-Marie-Tooth disease, Hypomagnesemia, Seizures, And Mental Retardation 2	Homozygous knockout die embryonically, *in vitro* data suggests regulation of Sertoli cell tight junctions	Heterozygote mutants have decreased cardiac contractility
Gpr37	G Protein-Coupled Receptor 37	Found in Endoplasmic Reticulum, translates signals into G-protein mediated intracellular effects	602583	N/A	Mutation associated with early onset Parkinson's disease and Autism Spectrum Disorder	Homozygous knockout mice are fertile but with impaired testis function- decreased proliferation and maturation of Sertoli cells, delay in sperm cell development, partial meiotic arrest of spermatocytes, increased spermatocyte apoptosis, increased *Dhh* expression	Reduced striatal dopamine
Tyro3	TYRO3 protein tyrosine kinase	Signal transduction- activated by GAS6 and Protein S	600341	N/A	Association with asthma	Homozygous *Tyro3* knockout mice are fertile but when all 3 members of the TAM family (*Tyro3, Ax, Mer*) are knocked out the resulting mice have azoospermia due to complete death of germ cells, caused by impaired Sertoli cell function	Seizures in aging mice
Arhgef10	Rho Guanine Nucleotide Exchange Factor 10	Regulates the activity of small Rho GTPases by stimulating the exchange of GDP for GTP	608136	N/A	Slowed nerve conduction velocity, Charcot-Marie-Tooth disease, associated with a risk of ischemic stroke	No	Social interaction impairment, altered platelet aggregation
Gas7	Growth arrest-specific 7	Enhances actin polymerisation and stabilise microtubules	603127	N/A	Associated with Schizophrenia risk	No in *Gas7* deficient mice (some protein function retained)	Deficient mice have motor function defects and decreased bone density

Table references: *Sox10:* (Herbarth et al., 1998; Inoue et al., 2004; Pingault et al., 2013; Pingault et al., 1998; Southard-Smith, Kos, & Pavan, 1998) *Sox9:* (Bi et al., 2001; Cox, Willatt, Homfray, & Woods, 2011; Foster et al., 1994; Gonen et al., 2017; Vidal, Chaboissier, de Rooij, & Schedl, 2001; Wagner et al., 1994) *Amh:* (Arango, Lovell-Badge, & Behringer, 1999; Carre-Eusebe et al., 1992; Mishina et al., 1996) *Dhh:* (Bitgood, Shen, & McMahon, 1996; Canto, Soderlund, Reyes, & Mendez, 2004; Umehara et al., 2000)*Serpine2:* (Luthi et al., 1997; Murer et al., 2001; Zhu et al., 2007) *Sh3gl2:* (Milosevic et al., 2011) *Tmem117:* (Tamaki et al., 2017) *Dtna:* (Ichida et al., 2001) (Wang et al., 2007) *Trpc3:* (Fogel, Hanson, & Becker, 2015; Rodriguez-Santiago, Mendoza-Torres, Jimenez-Bremont, & Lopez-Revilla, 2007) *Spint2:* (Heinz-Erian et al., 2009; Mitchell et al., 2001) *Mapk4:* (Rousseau et al., 2010) *Smtnl2:* (Gordon et al., 2013) *Slco3a1:* (Pan et al., 2018; Wei et al., 2014) *Rtn4rl1:* (Dickendesher et al., 2012) *Rnd2:* (Heng et al., 2008*) Efhd2:* (Brachs et al., 2014; Purohit et al., 2014) *Tmcc3:* (Sohn et al., 2016) *Tox:* (Wilkinson et al., 2002) *Mybl1:* (Bolcun-Filas et al., 2011; Toscani et al., 1997) *Abtb2:* (Roy & Pahan, 2013) *Limk1:* (Duan et al., 2018; Meng et al., 2002) *Entpd5: (*Fang et al., 2010; Read et al., 2009) *Ctsl:* (Maehr et al., 2005; Stypmann et al., 2002; Timmons, Rigby, & Poirier, 2002) *Msi1:* (Chavali et al., 2017; ErLin et al., 2015; Sakakibara et al., 2002) *Slc7a5:* (Baronas, Yang, Morales, Sipione, & Kurata, 2018; Tarlungeanu et al., 2016) *Glt25d1:* (Geister et al., 2019; Miyatake et al., 2018; Ye et al., 2018) *Ankrd13a:* (Kun-Rodrigues et al., 2015; Tanno, Yamaguchi, Goto, Ishido, & Komada, 2012) *Tacc1:* (Ghayad et al., 2009) *Ttyh3:* (Suzuki & Mizuno, 2004) *Tmem185b:* (Haitina, Fredriksson, Foord, Schioth, & Gloriam, 2009) *Nudt19:* (Shumar et al., 2018) *Dsp:* (Herbert Pratt et al., 2015; Norgett et al., 2000; Vasioukhin, Bowers, Bauer, Degenstein, & Fuchs, 2001) *Atp1a1:* (James et al., 1999; Lassuthova et al., 2018; Rajamanickam, Kastelic, & Thundathil, 2017; Schlingmann et al., 2018) *Gpr37:* (Fujita-Jimbo et al., 2012; La Sala et al., 2015; Marazziti et al., 2004) *Tyro3:* (Chan et al., 2016; Q. Lu et al., 1999; Q. Lu & Lemke, 2001) *Arhgef10:* (Boora et al., 2015; D. H. Lu et al., 2017; D. H. Lu et al., 2018) *Gas7: (Chao, Hung, & Chao, 2013; Huang, Chang, Su, Chao, & Lin-Chao, 2012; Z. Zhang et al., 2016)*
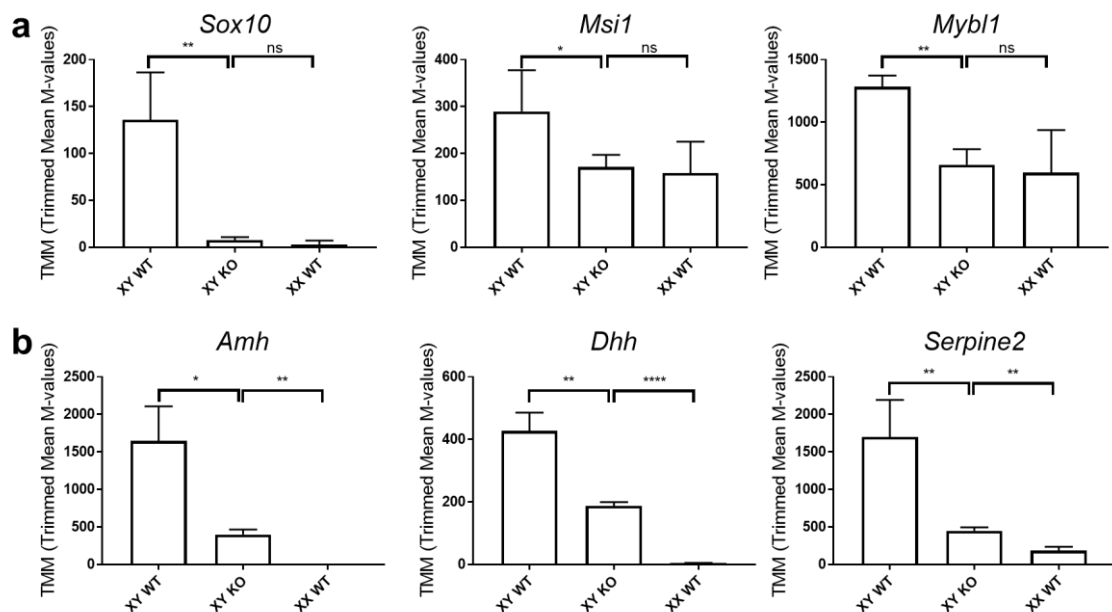
Figure 2.7. Representative histograms of candidate target gene RNA in gonads. Candidate target genes can be separated into two groups according to relative expression in XY KO versus XX WT. **(a)** Genes which are expressed at levels similar to XX WT. This represents 21/37 of the candidate genes. **(b)** Genes which are expressed at levels intermediate to XYWT and XX WT. This represents 16/37 of the candidate genes. RNAseq data is expressed as TMM (Trimmed Mean of *M* values) and is representative of n=3 with six pooled E13.5 gonads per sample. Error bars represent SEM. *P<0.05, **P<0.01 ***P<0.001, ****P<0.0001 (Unpaired Student's t-test). Ns, not significant.

2.4 Discussion

In males, Sertoli cells drive the differentiation of the other cell types of the testis but in the absence of *SOX9* they do not differentiate, resulting in female development even if *SRY* is present. To date, investigation of the role of *Sox9* in Sertoli cells has been difficult as *Sox9* null mice die at the onset of testis formation (E11.5), and testis development proceeds as normal in heterozygous mutants so conditional knockouts have been used to investigate its testicular role (F. Barrionuevo et al., 2006; F. Barrionuevo et al., 2009). The first example of mice lacking testicular *Sox9* are the *Cytokeratin 19-Cre/Sox9 flox* mice where *Sox9* was conditionally inactivated in the primordial gonad. *Sox9* null embryonic XY gonads were completely sex reversed, and developed into ovaries, which again makes investigation of the testicular role of *Sox9* difficult as Sertoli cells do not differentiate (F. Barrionuevo et al., 2006).

The *Amh-Cre;Sox9*^{*flox/flox*} mice are therefore a powerful model to investigate the effect of Sox9 in Sertoli cells (F. Barrionuevo et al., 2009). In this model Sertoli cells differentiate normally and Sox9 protein is detected at E12.5 but only a few Sertoli cells remain Sox9-positive by E13.5. Testis development in these mice is normal, however they develop sterility at 5-6 months of age indicating that Sox9 plays important roles in both the differentiation of the testis and the maintenance of testis function. RNAseq performed on these mice at E13.5 has been used to investigate which genes are immediately responsive to the loss of Sox9 and therefore are likely targeted by Sox9 during the development of the testis. 269 genes were found to be significantly dysregulated at E13.5 in the testis, 186 (69%) of which were down regulated in the knockout compared to the wildtype testis. Pathway analysis revealed that these down regulated, or in the wild type context, 'Sox9 activated' genes are involved in tube morphogenesis and organ development, a process incredibly important for the development of a functional testis (Combes et al., 2009). If these genes are important in the formation of the testis, they may be genes which are mutated in Disorders of Sex Development (DSD). Identification of the role which these 'Sox9 activated' genes play in testicular morphogenesis could therefore be important for diagnosing and managing these disorders.

As Sox9 is a transcription factor found only in Sertoli cells, it is unsurprising that many of the affected by its loss are also Sertoli cell enriched genes. Intersecting the 269 dysregulated genes with a dataset profiles which gene expression in key cell types of both male and female gonads revealed that the Sox9 responsive genes are significantly enriched in Sertoli cells (Jameson et al., 2012). This not only indicates that Sox9 plays largely a cell-autonomous role but it also highlights the power and sensitivity of this conditional *Sox9* knockout model as even though the RNAseq was performed on whole gonads and thus included all cell types of the gonad, the genes detected which were responsive to the loss of Sox9 and were largely Sertoli

cell specific. Four 'Sox9 activated' genes were enriched in Leydig cells and three were enriched in male Germ cells, albeit this enrichment was not statistically over-represented indicating that cell non-autonomous action is not a major function of Sox9 in the developing testis (see Appendix 2 for more details). However, this indirect action should not be discounted simply based on statistics and invites the investigation of the importance of these few genes which are dysregulated. Interestingly, three of these Leydig cell genes are involved in hedgehog signalling; *Ptch1, Hhip* and *Sostdc1*. *Ptch1* has a well-established role in sex determination. As a key ligand for Dhh on the Leydig cells, it conveys signals between the Sertoli and Leydig cells and is required for Leydig cell differentiation (Yao, Whoriskey, & Capel, 2002). Loss of Dhh also results in loss of Ptch1 protein (Bitgood et al., 1996). Given that *Dhh* is a Sox9 target gene, it is likely that Sox9 is influencing *Ptch1* expression via hedgehog signalling. The precise role of *Hhip* in the developing testis is unclear so far, but its cellular function has been well established as a negative regulator of hedgehog signalling (Chuang & McMahon, 1999; Olsen, Hsu, Glienke, Rubanyi, & Brooks, 2004). *Hhip* modulates the signals received by cells expressing Patched receptors by sequestering excess hedgehog proteins. *Sostdc1* also is a downstream target of hedgehog signalling, which may be required to prevent premature initiation of spermatogenesis as its downregulation is required at puberty for spermatogenic onset (Cho et al., 2011; Hammond, Brookes, & Dixon, 2018; Pradhan, Bhattacharya, Sarkar, & Majumdar, 2019). Thus, this reinforces that Sox9 is a key regulator of Hedgehog signalling in the developing testis.

To identify if Sox9 regulated genes are direct targets of Sox9 in the gonad, this RNAseq dataset was combined with Sox9 ChIPseq. The ChIPseq was performed in both the mouse and bovine as the testicular necessity of Sox9 is conserved among mammals. Thousands of genes were identified as bound by Sox9 in both the mouse (6430) and bovine (10604) models. Importantly, even when these datasets were combined (4082 genes in common), pathway analysis revealed that multiple pathways involved in the development and function of the male gonad were enriched. Other pathways enriched in this analysis may also point to Sertoli cell functions which Sox9 controls. This may begin to reveal how Sox9 divides its labour among target genes to drive key Sertoi cell processes. This analysis revealed the enrichment of multiple pathways controlling cell cycle and cell adhesion, both critical Sertoli cell functions (Lin, Barske, DeFalco, & Capel, 2017; Schmahl & Capel, 2003).

In mouse and bovine Sox9 ChIPseq datasets, 50% of the ChIPseq peaks were found in a region which represents less than 0.001% of the genome (-500-+500bp from the transcription start site) (McLean et al., 2010). This suggests that in the testis, Sox9 is largely acting at proximal promoters. This is not dissimilar to in mouse chondrocytes where 24.6% of peaks were within 500bp of the transcription start site(Ohba, He, Hojo, & McMahon, 2015). It is

important to note that in this dataset, 27656 Sox9 ChIP peaks were identified, reinforcing that the role and action of Sox9 in Sertoli cells and chondrocytes is very different (Bernard et al., 2003).

When the ChIPseq (4082 genes) and RNAseq (148 Sox9 activated genes) were intersected, 59 genes were identified as being both Sox9 bound and responsive (40% of the 'Sox9 activated' genes). Given that there are over 4000 genes identified as being 'bound' by Sox9 in the testis, the huge disparity between the number of genes bound and responsive indicates that there may be important genes which are not being downregulated in the knockout, pointing to compensatory or redundant mechanisms. The lack of phenotypic abnormality in the embryonic gonads also suggests this. When the *Amh-Cre;Sox9^flox/flox* mice are crossed onto a *Sox8* null background, inactivation of *Sox9* after sex determination leads to a more severe phenotype, whereby the Sertoli cells are reprogrammed into their female counterpart, granulosa cells (F. J. Barrionuevo et al., 2016). This shows that Sox8, a closely related Sox protein, can compensate for the loss of Sox9, indicative of redundancy between these two proteins. Thus, when both are present, they may also work together to regulate genes critical in testis development. Therefore, it may be useful in the future to repeat the RNAseq with this *Sox9/Sox8* knockout model.

A short-list of 37 Sox9 target genes which may be involved in DSD was created by combining the ChIPseq, RNAseq and the list of Sertoli cell enriched genes published in Jameson et al., (Jameson et al., 2012). This approach identified 4 characterised Sox9 target genes, validating the approach, and 33 novel targets which warrant further investigation. Comparison of the expression level of these 37 genes between the XY KO and XX WT allowed their classification into two groups. The first group of 21 genes represents genes which are similarly expressed between XY KO and XX WT gonads. While some of these genes showed very little to no expression in the XX gonad (such as *Sox10*), some were still expressed, like *Msi* and *Mybl1* indicating that in both sexes there are other gonadal regulators of expression. The second group of 16 genes represents genes whose expression was intermediate between XY WT and XX WT. This suggests that these genes are still partially active, even without Sox9, and thus are likely regulated by additional factors in the developing testis. In Sertoli cells, Sox9 often binds to chromatin with Dmrt1 and Gata4, a phenomenon dubbed the SCS (Sertoli Cell Signature) (Rahmoun et al., 2017). In (Rahmoun et al., 2017) a third group of genes was identified with XY KO expression lower than the XX WT gonads when the RNAseq was analysed. This pattern was not observed among the 37 target genes identified here suggesting that by combining the RNAseq and ChIPseq we may be identifying genes involved in Sertoli cell specific functions (Jameson et al., 2012; Rahmoun et al., 2017).

Of the 33 uncharacterised Sox9 target genes, seven had characterised knockout/knockdown models with fertility defects. Given that Sox9 regulates fertility in the postnatal testis it is not surprising that some of the putative targets have roles in spermatogenesis (F. Barrionuevo et al., 2009). Of these, most had not been investigated for their role in testis development but their role in spermatogenesis has been characterised which raises the question of whether these genes are also involved in the development of the testis. Many of the 33 genes have undefined roles in the testis with reproductive potential not yet reported. Furthermore, the robustness of the reproductive potential of the mouse testis should not be overlooked, especially given that *Sox9* in mice must be reduced below 23% of the expression of wild type to cause sex reversal (Gonen et al., 2017). This is opposed to the loss of only one allele (50%) in the human. As such loss of an important testicular development gene can be tolerated by the mouse testis and the report of the 'fertile' status may in fact be missing more subtle gonadal phenotypes. For example, the *Gpr37* mice are fertile by definition but have reduced testis weight (by about 15%), reduced epididymal sperm and reduced sperm motility (La Sala et al., 2015). Further inspection of the testes revealed that Gpr37 is a modulator of *Dhh* signalling as well as Sertoli cell maturation and proliferation. This emphasises the importance of investigating each of these 33 uncharacterised genes as potential DSD genes in the human.

Chapter 3:
NT2/D1 cells as a model for SOX9 function in the mammalian testis

3.1 Introduction

Among its most crucial functions as a key regulator of testis development, SOX9 drives the differentiation of Sertoli cells from the somatic cell population of the primitive gonad during embryogenesis. In turn, SOX9 activity within Sertoli cells plays a vital role in the differentiation of several other testicular cell lineages and morphogenesis of the testis. Following the upregulation of *SOX9*, Sertoli cells coalesce around germ cells and become encompassed by peritubular myoid cells to form the cords, which are then surrounded by steroidogenic Leydig cells (Svingen & Koopman, 2013). The morphogenesis of the testis requires Sertoli cells to proliferate before they migrate to surround primordial germ cells, gain polarity and form testicular cords (Barrionuevo, Burgos, & Jimenez, 2011; Hutchison et al., 2008). Ablation of *Sox9* from the developing mouse testis before sex determination results in complete sex reversal and thus, directly or indirectly *Sox9* is required for Sertoli cells to perform their critical functions (Barrionuevo et al., 2006).

While elegant mouse (and other organism) models have been useful in studying the function of critical sex determination genes based using knockout/transgenic approaches, limitations of using these models exclusively are emerging. Firstly, functional redundancy within SOX gene family members or genetic buffering (alternative pathways exist for the same functional outcome in an organism) can result in no phenotypic consequence (Barbaric, Miller, & Dear, 2007). As fertility is indispensable to the survival of a species, it is likely that there are many genes and pathways within the developing gonad that have acquired redundant functions to preserve reproductive function. Secondly, it is likely many genes contribute small, but beneficial effects toward testicular development (Barbaric et al., 2007). When considered at the level of an individual, these genes may provide marginal fitness improvement but at the level of a population provide significant selective advantage (Thatcher, Shaw, & Dickinson, 1998). This means that analysis of single gene mouse knockouts may not reveal anything obvious (Barbaric et al., 2007). Moreover, when inherent stochastic variability between individual mice is considered, finding subtle testicular phenotypes can become even more difficult. Differences of gene expression thresholds and genetic robustness between humans and mice are becoming apparent as more mice models are analysed (Bashamboo & McElreavey, 2016; Gonen, Quinn, O'Neill, Koopman, & Lovell-Badge, 2017).

With relevance to the mouse testis, *Sox9* transcript levels are required to decrease to 23% of that of wildtype before XY sex reversal is seen. In contrast, loss of only one copy (~50% function) in the human results the same XY sex reversal phenotype, reinforcing the need to consider gene dosage thresholds even when no obvious phenotype is observed in mice

(Gonen et al., 2017). Therefore, understanding the cellular functions of genes requires models that can complement mouse knockout approaches, and possibly reveal redundancies. This is needed to ensure proper analysis of variants of unknown significance and consequences of gene mutation thus providing an overarching view regarding the physiological relevance of mutation.

In this study, *in vitro* assay has been designed to model molecular mechanisms regulated by human *SOX9* in developing human Sertoli cells. N-Tera2cl.D1 (NT2/D1) cells are a well-characterised human Sertoli-like cell line which expresses *SOX9* and 30 other tested testis-determining genes (Knower et al., 2007). Originating from an embryonic human testicular carcinoma, but like urogenital XX and XY somatic cells, these cells have retained multipotency which presents challenges in avoiding undesirable cell (i.e. neuronal) lineage differentiation. In addition, a major limitation of the use of this line has been the well-characterised low rate of transfection (20%). As such, it has been speculated that negative results when using transfected NT2/D1 cells may be a reflection of this this limitation (Bernard, Sim, Knower, Vilain, & Harley, 2008). Therefore, the first aim of this study was to improve transfection efficiency to ensure sensitivity of the assays. Following this enhancement, NT2/D1 cells either overexpressing *SOX9* with an expression plasmid or *SOX9* knocked down with siRNA, human Sertoli cell functions were investigated to establish whether SOX9 plays a significant role in controlling proliferation, adhesion and the establishment of polarity of these cells.

3.2 Methods

*Cell culture and transient transfection - NT2/D1 cells were cultured in DMEM/F12 + GlutaMAX medium supplemented with 10% Fetal Bovine Serum and Antibiotic-Antimycotic (growth medium) in an atmosphere of 5% carbon dioxide at 37°C. All experiments repeated at least 3 times. Cells were seeded in a 6-well plate at a density of 3.6×10^5 cells per well. After 24 hours, all media was removed, and transfection reagents were added to the cells with 1ml of OPTI-MEM starve media. Following a 5-hour incubation, 500µl of transfection media was removed from each well and replaced with 2ml of growth medium. For over-expression analysis, cells were transfected using X-tremeGENE 9 with a total of 1µg of pcDNA3-*SOX9* ('SOX9') or the stoichiometrically equivalent amount of pcDNA3 control ('Control') expression plasmids in a 3:1 ratio with pEF-GFP in order to maximise selection for *SOX9* transfected cells during fluorescent activated cell sorting (FACS). For knockdown analyses, cells were transfected with 100nM *siSOX9* ('SiSOX9') or control *siRNA* ('Control') using Lipofectamine 2000 according to the manufacturer's instructions. Total RNA was extracted after 48 hours using TRI Reagent® following the manufacturer's procedure for a cell monolayer.

Quantitative RT-PCR (qRT-PCR)- 1µg of total RNA was reverse transcribed into cDNA using QuantiTect Reverse Transcription kit as per the manufacturer's instructions. 1 in 4 dilution of the cDNA product was PCR amplified using the QuantiTect SYBR® green Lightcycler RT-PCR kit. Real time quantitation of mRNA levels was conducted using the 7900HT Fast Real-Time PCR System (ThermoFisher Scientific). Primer sequences used are detailed in Appendix 1. Gene expression was normalized to *RPS29* levels using the delta-delta CT method. Statistical analysis has been performed using Graphpad Prism V7

Western Blot – Total cell protein was isolated post-transfection with radioimmunoprecipitation assay (RIPA) buffer, or for nuclear extractions using NE-PER kit (Pierce Biotechnology, Rockford USA), as per the manufacturer's instructions from whole cell populations. 5µg of protein was run on a 12% acrylamide gel in Towbins running buffer. After transfer to a PVDF membrane using Towbin's transfer buffer, the membrane was blocked with 5% skim milk powder in TBS-T for 1 hour. Primary antibody (Rabbit anti-SOX9 1:2000, Mouse anti-NEDD9 1:5000, TBP 1:5000 or Mouse anti-β-Tubulin 1:5000) was applied overnight at 4°C. The membrane was washed in TBS-T and then incubated in secondary (Donkey anti-Mouse 1:5000 or Goat anti-Rabbit 1:5000) for 1 hour at room temperature. The membranes were again washed in TBS-T and then imaged using ECL kit on a BioRad Chemidoc™. Image quantification has been performed using ImageJ software and statistical analysis has been performed using Graphpad Prism V7. Relative pixel densities of bands (with background subtracted) have been measured using the 'measurement' tool and values graphed have been normalized to the loading control.

Xcelligence – Real time adhesion, proliferation and migration assays were conducted using the Xcelligence system (ACEA) where cell number is calculated via electrical impedance across an electrode. The more cells attached to, or that pass through the gold electrode, the higher the electrical impedance measurement. 42 hours following transfection, NT2/D1 cells growth medium was replaced with starve (0% fetal calf serum) medium for 6 hours. For adhesion/proliferation assays, cells were seeded in proliferation assay plates (E-plates; John Morris Scientific) at a density of 1×10^4 cells per well with 5% fetal calf serum. Readings were taken on the Xcelligence machine every 15 seconds for the first 5 hours to measure adhesion followed by every 15 minutes for the next 43 hours. Analysis of adhesion encompassed 0-5 hours' time points. Analysis of proliferation encompassed 12-48 hour time points. For migration assays, 10% fetal calf serum was added in the lower well of migration assay plates as a chemoattractant (E-plates; John Morris Scientific) and cells were seeded in the upper well at a density of 2×10^4 with 1% fetal calf serum. Readings were taken every 15 minutes for

48 hours. Analysis encompassed 5-48 hours. All treatments were performed in quadruplicate to a total of three biological replicates. All data are expressed as rates of change.

Transepithelial Electrical Resistance (TEER) Assays – NT2/D1 cells were seeded at a density of 1×10^5 onto polyester bicameral chambers (12mm, 0.3µm pore; Sigma) 24 hours post transfection. Cells were allowed to attach overnight in 10% fetal calf serum before being washed with PBS and media replaced with 0.5% fetal calf serum. Cells were then incubated for a further 6 hours. Cells were then equilibrated on a warming plate set to 37 degrees within the culture hood for 30 minutes before TEER measurement. Following readings at 48 hours post transfection, cells were fixed for 7 minutes in 4% PFA for immunofluorescent analysis. These experiments were repeated at least 3 times. Results are reported as $\Omega.cm^2$.

Immunofluorescence, NT2/D1 cells – Membranes from TEER assays were carefully cut from inserts and placed, cells facing upwards in cell culture plate with wells just larger than the membrane. Or, cells were cultured on a UV sterilized coverslip within a 6-well plate. Both membranes and coverslips were fixed in 4% PFA for 7 minutes before being washed in PBS. After washing with PBS, were blocked with 5% Donkey Serum in 1x PBS with 0.1% Tween 20 for 1 hour. The block was removed and replaced with primary antibodies (Phospo-Histone H3 1:300, Laminin 1:200, N-Cadherin 1:25) and incubated for 2 hours at 37 degrees. Primary was washed off with 1x PBS with 0.1% Tween 20 and the membranes were incubated with the fluorescent-conjugated secondary antibody, (donkey anti-goat Alexa Fluor 594 1:1000 and donkey anti-rabbit Alexa Fluor 488 1:1000) for 1 hour at room temperature. Sections were washed in 1x PBS with 0.1% Tween 20, counterstained using DAPI, and then washed in 1x PBS and mounted using Dako Fluorescent Mounting Medium. Sections were imaged using fluorescence microscopy (Olympus Corp).

3.3 Results

Optimising NT2/D1 transfection: effect of starvation and cell density

In order to optimise the of transfection efficiency in NT2/D1 cells was, cell culture conditions were modified when transfecting 1µg of *GFP* expression plasmid, then assessed by FACS after 48 hours. Transfection efficiency was increased by 10% from approximately 20% to 30% when cells were transfected at a higher density (3.6×10^5) than previously (2×10^5) (**Figure 3.1a**) (P<0.01). Higher seeding density value was chosen based on an estimate of 70% confluency at the time of transfection (Nikcevic, Kovacevic-Grujicic, & Stevanovic, 2003) The addition of a starvation step for 5 hours following transfection further increased this rate to approximately 40% (**Figure 3.1a and 3.1b**) (P<0.05). Starvations exceeding 6 hours resulted

in decreased cell viability and under 3 hours did not affect transfection rates (data not shown). Increasing the concentration of transfected plasmid did not improve transfection efficiency, as over 1.5ug decreased cell viability (data not shown).
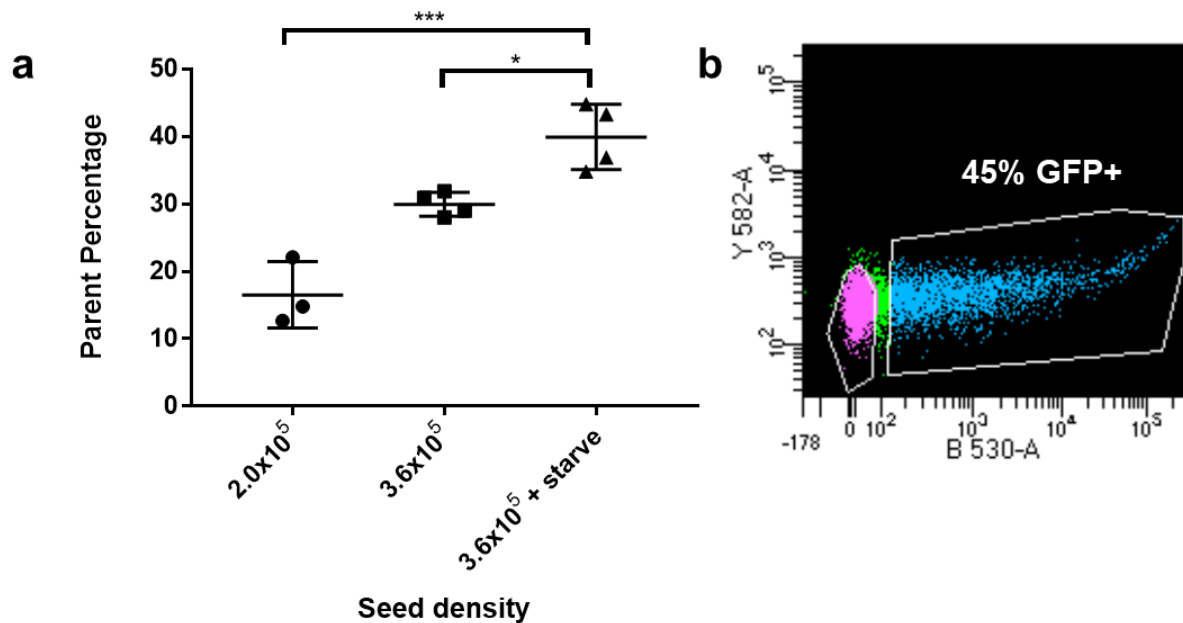
Figure 3.1. Transfection efficiency of NT2/D1 cells; effect of seeding density and starvation. **(a)** Increasing seed density and the addition of a 5-hour starvation at the time of transfection increased the transfection efficiency by 24% when NT2/D1 cells were transfected with 1ug of pEF-GFP plasmid and analysed by FACS after 48 hours. Circles show individual experiments with seeding density of 2.0×10^5, squares show seeding density of 3.6×10^5 snf triangles show seeding density of 3.6×10^5 plus starvation **(b)** Representation of the output generated by FACS with gating when transfection protocol is optimised. Pink shows GFP negative cells and blue shows GFP positive cells. Efficiencies are reported as percentage of the parent population and each test value graphed individually, with bars representing means and standard deviations. P-values are calculated using one-way ANOVA with Tukey's post hoc test, where the asterisks indicates significance: $*<0.05$, $***<0.001$.

Effect of over and under expression of *SOX9* in NT2/D1 cells on expression of target genes

In order to analyse the effects of *SOX9* alterations in NT2/D1 cells, cells were transfected with either *SOX9* expression plasmid to increase expression or *SOX9* siRNA to knockdown expression. QRT-PCR analysis of NT2/D1 cells transfected with the *SOX9*-over expression plasmid showed that when compared to empty vector, gene expression of endogenous *SOX9* itself was significantly increased by 35%, consistent with autoregulation (Gonen et al., 2017, Croft et al., 2018) (**Figure 3.2 a,** left). Western Blot analysis of whole cell extracts confirmed this result with an average 30% increase observed (**Figure 3.2 a,** middle and right). In whole cell extracts of empty vector transfected control NT2/D1 cells, the SOX9 protein levels are very low and making detection by Western Blot analysis difficult (Figure 3.2 a, middle). As the whole cell extract contains both the membrane-bound and cytoplasmic fractions of protein as well as the nuclear fraction it is possible that the increase in protein may reflect more protein being present outside of the nucleus and thus would have little physiological relevance as SOX9 action is as a transcription factor. Immunofluorescence confirmed the pattern of protein localisation is not altered and thus can be relevant to altering gene expression (**Figure 3.2 b**). SOX9 was knocked down in NT2/D1 cells using a siRNA and scrambled control, previously validated and used to test SOX9 cellular function (Alankarage et al., 2016, McDonald et al., 2012). In contrast, transcriptional analysis of *SOX9* knockdown cells showed that transcript *SOX9* transcript levels were downregulated by 46% compared to the control transfected cells (**Figure 3.2 c,** left). To improve SOX9 protein detection in the knockdown model, the Western blot was sensitised the enrich for SOX9 by analysing nuclear extracts. Again, Western blot of nuclear extracts confirmed this result with an average of 48% decrease in SOX9 protein (**Figure 3.2 c,** middle and right). To investigate whether altered *SOX9* expression in NT2/D1 cells had functional consequences to SOX9-target gene expression, mRNA levels of the well characterised target, *AMH* were assayed (Arango, Lovell-Badge, & Behringer, 1999). In NT2/D1 cells transfected with *SOX9*-over expression plasmid, *AMH* was up-regulated by 2-fold (**Figure 3.2 d,** left). In *SOX9* knockdown-treated cells however, *AMH* levels were reduced by 37% (**Figure 3.2 d** right). Together, these results confirm that NT2/D1 cells model events in Sertoli cells such as SOX9 regulation of *AMH*, and thus serves as a valuable *in vitro* model to investigate biological responses due to altered SOX9 expression in human Sertoli cells.
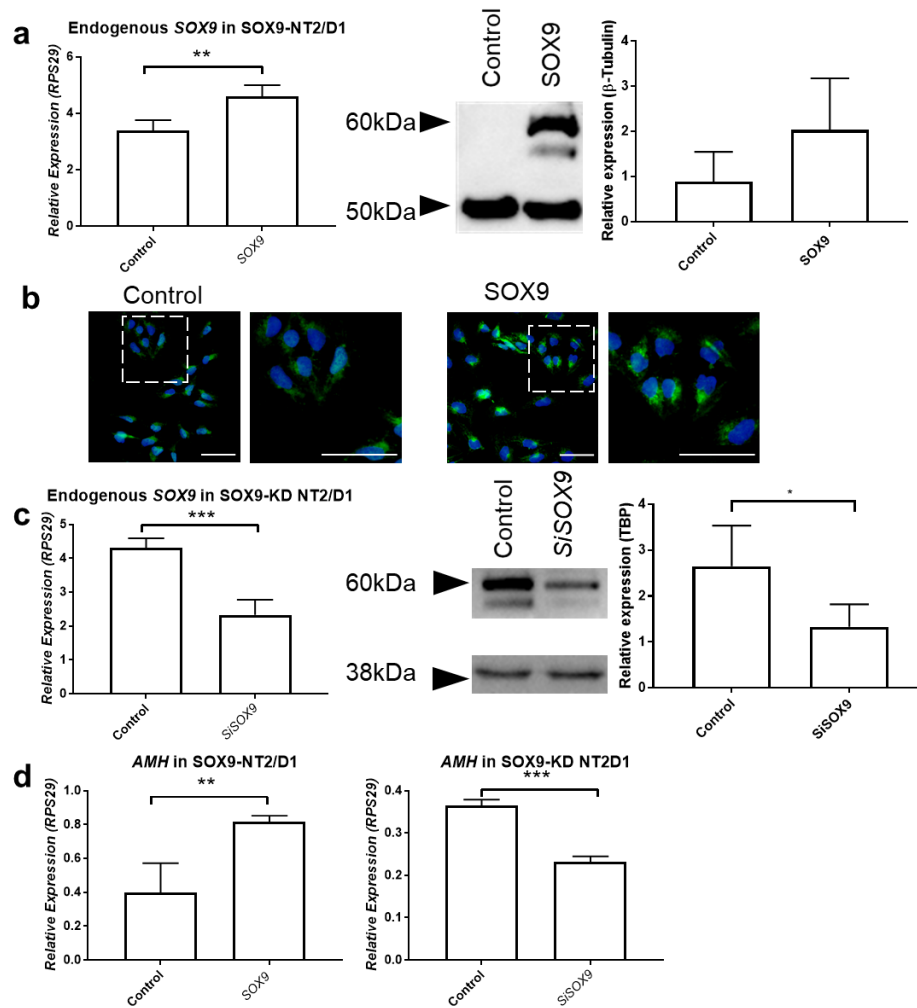
Figure 3.2. Manipulation of *SOX9* mRNA levels in NT2/D1 cells alters SOX9 Sertoli cell target gene expression (a) Left; Histogram of endogenous *SOX9* gene expression data from qRT-PCR in NT2/D1 cells over expressing SOX9 (*SOX9*)**.** Middle; Western blot analysis of SOX9 protein levels (60kDa) using whole cell extracts. β-Tubulin was used as a loading control (50kDa) (representative of n=3). Right; Histogram of Western Blot results **(b)** Immunofluorescence on NT2/D1 cells. SOX9 is in green and DAPI in blue. Scale bar represents 50µm. Dotted square on imaged depicts the area in zoom image Left; Control NT2/D1 cells, Right; *SOX9* over expressing NT2/D1 cells **(c)** Left; Histogram of endogenous *SOX9* gene expression data from qRT-PCR in NT2/D1 cells with *SOX9* knocked down (*SiSOX9*)**.** Middle; Western blot analysis using nuclear extracts of SOX9 protein levels (60kDa). TBP was used as a loading control (38kDa) (representative of n=3). Right; Histogram of Western blot results **(d)** Left; Histogram of *AMH* expression data from qRT-PCR in NT2/D1 cells over expressing *SOX9* (*SOX9*) and Right; NT2/D1 cells with *SOX9* knocked down (*SiSOX9*) All values were determined from at least 3 individual tests. Means are graphed with error bars representing standard deviation. P-values were calculated using a one-sided Student's T-test where the asterisk indicates significance: **<0.01, ***<0.001.

Analysis of the role SOX9 in adhesion, proliferation and the migration of NT2/D1 cells

Given that testis cord formation and maintenance requires adhesion of Sertoli cells both between themselves and with germ cells during testis development, we hypothesised that SOX9 would influence this process in NT2/D1 cells (Reviewed in (Mruk & Cheng, 2004)). To investigate this, Xcelligence assays were performed on *SOX9* knockdown and control NT2/D1 cells. To test adhesion, electrical impedance resulting from the adhesion of cells to the electrode was measured for 5 hours (**Figure 3.3 a,** left, blue shading). Cells with reduced *SOX9* expression showed a significantly reduced rate of adhesion ($P<0.05$) compared to control (**Figure 3.3 a,** middle). Proliferation is also required by embryonic Sertoli cells, to elongate the testis cords and create a nourishing environment for germ cells, with the number of Sertoli cells directly influencing sperm production potential in adult life (Reviewed in (Sharpe, McKinnell, Kivlin, & Fisher, 2003)). The same assay revealed the effect of *SOX9* on proliferation in NT2/D1 cells. Following the initial adhesion period, the rate of cell proliferation was measured. Here, electrical impedance increased as there were more cells present on the electrode correlating to a relative increase in cell number (**Figure 3.3 a,** left, unshaded). The rate of proliferation also significantly decreased compared to control ($P<0.05$) (**Figure 3.3 a,** right). Immunofluorescence to detect phospho-Histone H3 (PH3), a marker of proliferating cells, confirmed this result as more proliferating cells (red) are observed in the control than the *SOX9* knockdown NT2/D1 cells (**Figure 3.3 b**)

To organise into cords, Sertoli cells must migrate to encompass the germ cells (Nel-Themaat et al., 2011). Migration was therefore also investigated using Xcelligence assay. In this assay, electrical impedance is measured as cells move across an electrode towards an area of high chemical attraction (**Figure 3.3 c,** left). When *SOX9* expression was reduced, there was no change in rate of migration of NT2/D1 cells compared to control (**Figure 3.3 c,** right).
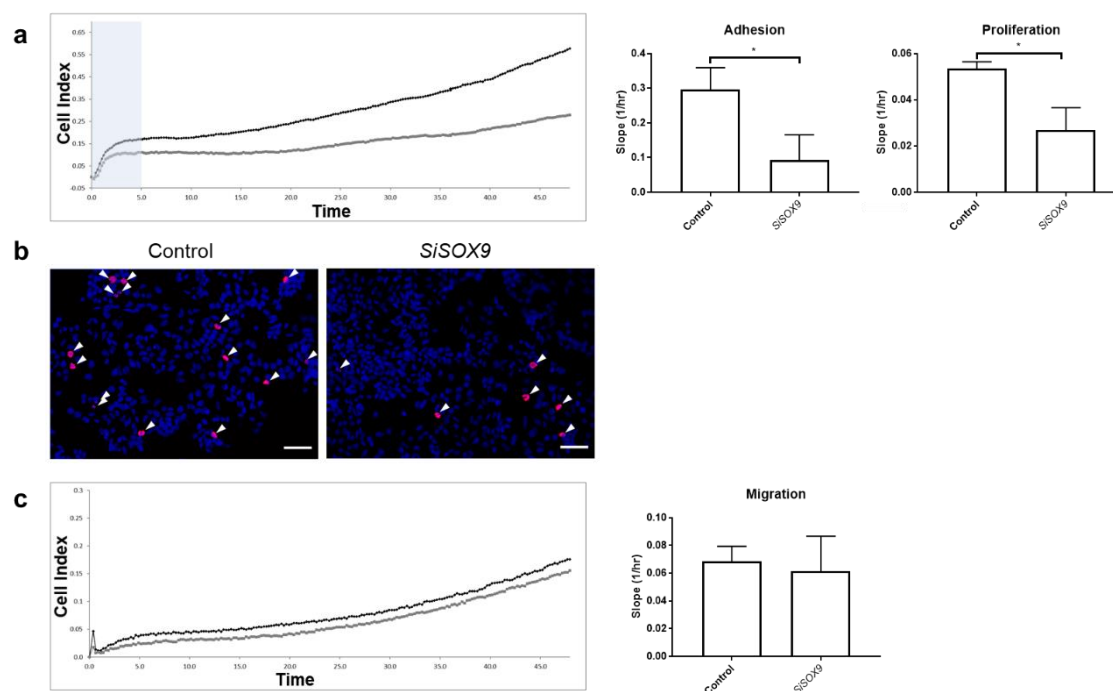
Figure 3.3. SOX9 controls adhesion and proliferation in Xcelligence assays. (a) Left; A representation of the output from the Xcelligence system measuring adhesion (blue shading) followed by proliferation (white background) of *SOX9* knockdown (grey) and control NT2/D1 cells (black). Middle; Histogram showing the rate of change of cell index of adhesion with control and *SOX9* knockdown NT2/D1 cells (SiSOX9) and, Right; Histogram showing the rate of change of cell index of proliferation. **(b)** Immunofluoresence for a proliferation marker, Phospho-histone H3 (red, white arrows) on control and *SOX9* knockdown NT2/D1 cells (*SiSOX9*). Nuclei are stained with DAPI (blue). Scale bars represent 500µm **(c)** Left; A representation of the output from the Xcelligence system measuring migration of *SOX9* knockdown (grey) and control NT2/D1 cells (black). Right; Histogram showing the rate of change of cell index of migration with control and *SOX9* knockdown NT2/D1 cells (SiSOX9) Electrical impedance was measured and reported as cell index for all Xcelligence tests. Histograms were made using rate of change (slope). Values were determined from 3 individual tests. Means are graphed with error bars representing standard deviation. P-values were calculated using one-sided Student's T-test where the asterisk indicates significance: *<0.05

Analysis of the role SOX9 in transepithelial resistance in NT2/D1 cells

By embryonic day 13 (E13) in mice, the testis cords have been defined, and are beginning to increase in length. This also marks the stage when Sertoli cells gain polarity and acquire an epithelial-like morphology where nuclei move closer to the basal lamina(Nel-Themaat et al., 2011). To test if SOX9 controls the establishment of polarity in NT2/D1 cells, transepithelial electrical resistance assays were used. This measures the permeability of a monolayer of cells, indicating the integrity of junctions between cells (Pattabiraman, Epstein, & Rao, 2013; Srinivasan et al., 2015). As junctions are essential components in the formation of polarity, this assay can be used to indicate both cell adhesion and polarity. To investigate if there is any change in transepithelial resistance, *SOX9* knockdown and control cells were seeded in a 12mm well inserts and assayed after 24 hours. *SOX9* knockdown resulted in significantly reduced transepithelial resistance compared to control (P<0.01) (**Figure 3.4a**). Immediately after resistance readings were taken, the inserts were fixed and immunofluorescence was carried out to investigate the possible contribution of two markers of Sertoli cell polarity in the developing testis, Laminin and N-Cadherin. Laminin showed weaker expression, while N-Cadherin expression was lost (**Figure 3.4b**).
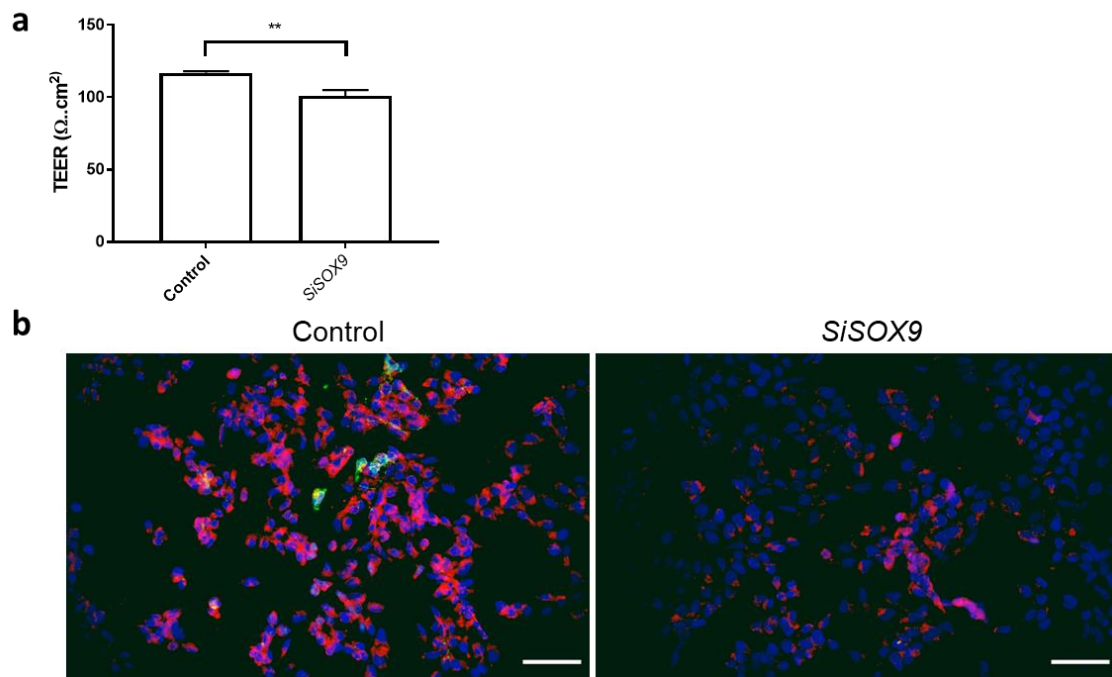
Figure 3.4. SOX9 controls transepithelial resistance in NT2/D1 cells. (a) Histogram of transepithelial resistance measurements comparing control and *SOX9* knockdown (*SiSOX9*) cells. Measurements were only made at 24 hours post seeding. Values were determined from 3 individual tests. Means are graphed with error bars representing standard deviation. P-values were calculated using a one-sided Student's T-test where the asterisk indicates significance: **<0.01. **(b)** Immunofluorescence on inserts fixed immediately after resistance was assayed for two polarity proteins expressed in Sertoli cells, Laminin (red) and N-Cadherin (green). Nuclei are stained with DAPI (blue). Scale bars represent 500µm.

3.4 Discussion

Regulation of gene transcription by SOX9 in the developing gonad is essential for testis development. By increasing the transfection efficiency of NT2/D1 cells, this study has established an *in vitro* model to demonstrate that SOX9 controls analagous cell functions to those of Sertoli cells in the developing testis. Previous studies using NT2/D1 cells as a model for human Sertoli cells have largely focussed on genetic regulation (Alankarage et al., 2016; de Santa Barbara, Moniot, Poulat, & Berta, 2000; Moniot et al., 2009; Rahmoun et al., 2017). However, this study shows that NT2/D1 cells can also be used to model Sertoli cellular behaviour and can thus be used in investigations of cellular function in the developing testis.

The low transfection rates of NT2/D1 cells have been a continual limitation for their use, and therefore serum starvation was considered a possible method to improve these rates. In many different cell culture approaches, serum starvation is a useful tool to synchronize the cell cycle, reduce cellular activities to basal levels and to induce quiescence. As a complement to transfection, serum starvation greatly increases efficiency in the pluripotent line, human embryonic stem cells (Liu, Zhang, & Peng, 2016; Wallenstein, Barminko, Schloss, & Yarmush, 2010). The addition of the serum starvation does not alter gene expression but if starved too long, cells will decrease in viability (Wallenstein et al., 2010). The transfection efficiency is thought to increase with starvation as the cells become synchronised in cell cycle, arresting the G0/G1 phase and thus many protocols have much longer starvation periods than has been applied here to ensure homogeneity (Migita et al., 2011; Wallenstein et al., 2010). A dramatic decrease in viability was observed if starvation was applied for longer than 6 hours in NT2/D1 cells. Therefore, cell cycle synchronisation by chemical methods, (and not starvation) may further improve this transfection rate. This would also allow the flexibility to arrest cells in different cell cycle phases, which may be more suitable when dealing with other cell lines. For example, Chinese hamster ovarian (CHO) cells transfect best after being arrested in S phase (Grosjean, Batard, Jordan, & Wurm, 2002).. Serum starvation may also aid in the movement of lipofectamine through the cell membrane and to the perinuclear region, which can take up to 4 hours (Cardarelli et al., 2016). The presence of serum can decrease the efficiency of how the lipoplexes form and while many transfection protocols take this into account with a short serum-free incubation, introduction of serum before the DNA has reached its cellular target may interrupt this process.

Despite an improved transfection rate, *SOX9* overexpression only led to a 35% increase in SOX9 protein levels in NT2/D1 cells. However, this increase was effective enough to increase the expression of the well characterised SOX9 target gene, *AMH* (Arango et al., 1999). It is

worth noting however that this increase in detected transcripts by RNAseq and qRT-PCR compares with a previous, less sensitive, microarray-based report where endogenous SOX9 levels did not reach a threshold of 1.25-fold increase when NT2/D1 cells were transfected with SOX9 expression plasmid (Ludbrook et al., 2016). Even with only a mild increase, this report found gene expression changes to 2626 genes, including known sex determining and testis function genes reiterating the potent potential of SOX9. Conversely, the siRNA-induced a decrease in SOX9 expression of 47% which resulted in the decrease of *AMH* expression. While this model does not necessarily show whether the control by SOX9 is direct, responsiveness of gene expression to the alterations in *SOX9* levels will indicate if the chosen target gene is in a pathway regulated by SOX9 in a Sertoli cell environment. The *SOX9* knockdown model has important biological relevance, because in humans, a reduction of *SOX9* levels by about 50%, caused by heterozygous *SOX9* mutation, is sufficiently severe to prevent testis development and cause XY sex reversal (Wagner et al., 1994). However, our model no sex reversal when probed by immunofluorescence for expression with the female transcription factor, *FOXL2*, in a preliminary analysis (data not shown, Abcam ab5096). This suggests that by decreasing *SOX9* in an intact, human Sertoli cell environment this model could be used to investigate Sertoli cell function but not to the point of trans-differentiation into granulosa-like cells.

We find that proliferation and adhesion are both controlled by SOX9 in NT2/D1 cells. To date, proliferation in embryonic Sertoli cells has largely been attributed to the growth factor, FGF9. In mice, Fgf9 is downstream of *Sox9* and plays a critical role in repressing the female pathway as well as proliferation via its receptor Fgfr2c (Kim et al., 2007; Schmahl, Kim, Colvin, Ornitz, & Capel, 2004; Willerton, Smith, Russell, & Mackay, 2004). Fgf9 acts early in the mouse testis to induce Sertoli cell proliferation, with defects appearing before cord formation in XY FGF9 homozygote knockout mice (Schmahl et al., 2004). Heterozygous mutation to *FGF9* in humans' results in bone malformations, however no patients have yet been detected with XY sex reversal begging the question of whether FGF9 controls Sertoli cell proliferation in humans (Rodriguez-Zabala et al., 2017). Therefore, it is highly likely that there are more factors controlling proliferation in human Sertoli cells to be discovered. Further to this, the molecular connection between *FGF9* and *SOX9* is yet to be identified. The NT2/D1 model presented here provides a system where FGF9 control of proliferation in human cells can be investigated and the relationship between *SOX9* and *FGF9* can be probed, as understanding not only the genes involved in testis development but their regulation provides key diagnostic information for Disorders of Sex Development (Gonen et al., 2018).

Paracrine regulators of Sertoli cells, such as Activin A , Insulin-like growth factor and FSH, are also critical for embryonic Sertoli cell proliferation (Allan et al., 2004; Froment et al., 2007; Meehan, Schlatt, O'Bryan, de Kretser, & Loveland, 2000; Nicholls et al., 2012). Despite this observation, Sertoli cells isolated from both human and mice testes will still proliferate in the absence of other cell types (Nicholls et al., 2012). Given that Sertoli cells have multiple non-autonomous proliferation mechanisms, it is possible that there are more cell autonomous mechanisms. Our model suggests these mechanisms are under the control of SOX9.

Cell adhesion and cell polarity are intimately related, as adhesion molecules often define the barriers that are required for polarity. Knockdown of *SOX9* in NT2/D1 cells suggests that SOX9 controls both. Adhesion of Sertoli cells to each other, and to germ cells has been closely investigated in the adult testis but not in the embryonic testis. The blood-testis barrier formed by tight junctions between Sertoli cells does not develop until puberty in mammals (Stanton, 2016). When mutated or ablated from mice, many of the central proteins that form these junctions do not apparently perturb testis development but still result in infertility, due to their postnatal role (Furuse, 2009). Despite having no reported role in embryonic development, these proteins, such as Cldn11, are still highly expressed in the developing mouse testis (Gow et al., 1999). In our model the decrease of *SOX9* results in a loss of N-Cadherin expression (encoded for by *CDH2*) and reduced laminin expression. The function of adherens junctions, which precedes the development of tight junctions, are yet to be investigated in the embryonic testis because total ablation of *Cdh1* and *Cdh2,* critical components of the adherens junctions in XY mice, is embryonic lethal soon after implantation (Larue, Ohsugi, Hirchenhain, & Kemler, 1994). Ablation of *Sox9* and the closely related *Sox8* from the embryonic testis causes both the decrease in expression of adherens molecules and a disruption in basal lamina expression (Barrionuevo et al., 2009; Georg, Barrionuevo, Wiech, & Scherer, 2012). Thus, our model provides a system to investigate both adhesion and polarity in human Sertoli cells. As SOX9 regulates this pathway, finding important components can come from investigating the genes downstream of SOX9.

Migration is another critical function of Sertoli cells in the developing testis. Our NT2/D1 model suggests that SOX9 does not play a role in regulating Sertoli cell migration, however this result may reflect limitations of this model. Firstly, Sox8 reinforces Sox9 expression during the development of the embryonic testis. In XY mice, *Sox8* is dispensable for testis development, however in the absence of *Sox9* it can compensate for the loss of gene regulation and somewhat maintain the developmental potential of the embryonic testis (Barrionuevo et al., 2009; Sock, Schmidt, Hermanns-Borgmeyer, Bosl, & Wegner, 2001). It is not until *Sox9* is ablated from Sertoli cells on a *Sox8* null background that disruption to cell junctions, and

upregulation of female markers was seen in the double knockout XY mice. This redundant mechanism is also at play in the human, and given *SOX8* is expressed in NT2/D1 cells is highly likely to affect NT2/D1 model as well (Knower et al., 2007; Portnoi et al., 2018). Another important consideration of this model is that the degree of knockdown may not be sufficient to disrupt critical functions. As these cells do still migrate, it is possible that this process is still under the control of SOX9. Exacerbating the loss of *SOX9* in this model may induce more severe phenotypes.

In conclusion, we have developed a model the investigate the role of SOX9 in Sertoli cells during testis development, specifically proliferation, migration, adhesion and polarity. Firstly, the transfection efficiency of NT2/D1 cells has been improved with the addition of a 5 hour starvation to the protocol and an increased seeding density. Despite this improvement, further *SOX9* knockdown may exacerbate phenotypes and development of alternative *in vitro* models should still be considered (Appendix 3). This study demonstrated that SOX9 controls cell proliferation suggesting that target genes of SOX9 likely regulate critical internal mechanisms of proliferation in Sertoli cells. Furthermore, SOX9 was shown to control both adhesion and polarity. As both functions are yet to be closely investigated in the developing testis, this model provides an environment for further examine the role of the genes SOX9 controls.

Chapter 4:

SOX9 controls proliferation in the developing mammalian testis via *NEDD9*

4.1 Introduction

Sex determination is the process during embryogenesis by which the bipotential gonad commits to developing as either an ovary (in the XX embryo) or a testis (in the XY embryo). Testis development is initiated by the expression of the Y-chromosome gene *SRY*, which activates expression of *SOX9*(Croft et al., 2018; Gonen et al., 2018; Sekido & Lovell-Badge, 2008). The transcription factor SOX9 orchestrates the differentiation and development of the testis from the biopotential gonad. Without SOX9, the gonad will develop as an ovary with the individual having the female phenotype (Vidal, Chaboissier, de Rooij, & Schedl, 2001; Wagner et al., 1994).

Disorders of Sex Development (DSD) encompass a wide range of conditions where chromosomal, gonadal or anatomical sex is atypical (Hughes et al., 2006). DSD encompasses a broad spectrum of conditions, including the development of ambiguous genitalia and complete sex reversal (1 in 4500 and 1 in 20,000 live births respectively (Reviewed in (Leon, Reyes, & Harley, 2019)). Despite over 20 years of research, over 50% of 46, XY DSD still fail to achieve molecular diagnosis which poses a major challenge for clinical management (Eggers et al., 2016; Ozen et al., 2017). This low diagnosis rate can be attributed to a lack of understanding regarding the molecular genetic mechanisms involved in the development of the testis and ovary.

As a transcription factor, SOX9 is a key regulator of the genes and pathways required for testis differentiation and development (Morais da Silva et al., 1996). In humans, mutation of *SOX9* coding or regulatory region can result in Campomelic Dysplasia with associated XY sex reversal (Foster et al., 1994; Wagner et al., 1994). SOX9 divides its labour among Sertoli cell genes in order to direct a multitude of cell phenotypes including cell proliferation, cell adhesion and cell migration (see Chapter 3). Mutation to direct transcriptional target genes of SOX9 can also cause DSD. One such target gene, *AMH* (anti-Müllerian hormone) is synthesised by the Sertoli cells to regress the female reproductive tract (Arango, Lovell-Badge, & Behringer, 1999; Cate et al., 1986). Mutation to *AMH* results in the persistence of the Müllerian ducts which develop as the oviducts, uterus and upper vagina. Only a handful of other SOX9 target genes have been identified in testis development including *PGDS, ETV5*, *DHH*, *CYP26B1* and *GDNF* (reviewed in Chapter 1). Collectively, these genes account for a few of the Sertoli cell functions required for testis development including amplification of *SOX9* expression (*PTGDS*), direct the differentiation of other testis cells (*DHH*), and protect the germ cells, (*ETV5, CYP26B1, GDNF*) (Alankarage et al., 2016; Kashimada et al., 2011; Meng et al., 2000; Moniot et al., 2009; Wilhelm et al., 2007; H. H. Yao, Whoriskey, & Capel, 2002). However, chromatin immunoprecipitation (ChIP) experiments predict that SOX9 could have over 5000

87

direct targets in the developing gonad, possibly regulating other Sertoli cell functions (Li, Zheng, & Lau, 2014; Rahmoun et al., 2017). Understanding these genes and the pathways they control will provide further insight into the molecular mechanisms of DSD.

This study shows that SOX9 directly regulates the expression of a testis-specific gene, Neural precursor cell expressed, developmentally downregulated 9 (*NEDD9*), during the development of the testis. Neural precursor cell expressed, developmentally downregulated 9, or NEDD9, is a non-catalytic scaffolding protein which acts to assemble many different complexes and therefore regulates several cellular functions including proliferation, adhesion and migration (Aquino et al., 2009; Miao et al., 2013; Singh, Cowell, Seo, O'Neill, & Golemis, 2007). Despite being identified as a sexually dimorphic gene over 10 years ago, the function of NEDD9 in testis development had not been elucidated (Nef et al., 2005). However, recent Sox9 ChIP sequencing identified *Nedd9* as a possible target of Sox9 in the bovine testis, inviting the investigation of its testicular function, and if it is relevant to human development (Rahmoun et al., 2017). Using the model developed in Chapter 3 of this thesis, this research shows that NEDD9 regulates proliferation in Sertoli cells, and possibly plays a role in the establishment of cell polarity.

4.2 Methods

Cell culture and transient transfection - NT2/D1 cells were cultured in DMEM/F12 + GlutaMAX medium supplemented with 10% Fetal Bovine Serum and Antibiotic-Antimycotic (growth medium) in an atmosphere of 5% carbon dioxide at 37°C. All experiments repeated at least 3 times. Cells were seeded in a 6-well plate at a density of 3.6×10^5 cells per well. After 24 hours, all media was removed, and transfection reagents were added to the cells with 1ml of OPTI-MEM starve media. Following a 5-hour incubation, 500µl of transfection media was removed from each well and replaced with 2ml of growth medium. For over-expression analysis, cells were transfected using X-tremeGENE 9 with a total of 1µg of pcDNA3-*SOX9* (*'SOX9'*) or pcDNA3 empty vector control ('Control') expression plasmids in a 3:1 ratio with pEF-GFP in order to maximise selection for *SOX9* transfected cells during fluorescent activated cell sorting (FACS). For knockdown analyses, cells were transfected with 100nM *siSOX9* (*'SiSOX9'*) or control (Control) *siRNA* or with 20nM total of *siNEDD9 A* and *siNEDD9 B* combined (*SiNEDD9*), as per (Humphreys et al., 2013) or negative control *siRNA* (Control) (see Appendix 1 for details) using Lipofectamine 2000 according to the manufacturer's instructions. Total RNA was extracted after 48 hours using TRI Reagent® following the manufacturer's procedure for a cell monolayer.

Quantitative RT-PCR (qRT-PCR)- 1µg of total RNA was reverse transcribed into cDNA using QuantiTect Reverse Transcription kit as per the manufacturer's instructions. 1 in 4 dilution of

the cDNA product was PCR amplified using the QuantiTect SYBR® green Lightcycler RT-PCR kit. Real time quantitation of mRNA levels was conducted using the 7900HT Fast Real-Time PCR System (ThermoFisher Scientific). Primer sequences used are detailed in Appendix 1. Gene expression was normalized to *RPS29* levels using the delta-delta CT method. Statistical analysis has been performed using Graphpad Prism V7

Western Blot – Total cell protein was isolated post-transfection with radioimmunoprecipitation assay (RIPA) buffer, or for nuclear extractions using NE-PER kit (Pierce Biotechnology, Rockford USA), as per the manufacturer's instructions from whole cell populations. 5µg of protein was run on a 12% acrylamide gel in Towbins running buffer. After transfer to a PVDF membrane using Towbin's transfer buffer, the membrane was blocked with 5% skim milk powder in TBS-T for 1 hour. Primary antibody (Mouse anti-NEDD9 1:5000 or Mouse anti-β-Tubulin 1:5000) was applied overnight at 4°C. The membrane was washed in TBS-T and then incubated in secondary (Donkey anti-Mouse 1:5000) for 1 hour at room temperature. The membranes were again washed in TBS-T and then imaged using ECL kit on a BioRad Chemidoc™. Image quantification has been performed using ImageJ software and statistical analysis has been performed using Graphpad Prism V7.

Chromatin Immunoprecipitation- NT2/D1 cells transfected with either pcDNA3-*SOX9* or pcDNA3 control expression vector (as above) were cross-linked with formaldehyde to a final concentration of 1%. Glycine was added to stop fixation to a final concentration of 0.125M. The cells were pelleted before resuspension in ChIP Lysis Buffer, and sonicated using the Covaris S220 Focused-ultrasonicator for 1.5 minutes (175.0 peak power; duty factor 30; 200 cycles/burst) to achieve a general fragment size of 200-500bp. DynabeadsTM Protein A were coupled with Rabbit anti-SOX9 and Rabbit polyclonal IgG. Sonicated chromatin was coupled with antibody and incubated overnight at 4oC. Beads were washed with ChIP-RIPA buffer and TE buffer and eluted in Elution Buffer. Chromatin was treated with Proteinase K.

DNA was purified by phenol:chloroform separation. 100% ethanol was added to precipitated DNA. Prior to immunoprecipitation, 20% of the sonicated chromatin was retained as total input chromatin and processed with the eluted immunoprecipitates. Chromatin was resuspended in 60µl TE buffer. The final ChIP precipitates and diluted input were analysed by qRT-PCR with the primers detailed in Appendix 1, using the Applied Biosystems 7900HT Fast Real-Time PCR system. Of the 60µl eluted from ChIP, 0.5µl of chromatin was added per well. Relative expression at each position was calculated as the ratio of the amount of PCR template in ChIP samples to that in input. IgG of the empty vector control (pcDNA3) was then set to 1 with all other samples calculated relative to this control.

Luciferase assay- Candidate 1.2 kb NEDD9 promoter (Hg19 Chr6:11,232,507-11,233,727) was generated by GeneScript between BglII and HindIII into Pgl4.10 luciferase vector (Promega). Luciferase assays were performed using COS-7 cells, as described in (Croft et al., 2018) with modifications; total 120ng of transcription factors per condition, 40ng of each transcription factor and 75ng of Ppgl4.10 luciferase, with 15ng of Renilla control. Firefly luciferase values assays were normalized to transfection control Renilla luciferase values and then to the average of the empty transcription factor vector control (pcDNA3.1). Standard error of the mean (s.e.m.) and 2way ANOVA were conducted from 4 biological replicates using Graphpad Prism V7

Xcelligence – Real time adhesion, proliferation and migration assays were conducted using the Xcelligence system (ACEA) where cell number is calculated via electrical impedance across an electrode. The more cells attached to, or that pass through the gold electrode, the higher the electrical impedance measurement. 42 hours following transfection, NT2/D1 cells growth medium was replaced with starve (0% fetal calf serum) medium for 6 hours. For adhesion/proliferation assays, cells were seeded in proliferation assay plates (E-plates; John Morris Scientific) at a density of $1x10^4$ cells per well with 5% fetal calf serum. Readings were taken on the Xcelligence machine every 15 seconds for the first 5 hours to measure adhesion followed by every 15 minutes for the next 43 hours. Analysis of adhesion encompassed 0-5 hours' time points. Analysis of proliferation encompassed 12-48 hour time points. For migration assays, 10% fetal calf serum was added in the lower well of migration assay plates as a chemoattractant (E-plates; John Morris Scientific) and cells were seeded in the upper well at a density of $2x10^4$ with 1% fetal calf serum. Readings were taken every 15 minutes for 48 hours. Analysis encompassed 5-48 hours. All treatments were performed in quadruplicate to a total of three biological replicates. All data are expressed as rates of change. Statistical analysis has been performed using Graphpad Prism V7.

Transepithelial Electrical Resistance (TEER) Assays – NT2/D1 cells were seeded at a density of $1x10^5$ onto polyester bicameral chambers (12mm, 0.3µm pore; Sigma) 24 hours post transfection. Cells were allowed to attach overnight in 10% fetal calf serum before being washed with PBS and media replaced with 0.5% fetal calf serum. Cells were then incubated for a further 6 hours. Cells were then equilibrated on a warming plate set to 37 degrees within the culture hood for 30 minutes before TEER measurement. Following readings at 48 hours post transfection, cells were fixed for 7 minutes in 4% PFA for immunofluorescent analysis. These experiments were repeated at least 3 times. Results are reported as $\Omega.cm^2$.

Immunofluorescence, NT2/D1 cells – Membranes from TEER assays were carefully cut from inserts and placed, cells facing upwards in cell culture plate with wells just larger than the

membrane. Or, cells were cultured on a UV sterilized coverslip within a 6 well plate. Both membranes and coverslips were fixed in 4% PFA for 7 minutes before being washed in PBS. After washing with PBS, were blocked with 5% Donkey Serum in 1× PBS with 0.1% Tween 20 for 1 hour. The block was removed and replaced with primary antibodies (Phospo-Histone H3 1:300) and incubated for 2 hours at 37 degrees. Primary was washed off with 1× PBS with 0.1% Tween 20 and the membranes were incubated with the fluorescent-conjugated secondary antibody, (donkey anti-rabbit Alexa Fluor 594 1:1000) for 1 hour at room temperature. Sections were washed in 1× PBS with 0.1% Tween 20, counterstained using DAPI, and then washed in 1× PBS and mounted using Dako Fluorescent Mounting Medium. Sections were imaged using fluorescence microscopy (Olympus Corp).

Nedd9 knockout mice- *Nedd9* knockout embryos were generated by A. Nikonova from the Golemis lab at the Fox Chase Cancer Centre in Philadelphia. After euthanasia by decapitation, embryos were fixed in 4% PFA, washed 3x with 1x PBS before being moved into 30% sucrose via a gradient. Embryos were shipped at room temperature for analysis by A. Symon. After dissection gonads were embedded in optimal cutting temperature (OCT) medium and snap frozen. Gonads were sectioned at a thickness of 8μm and mounted on slides by the Monash Histology Platform.

Amh-Cre Sox9$^{flox/flox}$ mice- Experiments on mice were carried out in strict adherence with the recommendations in the Australian code of practice for the care and use of animals for scientific purposes from the National Health and Medical Research Council. All procedures involving mice were approved by the MMCB animal ethics committee, Monash Medical Centre, Australia. Embryos from timed matings were firstly anaesthetised in ice-cold PBS before being euthanised by decapitation. Embryos were then fixed in overnight in 4% PFA at 4°C, then washed in 1x PBS. Embryos were then processed and embedded into paraffin by the Monash University Histology Platform. Sections were cut at 5μm and mounted onto slides

Immunofluorescence, gonads- Paraffin slides were baked at 60°C (30 minutes), deparaffinized in xylene, hydrated in 100% ethanol, and distilled in H$_2$O and PBS. OCT slides were thawed briefly at room temperature, then washed in 1x PBS. Antigen retrieval was performed by submerging slides in Antigen Citrate-based unmasking solution in the chamber of a pressure cooker and cooking for 2 minutes on high pressure. After 20 minutes the cooker was turned off and allowed to cool for 1 hour. Slides were then washed in 1x PBS. Sections were then blocked for 30 minutes with either 5% normal donkey serum or using MOM blocking solution (prepared according to the manufacturer's instructions) where primary antibodies were raised in the mouse and incubated overnight at 4°C with the following primary antibodies: anti-Amh 1:200, anti-Phospo-Histone H3 1:300, anti-Sox9 1:200, and anti-Nedd9 1:100 (for

details see Appendix 1). Sections were then washed three times in 1x PBS with 0.1% Tween 20 and incubated with the fluorescent-conjugated secondary antibodies (all at 1:1000), donkey anti-goat, donkey anti-rabbit, donkey anti-mouse Alexa Fluor 594, donkey anti-rabbit Alexa Fluor 488 (for details see Appendix 1), for 30 minutes at room temperature. Sections were washed in 1x PBS with 0.1% Tween 20, then incubated in 0.1% Sudan Black in 70% EtOH for 5 minutes to quench background autofluorescence. Sections were washed again 1x PBS with 0.1% Tween 20, counterstained using DAPI, and then washed again in 1x PBS then mounted using Dako Fluorescent Mounting Medium. Sections were imaged using fluorescence microscopy (Olympus Corp).

4.3 Results

Effect of *SOX9* on *NEDD9* expression in mouse Sertoli cells and NT2/D1 cells

Nedd9 is downregulated 1.6-fold in mouse testes where SOX9 has been ablated in an intact Sertoli cell environment (Amh-*Cre; Sox9*$^{flox/flox}$ mice) (Rahmoun et al., 2017). At embryonic day 15.5 (E15.5), Nedd9 protein is reduced in these testes too, reinforcing the biological relevance of this transcriptional response (**Figure 4.1 a**). While some residual expression remains, immunofluorescence intensity is decreased across the entire gonad, not just the Sertoli cells as was expected. In order to validate the *in vivo* findings NT2/D1 cells transfected with *SOX9* over expression plasmid were analysed to. QRT-PCR showed that in response to an increase in *SOX9, NEDD9* expression was significantly increased by 4.3-fold (**Figure 4.1 b**, left and right panel respectively), similar to in the tetracycline-induced *SOX9* over expression model developed by (Rahmoun et al., 2017). This transcriptional response was preserved in the *SOX9* knockdown cells, where *NEDD9* expression was decreased by 46% (**Figure 4.1 c**, left and right panel respectively). Together, these results show that Sertoli cell expression of *NEDD9* RNA and protein follows the expression of *SOX9,* as do characterised direct SOX9 target genes, and thus is a promising candidate for further investigation (Alankarage et al., 2016; Rahmoun et al., 2017).
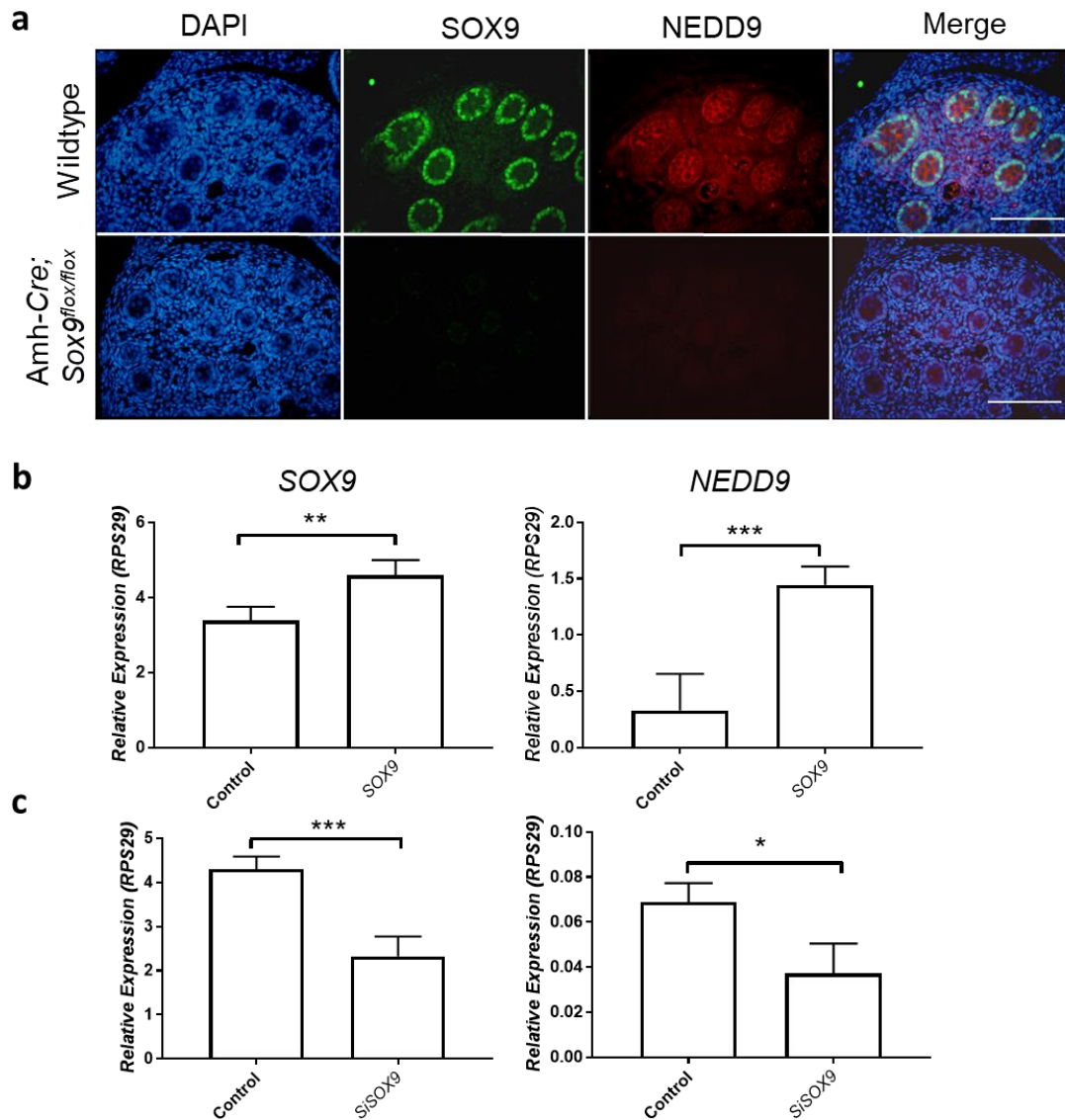
Figure 4.1. Manipulation of SOX9 expression in vitro and in vivo alters NEDD9 expression. (a) Immunofluorescence on E15.5 mouse testes with *Sox9* ablated Sertoli cells (Amh-*Cre; Sox9flox/flox*) and litter mate wildtype control (*Sox9flox/flox*). Sox9 staining is in green, Nedd9 staining is in red. Nuclei are stained blue with DAPI. Scale bars represent 250µm. **(b)** Left; Histogram of *SOX9* gene expression data from qRT-PCR in NT2/D1 cells over expressing SOX9 (*SOX9*) and Right; *NEDD9* gene expression from the same cells. **(c)** Left; Histogram of *SOX9* gene expression data from qRT-PCR in NT2/D1 cells with *SOX9* knocked down (*SiSOX9*) and Right; *NEDD9* gene expression from the same cells. Values were determined from at least 3 individual tests. Means are graphed with error bars representing standard deviation. P-values were calculated using a one-sided Student's T-test where the asterisks indicates significance: *<0.05, **<0.01, ***<0.001 **(e)**.

Analysis of SOX9 ChIP on the *NEDD9* promoter in NT2/D1 cells

SOX9 ChIP of embryonic bovine testes detected SOX9 bound to a 1.6kb region, covering the transcription start site of *NEDD9* and approximately 1.2kb upstream (**Figure 4.2 a** Bovine Sox9 ChIP peak) (Rahmoun et al., 2017). Sequence conservation in this region is high when mapped to the human genome (hg19) and the same features are evident (**Figure 4.2 a**, blue/red conservation track). Transcription factor binding sites can be predicted using a program called JASPAR which uses position frequency matrices to analyse DNA sequence (Mathelier et al., 2014). With high (0.8, or 80% similarity) stringency, JAPSPAR identified 6 possible SOX9 binding sites within this region (**Table 4.1** and depicted as A-F in pink in **Figure 4.2 a**). SOX9 has a signature of binding in the testis, where GATA4 and DMRT1 binding sites are also detected within 50 base pairs (Rahmoun et al., 2017). As JASPAR does not contain the DMRT1 motif, the motif was searched manually. Due to the high sequence similarity between DMRT1 and DMRT3 motif it will be referred to as DMRT sites (Murphy, Zarkower, & Bardwell, 2007). JASPAR analysis detected co-occurring GATA4 and DMRT sites within 50bp of SOX9 binding sites 1, 2, 4 and 6, while site 5 co-occurred with only a DMRT site. As these signature sites occur within a 1kb fragment encompassing the transcription start site at the proximal 5' promoter of *NEDD9*, the ChIP analysis was focussed here (**Figure 4.2 a**, NT2/D1 SOX9 ChIP analysis). Primer pairs tiling this region detected 4 fragments (primer pairs 2 and 3, 6, 9, 19) bound by SOX9 (**Figure 4.2 b**, blue bars). The blue circles on the schematic in **Figure 4.2 a** detail where these fragments align to relative to *NEDD9* and the Bovine Sox9 ChIP peak. Three of these regions align with predicted SOX9 binding sites (primer pairs 2 and 3, 6, 19). Further supporting this, DNAse hypersensitivity assay of human fetal testis and fetal ovary from the Roadmap Epigenomics Consortium shows that the chromatin from the human fetal testis is more open at this region and thus more likely to be actively regulated (**Figure 4.2 a**, green) (Roadmap Epigenomics et al., 2015). Together, these results demonstrate that it is highly likely that SOX9 binds to the proximal promoter of *NEDD9* to regulate transcription in a human Sertoli cell environment.

Table 4.1. SOX9 binding sites in *NEDD9* promoter detected by JASPAR.

	Relative Score (JASPAR)	Start	End	Genomic Location	Sequence
A	0.879893	1251	1259	Chr6:11233317-11233325	CTTTTGTTC
B	0.852654	751	759	Chr6:11232817-11232825	CCATTGAGT
C	0.852601	7	15	Chr6:11232073-11232081	TCATTGTGC
D	0.820211	890	898	Chr6:11232956-11232964	CCATTGGCT
E	0.813844	1677	1685	Chr6:11233743-11233751	GCAGTGTTC
F	0.812298	1379	1387	Chr6:11233445-11233453	TTTTTGTTC

Start and end sites are given relative to the input DNA (from bovine Sox9 ChIP peak aligned to hg19), which has been translated to a genomic location given in the human
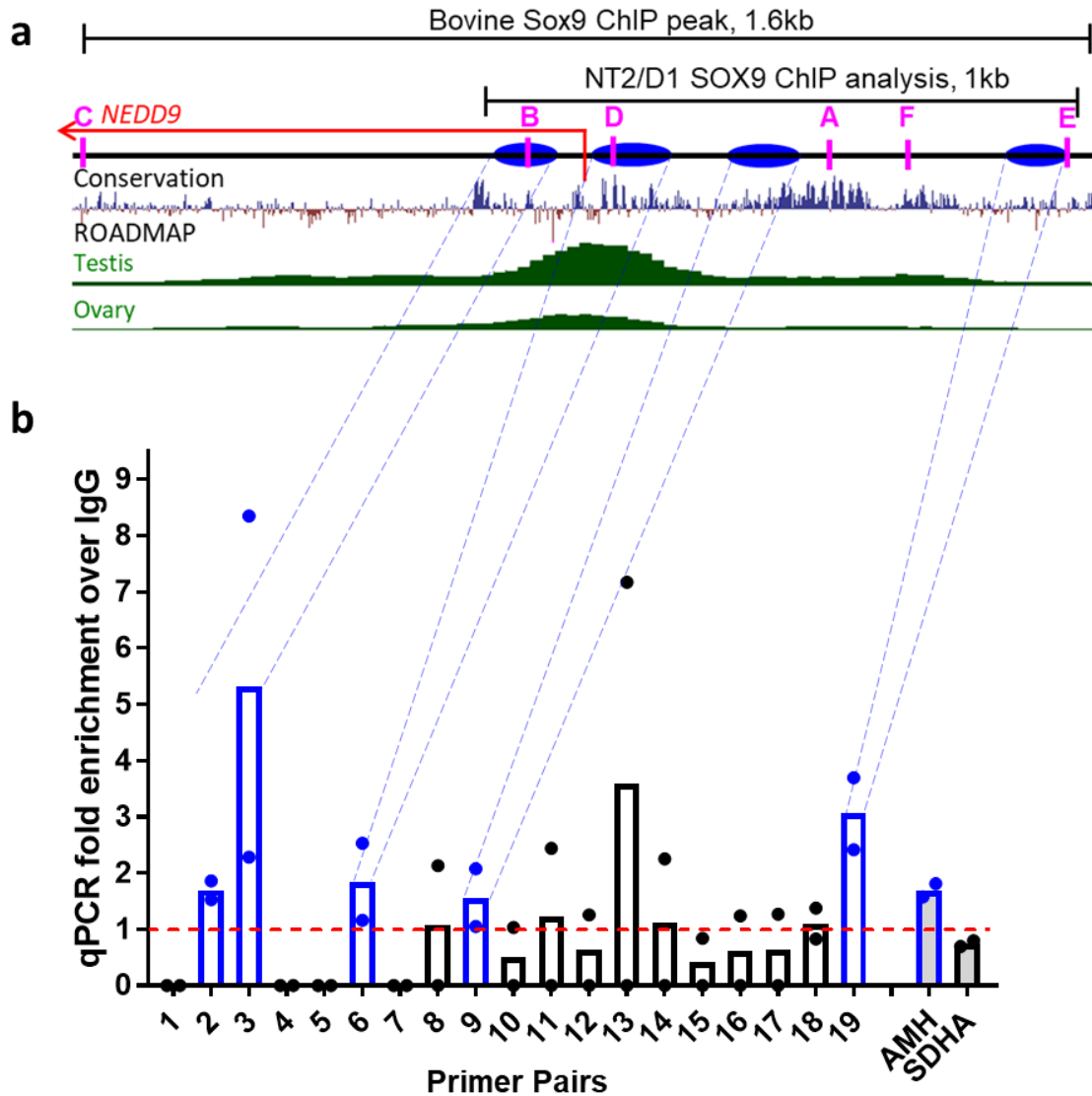
Figure 4.2. SOX9 binds the proximal promoter of *NEDD9*. (a) A schematic showing key regulatory features of the human genome where the 1.6kb bovine SOX9 ChIP peak maps to (chr6:11232066-11233752). Red arrow demonstrates transcription start site and direction of transcription. Conservation from UCSC genome browser is indicated by blue showing high conservation and red showing low conservation where the higher/lower the bar is the more conserved the region between 100 vertebrates. DNAse hypersensitivity assay from the ROADMAP Epigenomics consortium depicts open chromatin in the human fetal testis and fetal ovary where the higher the peak, the more open the region is. Letters A-F in pink mark the location of predicted SOX9 binding sites (see Table 1 for further detail). Blue ovals on the black DNA mark the location of the 4 regions detected as bound by SOX9 in NT2/D1 cells. **(b)** Fold enrichment of each of the tiling primer pairs for SOX9 vs IgG. Regions are considered likely bound (blue bars) when both replicates have an enrichment over 1 (red dotted line). AMH is shown as a well characterised positive control, and SDHA as a negative (Alankarage et al., 2016; Arango et al., 1999). N=2.

As ChIP experiments demonstrated that SOX9 binds to the human *NEDD9* promoter, luciferase assays were performed to test if SOX9 could activate the promoter in COS7 cells. Transfection of the reporter construct with SOX9 expression vector alone showed a modest but significant increase in luciferase activity when compared to the empty luciferase construct (**Figure 4.3**). Addition of other co-factors of SOX9; SF1, DMRT1 and GATA4, did not result in any further increase in luciferase activity suggesting that they do not cooperate at the *NEDD9* promoter. Addition of SF1 and DMRT1 alone did not induce any luciferase activity, and GATA4 alone showed activity significantly less than the empty vector. Of note, addition of all three Sertoli Cell Signature factors (SOX9, GATA4 and DMRT1) did not result in any significant activation of reporter construct. These results demonstrate that SOX9 is able to activate the *NEDD9* proximal promoter, likely in the absence of cofactors SF1, GATA4 and DMRT1.
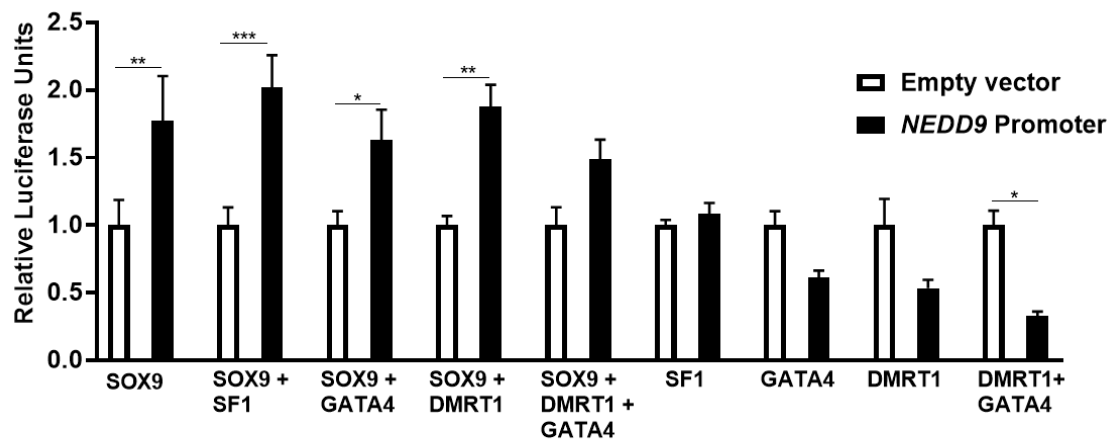
Figure 4.3. SOX9 activates the *NEDD9* promoter. Promoter activity of human *NEDD9* proximal promoter measured by luciferase assays in COS7 cells when transfected with combinations of SOX9, SF1, GATA4 and DMRT1 as detailed on the X axis. This activity is not significantly increased with the addition of SF1 or the Sertoli Cell Signature factors, GATA4 and DMRT1 (n=4). White bars represent empty vector control and black represents the *NEDD9* promoter. Error bars represent SEM. P values were calculated using 2way ANOVA where the asterisk indicates significance: *<0.05, **<0.01, ***<0.001.

Effect of *NEDD9* knockdown in NT2/D1 cells

To investigate the function of NEDD9 in human Sertoli cells, firstly *NEDD9* siRNA transfection on Sertoli cells was tested to show that expression could be reduced in NT2/D1 cells. Using siRNA treatment, *NEDD9* was reduced by 2.3-fold (P<0.01) (**Figure 4.4 a**, left). This reduction of transcripts correlated with loss of NEDD9 protein (**Figure 4.4 a,** middle and right). Some clusters of cells also changed morphology 48 hours after transfection to a more spherical shape, indicative of a cytoskeletal disruption (**Figure 4.4 b**) (Ribeiro, Reece, & Putney, 1997). This morphological change was particularly prevalent at the periphery of colonies. By observational analysis, these images also demonstrate a possible reduction in proliferation rate as the control cells are overgrowing whereas the siRNA treated cells are yet to reach confluency. Importantly, the decrease in NEDD9 did not lead to any change in SOX9 levels, so the NT2/D1 cell model could be used to elucidate the cellular consequence of *NEDD9* loss without any compounding effects from SOX9 loss (**Figure 4.4 c**).
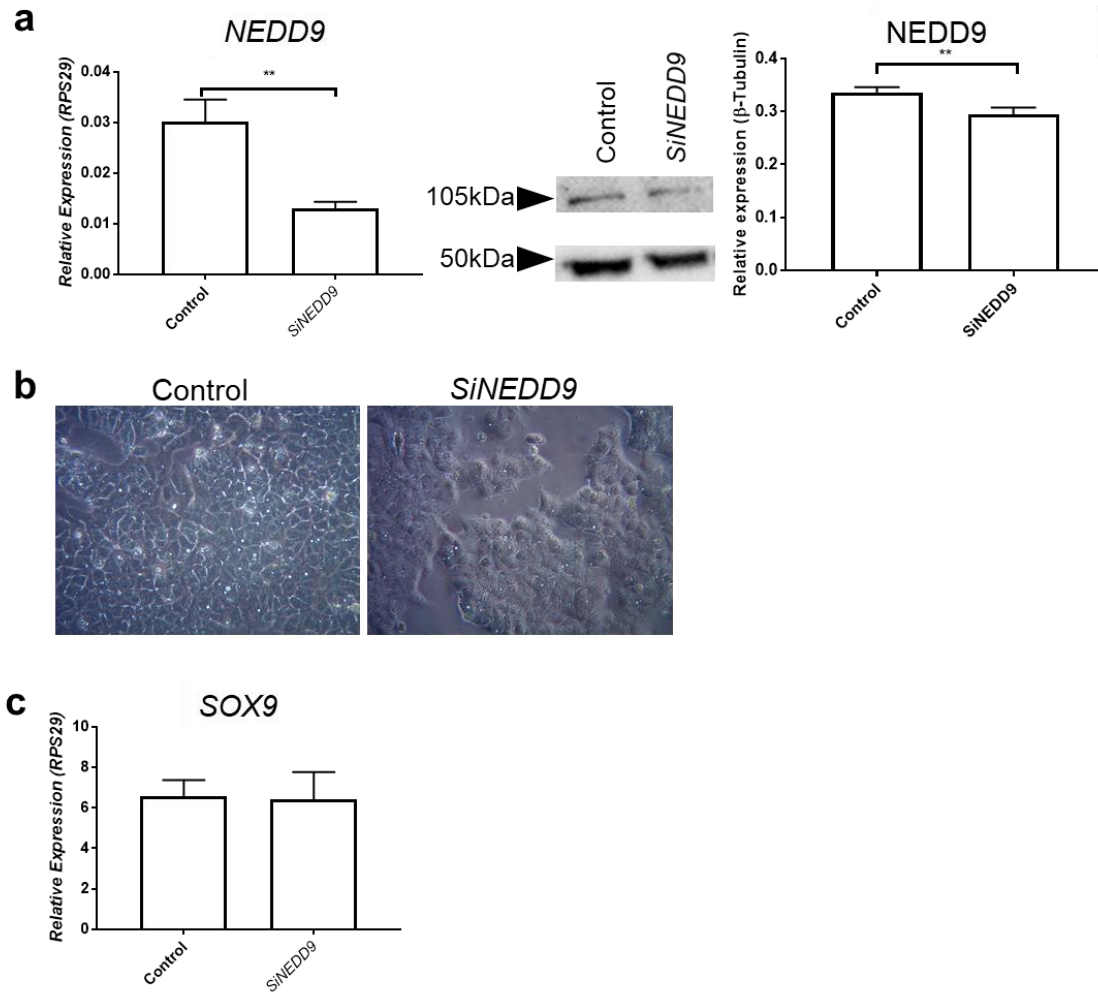
Figure 4.4. *NEDD9* knockdown in NT2/D1 cells. (a) Left; Histogram of *NEDD9* gene expression data from qRT-PCR in NT2/D1 cells with *NEDD9* knocked down (*SiNEDD9*) Middle; Western blot analysis using cytoplasmic extracts of NEDD9 protein levels (105kDa). β-Tubulin was used as a loading control (50kDa) (representative of n=3). Right; Histogram of Western blot results **(b)** Light microscopy of Control and *NEDD9* knockdown NT2/D1 cells 48 hours post transfection. **(c)** Histogram of *SOX9* gene expression data from qRT-PCR in NT2/D1 cells with *NEDD9* knocked down (*SiNEDD9*). Means are graphed with error bars representing standard deviation. P-values were calculated using a one-sided Student's T-test where the asterisk indicates significance: **<0.01.

Analysis of *NEDD9* regulation of Sertoli cell functions in NT2/D1 cells

A defining event during the differentiation of the testis is the formation of testis cords. The cords compartmentalise the testis and protect the germ cells from entering meiosis, and eventually create the environment crucial for sperm production (Svingen & Koopman, 2013). Sertoli cells are the regulatory hub for testis cord formation, driven by the expression of *SOX9* (Svingen & Koopman, 2013). To form cords, Sertoli cells must migrate to aggregate around germ cells where they adhere to each other (Mruk & Cheng, 2004; Nel-Themaat et al., 2011). Following this, the Sertoli cells establish polarity and proliferate to elongate the cords(Nel-Themaat et al., 2011; Sharpe, McKinnell, Kivlin, & Fisher, 2003). Given that NEDD9 has been implicated in all these functions, they were each assayed in NT2/D1 cells with *NEDD9* knocked down (Aquino et al., 2009; Izumchenko et al., 2009; Miao et al., 2013; Singh et al., 2007).

To investigate the role which *NEDD9* may play in human Sertoli cell function, Xcelligence assays were performed on *NEDD9* knockdown and control NT2/D1 cells. To test *NEDD9* involvement in adhesion, electrical impedance was measured for 5 hours immediately after seeding. Cells with reduced *NEDD9* expression showed no change in adhesion rate (**Figure 4.5 a**). Following this initial 5-hour adhesion period, proliferation of cells was measured in the same assay for a further 43 hours. The rate of proliferation was significantly reduced in *NEDD9* knockdown cells when compared to control (P<0.01) (**Figure 4.5 b,** left). Immunofluorescence to detect phospho-Histone H3 (PH3), a marker of proliferating cells confirmed that the proliferative capability of these cells was reduced (**Figure 4.5 b,** right).

Xcelligence assays were also used to investigate the contribution, if any, of *NEDD9* to Sertoli cell migration. In this assay, electrical impedance is measured as cells move across an electrode to an area with chemical attractant. There was no change in rate of migration when *NEDD9* expression was reduced in NT2/D1 cells (**Figure 4.5 c**).

To test if NEDD9 controls the establishment of polarity in NT2/D1 cells, transepithelial resistance assays were used. This assay measures the permeability of a monolayer of cells, which relates to the integrity of intercellular junctions (Pattabiraman, Epstein, & Rao, 2013; Srinivasan et al., 2015). To measure the contribution of NEDD9 to Sertoli cell polarity formation, *NEDD9* knockdown and control cells were seeded in 12mm well inserts and assayed after 24 hours. *NEDD9* knockdown cells showed in significantly reduced transepithelial resistance compared to control cells (p<0.0001), indicating a role for NEDD9 in the establishment of polarity in NT2/D1 cells (**Figure 4.5 d**).
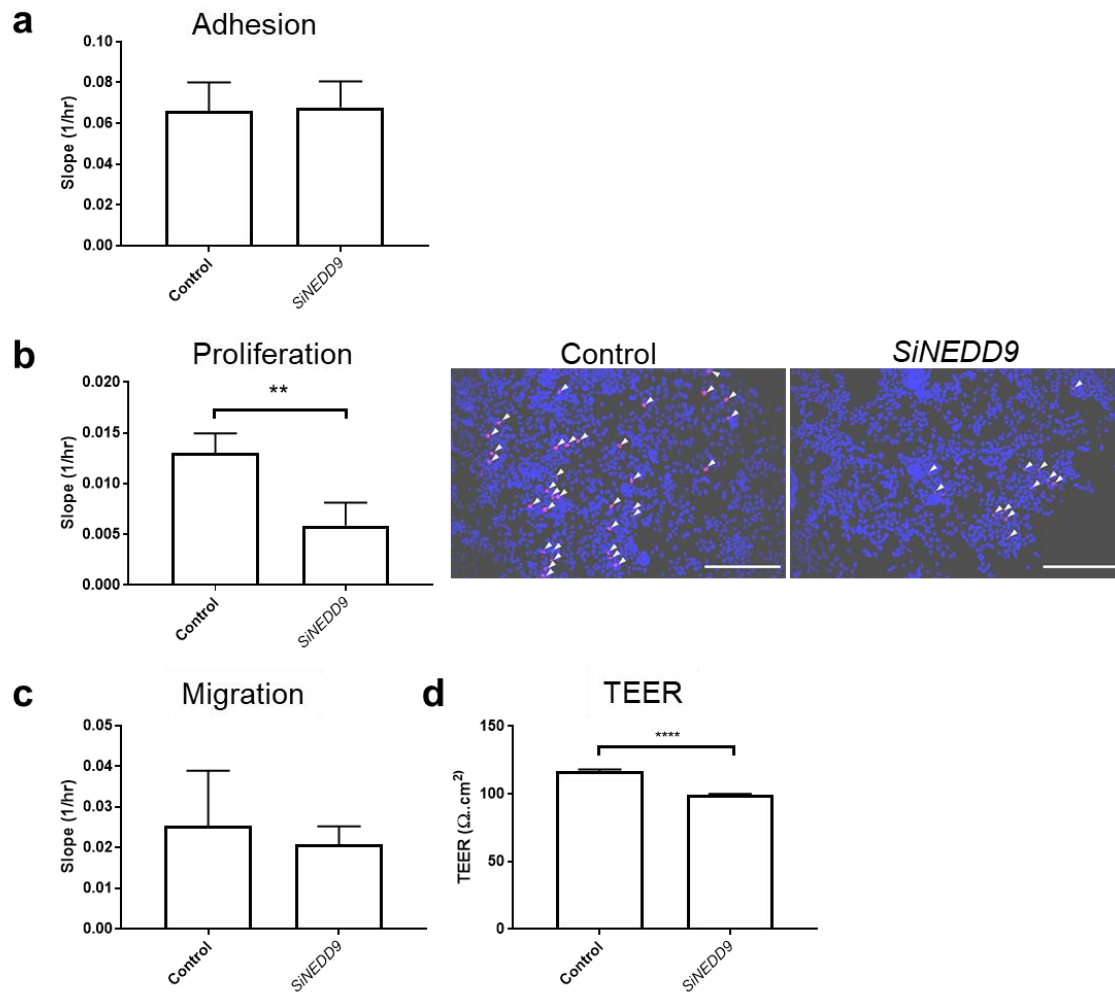
Figure 4.5. NEDD9 regulates proliferation and polarity, but not adhesion or migration in NT2/D1 cells. (a) Histogram showing rate of adhesion in control and *NEDD9* knockdown in NT2/D1 cells (*SiNEDD9*) measured by Xcelligence assay **(b)** Left; Histogram showing rate of proliferation in control and *NEDD9* knockdown in NT2/D1 cells (*SiNEDD9*) measured by Xcelligence assay. Middle; immunofluorescence for the proliferative marker, Phospho-Histone H3 (red staining and white arrows) and nuclei are stained blue with DAPI, on control NT2/D1 cells and Right; *NEDD9* knockdown NT2/D1 cells (*SiNEDD9*). Scale bars represent 2000µm **(c)** Histogram showing rate of migration in control and *NEDD9* knockdown in NT2/D1 cells (*SiNEDD9*) measured by Xcelligence assay **(d)** Histogram showing transepithelial resistance in control and *NEDD9* knockdown (*SiNEDD9*) NT2/D1 cells 24 hours post seeding measured in Ω.cm². All values were determined from at least 3 individual tests. Means are graphed with error bars representing standard deviation. P-values were calculated using a one-sided Student's T-test where the asterisk indicates significance: **<0.01, ****<0.0001.

Analysis of proliferation in embryonic *Nedd9* knockout testes

Given that *NEDD9* affected proliferation rate of NT2/D1 cells, the proliferative ability of Sertoli cells in developing mice testes was also assayed. Gonads from E13.5 mouse embryos with *Nedd9* completely ablated were dissected and morphologically analysed before being embedded and sectioned for analysis for immunofluorescence. Homozygous knockout *Nedd9* mice on a C57BL/6 background were reported to be fertile and viable, however it is worth noting that fertility can tolerate a significant decrease in testis weight and sperm count and thus "fertile and viable" should not rule out investigation (Schurmann et al., 2002; Seo et al., 2005). *Nedd9* knockout mice were generated from heterozygote crosses. Forty-seven embryos from 5 litters were analysed with a normal sex ratio. Of these embryos, 8 were *Nedd9* knockout (*Nedd9* KO). 2 of these embryos, from different litters, were XY meaning that only 4 knockout testes could be analysed. **Figure 4.6 a** (left and middle) shows brightfield images of heterozygous litter mate controls next to knockout testes. All 4 of these gonads were smaller than their litter mate heterozygous controls, as demonstrated by the histogram showing longitudinal measurements of the testes at their longest point (**Figure 4.6 a**, right). On average, the *Nedd9* knockout gonads were 15% smaller than the littermate controls. Immunofluorescence for the proliferative marker, PH3 (green) showed that relative to control (**Figure 4.6 b,** top left and right) proliferation was reduced throughout the entire gonad in the *Nedd9* KO, including within testis cords (yellow arrows) (**Figure 4.6 b,** bottom left and right). Anti-Mullerian hormone (red) was used to mark the testis cords. The gonad marked with the white star in **Figure 4.6 a** corresponds to the gonad in **Figure 4.6 b**. AMH staining in this gonad was weak and lacked definition, indicating severe malformation however in the *Nedd9* KO from litter b cord morphology appeared intact.
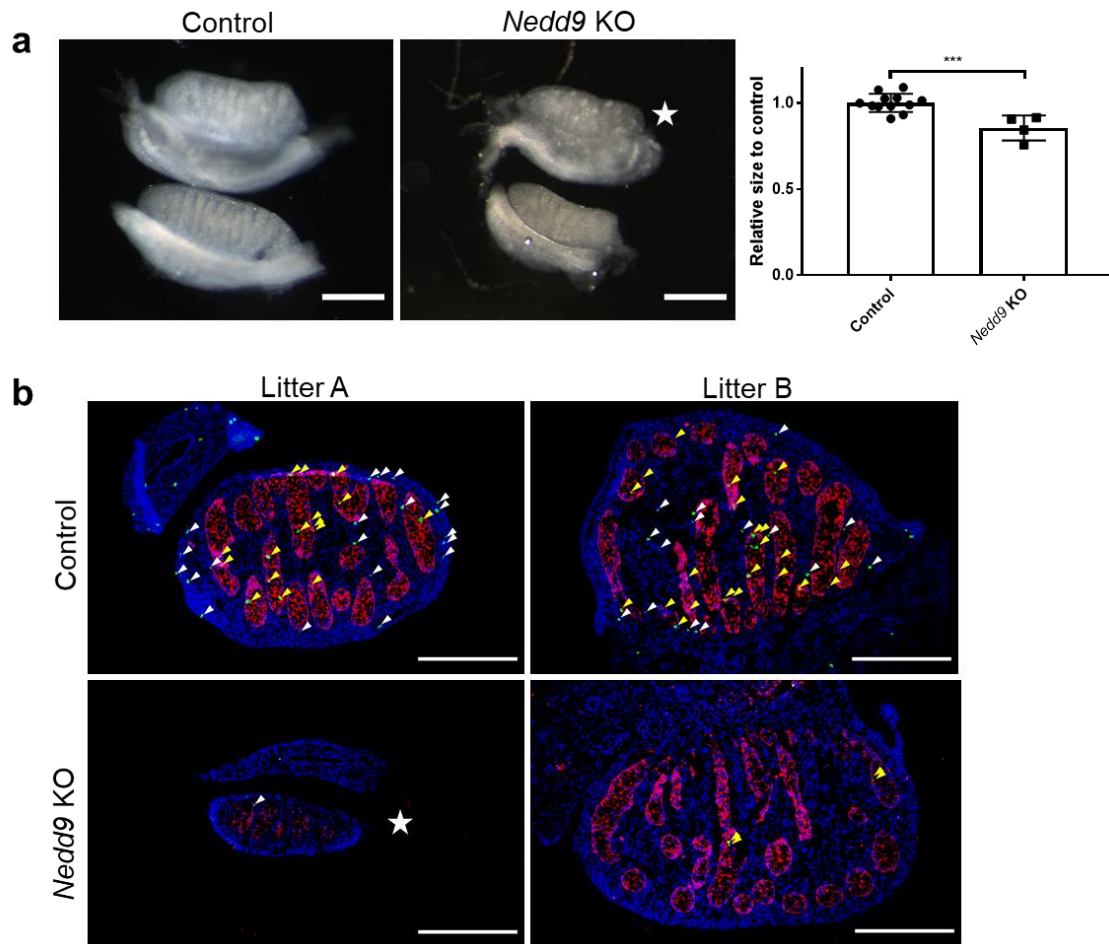
Figure 4.6. Cell proliferation is reduced in E13.5 *Nedd9* knockout gonads. (a) Left and Middle; Brightfield image showing heterozygous littermate control testes next to *NEDD9* knockout testes (*Nedd9* KO) Scale bars represent 100µm. Right; Histogram showing relative longitudinal measurements of the testes. Each data point represents the length of a gonad compared to the average length of littermate heterozygotes control gonads when they were measured from along the longest axis. Means are graphed with error bars representing standard deviation. P-values were calculated using a one-sided Student's T-test where the asterisk indicates significance: ***<0.001. **(b)** Gonads have been stained for the proliferative marker PH3 (green) and the Sertoli cell, testis cord marker AMH (red) in littermate control and *Nedd9* knockout testes (*Nedd9 KO*) from two representative litters, Litter A and Litter B. Nuclei are stained blue with DAPI. Proliferative cells are indicated with arrows. Yellow arrows mark proliferative cells within the testis cords and white arrows mark other proliferative cells of the testis. The star in and indicates the same gonad. Scale bars represent 100µm.

4.4 Discussion

Sertoli cells are central to the development of the testis. Not only do they drive the differentiation of themselves and the other key cell types of the testis, but they aggregate around the germ cells to form the hallmark feature of the male gonad, the testis cords (Svingen & Koopman, 2013). To form the cords the Sertoli cells must migrate and coalesce around the germ cells before they establish polarity (Nel-Themaat et al., 2011). Sertoli cell proliferation, from 24 hours after the cells begin to differentiate and throughout the entirety of embryonic testis development, is rapid compared to the ovary and essential for the testicular fate (Schmahl & Capel, 2003; Schmahl, Eicher, Washburn, & Capel, 2000). SOX9 is a key regulator of Sertoli cell differentiation, and thus the morphogenesis of the testis. Therefore, understanding the genes that SOX9 regulates during this period will improve our understanding of the genes and pathways that SOX9 initialises to form a testis.

Ablation of *Sox9* from an intact Sertoli cell environment in mice results in a 1.6-fold decrease in *Nedd9* expression at E13.5 (Rahmoun et al., 2017). Interestingly, *Nedd9* is still expressed at approximately 2.6-fold higher in the *Sox9* knockout testes than wildtype female levels indicating that in the testis, it is likely that other factors contribute to *Nedd9* regulation. Analysis of the expression profile of *Nedd9* at E13.5 in the developing testis shows that as well as being expressed in Sertoli cells, *Nedd9* is also expressed in endothelial cells and interstitial cells (Jameson et al., 2012). However, at E15.5 immunohistochemistry of Nedd9 in the testis was clearest in the Sertoli cells and Endothelial cells (**Figure 4.1**). At E15.5 it is also interesting to note that in the Sox9 knockout testes, Nedd9 expression appeared to decrease in all cell types of the testis, not just the Sertoli cells, indicating that other regulators of Nedd9 expression in other testicular cell types may also be under the control of Sox9. Similarly, in the NT2/D1 human Sertoli cell model, where knockdown of *SOX9* resulted in a 46% decrease of *NEDD9* but not a complete loss. This could be the result of other factors present which are positively regulating *NEDD9* in a Sertoli cell. Analysis of the ChIP peak detected in bovine revealed that 4 of the 6 binding sites detected co-occurred with the 'Sertoli Cell Signature' cofactors, GATA4 and DMRT, which could be coregulating *NEDD9* expression (Rahmoun et al., 2017). As Rahmoun et al., discovered this signature in both mice and bovine, it is likely conserved in other mammals and thus can be applied to a human model (Rahmoun et al., 2017). However, we could not rule out that this could be the result of an incomplete loss of *SOX9* using *siRNA* knockdown.

Luciferase assays in COS7 cells demonstrated that the addition of SOX9 was able to activate the *NEDD9* promoter. As SOX9 ChIP in NT2/D1 cells detected binding at 4 regions, this regulation is likely direct. Luciferase assays were performed in COS7 cells, a monkey kidney

cell line, because they don't express *SOX9, SRY* or *NR5A1* (SF1) (Sekido & Lovell-Badge, 2008). COS7 cells are also devoid of *GATA4* but do express *DMRT1* meaning that the possibility that SOX9 and DMRT1 are acting on the promoter together cannot be ruled out from these experiments (Wang et al., 2013; K. Yao, Lu, Cheng, & Zhou, 2006). It is worth noting however that addition of all three 'Sertoli Cell Signature' factors does not elicit any promoter activation, meaning it is unlikely that they are acting cooperatively to activate *NEDD9* expression in a Sertoli cell context. These luciferase assays also ruled out the possibility of SF1 cooperating with SOX9, as it has been known to at other testis-specific genes to regulate expression (Arango et al., 1999).

Clinically, NEDD9 is an important oncogenic factor, oft dysregulated in a range of metastases. As such, its regulation is complex and tissue dependent. While the post-translational regulation of NEDD9 has been investigated deeply, its transcriptional regulation is relatively underexplored. However, a range of expression inducing factors have been identified both experimentally and bioinformatically (**Figure 4.7**) (Shagisultanova, Gaponova, Gabbasov, Nicolas, & Golemis, 2015). As detailed in this figure, the *NEDD9* promoter contains many transcription factor binding sites. Of these factors, the most applicable to the testis is PAX5 which encodes a transcription factor found in the testis and regulated by transforming growth factor β, (TGFβ) a critical regulator of testis development and function (Pridans et al., 2008). Furthermore, NEDD9 is a well-characterised modulator of TGFβ signalling indicating the potential for a feedback loop to exist in the testis (Inamoto et al., 2007; Morimoto et al., 2014). By understanding its regulation and role in the developing testis, we are better poised to understand if or how it contributes to DSD. Furthermore, by identifying the proteins it interacts with in the testis, and the signals it relays we may be able to identify other genes mutated in DSD.

Despite its highly dimorphic expression, no testicular role for *NEDD9* had been reported. NEDD9 is an important part of the cytoskeletal network, acting to assemble complexes involved in migration, adhesion, cell cycle control (including proliferation and apoptosis) and polarity (Reviewed in (Shagisultanova et al., 2015)). Each of these biological processes are vital to the proper development of the testis.

Proliferation was significantly decreased in *NEDD9* knockdown NT2/D1 cells. This observation encouraged the deeper analysis of *Nedd9* knockout XY gonads. Morphological analysis revealed that *Nedd9* KO gonads were significantly smaller at E13.5 compared to their litter mates, and proliferation throughout the entire gonad was reduced. It is worth noting that *Nedd9* knockout mice are fertile. As long as, the gonads proliferate sufficiently within the critical window (E10.8-11.2), testes will develop normally, even if they are smaller (Schmahl & Capel,

2003). For example, ablation of the gene encoding follicle stimulating hormone (*Fsh*) and its receptor (*Fshr*) caused over 50% reduction in testis weight, and a reduction in Sertoli cell number yet, mice are still fertile (Abel et al., 2000; Kumar, Wang, Lu, & Matzuk, 1997). But, as the size of the Sertoli cell population in a testis directly correlates to the number of germ and Leydig cells, any reduction in Sertoli cell proliferation is likely to have adverse effects on fertility potential (Rebourcet et al., 2017). Furthermore, a 15% size reduction was also reported in *Gpr37* knockout mice, a candidate *SOX9* target gene (see Chapter 2), accompanied by dysregulated *Dhh* signalling and delayed sperm cell development yet these mice too are still fertile (La Sala et al., 2015). Thus, in future it is important not to discount disrupted testicular development based the ability of male to sire pups.

As the proper function of the gonads is essential to a species survival, it is unsurprising that there are multiple mechanisms regulating proliferation in the developing testis. Here we have shown that in a model of human Sertoli cells, SOX9 regulates the testis-specific expression of *NEDD9* via the proximal promoter. Using a *NEDD9* siRNA, and a mouse model we have demonstrated that loss of *NEDD9* results in decreased proliferation. This only correlated to a 15% decrease testis length, which is still within the functional capacity of the developing testis. Transepithelial resistance assays indicated that *NEDD9* may also regulate the ability of NT2/D1 cells to establish polarity. Future experiments using *Nedd9* knockout mice should further investigate these using markers of polarity in the embryonic testis and of junctional proteins.
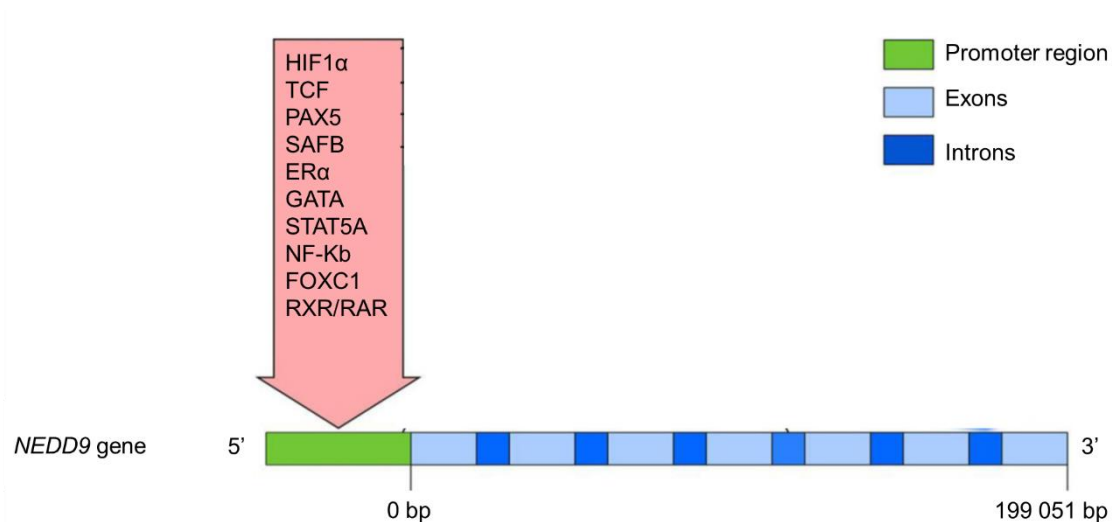
Figure 4.7 Schematic representation of NEDD9 gene and mRNA. Relative sizes are not to scale. Inside the pink arrow are factors inducing transcription of NEDD9. RXR- retinoid X receptor, RAR- retinoic acid receptor. Figure adapted from (Shagisultanova et al., 2015)

Chapter 5:

General Discussion and Conclusions

5.1 Introduction

The transcription factor SOX9 is indispensable to the development and function of the mammalian testis. Loss or mutation to *SOX9* can result in gonadal dysgenesis encompassing a wide spectrum of phenotypes ranging from complete XY sex reversal through to fertility defects. Moreover, ectopic *SOX9* expression in the XX gonads leads to the initiation of the male pathway, despite the male sex determining factor, *SRY* being absent. Thus, SOX9 is both necessary and sufficient for the development of the testis. The discovery of downstream target genes of SOX9 in the testis will improve our understanding of the genes involved orchestrating sex determination and development. As such, SOX9 target genes are also candidate DSD genes. While many datasets detailing expression of gonadal genes at various developmental time-points have now been published, our understanding of how SOX9 regulates the development and function of the mammalian testis remains surprisingly unclear (Beverdam & Koopman, 2006; Cory, Boyer, Pilon, Lussier, & Silversides, 2007; Del Valle et al., 2017; Jameson et al., 2012; Li, Zheng, & Lau, 2014; Nef et al., 2005; Stevant & Nef, 2018). The primary aim of this thesis was to discover novel target genes of SOX9 in the testis.

Datasets analysing the transcriptomes and transcription factor binding in the developing gonad are the first step to functionally characterising any novel genes and their role (if any) in DSD. With Next Generation sequencing, the availability of these datasets is increasing exponentially. Analysis of these datasets can begin to create a concise view of the mechanisms of testicular development by identifying genes and molecular pathways that direct either the testicular or ovarian fate. A major challenge however lies in our ability to elucidate what role these genes have in testis development at both a cellular and a whole-organ level. Particularly when referring to sex determination and development, mice have proven to be an excellent model. However, a significant emerging limitation is the difference in threshold protein function needed to illicit an obvious phenotype between mice and humans. Mice require only 23% of *Sox9* levels relative to wild type for testis development to proceed as normal, whereas in humans this is at least 50% (Gonen, Quinn, O'Neill, Koopman, & Lovell-Badge, 2017). Thus, the generation of a human model of testicular function is necessary to continue investigating the role of candidate genes in gonadal development and DSD.

This thesis describes studies conducted to investigate novel targets of SOX9 in the developing mammalian testis. By combining Sertoli cell-*Sox9* knockout RNAseq with Sox9 ChIPseq data from mice, 37 candidate Sox9 target genes have been identified, and evaluated bioinformatically and with literature for their potential roles in gonadogenesis (Chapter 2). In Chapter 3 a model and analytical approach for investigating Sertoli cell SOX9 function has

been developed using the human NT2/D1 cell line. This model has been used to elucidate the role of a strong candidate SOX9 target gene, *NEDD9,* in the developing testis (Chapter 4).

5.2 SOX9 divides its labour among target genes to regulate multiple pathways in testis development

The combination of RNAseq from *Sox9* knockout mouse testes with mouse Sox9 ChIPseq allowed the identification of 37 target genes with a wide variety of putative functions in Sertoli cells. Four of these genes, *Amh, Dhh, Sox10* and *Sox9* itself are published Sox9 target genes with defined roles in sex determination and development, and their identification validated the approach taken. However, other genes reported to be regulated by Sox9, such as *Gdnf, Etv5* and *Cyp26b1* were not in the 37, highlighting that the stringency adopted in filtering these datasets may be missing important testicular factors including paracrine or other growth factors.

Part of the filtering strategy was the use of a published 'Sertoli cell enriched' microarray screen of key cell populations of the male and female mouse gonads in embryonic development (Jameson et al., 2012). This filter was applied to genes both downregulated in the *Sox9* knockout testes and bound in the Sox9 ChIPseq. Sertoli cells are the central hub of testis development, directing the differentiation of the other cell types of the testis (Svingen & Koopman, 2013). This meant that the genes identified are more likely to be direct targets, as *Sox9* is only present in Sertoli cells. This step excluded 22 genes which reassuringly did not include key regulated sex determining or testis development genes, further validating the rigorous filtering process (Appendix 1). However, this microarray only contains expression data for 12,015 genes, limiting the number of genes with profiles available. Of the 269 differentially regulated genes, 78 genes were excluded from analysis due to not being included in the microarray. None of these 78 genes have known or suspected sex determining functions, supporting this exclusion. Of these 78 genes, 26 (33%) were aligned to predicted genes with no assigned functions. Of the remaining 52 genes, only 8 were identified as being bound in the Sox9 ChIPseq. These included *Trim7, Tuba1c, Kcnn2, Olfml2a, Ppp4r1l-ps, Col27a1, Ptpn5* and *Ssbp4. Col27a1* is already a well-characterised Sox9 target gene during chondrogenesis although no testicular role has been identified (Jenkins, Moss, Pace, & Bridgewater, 2005). Therefore, it cannot be ruled out that among the remaining 52 genes there may be intriguing putative target genes and thus future studies should not rule out this possibility.

Powerful filtering was achieved by combining Mouse and Bovine ChIPseq datasets to improve the signal to noise ratio. By excluding genes only bound in the mouse ChIP, the characterised target *Gdnf* was excluded along with other interesting factors expressed in the testis such as

Nkd2 and *Qsox2* (Barseghyan et al., 2018; Kuo et al., 2017; Meng et al., 2000). Exclusion of genes only bound in the bovine ChIP also excluded the characterised targets *Pgds* and *Gstm6* and excluded numerous interesting testis-expressed genes such as *Lgr5*, *Rcan1* and *Nedd9* (Barseghyan et al., 2018; Beverdam & Koopman, 2006; Beverdam et al., 2009; Nef et al., 2005). Given the differences between mice and human sex determination already highlighted in this thesis, there are clear limitations of analysing completely conserved Sox9 function between mouse and bovine testes. Thus, while the stringency of the filtering process adopted in Chapter 2 has provided a robust list of candidate *Sox9* target genes that may also be mutated in DSD, it is not exhaustive so other targets likely exist. For example, *Nedd9* was chosen for examination in this thesis based on RNAseq data alone (ChIPseq data was unavailable at the commencement of this thesis, and only bovine was confirmatory) By relaxing the ChIPseq filtering process and including genes bound either Sox9 ChIPseq, another 60 genes could be added to the putative target gene list (detailed in Appendix 2).

5.3 NT2/D1 cells, a human Sertoli-like cell line, as a model of Sertoli cell gene function

NT2/D1 cells have been established as a human Sertoli-like cell line, expressing male gonadal supporting cell specific genes and not expressing female gonadal supporting cell genes (Knower et al., 2007). These cells have been used to investigate a variety of processes important for sex development, including the nuclear localisation of SOX9 and the regulation of SOX9 target genes (Alankarage et al., 2016; Argentaro et al., 2003; De Santa Barbara et al., 1998; Knower et al., 2011; L. Ludbrook, Alankarage, Bagheri-Fam, & Harley, 2016; Malki et al., 2005; Moniot et al., 2009). As a human cell line, they provide a human model to help understand cellular function of genes implicated in DSD. By over-expressing *SOX9* with an expression plasmid, or knocking down *SOX9* with siRNA, the action of the transcription factor can be more deeply investigated. Furthermore, we can model XY female DSDs involving *SOX9* mutation/deletion. However, a limitation of the use of the NT2/D1 model to date has been its poor transfection efficiency at around 20-30% (Alankarage et al., 2016; L. Ludbrook et al., 2016; L. M. Ludbrook et al., 2012). Thus, this study provided an important enhancement to the power of the NT2/D1 model by improving the transfection efficiency to over 40%. This improvement meant that without FACS, cells could be confidently transfected without GFP co-transfection and used directly in live cell behaviour assays to probe key Sertoli cell functions like proliferation, migration and establishment of polarity. Further improving this transfection efficiency, possibly by optimising the transfection reagent used, could further exacerbate the change in functions seen and may reveal other cellular behaviours controlled by SOX9.

The analytical approach of combining Xcelligence, transepithelial assays and immunofluorescence to assay *SOX9* function in Sertoli cells provides a novel method to

investigate how genes under the control of *SOX9* regulate key behaviours of Sertoli cells. By comparing changes in cell function between the knock down of *SOX9* candidate target genes and *SOX9* itself in NT2/D1 cells, we can begin to draw conclusions about how SOX9 regulates cell functions via these candidate genes in the developing testis. The use of a human cell culture model circumvents the emerging challenges in using mice exclusively as a model of sex determination and gonadal development. However, as NT2/D1 are a homogenous cell population, SOX9 targets which regulate the differentiation of other cell types, such as *DHH* which acts upon Leydig cells*,* may not show significant functional alterations as these are based largely upon identifying cell-autonomous functions. Thus, it may be important to design a co-culture model with Leydig cells for example, or to collect the secreted NT2/D1 media for analysis, based on putative gene function.

Analysing the function of SOX9 target genes in Sertoli cells relies on the availability and efficiency of siRNAs. Generally, physiological relevance is not reached until a minimum of 50% knockdown in achieved (equivalent to heterozygous loss of function), although subtle phenotypes may be revealed with a less efficient siRNA knockdown. In Chapter 3, 46% loss of *SOX9* revealed that SOX9 is controlling cell proliferation, adhesion and the establishment of polarity but surprisingly, no change in migration rate was identified. By further exacerbating this loss, other functions like migration may be revealed. To overcome the challenge of both siRNA availability and efficiency, and the limitations of *Sox9* mouse hypomorphs research to create an alternative model based on a NT2/D1 cell line that stably expresses *Cas9* was successfully initiated (Appendix 3). This created a population of cells which will utilise CRISPR/Cas9 gene editing to knock down or even completely knockout gene expression. This approach will circumvent the reliance on siRNA availability and allow for the rapid screening of multiple guide RNAs (sgRNA) to achieve the maximum knockdown effect. In the case of *SOX9* reduction, this may even result in XY sex reversal at a cellular level, a phenomenon not yet observed in these cells.

5.4 *NEDD9* in the developing testis

The final experimental chapter of this thesis evaluated *NEDD9* as a SOX9 target gene. *Nedd9* expression had been reported in the embryonic mouse testis, but its function was not known (Nef et al., 2005; Rahmoun et al., 2017). Recently however, both Sox9 and Sox10 were shown to regulate *Nedd9* directly in avian neural crest cells and human melanomas (Liu et al., 2017; Yang et al., 2019). These reports support the Sox9-Nedd9 relationship that was identified in this thesis in fetal testis using large datasets. NT2/D1 cells were utilised as a model of male sex determination to show the direct regulation of *NEDD9* by SOX9 via targeted chromatin immunoprecipitation. Binding was detected in a region that bioinformatic analyses revealed to

contain multiple SOX9 binding sites in support of the *in vivo* mouse and bovine Sox9 ChIPseq data. The assayed region was also activated by SOX9 in *in vitro* luciferase assays, confirming the positive regulation of *NEDD9* by SOX9. To confirm the importance of the SOX9 binding to the promoter, mutation of the identified binding sites in luciferase assay is required.

In mice the loss of *Sox9* from embryonic testes at E13.5 resulted in decreased expression of *Nedd9*, indicating that *Nedd9* is regulated by Sox9 *in vivo.* However, there is residual *Nedd9* expression, which suggests the possibility that Sox9 is not the sole regulator in embryonic Sertoli cells. Evidence suggests that there is a Sertoli cell signature of binding where Dmrt1 and Gata4 co-regulate important testicular factors with Sox9 (Rahmoun et al., 2017). This possibility was explored and while putative binding sites for both transcription factors were identified bioinformatically on the *NEDD9* promoter, these did not show activation by DMRT1 and/or GATA4. Thus, it cannot be discounted that other factors are regulating *Nedd9* expression in the developing testis. Additionally, as *Nedd9* is expressed in other cell types of the testis (endothelial and Leydig cells) it is possible that the incomplete loss is due to retained expression in other cell types of the testis (Jameson et al., 2012).

Functional assays in NT2/D1 cells using siRNA, Xcelligence and transepithelial resistance assays demonstrated that NEDD9 controls proliferation and establishment of cell polarity. This data initiated a collaboration with a group at Fox Chase Cancer Centre in Philadelphia, USA that owns a colony of *Nedd9* knockout mice (Seo et al., 2005) (Izumchenko et al., 2009).This collaboration generated E13.5 *Nedd9* knockout embryos that were analysed as part of this thesis study. Of 47 embryos from heterozygous crosses, only 8 were *Nedd9* knockout embryos of which 2 were XY embryos, meaning that 4 testes were available. Given this skewed ratio of mutants and XY embryos, a longitudinal study of the offspring produced may reveal if the reproductive potential of mice is affected with a loss of *Nedd9*. These XY KO testes showed reduced size and reduced numbers of proliferative cells across the whole gonad, as indicated by PH3 immunostaining, consistent with the findings in NT2/D1 cells. A reduction in testis size can still have functional effect, even when only modest, as a reduction in testis weight is associated to a reduction in sperm count. Furthermore, Sertoli cell number is closely correlated to germ cell number in the mouse testis (Rebourcet et al., 2017). However the robustness of the mouse testis ensures that even with a 30% reduction in testis weight and 60% reduction in sperm count no fertility defects are apparent highlighting the point that murine fertility status may not be a reliable indicator of gonadal phenotypes (Kumar et al., 2001; Schurmann et al., 2002). In contrast, sperm production in the human testis may be more sensitive to a reduction in testis size as even a 20% decrease in testis volume is associated with a loss of fertility (Bujan et al., 1989; Condorelli, Calogero, & La Vignera, 2013; Pasqualotto et al., 2005). This means that *NEDD9* may have a functional role in humans, despite no fertility

defect being detected so far in mice. However, with only 4 testes from 2 animals analysed this can only be considered a preliminary analysis and investigation with markers of polarity, such as laminin, e-cadherin and n-cadherin, is needed to assess the possible loss of Sertoli cell polarity in *Nedd9* knockout testes (Lin, Barske, DeFalco, & Capel, 2017).

5.5 Future Directions

This thesis uncovered a number of putative testicular SOX9 target genes and thus a number of genes potentially involved in DSD. In Chapter 2, 33 genes with no characterised testicular function were identified. These genes have enriched expression in Sertoli cells, are bound by and are positively regulated by Sox9 in mouse testes. Future studies should continue to focus on the role of these genes in the developing testis and if they contribute to Disorders of Sex Development. This thesis outlines a robust method to evaluate candidate target genes whereby their cellular function can be analysed using NT2/D1 cells with a combination of protein assays (immunohistochemistry, western blotting), cell function assays (Xcelligence, Transepitelial Resistance assays) and Chromatin assays (Bioinformatic analysis and ChIP assays). Conclusions from this analytical process can be used to direct an analysis in mice carrying deletions and targeted mutations, allowing for more subtle phenotypes to be detected such as in Chapter 4 where preliminary analysis of *Nedd9* knockout testes suggest a 15% reduction in size.

While many of the genes identified in Chapter 2 code for cytoskeletal components or proteins that interact with the cytoskeleton (similar to *Nedd9*), genes with a wide variety of functions have been identified including transcription factors (*Tox, Mybl1*), signal transduction molecules (*Mapk4, Tyro3*) and even a post-transcriptional gene editing component (*Msi1*) to name a few. As embryonic Sertoli cells have a wide variety of essential functions (**Figure 5.1**) this is not surprising, but it is an important consideration for future experiments. With each type of molecule investigated it will be important to adjust the *in vitro* tests conducted accordingly to ensure that Sertoli cell function is being assayed in the most appropriate way. For example, when researching the transcription factors and signal transduction molecules it will also be important to consider which genes and pathways they are in turn regulating through the use of experiments like ChIP and phosphorylation assays. For the post-transcriptional gene editing component, it will be important to find out what molecules are targeted for editing to consider how this contributes to the essential functions of embryonic Sertoli cells. Furthermore, these tests largely consider cell-autonomous effects. As Sertoli cells are central to the development of the entire testis and differentiation of the other cell types (Svingen and Koopman 2013), future experiments incorporating co-culture with other cell types will be important. It will be

interesting to consider how manipulation of these Sertoli cell genes affects the function of Leydig cells and germ cells for example.

In chondrocytes, SOX9 can act as a transcriptional activator or repressor depending on the partner proteins bound (Lefebvre & Dvir-Ginzberg, 2017; Tan et al., 2018). An interesting question raised by the analysis in Chapter 2 is whether Sox9 can act as a transcriptional repressor in the developing testis too. Pathway analysis of the Sox9 repressed genes suggests that this is not a major testicular role with enriched pathways relating to cardiac function. This does not mean that it is not an important role for Sox9 in the testis however and still warrants an investigation. Analysis of the genes that were repressed by Sox9 revealed that 10 genes were 'enriched' in normal Granulosa cell populations, suggesting that they may have pro-ovarian function, and again may be involved in DSD when mutated.

Chapter 3 of this thesis addressed a key challenge in assessing candidate DSD genes for their cellular function in the development of the testis by developing methods of assaying Sertoli cell function. In Chapter 3, SOX9 was knocked down and changes to Sertoli cell functions were assessed. In Chapter 4, this model was applied to assess the function of a candidate target gene, NEDD9 and was able to successfully predict a function in Sertoli cells in vivo (proliferation). Whilst providing convincing results, the current use of NT2/D1 cells in these assays has its caveats, mainly stemming from the use of siRNA to knockdown the gene of interest. The use of siRNA relies on the ability of the designed nucleotide to hijack the cells RNA interference machinery and post-transcriptionally target mRNA for degradation. Unfortunately, the reduction achieved with siRNA may not be physiologically relevant for enough to elicit a clear cell behavioural change. Furthermore, the RNA interference machinery is mostly found in the cytoplasm meaning that long non-coding RNAs cannot be targeted by this method (Bassett et al., 2014). This warrants the development of a more robust model for knocking down SOX9 in NT2/D1 cells, as outlined in section 5.3. Appendix 3 has begun to address this challenge with the development of a stable Cas9-expressing NT2/D1 cell line which can be used to reliably excise Sox9 from the genome using Clustered Regularly Interspaced Short Palindromic Repeats (CRISPR). Future experiments should continue to develop and validate this approach. CRISPR is not without its caveats however, with the potential for off target deletions now well documented. Therefore, by having both models available, the appropriate direction can be taken given the gene of interest.

Finally, this thesis has identified NEDD9 as a SOX9 target in Sertoli cells and has identified a possible role for NEDD9 in controlling proliferation in the testis. Unfortunately, only a small sample size of mutant mice was able to be collected and analysed. Future experiments involving the use of fresh Nedd9 knockout gonad tissue will be important so that multiple

proliferative markers can be assessed over a wide range of time periods, including at birth, puberty and in adulthood. Furthermore, experiments involving the monitoring of the fertility of these male mice will be interesting. So far, no reproductive defects have been reported but litter sizes and pregnancy efficiency are yet to be reported on in Nedd9 knockout mice. Additionally, NEDD9 should be investigated as a DSD gene in humans. While mouse fertility is very resilient to reductions in testicular size, human fertility and testis function is directly regulated to testicular size (Condorelli et al., 2013).

5.6 Conclusions

This thesis has investigated target genes of SOX9 in the developing testis. Transcriptomic analyses and and cell phenotyping indicated that SOX9 divides its labour (i.e. various Sertoli cell functions) among target genes in the developing testis. Many characteristics of embryonic Sertoli cells required for fertile male development have been identified, and some of these have been linked to SOX9 via target genes (**Figure 5.1**) (Nel-Themaat et al., 2011). Given that *SOX9* is both necessary and sufficient to induce the formation of the testis, and thus embryonic Sertoli cell behaviours, it is likely that as more target genes are discovered and their functions characterised, SOX9 will be connected to all of these behaviours. One such gene, *NEDD9*, has been identified as a testicular target of *SOX9*. *NEDD9* likely controls cell proliferation cell polarity in Sertoli cells. Using a stringent filtering approach 37 candidate genes were identified, some with established functions in the testis, or known to be involved in fertility. Given that production of sperm is critical to the function of the testis and fertile male development; it is unsurprising that SOX9 target genes are involved in the establishment or maintenance of fertility. Therefore, it is plausible to suggest that the key function of SOX9 in the testis is to regulate fertility through Sertoli cell function and maintenance. This regulation covers all functional aspects, from the establishment of the male gonad to the repression of the female genetic pathway and even the post-natal maintenance of an appropriate environment for spermatogenesis (Barrionuevo et al., 2009).

Despite many advances in the sex determination field, including the use of Next Generation sequencing, the diagnostic odyssey for patients with DSD still remains vast. Current estimations of diagnosis rates are near 50% meaning that many patients and families are still left with the unknown (Barseghyan et al., 2018; Eggers et al., 2016). Improved diagnostic ability means improved genetic counselling, better understanding of reproductive options for the family, improved monitoring of associated risks and a cathartic effect (Lee et al., 2016). By investigating target genes of SOX9 in the developing testis, it is highly likely we will be able to improve these diagnostic rates (Barseghyan et al., 2018). It is hoped that by identifying and

characterising these target genes the mechanisms governing human testis development can be better understood to enable easier diagnosis of DSD.

Embryonic Sertoli Cell Behaviours		SOX9 Target Genes
Proliferation		*NEDD9, FGF9, FGFR2*
Polarity establishment		*NEDD9?*
Maintenance of *SOX9* expression		*SOX9, PGDS, PGD2, FGF9, FGFR2*
Differentiation of other testis cell types		*DHH*
Regression of female structures		*AMH*
Maintenance/Protection of stem cells		*ETV5, GDNF, CYP26B1, GSTM6, FGF9*
Repression of female pathway		*FGF9, FGFR2*
Cell adhesion		
Migration		
Mesenchyme to Epithelial transition		
Unknown functions?		*CBLN4, PADI2,* ***Unknown genes***

Fertile Male Development connects to all behaviours.

Figure 5.1. SOX9 directs Sertoli cell behaviours by dividing its labour among target genes. Known SOX9 target genes have many roles in embryonic testis but there are many unknown genes to be characterised. On the left, embryonic Sertoli cell behaviours are listed. These are connected to characterised SOX9 target genes on the right, implicating SOX9 as a contributor to the behaviour. Cell adhesion, migration and Mesenchyme to Epithelial transition are yet to be linked to SOX9 target genes. *NEDD9* has been included as a contributor to proliferation and possible contributor to polarity establishment. Combined, these Sertoli cell behaviours are required for fertile male development. (Arango, Lovell-Badge, & Behringer, 1999; Barrionuevo et al., 2009; Beverdam et al., 2009; Bradford et al., 2009; Kashimada et al., 2011; Lin et al., 2017; Moniot et al., 2009; Nel-Themaat et al., 2011; Sekido & Lovell-Badge, 2013; Tsuji-Hosokawa et al., 2018)

References

References

Abel, M. H., Wootton, A. N., Wilkins, V., Huhtaniemi, I., Knight, P. G., & Charlton, H. M. (2000). The effect of a null mutation in the follicle-stimulating hormone receptor gene on mouse reproduction. Endocrinology, 141(5), 1795-1803. doi:10.1210/endo.141.5.7456

Achermann, J. C., Ito, M., Ito, M., Hindmarsh, P. C., & Jameson, J. L. (1999). A mutation in the gene encoding steroidogenic factor-1 causes XY sex reversal and adrenal failure in humans. Nat Genet, 22(2), 125-126. doi:10.1038/9629

Adam, R. C., Yang, H., Rockowitz, S., Larsen, S. B., Nikolova, M., Oristian, D. S., . . . Fuchs, E. (2015). Pioneer factors govern super-enhancer dynamics in stem cell plasticity and lineage choice. Nature, 521(7552), 366-370. doi:10.1038/nature14289

Alankarage, D., Lavery, R., Svingen, T., Kelly, S., Ludbrook, L., Bagheri-Fam, S., . . . Harley, V. (2016). SOX9 regulates expression of the male fertility gene Ets variant factor 5 (ETV5) during mammalian sex development. Int J Biochem Cell Biol, 79, 41-51. doi:10.1016/j.biocel.2016.08.005

Allali, S., Muller, J. B., Brauner, R., Lourenco, D., Boudjenah, R., Karageorgou, V., . . . Bashamboo, A. (2011). Mutation analysis of NR5A1 encoding steroidogenic factor 1 in 77 patients with 46, XY disorders of sex development (DSD) including hypospadias. PLoS One, 6(10), e24117. doi:10.1371/journal.pone.0024117

Allan, C. M., Garcia, A., Spaliviero, J., Zhang, F. P., Jimenez, M., Huhtaniemi, I., & Handelsman, D. J. (2004). Complete Sertoli cell proliferation induced by follicle-stimulating hormone (FSH) independently of luteinizing hormone activity: evidence from genetic models of isolated FSH action. Endocrinology, 145(4), 1587-1593. doi:10.1210/en.2003-1164

Aquino, J. B., Lallemend, F., Marmigere, F., Adameyko, II, Golemis, E. A., & Ernfors, P. (2009). The retinoic acid inducible Cas-family signaling protein Nedd9 regulates neural crest cell migration by modulating adhesion and actin dynamics. Neuroscience, 162(4), 1106-1119. doi:10.1016/j.neuroscience.2009.05.035

Arango, N. A., Lovell-Badge, R., & Behringer, R. R. (1999). Targeted mutagenesis of the endogenous mouse Mis gene promoter: in vivo definition of genetic pathways of vertebrate sexual development. Cell, 99(4), 409-419.

Argentaro, A., Sim, H., Kelly, S., Preiss, S., Clayton, A., Jans, D. A., & Harley, V. R. (2003). A SOX9 defect of calmodulin-dependent nuclear import in campomelic dysplasia/autosomal sex reversal. J Biol Chem, 278(36), 33839-33847. doi:10.1074/jbc.M302078200

Bagheri-Fam, S., Bird, A. D., Zhao, L., Ryan, J. M., Yong, M., Wilhelm, D., . . . Harley, V. R. (2017). Testis Determination Requires a Specific FGFR2 Isoform to Repress FOXL2. Endocrinology, 158(11), 3832-3843. doi:10.1210/en.2017-00674

Bagheri-Fam, S., Ono, M., Li, L., Zhao, L., Ryan, J., Lai, R., . . . Harley, V. R. (2015). FGFR2 mutation in 46,XY sex reversal with craniosynostosis. Hum Mol Genet, 24(23), 6699-6710. doi:10.1093/hmg/ddv374

Bagheri-Fam, S., Sim, H., Bernard, P., Jayakody, I., Taketo, M. M., Scherer, G., & Harley, V. R. (2008). Loss of Fgfr2 leads to partial XY sex reversal. Dev Biol, 314(1), 71-83. doi:10.1016/j.ydbio.2007.11.010

Barbaric, I., Miller, G., & Dear, T. N. (2007). Appearances can be deceiving: phenotypes of knockout mice. Brief Funct Genomic Proteomic, 6(2), 91-103. doi:10.1093/bfgp/elm008

Baronas, V. A., Yang, R. Y., Morales, L. C., Sipione, S., & Kurata, H. T. (2018). Slc7a5 regulates Kv1.2 channels and modifies functional outcomes of epilepsy-linked channel mutations. Nat Commun, 9(1), 4417. doi:10.1038/s41467-018-06859-x

Barrionuevo, F., Bagheri-Fam, S., Klattig, J., Kist, R., Taketo, M. M., Englert, C., & Scherer, G. (2006). Homozygous inactivation of Sox9 causes complete XY sex reversal in mice. Biol Reprod, 74(1), 195-201. doi:10.1095/biolreprod.105.045930

Barrionuevo, F., Burgos, M., & Jimenez, R. (2011). Origin and function of embryonic Sertoli cells. Biomol Concepts, 2(6), 537-547. doi:10.1515/BMC.2011.044

Barrionuevo, F., Georg, I., Scherthan, H., Lecureuil, C., Guillou, F., Wegner, M., & Scherer, G. (2009). Testis cord differentiation after the sex determination stage is independent of Sox9 but fails in the combined absence of Sox9 and Sox8. Dev Biol, 327(2), 301-312. doi:10.1016/j.ydbio.2008.12.011

Barrionuevo, F., & Scherer, G. (2010). SOX E genes: SOX9 and SOX8 in mammalian testis development. Int J Biochem Cell Biol, 42(3), 433-436. doi:10.1016/j.biocel.2009.07.015

Barrionuevo, F. J., Hurtado, A., Kim, G. J., Real, F. M., Bakkali, M., Kopp, J. L., . . . Jimenez, R. (2016). Sox9 and Sox8 protect the adult testis from male-to-female genetic reprogramming and complete degeneration. Elife, 5. doi:10.7554/eLife.15635

Barseghyan, H., Symon, A., Zadikyan, M., Almalvez, M., Segura, E. E., Eskin, A., . . . Vilain, E. (2018). Identification of novel candidate genes for 46,XY disorders of sex development (DSD) using a C57BL/6J-Y (POS) mouse model. Biol Sex Differ, 9(1), 8. doi:10.1186/s13293-018-0167-9

Barsoum, I. B., Bingham, N. C., Parker, K. L., Jorgensen, J. S., & Yao, H. H. (2009). Activation of the Hedgehog pathway in the mouse fetal ovary leads to ectopic appearance of fetal Leydig cells and female pseudohermaphroditism. Dev Biol, 329(1), 96-103. doi:10.1016/j.ydbio.2009.02.025

Bashamboo, A., Brauner, R., Bignon-Topalovic, J., Lortat-Jacob, S., Karageorgou, V., Lourenco, D., . . . McElreavey, K. (2014). Mutations in the FOG2/ZFPM2 gene are associated with anomalies of human testis determination. Hum Mol Genet, 23(14), 3657-3665. doi:10.1093/hmg/ddu074

Bashamboo, A., & McElreavey, K. (2015). Human sex-determination and disorders of sex-development (DSD). Semin Cell Dev Biol, 45, 77-83. doi:10.1016/j.semcdb.2015.10.030

Bashamboo, A., & McElreavey, K. (2016). Mechanism of Sex Determination in Humans: Insights from Disorders of Sex Development. Sex Dev, 10(5-6), 313-325. doi:10.1159/000452637

Bassett, A. R., Akhtar, A., Barlow, D. P., Bird, A. P., Brockdorff, N., Duboule, D., . . . Ponting, C. P. (2014). Considerations when investigating lncRNA function in vivo. Elife, 3, e03058. doi:10.7554/eLife.03058

Benko, S., Fantes, J. A., Amiel, J., Kleinjan, D. J., Thomas, S., Ramsay, J., . . . Lyonnet, S. (2009). Highly conserved non-coding elements on either side of SOX9 associated with Pierre Robin sequence. Nat Genet, 41(3), 359-364. doi:10.1038/ng.329

Bernard, P., Ryan, J., Sim, H., Czech, D. P., Sinclair, A. H., Koopman, P., & Harley, V. R. (2012). Wnt signaling in ovarian development inhibits Sf1 activation of Sox9 via the Tesco enhancer. Endocrinology, 153(2), 901-912. doi:10.1210/en.2011-1347

Bernard, P., Sim, H., Knower, K., Vilain, E., & Harley, V. (2008). Human SRY inhibits beta-catenin-mediated transcription. Int J Biochem Cell Biol, 40(12), 2889-2900. doi:10.1016/j.biocel.2008.06.006

Bernard, P., Tang, P., Liu, S., Dewing, P., Harley, V. R., & Vilain, E. (2003). Dimerization of SOX9 is required for chondrogenesis, but not for sex determination. Hum Mol Genet, 12(14), 1755-1765.

Berta, P., Hawkins, J. R., Sinclair, A. H., Taylor, A., Griffiths, B. L., Goodfellow, P. N., & Fellous, M. (1990). Genetic evidence equating SRY and the testis-determining factor. Nature, 348(6300), 448-450. doi:10.1038/348448A0

Beverdam, A., & Koopman, P. (2006). Expression profiling of purified mouse gonadal somatic cells during the critical time window of sex determination reveals novel candidate genes for human sexual dysgenesis syndromes. Hum Mol Genet, 15(3), 417-431. doi:10.1093/hmg/ddi463

Beverdam, A., Svingen, T., Bagheri-Fam, S., Bernard, P., McClive, P., Robson, M., . . . Koopman, P. (2009). Sox9-dependent expression of Gstm6 in Sertoli cells during testis development in mice. Reproduction, 137(3), 481-486. doi:10.1530/REP-08-0336

Bi, W., Huang, W., Whitworth, D. J., Deng, J. M., Zhang, Z., Behringer, R. R., & de Crombrugghe, B. (2001). Haploinsufficiency of Sox9 results in defective cartilage primordia and premature skeletal mineralization. Proc Natl Acad Sci U S A, 98(12), 6698-6703. doi:10.1073/pnas.111092198

Biason-Lauber, A., Konrad, D., Meyer, M., DeBeaufort, C., & Schoenle, E. J. (2009). Ovaries and female phenotype in a girl with 46,XY karyotype and mutations in the CBX2 gene. Am J Hum Genet, 84(5), 658-663. doi:10.1016/j.ajhg.2009.03.016

Birk, O. S., Casiano, D. E., Wassif, C. A., Cogliati, T., Zhao, L., Zhao, Y., . . . Westphal, H. (2000). The LIM homeobox gene Lhx9 is essential for mouse gonad formation. Nature, 403(6772), 909-913. doi:10.1038/35002622

Bishop, C. E., Whitworth, D. J., Qin, Y., Agoulnik, A. I., Agoulnik, I. U., Harrison, W. R., . . . Overbeek, P. A. (2000). A transgenic insertion upstream of sox9 is associated with dominant XX sex reversal in the mouse. Nat Genet, 26(4), 490-494. doi:10.1038/82652

Bitgood, M. J., Shen, L., & McMahon, A. P. (1996). Sertoli cell signaling by Desert hedgehog regulates the male germline. Curr Biol, 6(3), 298-304. doi:10.1016/s0960-9822(02)00480-3

Boettcher, M., & McManus, M. T. (2015). Choosing the Right Tool for the Job: RNAi, TALEN, or CRISPR. Mol Cell, 58(4), 575-585. doi:10.1016/j.molcel.2015.04.028

Bogani, D., Siggers, P., Brixey, R., Warr, N., Beddow, S., Edwards, J., . . . Greenfield, A. (2009). Loss of mitogen-activated protein kinase kinase kinase 4 (MAP3K4) reveals a requirement for MAPK signalling in mouse sex determination. PLoS Biol, 7(9), e1000196. doi:10.1371/journal.pbio.1000196

Bolcun-Filas, E., Bannister, L. A., Barash, A., Schimenti, K. J., Hartford, S. A., Eppig, J. J., . . . Schimenti, J. C. (2011). A-MYB (MYBL1) transcription factor is a master regulator of male meiosis. Development, 138(15), 3319-3330. doi:10.1242/dev.067645

Boora, G. K., Kulkarni, A. A., Kanwar, R., Beyerlein, P., Qin, R., Banck, M. S., . . . Beutler, A. S. (2015). Association of the Charcot-Marie-Tooth disease gene ARHGEF10 with paclitaxel

induced peripheral neuropathy in NCCTG N08CA (Alliance). J Neurol Sci, 357(1-2), 35-40. doi:10.1016/j.jns.2015.06.056

Bouma, G. J., Washburn, L. L., Albrecht, K. H., & Eicher, E. M. (2007). Correct dosage of Fog2 and Gata4 transcription factors is critical for fetal testis development in mice. Proc Natl Acad Sci U S A, 104(38), 14994-14999. doi:10.1073/pnas.0701677104

Bowles, J., Feng, C. W., Ineson, J., Miles, K., Spiller, C. M., Harley, V. R., . . . Koopman, P. (2018). Retinoic Acid Antagonizes Testis Development in Mice. Cell Rep, 24(5), 1330-1341. doi:10.1016/j.celrep.2018.06.111

Bowles, J., Feng, C. W., Spiller, C., Davidson, T. L., Jackson, A., & Koopman, P. (2010). FGF9 suppresses meiosis and promotes male germ cell fate in mice. Dev Cell, 19(3), 440-449. doi:10.1016/j.devcel.2010.08.010

Bowles, J., Knight, D., Smith, C., Wilhelm, D., Richman, J., Mamiya, S., . . . Koopman, P. (2006). Retinoid signaling determines germ cell fate in mice. Science, 312(5773), 596-600. doi:10.1126/science.1125691

Bowles, J., Schepers, G., & Koopman, P. (2000). Phylogeny of the SOX family of developmental transcription factors based on sequence and structural indicators. Dev Biol, 227(2), 239-255. doi:10.1006/dbio.2000.9883

Brachs, S., Turqueti-Neves, A., Stein, M., Reimer, D., Brachvogel, B., Bosl, M., . . . Mielenz, D. (2014). Swiprosin-1/EFhd2 limits germinal center responses and humoral type 2 immunity. Eur J Immunol, 44(11), 3206-3219. doi:10.1002/eji.201444479

Bradford, S. T., Hiramatsu, R., Maddugoda, M. P., Bernard, P., Chaboissier, M. C., Sinclair, A., . . . Wilhelm, D. (2009). The cerebellin 4 precursor gene is a direct target of SRY and SOX9 in mice. Biol Reprod, 80(6), 1178-1188. doi:10.1095/biolreprod.108.071480

Bradford, S. T., Wilhelm, D., Bandiera, R., Vidal, V., Schedl, A., & Koopman, P. (2009). A cell-autonomous role for WT1 in regulating Sry in vivo. Hum Mol Genet, 18(18), 3429-3438. doi:10.1093/hmg/ddp283

Brennan, J., & Capel, B. (2004). One tissue, two fates: molecular genetic events that underlie testis versus ovary development. Nat Rev Genet, 5(7), 509-521. doi:10.1038/nrg1381

Brennan, J., Tilmann, C., & Capel, B. (2003). Pdgfr-alpha mediates testis cord organization and fetal Leydig cell development in the XY gonad. Genes Dev, 17(6), 800-810. doi:10.1101/gad.1052503

Britsch, S., Goerich, D. E., Riethmacher, D., Peirano, R. I., Rossner, M., Nave, K. A., . . . Wegner, M. (2001). The transcription factor Sox10 is a key regulator of peripheral glial development. Genes Dev, 15(1), 66-78. doi:10.1101/gad.186601

Bujan, L., Mieusset, R., Mansat, A., Moatti, J. P., Mondinat, C., & Pontonnier, F. (1989). Testicular size in infertile men: relationship to semen characteristics and hormonal blood levels. Br J Urol, 64(6), 632-637. doi:10.1111/j.1464-410x.1989.tb05325.x

Bullejos, M., & Koopman, P. (2001). Spatially dynamic expression of Sry in mouse genital ridges. Dev Dyn, 221(2), 201-205. doi:10.1002/dvdy.1134

Bullejos, M., & Koopman, P. (2005). Delayed Sry and Sox9 expression in developing mouse gonads underlies B6-Y(DOM) sex reversal. Dev Biol, 278(2), 473-481. doi:10.1016/j.ydbio.2004.11.030

Burgoyne, P. S., Buehr, M., & McLaren, A. (1988). XY follicle cells in ovaries of XX----XY female mouse chimaeras. Development, 104(4), 683-688.

Canto, P., Soderlund, D., Reyes, E., & Mendez, J. P. (2004). Mutations in the desert hedgehog (DHH) gene in patients with 46,XY complete pure gonadal dysgenesis. J Clin Endocrinol Metab, 89(9), 4480-4483. doi:10.1210/jc.2004-0863

Capel, B. (2017). Vertebrate sex determination: evolutionary plasticity of a fundamental switch. Nat Rev Genet, 18(11), 675-689. doi:10.1038/nrg.2017.60

Cardarelli, F., Digiacomo, L., Marchini, C., Amici, A., Salomone, F., Fiume, G., . . . Caracciolo, G. (2016). The intracellular trafficking mechanism of Lipofectamine-based transfection reagents and its implication for gene delivery. Sci Rep, 6, 25879. doi:10.1038/srep25879

Carre-Eusebe, D., Imbeaud, S., Harbison, M., New, M. I., Josso, N., & Picard, J. Y. (1992). Variants of the anti-Mullerian hormone gene in a compound heterozygote with the persistent Mullerian duct syndrome and his family. Hum Genet, 90(4), 389-394. doi:10.1007/bf00220465

Cate, R. L., Mattaliano, R. J., Hession, C., Tizard, R., Farber, N. M., Cheung, A., . . . et al. (1986). Isolation of the bovine and human genes for Mullerian inhibiting substance and expression of the human gene in animal cells. Cell, 45(5), 685-698.

Chaboissier, M. C., Kobayashi, A., Vidal, V. I., Lutzkendorf, S., van de Kant, H. J., Wegner, M., . . . Schedl, A. (2004). Functional analysis of Sox8 and Sox9 during sex determination in the mouse. Development, 131(9), 1891-1901. doi:10.1242/dev.01087

Chan, P. Y., Carrera Silva, E. A., De Kouchkovsky, D., Joannas, L. D., Hao, L., Hu, D., . . . Rothlin, C. V. (2016). The TAM family receptor tyrosine kinase TYRO3 is a negative regulator of type 2 immunity. Science, 352(6281), 99-103. doi:10.1126/science.aaf1358

Chao, C. C., Hung, F. C., & Chao, J. J. (2013). Gas7 is required for mesenchymal stem cell-derived bone development. Stem Cells Int, 2013, 137010. doi:10.1155/2013/137010

Chavali, P. L., Stojic, L., Meredith, L. W., Joseph, N., Nahorski, M. S., Sanford, T. J., . . . Gergely, F. (2017). Neurodevelopmental protein Musashi-1 interacts with the Zika genome and promotes viral replication. Science, 357(6346), 83-88. doi:10.1126/science.aam9243

Chen, C., Ouyang, W., Grigura, V., Zhou, Q., Carnes, K., Lim, H., . . . Murphy, K. M. (2005). ERM is required for transcriptional control of the spermatogonial stem cell niche. Nature, 436(7053), 1030-1034. doi:10.1038/nature03894

Chen, M., Wang, X., Wang, Y., Zhang, L., Xu, B., Lv, L., . . . Gao, F. (2014). Wt1 is involved in leydig cell steroid hormone biosynthesis by regulating paracrine factor expression in mice. Biol Reprod, 90(4), 71. doi:10.1095/biolreprod.113.114702

Chen, M., Zhang, L., Cui, X., Lin, X., Li, Y., Wang, Y., . . . Gao, F. (2017). Wt1 directs the lineage specification of sertoli and granulosa cells by repressing Sf1 expression. Development, 144(1), 44-53. doi:10.1242/dev.144105

Cho, S. W., Kwak, S., Woolley, T. E., Lee, M. J., Kim, E. J., Baker, R. E., . . . Jung, H. S. (2011). Interactions between Shh, Sostdc1 and Wnt signaling and a new feedback loop for spatial patterning of the teeth. Development, 138(9), 1807-1816. doi:10.1242/dev.056051

Chuang, P. T., & McMahon, A. P. (1999). Vertebrate Hedgehog signalling modulated by induction of a Hedgehog-binding protein. Nature, 397(6720), 617-621. doi:10.1038/17611

Clark, A. M., Garland, K. K., & Russell, L. D. (2000). Desert hedgehog (Dhh) gene is required in the mouse testis for formation of adult-type Leydig cells and normal development of peritubular cells and seminiferous tubules. Biol Reprod, 63(6), 1825-1838.

Colvin, J. S., Green, R. P., Schmahl, J., Capel, B., & Ornitz, D. M. (2001). Male-to-female sex reversal in mice lacking fibroblast growth factor 9. Cell, 104(6), 875-889.

Combes, A. N., Lesieur, E., Harley, V. R., Sinclair, A. H., Little, M. H., Wilhelm, D., & Koopman, P. (2009). Three-dimensional visualization of testis cord morphogenesis, a novel tubulogenic mechanism in development. Dev Dyn, 238(5), 1033-1041. doi:10.1002/dvdy.21925

Combes, A. N., Wilhelm, D., Davidson, T., Dejana, E., Harley, V., Sinclair, A., & Koopman, P. (2009). Endothelial cell migration directs testis cord formation. Dev Biol, 326(1), 112-120. doi:10.1016/j.ydbio.2008.10.040

Condorelli, R., Calogero, A. E., & La Vignera, S. (2013). Relationship between Testicular Volume and Conventional or Nonconventional Sperm Parameters. Int J Endocrinol, 2013, 145792. doi:10.1155/2013/145792

Cool, J., & Capel, B. (2009). Mixed signals: development of the testis. Semin Reprod Med, 27(1), 5-13. doi:10.1055/s-0028-1108005

Cool, J., DeFalco, T. J., & Capel, B. (2011). Vascular-mesenchymal cross-talk through Vegf and Pdgf drives organ patterning. Proc Natl Acad Sci U S A, 108(1), 167-172. doi:10.1073/pnas.1010299108

Cory, A. T., Boyer, A., Pilon, N., Lussier, J. G., & Silversides, D. W. (2007). Presumptive pre-Sertoli cells express genes involved in cell proliferation and cell signalling during a critical window in early testis differentiation. Mol Reprod Dev, 74(12), 1491-1504. doi:10.1002/mrd.20722

Coveney, D., Cool, J., Oliver, T., & Capel, B. (2008). Four-dimensional analysis of vascularization during primary development of an organ, the gonad. Proc Natl Acad Sci U S A, 105(20), 7212-7217. doi:10.1073/pnas.0707674105

Cox, J. J., Willatt, L., Homfray, T., & Woods, C. G. (2011). A SOX9 duplication and familial 46,XX developmental testicular disorder. N Engl J Med, 364(1), 91-93. doi:10.1056/NEJMc1010311

Croft, B., Ayers, K., Sinclair, A., & Ohnesorg, T. (2016). Review disorders of sex development: The evolving role of genomics in diagnosis and gene discovery. Birth Defects Res C Embryo Today, 108(4), 337-350. doi:10.1002/bdrc.21148

Croft, B., Ohnesorg, T., Hewitt, J., Bowles, J., Quinn, A., Tan, J., . . . Sinclair, A. (2018). Human sex reversal is caused by duplication or deletion of core enhancers upstream of SOX9. Nat Commun, 9(1), 5319. doi:10.1038/s41467-018-07784-9

Cupp, A. S., Tessarollo, L., & Skinner, M. K. (2002). Testis developmental phenotypes in neurotropin receptor trkA and trkC null mutations: role in formation of seminiferous cords and germ cell survival. Biol Reprod, 66(6), 1838-1845.

Cupp, A. S., Uzumcu, M., & Skinner, M. K. (2003). Chemotactic role of neurotropin 3 in the embryonic testis that facilitates male sex determination. Biol Reprod, 68(6), 2033-2037. doi:10.1095/biolreprod.102.012617

Das, D. K., Sanghavi, D., Gawde, H., Idicula-Thomas, S., & Vasudevan, L. (2011). Novel homozygous mutations in Desert hedgehog gene in patients with 46,XY complete gonadal dysgenesis and prediction of its structural and functional implications by computational methods. Eur J Med Genet, 54(6), e529-534. doi:10.1016/j.ejmg.2011.04.010

De Santa Barbara, P., Bonneaud, N., Boizet, B., Desclozeaux, M., Moniot, B., Sudbeck, P., . . . Berta, P. (1998). Direct interaction of SRY-related protein SOX9 and steroidogenic factor 1 regulates transcription of the human anti-Mullerian hormone gene. Mol Cell Biol, 18(11), 6653-6665. doi:10.1128/mcb.18.11.6653

de Santa Barbara, P., Mejean, C., Moniot, B., Malcles, M. H., Berta, P., & Boizet-Bonhoure, B. (2001). Steroidogenic factor-1 contributes to the cyclic-adenosine monophosphate down-regulation of human SRY gene expression. Biol Reprod, 64(3), 775-783.

de Santa Barbara, P., Moniot, B., Poulat, F., & Berta, P. (2000). Expression and subcellular localization of SF-1, SOX9, WT1, and AMH proteins during early human testicular development. Dev Dyn, 217(3), 293-298. doi:10.1002/(SICI)1097-0177(200003)217:3<293::AID-DVDY7>3.0.CO;2-P

DeFalco, T., Takahashi, S., & Capel, B. (2011). Two distinct origins for Leydig cell progenitors in the fetal testis. Dev Biol, 352(1), 14-26. doi:10.1016/j.ydbio.2011.01.011

Del Valle, I., Buonocore, F., Duncan, A. J., Lin, L., Barenco, M., Parnaik, R., . . . Achermann, J. C. (2017). A genomic atlas of human adrenal and gonad development. Wellcome Open Res, 2, 25. doi:10.12688/wellcomeopenres.11253.2

Dickendesher, T. L., Baldwin, K. T., Mironova, Y. A., Koriyama, Y., Raiker, S. J., Askew, K. L., . . . Giger, R. J. (2012). NgR1 and NgR3 are receptors for chondroitin sulfate proteoglycans. Nat Neurosci, 15(5), 703-712. doi:10.1038/nn.3070

Duan, X., Zhang, H. L., Wu, L. L., Liu, M. Y., Pan, M. H., Ou, X. H., & Sun, S. C. (2018). Involvement of LIMK1/2 in actin assembly during mouse embryo development. Cell Cycle, 17(11), 1381-1389. doi:10.1080/15384101.2018.1482138

Eggers, S., Sadedin, S., van den Bergen, J. A., Robevska, G., Ohnesorg, T., Hewitt, J., . . . Sinclair, A. H. (2016). Disorders of sex development: insights from targeted gene sequencing of a large international patient cohort. Genome Biol, 17(1), 243. doi:10.1186/s13059-016-1105-y

ErLin, S., WenJie, W., LiNing, W., BingXin, L., MingDe, L., Yan, S., & RuiFa, H. (2015). Musashi-1 maintains blood-testis barrier structure during spermatogenesis and regulates stress granule formation upon heat stress. Mol Biol Cell, 26(10), 1947-1956. doi:10.1091/mbc.E14-11-1497

Fang, M., Shen, Z., Huang, S., Zhao, L., Chen, S., Mak, T. W., & Wang, X. (2010). The ER UDPase ENTPD5 promotes protein N-glycosylation, the Warburg effect, and proliferation in the PTEN pathway. Cell, 143(5), 711-724. doi:10.1016/j.cell.2010.10.010

Fogel, B. L., Hanson, S. M., & Becker, E. B. (2015). Do mutations in the murine ataxia gene TRPC3 cause cerebellar ataxia in humans? Mov Disord, 30(2), 284-286. doi:10.1002/mds.26096

Foster, J. W., Dominguez-Steglich, M. A., Guioli, S., Kwok, C., Weller, P. A., Stevanovic, M., . . . et al. (1994). Campomelic dysplasia and autosomal sex reversal caused by mutations in an SRY-related gene. Nature, 372(6506), 525-530. doi:10.1038/372525a0

Frasier, S. D., Bashore, R. A., & Mosier, H. D. (1964). Gonadoblastoma Associated with Pure Gonadal Dysgenesis in Monozygous Twins. J Pediatr, 64, 740-745.

Froment, P., Vigier, M., Negre, D., Fontaine, I., Beghelli, J., Cosset, F. L., . . . Durand, P. (2007). Inactivation of the IGF-I receptor gene in primary Sertoli cells highlights the autocrine effects of IGF-I. J Endocrinol, 194(3), 557-568. doi:10.1677/JOE-07-0258

Fujimoto, Y., Tanaka, S. S., Yamaguchi, Y. L., Kobayashi, H., Kuroki, S., Tachibana, M., . . . Nishinakamura, R. (2013). Homeoproteins Six1 and Six4 regulate male sex determination and mouse gonadal development. Dev Cell, 26(4), 416-430. doi:10.1016/j.devcel.2013.06.018

Fujita-Jimbo, E., Yu, Z. L., Li, H., Yamagata, T., Mori, M., Momoi, T., & Momoi, M. Y. (2012). Mutation in Parkinson disease-associated, G-protein-coupled receptor 37 (GPR37/PaelR) is related to autism spectrum disorder. PLoS One, 7(12), e51155. doi:10.1371/journal.pone.0051155

Furuse, M. (2009). Knockout animals and natural mutations as experimental and diagnostic tool for studying tight junction functions in vivo. Biochim Biophys Acta, 1788(4), 813-819. doi:10.1016/j.bbamem.2008.07.017

Gao, F., Maiti, S., Alam, N., Zhang, Z., Deng, J. M., Behringer, R. R., . . . Huff, V. (2006). The Wilms tumor gene, Wt1, is required for Sox9 expression and maintenance of tubular architecture in the developing testis. Proc Natl Acad Sci U S A, 103(32), 11987-11992. doi:10.1073/pnas.0600994103

Garcia-Moreno, S. A., Lin, Y. T., Futtner, C. R., Salamone, I. M., Capel, B., & Maatouk, D. M. (2019). CBX2 is required to stabilize the testis pathway by repressing Wnt signaling. PLoS Genet, 15(5), e1007895. doi:10.1371/journal.pgen.1007895

Garside, V. C., Cullum, R., Alder, O., Lu, D. Y., Vander Werff, R., Bilenky, M., . . . Hoodless, P. A. (2015). SOX9 modulates the expression of key transcription factors required for heart valve development. Development, 142(24), 4340-4350. doi:10.1242/dev.125252

Gasca, S., Canizares, J., De Santa Barbara, P., Mejean, C., Poulat, F., Berta, P., & Boizet-Bonhoure, B. (2002). A nuclear export signal within the high mobility group domain regulates the nucleocytoplasmic translocation of SOX9 during sexual determination. Proc Natl Acad Sci U S A, 99(17), 11199-11204. doi:10.1073/pnas.172383099

Geister, K. A., Lopez-Jimenez, A. J., Houghtaling, S., Ho, T. H., Vanacore, R., & Beier, D. R. (2019). Loss of function of Colgalt1 disrupts collagen post-translational modification and causes musculoskeletal defects. Dis Model Mech, 12(6). doi:10.1242/dmm.037176

Georg, I., Barrionuevo, F., Wiech, T., & Scherer, G. (2012). Sox9 and Sox8 are required for basal lamina integrity of testis cords and for suppression of FOXL2 during embryonic testis development in mice. Biol Reprod, 87(4), 99. doi:10.1095/biolreprod.112.101907

Ghayad, S. E., Vendrell, J. A., Bieche, I., Spyratos, F., Dumontet, C., Treilleux, I., . . . Cohen, P. A. (2009). Identification of TACC1, NOV, and PTTG1 as new candidate genes associated with endocrine therapy resistance in breast cancer. J Mol Endocrinol, 42(2), 87-103. doi:10.1677/JME-08-0076

Gierl, M. S., Gruhn, W. H., von Seggern, A., Maltry, N., & Niehrs, C. (2012). GADD45G functions in male sex determination by promoting p38 signaling and Sry expression. Dev Cell, 23(5), 1032-1042. doi:10.1016/j.devcel.2012.09.014

Ginsburg, M., Snow, M. H., & McLaren, A. (1990). Primordial germ cells in the mouse embryo during gastrulation. Development, 110(2), 521-528.

Gnessi, L., Emidi, A., Jannini, E. A., Carosa, E., Maroder, M., Arizzi, M., . . . Spera, G. (1995). Testicular development involves the spatiotemporal control of PDGFs and PDGF receptors gene expression and action. J Cell Biol, 131(4), 1105-1121.

Gonen, N., Futtner, C. R., Wood, S., Garcia-Moreno, S. A., Salamone, I. M., Samson, S. C., . . . Lovell-Badge, R. (2018). Sex reversal following deletion of a single distal enhancer of Sox9. Science, 360(6396), 1469-1473. doi:10.1126/science.aas9408

Gonen, N., & Lovell-Badge, R. (2019). The regulation of Sox9 expression in the gonad. Curr Top Dev Biol, 134, 223-252. doi:10.1016/bs.ctdb.2019.01.004

Gonen, N., Quinn, A., O'Neill, H. C., Koopman, P., & Lovell-Badge, R. (2017). Correction: Normal Levels of Sox9 Expression in the Developing Mouse Testis Depend on the TES/TESCO Enhancer, but This Does Not Act Alone. PLoS Genet, 13(2), e1006584. doi:10.1371/journal.pgen.1006584

Gordon, C. T., Attanasio, C., Bhatia, S., Benko, S., Ansari, M., Tan, T. Y., . . . Lyonnet, S. (2014). Identification of novel craniofacial regulatory domains located far upstream of SOX9 and disrupted in Pierre Robin sequence. Hum Mutat, 35(8), 1011-1020. doi:10.1002/humu.22606

Gordon, C. T., Tan, T. Y., Benko, S., Fitzpatrick, D., Lyonnet, S., & Farlie, P. G. (2009). Long-range regulation at the SOX9 locus in development and disease. J Med Genet, 46(10), 649-656. doi:10.1136/jmg.2009.068361

Gordon, E. A., Whisenant, T. C., Zeller, M., Kaake, R. M., Gordon, W. M., Krotee, P., . . . Bardwell, L. (2013). Combining docking site and phosphosite predictions to find new substrates: identification of smoothelin-like-2 (SMTNL2) as a c-Jun N-terminal kinase (JNK) substrate. Cell Signal, 25(12), 2518-2529. doi:10.1016/j.cellsig.2013.08.004

Gow, A., Southwood, C. M., Li, J. S., Pariali, M., Riordan, G. P., Brodie, S. E., . . . Lazzarini, R. A. (1999). CNS myelin and sertoli cell tight junction strands are absent in Osp/claudin-11 null mice. Cell, 99(6), 649-659.

Granados, A., Alaniz, V. I., Mohnach, L., Barseghyan, H., Vilain, E., Ostrer, H., . . . Keegan, C. E. (2017). MAP3K1-related gonadal dysgenesis: Six new cases and review of the literature. Am J Med Genet C Semin Med Genet, 175(2), 253-259. doi:10.1002/ajmg.c.31559

Grosjean, F., Batard, P., Jordan, M., & Wurm, F. M. (2002). S-phase synchronized CHO cells show elevated transfection efficiency and expression using CaPi. Cytotechnology, 38(1-3), 57-62. doi:10.1023/A:1021197830091

Gubbay, J., Collignon, J., Koopman, P., Capel, B., Economou, A., Munsterberg, A., . . . Lovell-Badge, R. (1990). A gene mapping to the sex-determining region of the mouse Y chromosome is a member of a novel family of embryonically expressed genes. Nature, 346(6281), 245-250. doi:10.1038/346245a0

Hacker, A., Capel, B., Goodfellow, P., & Lovell-Badge, R. (1995). Expression of Sry, the mouse sex determining gene. Development, 121(6), 1603-1614.

Hadley, M. A., Byers, S. W., Suarez-Quian, C. A., Kleinman, H. K., & Dym, M. (1985). Extracellular matrix regulates Sertoli cell differentiation, testicular cord formation, and germ cell development in vitro. J Cell Biol, 101(4), 1511-1522.

Haitina, T., Fredriksson, R., Foord, S. M., Schioth, H. B., & Gloriam, D. E. (2009). The G protein-coupled receptor subset of the dog genome is more similar to that in humans than rodents. BMC Genomics, 10, 24. doi:10.1186/1471-2164-10-24

Hammes, A., Guo, J. K., Lutsch, G., Leheste, J. R., Landrock, D., Ziegler, U., . . . Schedl, A. (2001). Two splice variants of the Wilms' tumor 1 gene have distinct functions during sex determination and nephron formation. Cell, 106(3), 319-329.

Hammond, N. L., Brookes, K. J., & Dixon, M. J. (2018). Ectopic Hedgehog Signaling Causes Cleft Palate and Defective Osteogenesis. J Dent Res, 97(13), 1485-1493. doi:10.1177/0022034518785336

Haning, R. V., Jr., Chesney, R. W., Moorthy, A. V., & Gilbert, E. F. (1985). A syndrome of chronic renal failure and XY gonadal dysgenesis in young phenotypic females without genital ambiguity. Am J Kidney Dis, 6(1), 40-48.

Hanley, N. A., Hagan, D. M., Clement-Jones, M., Ball, S. G., Strachan, T., Salas-Cortes, L., . . . Wilson, D. I. (2000). SRY, SOX9, and DAX1 expression patterns during human sex determination and gonadal development. Mech Dev, 91(1-2), 403-407.

Harley, V. R., & Goodfellow, P. N. (1994). The biochemical role of SRY in sex determination. Mol Reprod Dev, 39(2), 184-193. doi:10.1002/mrd.1080390211

Harrison, S. M., Granberg, C. F., Keays, M., Hill, M., Grimsby, G. M., & Baker, L. A. (2014). DNA copy number variations in patients with 46,XY disorders of sex development. J Urol, 192(6), 1801-1806. doi:10.1016/j.juro.2014.06.040

Hata, K., Nishimura, R., Muramatsu, S., Matsuda, A., Matsubara, T., Amano, K., . . . Yoneda, T. (2008). Paraspeckle protein p54nrb links Sox9-mediated transcription with RNA processing during chondrogenesis in mice. J Clin Invest, 118(9), 3098-3108. doi:10.1172/JCI31373

Heinz-Erian, P., Muller, T., Krabichler, B., Schranz, M., Becker, C., Ruschendorf, F., . . . Janecke, A. R. (2009). Mutations in SPINT2 cause a syndromic form of congenital sodium diarrhea. Am J Hum Genet, 84(2), 188-196. doi:10.1016/j.ajhg.2009.01.004

Heng, J. I., Nguyen, L., Castro, D. S., Zimmer, C., Wildner, H., Armant, O., . . . Guillemot, F. (2008). Neurogenin 2 controls cortical neuron migration through regulation of Rnd2. Nature, 455(7209), 114-118. doi:10.1038/nature07198

Herbarth, B., Pingault, V., Bondurand, N., Kuhlbrodt, K., Hermans-Borgmeyer, I., Puliti, A., . . . Wegner, M. (1998). Mutation of the Sry-related Sox10 gene in Dominant megacolon, a mouse model for human Hirschsprung disease. Proc Natl Acad Sci U S A, 95(9), 5161-5165. doi:10.1073/pnas.95.9.5161

Herbert Pratt, C., Potter, C. S., Fairfield, H., Reinholdt, L. G., Bergstrom, D. E., Harris, B. S., . . . Sundberg, J. P. (2015). Dsp rul: a spontaneous mouse mutation in desmoplakin as a model of Carvajal-Huerta syndrome. Exp Mol Pathol, 98(2), 164-172. doi:10.1016/j.yexmp.2015.01.015

Hiramatsu, R., Matoba, S., Kanai-Azuma, M., Tsunekawa, N., Katoh-Fukui, Y., Kurohmaru, M., . . . Kanai, Y. (2009). A critical time window of Sry action in gonadal sex determination in mice. Development, 136(1), 129-138. doi:10.1242/dev.029587

Hu, Y. C., Okumura, L. M., & Page, D. C. (2013). Gata4 is required for formation of the genital ridge in mice. PLoS Genet, 9(7), e1003629. doi:10.1371/journal.pgen.1003629

Huang, B. T., Chang, P. Y., Su, C. H., Chao, C. C., & Lin-Chao, S. (2012). Gas7-deficient mouse reveals roles in motor function and muscle fiber composition during aging. PLoS One, 7(5), e37702. doi:10.1371/journal.pone.0037702

Huang, Y. H., Jankowski, A., Cheah, K. S., Prabhakar, S., & Jauch, R. (2015). SOXE transcription factors form selective dimers on non-compact DNA motifs through multifaceted interactions between dimerization and high-mobility group domains. Sci Rep, 5, 10398. doi:10.1038/srep10398

Hughes, I. A., Houk, C., Ahmed, S. F., Lee, P. A., Group, L. C., & Group, E. C. (2006). Consensus statement on management of intersex disorders. Arch Dis Child, 91(7), 554-563. doi:10.1136/adc.2006.098319

Hughes, I. A., Houk, C., Ahmed, S. F., Lee, P. A., & Lawson Wilkins Pediatric Endocrine Society/European Society for Paediatric Endocrinology Consensus, G. (2006). Consensus statement on management of intersex disorders. J Pediatr Urol, 2(3), 148-162. doi:10.1016/j.jpurol.2006.03.004

Hutchison, G. R., Scott, H. M., Walker, M., McKinnell, C., Ferrara, D., Mahood, I. K., & Sharpe, R. M. (2008). Sertoli cell development and function in an animal model of testicular dysgenesis syndrome. Biol Reprod, 78(2), 352-360. doi:10.1095/biolreprod.107.064006

Ichida, F., Tsubata, S., Bowles, K. R., Haneda, N., Uese, K., Miyawaki, T., . . . Towbin, J. A. (2001). Novel gene mutations in patients with left ventricular noncompaction or Barth syndrome. Circulation, 103(9), 1256-1263. doi:10.1161/01.cir.103.9.1256

Inamoto, S., Iwata, S., Inamoto, T., Nomura, S., Sasaki, T., Urasaki, Y., . . . Morimoto, C. (2007). Crk-associated substrate lymphocyte type regulates transforming growth factor-beta signaling by inhibiting Smad6 and Smad7. Oncogene, 26(6), 893-904. doi:10.1038/sj.onc.1209848

Inoue, K., Khajavi, M., Ohyama, T., Hirabayashi, S., Wilson, J., Reggin, J. D., . . . Lupski, J. R. (2004). Molecular mechanism for distinct neurological phenotypes conveyed by allelic truncating mutations. Nat Genet, 36(4), 361-369. doi:10.1038/ng1322

Ishigami, A., Ohsawa, T., Asaga, H., Akiyama, K., Kuramoto, M., & Maruyama, N. (2002). Human peptidylarginine deiminase type II: molecular cloning, gene organization, and expression in human skin. Arch Biochem Biophys, 407(1), 25-31. doi:10.1016/s0003-9861(02)00516-7

Izumchenko, E., Singh, M. K., Plotnikova, O. V., Tikhmyanova, N., Little, J. L., Serebriiskii, I. G., . . . Golemis, E. A. (2009). NEDD9 promotes oncogenic signaling in mammary tumor development. Cancer Res, 69(18), 7198-7206. doi:10.1158/0008-5472.CAN-09-0795

Jakob, S., & Lovell-Badge, R. (2011). Sex determination and the control of Sox9 expression in mammals. FEBS J, 278(7), 1002-1009. doi:10.1111/j.1742-4658.2011.08029.x

James, P. F., Grupp, I. L., Grupp, G., Woo, A. L., Askew, G. R., Croyle, M. L., . . . Lingrel, J. B. (1999). Identification of a specific role for the Na,K-ATPase alpha 2 isoform as a regulator of calcium in the heart. Mol Cell, 3(5), 555-563.

Jameson, S. A., Lin, Y. T., & Capel, B. (2012). Testis development requires the repression of Wnt4 by Fgf signaling. Dev Biol, 370(1), 24-32. doi:10.1016/j.ydbio.2012.06.009

Jameson, S. A., Natarajan, A., Cool, J., DeFalco, T., Maatouk, D. M., Mork, L., . . . Capel, B. (2012). Temporal transcriptional profiling of somatic and germ cells reveals biased lineage

priming of sexual fate in the fetal mouse gonad. PLoS Genet, 8(3), e1002575. doi:10.1371/journal.pgen.1002575

Jenkins, E., Moss, J. B., Pace, J. M., & Bridgewater, L. C. (2005). The new collagen gene COL27A1 contains SOX9-responsive enhancer elements. Matrix Biol, 24(3), 177-184. doi:10.1016/j.matbio.2005.02.004

Johnen, H., Gonzalez-Silva, L., Carramolino, L., Flores, J. M., Torres, M., & Salvador, J. M. (2013). Gadd45g is essential for primary sex determination, male fertility and testis development. PLoS One, 8(3), e58751. doi:10.1371/journal.pone.0058751

Kadaja, M., Keyes, B. E., Lin, M., Pasolli, H. A., Genander, M., Polak, L., . . . Fuchs, E. (2014). SOX9: a stem cell transcriptional regulator of secreted niche signaling factors. Genes Dev, 28(4), 328-341. doi:10.1101/gad.233247.113

Kamachi, Y., Uchikawa, M., & Kondoh, H. (2000). Pairing SOX off: with partners in the regulation of embryonic development. Trends Genet, 16(4), 182-187.

Kashimada, K., Svingen, T., Feng, C. W., Pelosi, E., Bagheri-Fam, S., Harley, V. R., . . . Koopman, P. (2011). Antagonistic regulation of Cyp26b1 by transcription factors SOX9/SF1 and FOXL2 during gonadal development in mice. FASEB J, 25(10), 3561-3569. doi:10.1096/fj.11-184333

Kastury, K., Druck, T., Huebner, K., Barletta, C., Acampora, D., Simeone, A., . . . Boncinelli, E. (1994). Chromosome locations of human EMX and OTX genes. Genomics, 22(1), 41-45. doi:10.1006/geno.1994.1343

Kato, T., Miyata, K., Sonobe, M., Yamashita, S., Tamano, M., Miura, K., . . . Takada, S. (2013). Production of Sry knockout mouse using TALEN via oocyte injection. Sci Rep, 3, 3136. doi:10.1038/srep03136

Katoh-Fukui, Y., Miyabayashi, K., Komatsu, T., Owaki, A., Baba, T., Shima, Y., . . . Morohashi, K. (2012). Cbx2, a polycomb group gene, is required for Sry gene expression in mice. Endocrinology, 153(2), 913-924. doi:10.1210/en.2011-1055

Katoh-Fukui, Y., Tsuchiya, R., Shiroishi, T., Nakahara, Y., Hashimoto, N., Noguchi, K., & Higashinakagawa, T. (1998). Male-to-female sex reversal in M33 mutant mice. Nature, 393(6686), 688-692. doi:10.1038/31482

Kent, J., Wheatley, S. C., Andrews, J. E., Sinclair, A. H., & Koopman, P. (1996). A male-specific role for SOX9 in vertebrate sex determination. Development, 122(9), 2813-2822.

Kim, G. J., Sock, E., Buchberger, A., Just, W., Denzer, F., Hoepffner, W., . . . Scherer, G. (2015). Copy number variation of two separate regulatory regions upstream of SOX9 causes isolated 46,XY or 46,XX disorder of sex development. J Med Genet, 52(4), 240-247. doi:10.1136/jmedgenet-2014-102864

Kim, Y., Bingham, N., Sekido, R., Parker, K. L., Lovell-Badge, R., & Capel, B. (2007). Fibroblast growth factor receptor 2 regulates proliferation and Sertoli differentiation during male sex determination. Proc Natl Acad Sci U S A, 104(42), 16558-16563. doi:10.1073/pnas.0702581104

Kim, Y., Kobayashi, A., Sekido, R., DiNapoli, L., Brennan, J., Chaboissier, M. C., . . . Capel, B. (2006). Fgf9 and Wnt4 act as antagonistic signals to regulate mammalian sex determination. PLoS Biol, 4(6), e187. doi:10.1371/journal.pbio.0040187

Kinberg, J. A., Angle, C. R., & Wilson, R. B. (1987). Nephropathy-gonadal dysgenesis, type 2: renal failure in three siblings with XY dysgenesis in one. Am J Kidney Dis, 9(6), 507-510.

Klamt, B., Koziell, A., Poulat, F., Wieacker, P., Scambler, P., Berta, P., & Gessler, M. (1998). Frasier syndrome is caused by defective alternative splicing of WT1 leading to an altered ratio of WT1 +/-KTS splice isoforms. Hum Mol Genet, 7(4), 709-714.

Knebelmann, B., Boussin, L., Guerrier, D., Legeai, L., Kahn, A., Josso, N., & Picard, J. Y. (1991). Anti-Mullerian hormone Bruxelles: a nonsense mutation associated with the persistent Mullerian duct syndrome. Proc Natl Acad Sci U S A, 88(9), 3767-3771. doi:10.1073/pnas.88.9.3767

Knower, K. C., Kelly, S., Ludbrook, L. M., Bagheri-Fam, S., Sim, H., Bernard, P., . . . Harley, V. R. (2011). Failure of SOX9 regulation in 46XY disorders of sex development with SRY, SOX9 and SF1 mutations. PLoS One, 6(3), e17751. doi:10.1371/journal.pone.0017751

Knower, K. C., Sim, H., McClive, P. J., Bowles, J., Koopman, P., Sinclair, A. H., & Harley, V. R. (2007). Characterisation of urogenital ridge gene expression in the human embryonal carcinoma cell line NT2/D1. Sex Dev, 1(2), 114-126. doi:10.1159/000100033

Kohler, B., Lin, L., Ferraz-de-Souza, B., Wieacker, P., Heidemann, P., Schroder, V., . . . Achermann, J. C. (2008). Five novel mutations in steroidogenic factor 1 (SF1, NR5A1) in 46,XY patients with severe underandrogenization but without adrenal insufficiency. Hum Mutat, 29(1), 59-64. doi:10.1002/humu.20588

Koopman, P., Gubbay, J., Vivian, N., Goodfellow, P., & Lovell-Badge, R. (1991). Male development of chromosomally female mice transgenic for Sry. Nature, 351(6322), 117-121. doi:10.1038/351117a0

Koopman, P., Munsterberg, A., Capel, B., Vivian, N., & Lovell-Badge, R. (1990). Expression of a candidate sex-determining gene during mouse testis differentiation. Nature, 348(6300), 450-452. doi:10.1038/348450a0

Kosicki, M., Tomberg, K., & Bradley, A. (2018). Erratum: Repair of double-strand breaks induced by CRISPR-Cas9 leads to large deletions and complex rearrangements. Nat Biotechnol, 36(9), 899. doi:10.1038/nbt0918-899c

Koubova, J., Menke, D. B., Zhou, Q., Capel, B., Griswold, M. D., & Page, D. C. (2006). Retinoic acid regulates sex-specific timing of meiotic initiation in mice. Proc Natl Acad Sci U S A, 103(8), 2474-2479. doi:10.1073/pnas.0510813103

Kreidberg, J. A., Sariola, H., Loring, J. M., Maeda, M., Pelletier, J., Housman, D., & Jaenisch, R. (1993). WT-1 is required for early kidney development. Cell, 74(4), 679-691.

Kumar, T. R., Varani, S., Wreford, N. G., Telfer, N. M., de Kretser, D. M., & Matzuk, M. M. (2001). Male reproductive phenotypes in double mutant mice lacking both FSHbeta and activin receptor IIA. Endocrinology, 142(8), 3512-3518. doi:10.1210/endo.142.8.8336

Kumar, T. R., Wang, Y., Lu, N., & Matzuk, M. M. (1997). Follicle stimulating hormone is required for ovarian follicle maturation but not male fertility. Nat Genet, 15(2), 201-204. doi:10.1038/ng0297-201

Kun-Rodrigues, C., Ganos, C., Guerreiro, R., Schneider, S. A., Schulte, C., Lesage, S., . . . Bras, J. (2015). A systematic screening to identify de novo mutations causing sporadic early-onset Parkinson's disease. Hum Mol Genet, 24(23), 6711-6720. doi:10.1093/hmg/ddv376

Kuo, Y. W., Joshi, R., Wang, T. E., Chang, H. W., Li, S. H., Hsiao, C. N., & Tsai, P. J. (2017). Identification, characterization and purification of porcine Quiescin Q6-Sulfydryl Oxidase 2 protein. BMC Vet Res, 13(1), 205. doi:10.1186/s12917-017-1125-1

La Sala, G., Marazziti, D., Di Pietro, C., Golini, E., Matteoni, R., & Tocchini-Valentini, G. P. (2015). Modulation of Dhh signaling and altered Sertoli cell function in mice lacking the GPR37-prosaposin receptor. FASEB J, 29(5), 2059-2069. doi:10.1096/fj.14-269209

Larney, C., Bailey, T. L., & Koopman, P. (2014). Switching on sex: transcriptional regulation of the testis-determining gene Sry. Development, 141(11), 2195-2205. doi:10.1242/dev.107052

Larue, L., Ohsugi, M., Hirchenhain, J., & Kemler, R. (1994). E-cadherin null mutant embryos fail to form a trophectoderm epithelium. Proc Natl Acad Sci U S A, 91(17), 8263-8267.

Lassuthova, P., Rebelo, A. P., Ravenscroft, G., Lamont, P. J., Davis, M. R., Manganelli, F., . . . Zuchner, S. (2018). Mutations in ATP1A1 Cause Dominant Charcot-Marie-Tooth Type 2. Am J Hum Genet, 102(3), 505-514. doi:10.1016/j.ajhg.2018.01.023

Laue, K., Pogoda, H. M., Daniel, P. B., van Haeringen, A., Alanay, Y., von Ameln, S., . . . Robertson, S. P. (2011). Craniosynostosis and multiple skeletal anomalies in humans and zebrafish result from a defect in the localized degradation of retinoic acid. Am J Hum Genet, 89(5), 595-606. doi:10.1016/j.ajhg.2011.09.015

Lavery, R., Lardenois, A., Ranc-Jianmotamedi, F., Pauper, E., Gregoire, E. P., Vigier, C., . . . Chaboissier, M. C. (2011). XY Sox9 embryonic loss-of-function mouse mutants show complete sex reversal and produce partially fertile XY oocytes. Dev Biol, 354(1), 111-122. doi:10.1016/j.ydbio.2011.03.029

Lee, P. A., Nordenstrom, A., Houk, C. P., Ahmed, S. F., Auchus, R., Baratz, A., . . . Global, D. S. D. U. C. (2016). Global Disorders of Sex Development Update since 2006: Perceptions, Approach and Care. Horm Res Paediatr, 85(3), 158-180. doi:10.1159/000442975

Lefebvre, V., Dumitriu, B., Penzo-Mendez, A., Han, Y., & Pallavi, B. (2007). Control of cell fate and differentiation by Sry-related high-mobility-group box (Sox) transcription factors. Int J Biochem Cell Biol, 39(12), 2195-2214. doi:10.1016/j.biocel.2007.05.019

Leon, N. Y., Reyes, A. P., & Harley, V. R. (2019). A clinical algorithm to diagnose differences of sex development. Lancet Diabetes Endocrinol, 7(7), 560-574. doi:10.1016/S2213-8587(18)30339-5

Li, H., MacLean, G., Cameron, D., Clagett-Dame, M., & Petkovich, M. (2009). Cyp26b1 expression in murine Sertoli cells is required to maintain male germ cells in an undifferentiated state during embryogenesis. PLoS One, 4(10), e7501. doi:10.1371/journal.pone.0007501

Li, Y., Zheng, M., & Lau, Y. F. (2014). The sex-determining factors SRY and SOX9 regulate similar target genes and promote testis cord formation during testicular differentiation. Cell Rep, 8(3), 723-733. doi:10.1016/j.celrep.2014.06.055

Lin, L., Philibert, P., Ferraz-de-Souza, B., Kelberman, D., Homfray, T., Albanese, A., . . . Achermann, J. C. (2007). Heterozygous missense mutations in steroidogenic factor 1 (SF1/Ad4BP, NR5A1) are associated with 46,XY disorders of sex development with normal adrenal function. J Clin Endocrinol Metab, 92(3), 991-999. doi:10.1210/jc.2006-1672

Lin, Y. T., Barske, L., DeFalco, T., & Capel, B. (2017). Numb regulates somatic cell lineage commitment during early gonadogenesis in mice. Development, 144(9), 1607-1618. doi:10.1242/dev.149203

Lin, Y. T., & Capel, B. (2015). Cell fate commitment during mammalian sex determination. Curr Opin Genet Dev, 32, 144-152. doi:10.1016/j.gde.2015.03.003

Lindeman, R. E., Gearhart, M. D., Minkina, A., Krentz, A. D., Bardwell, V. J., & Zarkower, D. (2015). Sexual cell-fate reprogramming in the ovary by DMRT1. Curr Biol, 25(6), 764-771. doi:10.1016/j.cub.2015.01.034

Liu, J. A., Rao, Y., Cheung, M. P. L., Hui, M. N., Wu, M. H., Chan, L. K., . . . Cheung, M. (2017). Asymmetric localization of DLC1 defines avian trunk neural crest polarity for directional delamination and migration. Nat Commun, 8(1), 1185. doi:10.1038/s41467-017-01107-0

Liu, S. S., Zhang, C. Z., & Peng, G. (2016). Effects of starvation on the expression of feeding related neuropeptides in the larval zebrafish hypothalamus. Yi Chuan, 38(9), 821-830. doi:10.16288/j.yczz.16-087

Lourenco, D., Brauner, R., Rybczynska, M., Nihoul-Fekete, C., McElreavey, K., & Bashamboo, A. (2011). Loss-of-function mutation in GATA4 causes anomalies of human testicular development. Proc Natl Acad Sci U S A, 108(4), 1597-1602. doi:10.1073/pnas.1010257108

Lu, D. H., Hsu, C. C., Huang, S. W., Tu, H. J., Huang, T. F., Liou, H. C., . . . Gau, S. S. (2017). ARHGEF10 knockout inhibits platelet aggregation and protects mice from thrombus formation. J Thromb Haemost, 15(10), 2053-2064. doi:10.1111/jth.13799

Lu, D. H., Liao, H. M., Chen, C. H., Tu, H. J., Liou, H. C., Gau, S. S., & Fu, W. M. (2018). Impairment of social behaviors in Arhgef10 knockout mice. Mol Autism, 9, 11. doi:10.1186/s13229-018-0197-5

Lu, Q., Gore, M., Zhang, Q., Camenisch, T., Boast, S., Casagranda, F., . . . Lemke, G. (1999). Tyro-3 family receptors are essential regulators of mammalian spermatogenesis. Nature, 398(6729), 723-728. doi:10.1038/19554

Lu, Q., & Lemke, G. (2001). Homeostatic regulation of the immune system by receptor tyrosine kinases of the Tyro 3 family. Science, 293(5528), 306-311. doi:10.1126/science.1061663

Ludbrook, L., Alankarage, D., Bagheri-Fam, S., & Harley, V. (2016). Dataset of differentially expressed genes from SOX9 over-expressing NT2/D1 cells. Data Brief, 9, 194-198. doi:10.1016/j.dib.2016.08.047

Ludbrook, L. M., Bernard, P., Bagheri-Fam, S., Ryan, J., Sekido, R., Wilhelm, D., . . . Harley, V. R. (2012). Excess DAX1 leads to XY ovotesticular disorder of sex development (DSD) in mice by inhibiting steroidogenic factor-1 (SF1) activation of the testis enhancer of SRY-box-9 (Sox9). Endocrinology, 153(4), 1948-1958. doi:10.1210/en.2011-1428

Luo, X., Ikeda, Y., & Parker, K. L. (1994). A cell-specific nuclear receptor is essential for adrenal and gonadal development and sexual differentiation. Cell, 77(4), 481-490.

Luthi, A., Van der Putten, H., Botteri, F. M., Mansuy, I. M., Meins, M., Frey, U., . . . Monard, D. (1997). Endogenous serine protease inhibitor modulates epileptic activity and hippocampal long-term potentiation. J Neurosci, 17(12), 4688-4699.

Maatouk, D. M., DiNapoli, L., Alvers, A., Parker, K. L., Taketo, M. M., & Capel, B. (2008). Stabilization of beta-catenin in XY gonads causes male-to-female sex-reversal. Hum Mol Genet, 17(19), 2949-2955. doi:10.1093/hmg/ddn193

Maatouk, D. M., Natarajan, A., Shibata, Y., Song, L., Crawford, G. E., Ohler, U., & Capel, B. (2017). Genome-wide identification of regulatory elements in Sertoli cells. Development, 144(4), 720-730. doi:10.1242/dev.142554

Maehr, R., Mintern, J. D., Herman, A. E., Lennon-Dumenil, A. M., Mathis, D., Benoist, C., & Ploegh, H. L. (2005). Cathepsin L is essential for onset of autoimmune diabetes in NOD mice. J Clin Invest, 115(10), 2934-2943. doi:10.1172/JCI25485

Maggio, I., Holkers, M., Liu, J., Janssen, J. M., Chen, X., & Goncalves, M. A. (2014). Adenoviral vector delivery of RNA-guided CRISPR/Cas9 nuclease complexes induces targeted mutagenesis in a diverse array of human cells. Sci Rep, 4, 5105. doi:10.1038/srep05105

Mali, P., Yang, L., Esvelt, K. M., Aach, J., Guell, M., DiCarlo, J. E., . . . Church, G. M. (2013). RNA-guided human genome engineering via Cas9. Science, 339(6121), 823-826. doi:10.1126/science.1232033

Malki, S., Nef, S., Notarnicola, C., Thevenet, L., Gasca, S., Mejean, C., . . . Boizet-Bonhoure, B. (2005). Prostaglandin D2 induces nuclear import of the sex-determining factor SOX9 via its cAMP-PKA phosphorylation. EMBO J, 24(10), 1798-1809. doi:10.1038/sj.emboj.7600660

Marazziti, D., Golini, E., Mandillo, S., Magrelli, A., Witke, W., Matteoni, R., & Tocchini-Valentini, G. P. (2004). Altered dopamine signaling and MPTP resistance in mice lacking the Parkinson's disease-associated GPR37/parkin-associated endothelin-like receptor. Proc Natl Acad Sci U S A, 101(27), 10189-10194. doi:10.1073/pnas.0403661101

Martinez de LaPiscina, I., de Mingo, C., Riedl, S., Rodriguez, A., Pandey, A. V., Fernandez-Cancio, M., . . . Fluck, C. E. (2018). GATA4 Variants in Individuals With a 46,XY Disorder of Sex Development (DSD) May or May Not Be Associated With Cardiac Defects Depending on Second Hits in Other DSD Genes. Front Endocrinol (Lausanne), 9, 142. doi:10.3389/fendo.2018.00142

Mathelier, A., Zhao, X., Zhang, A. W., Parcy, F., Worsley-Hunt, R., Arenillas, D. J., . . . Wasserman, W. W. (2014). JASPAR 2014: an extensively expanded and updated open-access database of transcription factor binding profiles. Nucleic Acids Res, 42(Database issue), D142-147. doi:10.1093/nar/gkt997

Matsuo, I., Suda, Y., Yoshida, M., Ueki, T., Kimura, C., Kuratani, S., & Aizawa, S. (1997). Otx and Emx functions in patterning of the vertebrate rostral head. Cold Spring Harb Symp Quant Biol, 62, 545-553.

Matzuk, M. M., & Lamb, D. J. (2008). The biology of infertility: research advances and clinical challenges. Nat Med, 14(11), 1197-1213. doi:10.1038/nm.f.1895

McDowall, S., Argentaro, A., Ranganathan, S., Weller, P., Mertin, S., Mansour, S., . . . Harley, V. (1999). Functional and structural studies of wild type SOX9 and mutations causing campomelic dysplasia. J Biol Chem, 274(34), 24023-24030.

McLaren, A. (2003). Primordial germ cells in the mouse. Dev Biol, 262(1), 1-15.

McLean, C. Y., Bristor, D., Hiller, M., Clarke, S. L., Schaar, B. T., Lowe, C. B., . . . Bejerano, G. (2010). GREAT improves functional interpretation of cis-regulatory regions. Nat Biotechnol, 28(5), 495-501. doi:10.1038/nbt.1630

Meehan, T., Schlatt, S., O'Bryan, M. K., de Kretser, D. M., & Loveland, K. L. (2000). Regulation of germ cell and Sertoli cell development by activin, follistatin, and FSH. Dev Biol, 220(2), 225-237. doi:10.1006/dbio.2000.9625

Mendonca, B. B., Domenice, S., Arnhold, I. J., & Costa, E. M. (2009). 46,XY disorders of sex development (DSD). Clin Endocrinol (Oxf), 70(2), 173-187. doi:CEN3392 [pii]

10.1111/j.1365-2265.2008.03392.x [doi]

Meng, X., Lindahl, M., Hyvonen, M. E., Parvinen, M., de Rooij, D. G., Hess, M. W., . . . Sariola, H. (2000). Regulation of cell fate decision of undifferentiated spermatogonia by GDNF. Science, 287(5457), 1489-1493. doi:10.1126/science.287.5457.1489

Meng, Y., Zhang, Y., Tregoubov, V., Janus, C., Cruz, L., Jackson, M., . . . Jia, Z. (2002). Abnormal spine morphology and enhanced LTP in LIMK-1 knockout mice. Neuron, 35(1), 121-133.

Merchant-Larios, H., & Centeno, B. (1981). Morphogenesis of the ovary from the sterile W/Wv mouse. Prog Clin Biol Res, 59B, 383-392.

Mertin, S., McDowall, S. G., & Harley, V. R. (1999). The DNA-binding specificity of SOX9 and other SOX proteins. Nucleic Acids Res, 27(5), 1359-1364.

Mi, H., Muruganujan, A., & Thomas, P. D. (2013). PANTHER in 2013: modeling the evolution of gene function, and other gene attributes, in the context of phylogenetic trees. Nucleic Acids Res, 41(Database issue), D377-386. doi:10.1093/nar/gks1118

Miao, Y., Li, A. L., Wang, L., Fan, C. F., Zhang, X. P., Xu, H. T., . . . Wang, E. H. (2013). Overexpression of NEDD9 is associated with altered expression of E-Cadherin, beta-Catenin and N-Cadherin and predictive of poor prognosis in non-small cell lung cancer. Pathol Oncol Res, 19(2), 281-286. doi:10.1007/s12253-012-9580-2

Michala, L., & Creighton, S. M. (2010). The XY female. Best Pract Res Clin Obstet Gynaecol, 24(2), 139-148. doi:10.1016/j.bpobgyn.2009.09.009

Migita, S., Hanagata, N., Tsuya, D., Yamazaki, T., Sugimoto, Y., & Ikoma, T. (2011). Transfection efficiency for size-separated cells synchronized in cell cycle by microfluidic device. Biomed Microdevices, 13(4), 725-729. doi:10.1007/s10544-011-9542-6

Milosevic, I., Giovedi, S., Lou, X., Raimondi, A., Collesi, C., Shen, H., . . . De Camilli, P. (2011). Recruitment of endophilin to clathrin-coated pit necks is required for efficient vesicle uncoating after fission. Neuron, 72(4), 587-601. doi:10.1016/j.neuron.2011.08.029

Mishina, Y., Rey, R., Finegold, M. J., Matzuk, M. M., Josso, N., Cate, R. L., & Behringer, R. R. (1996). Genetic analysis of the Mullerian-inhibiting substance signal transduction pathway in mammalian sexual differentiation. Genes Dev, 10(20), 2577-2587. doi:10.1101/gad.10.20.2577

Mitchell, K. J., Pinson, K. I., Kelly, O. G., Brennan, J., Zupicich, J., Scherz, P., . . . Skarnes, W. C. (2001). Functional analysis of secreted and transmembrane proteins critical to mouse development. Nat Genet, 28(3), 241-249. doi:10.1038/90074

Miyamoto, N., Yoshida, M., Kuratani, S., Matsuo, I., & Aizawa, S. (1997). Defects of urogenital development in mice lacking Emx2. Development, 124(9), 1653-1664.

Miyamoto, Y., Taniguchi, H., Hamel, F., Silversides, D. W., & Viger, R. S. (2008). A GATA4/WT1 cooperation regulates transcription of genes required for mammalian sex determination and differentiation. BMC Mol Biol, 9, 44. doi:10.1186/1471-2199-9-44

Miyatake, S., Schneeberger, S., Koyama, N., Yokochi, K., Ohmura, K., Shiina, M., . . . Matsumoto, N. (2018). Biallelic COLGALT1 variants are associated with cerebral small vessel disease. Ann Neurol, 84(6), 843-853. doi:10.1002/ana.25367

Molyneaux, K., & Wylie, C. (2004). Primordial germ cell migration. Int J Dev Biol, 48(5-6), 537-544. doi:10.1387/ijdb.041833km

Moniot, B., Declosmenil, F., Barrionuevo, F., Scherer, G., Aritake, K., Malki, S., . . . Poulat, F. (2009). The PGD2 pathway, independently of FGF9, amplifies SOX9 activity in Sertoli cells during male sexual differentiation. Development, 136(11), 1813-1821. doi:10.1242/dev.032631

Montazer-Torbati, F., Kocer, A., Auguste, A., Renault, L., Charpigny, G., Pailhoux, E., & Pannetier, M. (2010). A study of goat SRY protein expression suggests putative new roles for this gene in the developing testis of a species with long-lasting SRY expression. Dev Dyn, 239(12), 3324-3335. doi:10.1002/dvdy.22452

Morais da Silva, S., Hacker, A., Harley, V., Goodfellow, P., Swain, A., & Lovell-Badge, R. (1996). Sox9 expression during gonadal development implies a conserved role for the gene in testis differentiation in mammals and birds. Nat Genet, 14(1), 62-68. doi:10.1038/ng0996-62

Morimoto, K., Tanaka, T., Nitta, Y., Ohnishi, K., Kawashima, H., & Nakatani, T. (2014). NEDD9 crucially regulates TGF-beta-triggered epithelial-mesenchymal transition and cell invasion in prostate cancer cells: involvement in cancer progressiveness. Prostate, 74(8), 901-910. doi:10.1002/pros.22809

Morrow, C. M., Tyagi, G., Simon, L., Carnes, K., Murphy, K. M., Cooke, P. S., . . . Hess, R. A. (2009). Claudin 5 expression in mouse seminiferous epithelium is dependent upon the transcription factor ets variant 5 and contributes to blood-testis barrier function. Biol Reprod, 81(5), 871-879. doi:10.1095/biolreprod.109.077040

Mruk, D. D., & Cheng, C. Y. (2004). Sertoli-Sertoli and Sertoli-germ cell interactions and their significance in germ cell movement in the seminiferous epithelium during spermatogenesis. Endocr Rev, 25(5), 747-806. doi:10.1210/er.2003-0022

Murer, V., Spetz, J. F., Hengst, U., Altrogge, L. M., de Agostini, A., & Monard, D. (2001). Male fertility defects in mice lacking the serine protease inhibitor protease nexin-1. Proc Natl Acad Sci U S A, 98(6), 3029-3033. doi:10.1073/pnas.051630698

Murphy, M. W., Zarkower, D., & Bardwell, V. J. (2007). Vertebrate DM domain proteins bind similar DNA sequences and can heterodimerize on DNA. BMC Mol Biol, 8, 58. doi:10.1186/1471-2199-8-58

Nation, T. R., Balic, A., Southwell, B. R., Newgreen, D. F., & Hutson, J. M. (2009). The hormonal control of testicular descent. Pediatr Endocrinol Rev, 7(1), 22-31.

Nef, S., Schaad, O., Stallings, N. R., Cederroth, C. R., Pitetti, J. L., Schaer, G., . . . Vassalli, J. D. (2005). Gene expression during sex determination reveals a robust female genetic

program at the onset of ovarian development. Dev Biol, 287(2), 361-377. doi:10.1016/j.ydbio.2005.09.008

Nef, S., Stevant, I., & Greenfield, A. (2019). Characterizing the bipotential mammalian gonad. Curr Top Dev Biol, 134, 167-194. doi:10.1016/bs.ctdb.2019.01.002

Nef, S., Verma-Kurvari, S., Merenmies, J., Vassalli, J. D., Efstratiadis, A., Accili, D., & Parada, L. F. (2003). Testis determination requires insulin receptor family function in mice. Nature, 426(6964), 291-295. doi:10.1038/nature02059

Neirijnck, Y., Calvel, P., Kilcoyne, K. R., Kuhne, F., Stevant, I., Griffeth, R. J., . . . Nef, S. (2018). Insulin and IGF1 receptors are essential for the development and steroidogenic function of adult Leydig cells. FASEB J, 32(6), 3321-3335. doi:10.1096/fj.201700769RR

Nel-Themaat, L., Jang, C. W., Stewart, M. D., Akiyama, H., Viger, R. S., & Behringer, R. R. (2011). Sertoli cell behaviors in developing testis cords and postnatal seminiferous tubules of the mouse. Biol Reprod, 84(2), 342-350. doi:10.1095/biolreprod.110.086900

Nicholls, P. K., Stanton, P. G., Chen, J. L., Olcorn, J. S., Haverfield, J. T., Qian, H., . . . Harrison, C. A. (2012). Activin signaling regulates Sertoli cell differentiation and function. Endocrinology, 153(12), 6065-6077. doi:10.1210/en.2012-1821

Nikcevic, G., Kovacevic-Grujicic, N., & Stevanovic, M. (2003). Improved transfection efficiency of cultured human cells. Cell Biol Int, 27(9), 735-737.

Nordenvall, A. S., Frisen, L., Nordenstrom, A., Lichtenstein, P., & Nordenskjold, A. (2014). Population based nationwide study of hypospadias in Sweden, 1973 to 2009: incidence and risk factors. J Urol, 191(3), 783-789. doi:10.1016/j.juro.2013.09.058

Norgett, E. E., Hatsell, S. J., Carvajal-Huerta, L., Cabezas, J. C., Common, J., Purkis, P. E., . . . Kelsell, D. P. (2000). Recessive mutation in desmoplakin disrupts desmoplakin-intermediate filament interactions and causes dilated cardiomyopathy, woolly hair and keratoderma. Hum Mol Genet, 9(18), 2761-2766. doi:10.1093/hmg/9.18.2761

O'Bryan, M. K., Grealy, A., Stahl, P. J., Schlegel, P. N., McLachlan, R. I., & Jamsai, D. (2012). Genetic variants in the ETV5 gene in fertile and infertile men with nonobstructive azoospermia associated with Sertoli cell-only syndrome. Fertil Steril, 98(4), 827-835 e821-823. doi:10.1016/j.fertnstert.2012.06.013

O'Bryan, M. K., Takada, S., Kennedy, C. L., Scott, G., Harada, S., Ray, M. K., . . . Mishina, Y. (2008). Sox8 is a critical regulator of adult Sertoli cell function and male fertility. Dev Biol, 316(2), 359-370. doi:10.1016/j.ydbio.2008.01.042

Ogawa, Y., Terao, M., Hara, S., Tamano, M., Okayasu, H., Kato, T., & Takada, S. (2018). Mapping of a responsible region for sex reversal upstream of Sox9 by production of mice with serial deletion in a genomic locus. Sci Rep, 8(1), 17514. doi:10.1038/s41598-018-35746-0

Ohba, S., He, X., Hojo, H., & McMahon, A. P. (2015). Distinct Transcriptional Programs Underlie Sox9 Regulation of the Mammalian Chondrocyte. Cell Rep, 12(2), 229-243. doi:10.1016/j.celrep.2015.06.013

Olsen, C. L., Hsu, P. P., Glienke, J., Rubanyi, G. M., & Brooks, A. R. (2004). Hedgehog-interacting protein is highly expressed in endothelial cells but down-regulated during angiogenesis and in several human tumors. BMC Cancer, 4, 43. doi:10.1186/1471-2407-4-43

Ono, M., & Harley, V. R. (2013). Disorders of sex development: new genes, new concepts. Nat Rev Endocrinol, 9(2), 79-91. doi:10.1038/nrendo.2012.235

Ottolenghi, C., Moreira-Filho, C., Mendonca, B. B., Barbieri, M., Fellous, M., Berkovitz, G. D., & McElreavey, K. (2001). Absence of mutations involving the LIM homeobox domain gene LHX9 in 46,XY gonadal agenesis and dysgenesis. J Clin Endocrinol Metab, 86(6), 2465-2469. doi:10.1210/jcem.86.6.7539

Ozen, S., Onay, H., Atik, T., Solmaz, A. E., Ozkinay, F., Goksen, D., & Darcan, S. (2017). Rapid Molecular Genetic Diagnosis with Next-Generation Sequencing in 46,XY Disorders of Sex Development Cases: Efficiency and Cost Assessment. Horm Res Paediatr, 87(2), 81-87. doi:10.1159/000452995

Pan, Q., Zhang, X., Zhang, L., Cheng, Y., Zhao, N., Li, F., . . . Chai, J. (2018). Solute Carrier Organic Anion Transporter Family Member 3A1 Is a Bile Acid Efflux Transporter in Cholestasis. Gastroenterology, 155(5), 1578-1592 e1516. doi:10.1053/j.gastro.2018.07.031

Park, S. Y., Meeks, J. J., Raverot, G., Pfaff, L. E., Weiss, J., Hammer, G. D., & Jameson, J. L. (2005). Nuclear receptors Sf1 and Dax1 function cooperatively to mediate somatic cell differentiation during testis development. Development, 132(10), 2415-2423. doi:10.1242/dev.01826

Pasqualotto, F. F., Lucon, A. M., de Goes, P. M., Sobreiro, B. P., Hallak, J., Pasqualotto, E. B., & Arap, S. (2005). Semen profile, testicular volume, and hormonal levels in infertile patients with varicoceles compared with fertile men with and without varicoceles. Fertil Steril, 83(1), 74-77. doi:10.1016/j.fertnstert.2004.06.047

Pattabiraman, P. P., Epstein, D. L., & Rao, P. V. (2013). Regulation of Adherens Junctions in Trabecular Meshwork Cells by Rac GTPase and their influence on Intraocular Pressure. J Ocul Biol, 1(1). doi:10.13188/2334-2838.1000002

Pearlman, A., Loke, J., Le Caignec, C., White, S., Chin, L., Friedman, A., . . . Ostrer, H. (2010). Mutations in MAP3K1 cause 46,XY disorders of sex development and implicate a common signal transduction pathway in human testis determination. Am J Hum Genet, 87(6), 898-904. doi:10.1016/j.ajhg.2010.11.003

Peirano, R. I., & Wegner, M. (2000). The glial transcription factor Sox10 binds to DNA both as monomer and dimer with different functional consequences. Nucleic Acids Res, 28(16), 3047-3055. doi:10.1093/nar/28.16.3047

Pelletier, J., Bruening, W., Li, F. P., Haber, D. A., Glaser, T., & Housman, D. E. (1991). WT1 mutations contribute to abnormal genital system development and hereditary Wilms' tumour. Nature, 353(6343), 431-434. doi:10.1038/353431a0

Philibert, P., Boizet-Bonhoure, B., Bashamboo, A., Paris, F., Aritake, K., Urade, Y., . . . Poulat, F. (2013). Unilateral cryptorchidism in mice mutant for Ptgds. Hum Mutat, 34(2), 278-282. doi:10.1002/humu.22231

Pierucci-Alves, F., Clark, A. M., & Russell, L. D. (2001). A developmental study of the Desert hedgehog-null mouse testis. Biol Reprod, 65(5), 1392-1402.

Pilon, N., Daneau, I., Paradis, V., Hamel, F., Lussier, J. G., Viger, R. S., & Silversides, D. W. (2003). Porcine SRY promoter is a target for steroidogenic factor 1. Biol Reprod, 68(4), 1098-1106. doi:10.1095/biolreprod.102.010884

Pingault, V., Bodereau, V., Baral, V., Marcos, S., Watanabe, Y., Chaoui, A., . . . Bondurand, N. (2013). Loss-of-function mutations in SOX10 cause Kallmann syndrome with deafness. Am J Hum Genet, 92(5), 707-724. doi:10.1016/j.ajhg.2013.03.024

Pingault, V., Bondurand, N., Kuhlbrodt, K., Goerich, D. E., Prehu, M. O., Puliti, A., . . . Goossens, M. (1998). SOX10 mutations in patients with Waardenburg-Hirschsprung disease. Nat Genet, 18(2), 171-173. doi:10.1038/ng0298-171

Pitetti, J. L., Calvel, P., Romero, Y., Conne, B., Truong, V., Papaioannou, M. D., . . . Nef, S. (2013). Insulin and IGF1 receptors are essential for XX and XY gonadal differentiation and adrenal development in mice. PLoS Genet, 9(1), e1003160. doi:10.1371/journal.pgen.1003160

Polanco, J. C., Wilhelm, D., Davidson, T. L., Knight, D., & Koopman, P. (2010). Sox10 gain-of-function causes XX sex reversal in mice: implications for human 22q-linked disorders of sex development. Hum Mol Genet, 19(3), 506-516. doi:10.1093/hmg/ddp520

Portnoi, M. F., Dumargne, M. C., Rojo, S., Witchel, S. F., Duncan, A. J., Eozenou, C., . . . Bashamboo, A. (2018). Mutations involving the SRY-related gene SOX8 are associated with a spectrum of human reproductive anomalies. Hum Mol Genet, 27(7), 1228-1240. doi:10.1093/hmg/ddy037

Pradhan, B. S., Bhattacharya, I., Sarkar, R., & Majumdar, S. S. (2019). Downregulation of Sostdc1 in Testicular Sertoli Cells is Prerequisite for Onset of Robust Spermatogenesis at Puberty. Sci Rep, 9(1), 11458. doi:10.1038/s41598-019-47930-x

Pridans, C., Holmes, M. L., Polli, M., Wettenhall, J. M., Dakic, A., Corcoran, L. M., . . . Nutt, S. L. (2008). Identification of Pax5 target genes in early B cell differentiation. J Immunol, 180(3), 1719-1728. doi:10.4049/jimmunol.180.3.1719

Purohit, P., Perez-Branguli, F., Prots, I., Borger, E., Gunn-Moore, F., Welzel, O., . . . Mielenz, D. (2014). The Ca2+ sensor protein swiprosin-1/EFhd2 is present in neurites and involved in kinesin-mediated transport in neurons. PLoS One, 9(8), e103976. doi:10.1371/journal.pone.0103976

Qin, Y., & Bishop, C. E. (2005). Sox9 is sufficient for functional testis development producing fertile male mice in the absence of Sry. Hum Mol Genet, 14(9), 1221-1229. doi:10.1093/hmg/ddi133

Qin, Y., Kong, L. K., Poirier, C., Truong, C., Overbeek, P. A., & Bishop, C. E. (2004). Long-range activation of Sox9 in Odd Sex (Ods) mice. Hum Mol Genet, 13(12), 1213-1218. doi:10.1093/hmg/ddh141

Rahmoun, M., Lavery, R., Laurent-Chaballier, S., Bellora, N., Philip, G. K., Rossitto, M., . . . Poulat, F. (2017). In mammalian foetal testes, SOX9 regulates expression of its target genes by binding to genomic regions with conserved signatures. Nucleic Acids Res, 45(12), 7191-7211. doi:10.1093/nar/gkx328

Rajamanickam, G. D., Kastelic, J. P., & Thundathil, J. C. (2017). The ubiquitous isoform of Na/K-ATPase (ATP1A1) regulates junctional proteins, connexin 43 and claudin 11 via Src-EGFR-ERK1/2-CREB pathway in rat Sertoli cells. Biol Reprod, 96(2), 456-468. doi:10.1095/biolreprod.116.141267

Ran, F. A., Hsu, P. D., Wright, J., Agarwala, V., Scott, D. A., & Zhang, F. (2013). Genome engineering using the CRISPR-Cas9 system. Nat Protoc, 8(11), 2281-2308. doi:10.1038/nprot.2013.143

Read, R., Hansen, G., Kramer, J., Finch, R., Li, L., & Vogel, P. (2009). Ectonucleoside triphosphate diphosphohydrolase type 5 (Entpd5)-deficient mice develop progressive hepatopathy, hepatocellular tumors, and spermatogenic arrest. Vet Pathol, 46(3), 491-504. doi:10.1354/vp.08-VP-0201-R-AM

Rebourcet, D., Darbey, A., Monteiro, A., Soffientini, U., Tsai, Y. T., Handel, I., . . . O'Shaughnessy, P. J. (2017). Sertoli Cell Number Defines and Predicts Germ and Leydig Cell Population Sizes in the Adult Mouse Testis. Endocrinology, 158(9), 2955-2969. doi:10.1210/en.2017-00196

Ribeiro, C. M., Reece, J., & Putney, J. W., Jr. (1997). Role of the cytoskeleton in calcium signaling in NIH 3T3 cells. An intact cytoskeleton is required for agonist-induced [Ca2+]i signaling, but not for capacitative calcium entry. J Biol Chem, 272(42), 26555-26561.

Riccardi, V. M., Sujansky, E., Smith, A. C., & Francke, U. (1978). Chromosomal imbalance in the Aniridia-Wilms' tumor association: 11p interstitial deletion. Pediatrics, 61(4), 604-610.

Richardson, B. E., & Lehmann, R. (2010). Mechanisms guiding primordial germ cell migration: strategies from different organisms. Nat Rev Mol Cell Biol, 11(1), 37-49. doi:10.1038/nrm2815

Roadmap Epigenomics, C., Kundaje, A., Meuleman, W., Ernst, J., Bilenky, M., Yen, A., . . . Kellis, M. (2015). Integrative analysis of 111 reference human epigenomes. Nature, 518(7539), 317-330. doi:10.1038/nature14248

Robinson, M. D., & Oshlack, A. (2010). A scaling normalization method for differential expression analysis of RNA-seq data. Genome Biol, 11(3), R25. doi:10.1186/gb-2010-11-3-r25

Rodriguez-Santiago, M., Mendoza-Torres, M., Jimenez-Bremont, J. F., & Lopez-Revilla, R. (2007). Knockout of the trcp3 gene causes a recessive neuromotor disease in mice. Biochem Biophys Res Commun, 360(4), 874-879. doi:10.1016/j.bbrc.2007.06.150

Rodriguez-Zabala, M., Aza-Carmona, M., Rivera-Pedroza, C. I., Belinchon, A., Guerrero-Zapata, I., Barraza-Garcia, J., . . . Heath, K. E. (2017). FGF9 mutation causes craniosynostosis along with multiple synostoses. Hum Mutat, 38(11), 1471-1476. doi:10.1002/humu.23292

Ross, A. J., Tilman, C., Yao, H., MacLaughlin, D., & Capel, B. (2003). AMH induces mesonephric cell migration in XX gonads. Mol Cell Endocrinol, 211(1-2), 1-7.

Rousseau, J., Klinger, S., Rachalski, A., Turgeon, B., Deleris, P., Vigneault, E., . . . Meloche, S. (2010). Targeted inactivation of Mapk4 in mice reveals specific nonredundant functions of Erk3/Erk4 subfamily mitogen-activated protein kinases. Mol Cell Biol, 30(24), 5752-5763. doi:10.1128/MCB.01147-10

Roy, A., & Pahan, K. (2013). Ankyrin repeat and BTB/POZ domain containing protein-2 inhibits the aggregation of alpha-synuclein: implications for Parkinson's disease. FEBS Lett, 587(21), 3567-3574. doi:10.1016/j.febslet.2013.09.020

Sadovsky, Y., Crawford, P. A., Woodson, K. G., Polish, J. A., Clements, M. A., Tourtellotte, L. M., . . . Milbrandt, J. (1995). Mice deficient in the orphan receptor steroidogenic factor 1 lack adrenal glands and gonads but express P450 side-chain-cleavage enzyme in the placenta and have normal embryonic serum levels of corticosteroids. Proc Natl Acad Sci U S A, 92(24), 10939-10943. doi:10.1073/pnas.92.24.10939

Sakakibara, S., Nakamura, Y., Yoshida, T., Shibata, S., Koike, M., Takano, H., . . . Okano, H. (2002). RNA-binding protein Musashi family: roles for CNS stem cells and a subpopulation of ependymal cells revealed by targeted disruption and antisense ablation. Proc Natl Acad Sci U S A, 99(23), 15194-15199. doi:10.1073/pnas.232087499

Salz, H. K. (2011). Sex determination in insects: a binary decision based on alternative splicing. Curr Opin Genet Dev, 21(4), 395-400. doi:10.1016/j.gde.2011.03.001

Schepers, G., Wilson, M., Wilhelm, D., & Koopman, P. (2003). SOX8 is expressed during testis differentiation in mice and synergizes with SF1 to activate the Amh promoter in vitro. J Biol Chem, 278(30), 28101-28108. doi:10.1074/jbc.M304067200

Schlingmann, K. P., Bandulik, S., Mammen, C., Tarailo-Graovac, M., Holm, R., Baumann, M., . . . Konrad, M. (2018). Germline De Novo Mutations in ATP1A1 Cause Renal Hypomagnesemia, Refractory Seizures, and Intellectual Disability. Am J Hum Genet, 103(5), 808-816. doi:10.1016/j.ajhg.2018.10.004

Schmahl, J., & Capel, B. (2003). Cell proliferation is necessary for the determination of male fate in the gonad. Dev Biol, 258(2), 264-276.

Schmahl, J., Eicher, E. M., Washburn, L. L., & Capel, B. (2000). Sry induces cell proliferation in the mouse gonad. Development, 127(1), 65-73.

Schmahl, J., Kim, Y., Colvin, J. S., Ornitz, D. M., & Capel, B. (2004). Fgf9 induces proliferation and nuclear localization of FGFR2 in Sertoli precursors during male sex determination. Development, 131(15), 3627-3636. doi:10.1242/dev.01239

Schmidt, D., Ovitt, C. E., Anlag, K., Fehsenfeld, S., Gredsted, L., Treier, A. C., & Treier, M. (2004). The murine winged-helix transcription factor Foxl2 is required for granulosa cell differentiation and ovary maintenance. Development, 131(4), 933-942. doi:10.1242/dev.00969

Schurmann, A., Koling, S., Jacobs, S., Saftig, P., Krauss, S., Wennemuth, G., . . . Joost, H. G. (2002). Reduced sperm count and normal fertility in male mice with targeted disruption of the ADP-ribosylation factor-like 4 (Arl4) gene. Mol Cell Biol, 22(8), 2761-2768.

Seeherunvong, T., Perera, E. M., Bao, Y., Benke, P. J., Benigno, A., Donahue, R. P., & Berkovitz, G. D. (2004). 46,XX sex reversal with partial duplication of chromosome arm 22q. Am J Med Genet A, 127A(2), 149-151. doi:10.1002/ajmg.a.20630

Sekido, R., & Lovell-Badge, R. (2008). Sex determination involves synergistic action of SRY and SF1 on a specific Sox9 enhancer. Nature, 453(7197), 930-934. doi:10.1038/nature06944

Sekido, R., & Lovell-Badge, R. (2013). Genetic control of testis development. Sex Dev, 7(1-3), 21-32. doi:10.1159/000342221

Seo, S., Asai, T., Saito, T., Suzuki, T., Morishita, Y., Nakamoto, T., . . . Hirai, H. (2005). Crk-associated substrate lymphocyte type is required for lymphocyte trafficking and marginal zone B cell maintenance. J Immunol, 175(6), 3492-3501.

Shagisultanova, E., Gaponova, A. V., Gabbasov, R., Nicolas, E., & Golemis, E. A. (2015). Preclinical and clinical studies of the NEDD9 scaffold protein in cancer and other diseases. Gene, 567(1), 1-11. doi:10.1016/j.gene.2015.04.086

Sharpe, R. M., McKinnell, C., Kivlin, C., & Fisher, J. S. (2003). Proliferation and functional maturation of Sertoli cells, and their relevance to disorders of testis function in adulthood. Reproduction, 125(6), 769-784.

Shumar, S. A., Kerr, E. W., Geldenhuys, W. J., Montgomery, G. E., Fagone, P., Thirawatananond, P., . . . Leonardi, R. (2018). Nudt19 is a renal CoA diphosphohydrolase with biochemical and regulatory properties that are distinct from the hepatic Nudt7 isoform. J Biol Chem, 293(11), 4134-4148. doi:10.1074/jbc.RA117.001358

Simon, L., Ekman, G. C., Garcia, T., Carnes, K., Zhang, Z., Murphy, T., . . . Hofmann, M. C. (2010). ETV5 regulates sertoli cell chemokines involved in mouse stem/progenitor spermatogonia maintenance. Stem Cells, 28(10), 1882-1892. doi:10.1002/stem.508

Sinclair, A. H., Berta, P., Palmer, M. S., Hawkins, J. R., Griffiths, B. L., Smith, M. J., . . . Goodfellow, P. N. (1990). A gene from the human sex-determining region encodes a protein with homology to a conserved DNA-binding motif. Nature, 346(6281), 240-244. doi:10.1038/346240a0

Singh, M., Cowell, L., Seo, S., O'Neill, G., & Golemis, E. (2007). Molecular basis for HEF1/NEDD9/Cas-L action as a multifunctional co-ordinator of invasion, apoptosis and cell cycle. Cell Biochem Biophys, 48(1), 54-72.

Skakkebaek, N. E., Rajpert-De Meyts, E., & Main, K. M. (2001). Testicular dysgenesis syndrome: an increasingly common developmental disorder with environmental aspects. Hum Reprod, 16(5), 972-978.

Small, C. L., Shima, J. E., Uzumcu, M., Skinner, M. K., & Griswold, M. D. (2005). Profiling gene expression during the differentiation and development of the murine embryonic gonad. Biol Reprod, 72(2), 492-501. doi:10.1095/biolreprod.104.033696

Sock, E., Schmidt, K., Hermanns-Borgmeyer, I., Bosl, M. R., & Wegner, M. (2001). Idiopathic weight reduction in mice deficient in the high-mobility-group transcription factor Sox8. Mol Cell Biol, 21(20), 6951-6959. doi:10.1128/MCB.21.20.6951-6959.2001

Sohn, W. J., Kim, J. Y., Kim, D., Park, J. A., Lee, Y., & Kwon, H. J. (2016). Expression and characterization of transmembrane and coiled-coil domain family 3. BMB Rep, 49(11), 629-634. doi:10.5483/bmbrep.2016.49.11.151

Southard-Smith, E. M., Kos, L., & Pavan, W. J. (1998). Sox10 mutation disrupts neural crest development in Dom Hirschsprung mouse model. Nat Genet, 18(1), 60-64. doi:10.1038/ng0198-60

Spiller, C. M., & Bowles, J. (2015). Sex determination in mammalian germ cells. Asian J Androl, 17(3), 427-432. doi:10.4103/1008-682X.150037

Srinivasan, B., Kolli, A. R., Esch, M. B., Abaci, H. E., Shuler, M. L., & Hickman, J. J. (2015). TEER measurement techniques for in vitro barrier model systems. J Lab Autom, 20(2), 107-126. doi:10.1177/2211068214561025

Stanton, P. G. (2016). Regulation of the blood-testis barrier. Semin Cell Dev Biol, 59, 166-173. doi:10.1016/j.semcdb.2016.06.018

Stevant, I., & Nef, S. (2018). Single cell transcriptome sequencing: A new approach for the study of mammalian sex determination. Mol Cell Endocrinol, 468, 11-18. doi:10.1016/j.mce.2018.01.013

Stolt, C. C., Schlierf, A., Lommes, P., Hillgartner, S., Werner, T., Kosian, T., . . . Wegner, M. (2006). SoxD proteins influence multiple stages of oligodendrocyte development and modulate SoxE protein function. Dev Cell, 11(5), 697-709. doi:10.1016/j.devcel.2006.08.011

Stypmann, J., Glaser, K., Roth, W., Tobin, D. J., Petermann, I., Matthias, R., . . . Reinheckel, T. (2002). Dilated cardiomyopathy in mice deficient for the lysosomal cysteine peptidase cathepsin L. Proc Natl Acad Sci U S A, 99(9), 6234-6239. doi:10.1073/pnas.092637699

Sudbeck, P., Schmitz, M. L., Baeuerle, P. A., & Scherer, G. (1996). Sex reversal by loss of the C-terminal transactivation domain of human SOX9. Nat Genet, 13(2), 230-232. doi:10.1038/ng0696-230

Suzuki, M., & Mizuno, A. (2004). A novel human Cl(-) channel family related to Drosophila flightless locus. J Biol Chem, 279(21), 22461-22468. doi:10.1074/jbc.M313813200

Svingen, T., & Koopman, P. (2007). Involvement of homeobox genes in mammalian sexual development. Sex Dev, 1(1), 12-23. doi:10.1159/000096235

Svingen, T., & Koopman, P. (2013). Building the mammalian testis: origins, differentiation, and assembly of the component cell populations. Genes Dev, 27(22), 2409-2426. doi:10.1101/gad.228080.113

Symon, A., & Harley, V. (2017). SOX9: A genomic view of tissue specific expression and action. Int J Biochem Cell Biol, 87, 18-22. doi:10.1016/j.biocel.2017.03.005

Tamaki, T., Kamatsuka, K., Sato, T., Morooka, S., Otsuka, K., Hattori, M., & Sugiyama, T. (2017). A novel transmembrane protein defines the endoplasmic reticulum stress-induced cell death pathway. Biochem Biophys Res Commun, 486(1), 149-155. doi:10.1016/j.bbrc.2017.03.017

Tanno, H., Yamaguchi, T., Goto, E., Ishido, S., & Komada, M. (2012). The Ankrd 13 family of UIM-bearing proteins regulates EGF receptor endocytosis from the plasma membrane. Mol Biol Cell, 23(7), 1343-1353. doi:10.1091/mbc.E11-09-0817

Tarlungeanu, D. C., Deliu, E., Dotter, C. P., Kara, M., Janiesch, P. C., Scalise, M., . . . Novarino, G. (2016). Impaired Amino Acid Transport at the Blood Brain Barrier Is a Cause of Autism Spectrum Disorder. Cell, 167(6), 1481-1494 e1418. doi:10.1016/j.cell.2016.11.013

Tevosian, S. G., Albrecht, K. H., Crispino, J. D., Fujiwara, Y., Eicher, E. M., & Orkin, S. H. (2002). Gonadal differentiation, sex determination and normal Sry expression in mice require direct interaction between transcription partners GATA4 and FOG2. Development, 129(19), 4627-4634.

Thatcher, J. W., Shaw, J. M., & Dickinson, W. J. (1998). Marginal fitness contributions of nonessential genes in yeast. Proc Natl Acad Sci U S A, 95(1), 253-257.

Tilmann, C., & Capel, B. (1999). Mesonephric cell migration induces testis cord formation and Sertoli cell differentiation in the mammalian gonad. Development, 126(13), 2883-2890.

Timmons, P. M., Rigby, P. W., & Poirier, F. (2002). The murine seminiferous epithelial cycle is pre-figured in the Sertoli cells of the embryonic testis. Development, 129(3), 635-647.

Toscani, A., Mettus, R. V., Coupland, R., Simpkins, H., Litvin, J., Orth, J., . . . Reddy, E. P. (1997). Arrest of spermatogenesis and defective breast development in mice lacking A-myb. Nature, 386(6626), 713-717. doi:10.1038/386713a0

Tsuji-Hosokawa, A., Kashimada, K., Kato, T., Ogawa, Y., Nomura, R., Takasawa, K., . . . Morio, T. (2018). Peptidyl arginine deiminase 2 (Padi2) is expressed in Sertoli cells in a specific manner and regulated by SOX9 during testicular development. Sci Rep, 8(1), 13263. doi:10.1038/s41598-018-31376-8

Tyagi, G., Carnes, K., Morrow, C., Kostereva, N. V., Ekman, G. C., Meling, D. D., . . . Cooke, P. S. (2009). Loss of Etv5 decreases proliferation and RET levels in neonatal mouse testicular germ cells and causes an abnormal first wave of spermatogenesis. Biol Reprod, 81(2), 258-266. doi:10.1095/biolreprod.108.075200

Uda, M., Ottolenghi, C., Crisponi, L., Garcia, J. E., Deiana, M., Kimber, W., . . . Pilia, G. (2004). Foxl2 disruption causes mouse ovarian failure by pervasive blockage of follicle development. Hum Mol Genet, 13(11), 1171-1181. doi:10.1093/hmg/ddh124

Uhlenhaut, N. H., Jakob, S., Anlag, K., Eisenberger, T., Sekido, R., Kress, J., . . . Treier, M. (2009). Somatic sex reprogramming of adult ovaries to testes by FOXL2 ablation. Cell, 139(6), 1130-1142. doi:10.1016/j.cell.2009.11.021

Umehara, F., Tate, G., Itoh, K., Yamaguchi, N., Douchi, T., Mitsuya, T., & Osame, M. (2000). A novel mutation of desert hedgehog in a patient with 46,XY partial gonadal dysgenesis accompanied by minifascicular neuropathy. Am J Hum Genet, 67(5), 1302-1305. doi:10.1016/S0002-9297(07)62958-9

Ungewitter, E. K., & Yao, H. H. (2013). How to make a gonad: cellular mechanisms governing formation of the testes and ovaries. Sex Dev, 7(1-3), 7-20. doi:10.1159/000338612

Vasioukhin, V., Bowers, E., Bauer, C., Degenstein, L., & Fuchs, E. (2001). Desmoplakin is essential in epidermal sheet formation. Nat Cell Biol, 3(12), 1076-1085. doi:10.1038/ncb1201-1076

Vidal, V. P., Chaboissier, M. C., de Rooij, D. G., & Schedl, A. (2001). Sox9 induces testis development in XX transgenic mice. Nat Genet, 28(3), 216-217. doi:10.1038/90046

Viger, R. S., Mertineit, C., Trasler, J. M., & Nemer, M. (1998). Transcription factor GATA-4 is expressed in a sexually dimorphic pattern during mouse gonadal development and is a potent activator of the Mullerian inhibiting substance promoter. Development, 125(14), 2665-2675.

Wagner, T., Wirth, J., Meyer, J., Zabel, B., Held, M., Zimmer, J., . . . Scherer, G. (1994). Autosomal sex reversal and campomelic dysplasia are caused by mutations in and around the SRY-related gene SOX9. Cell, 79(6), 1111-1120.

Wallenstein, E. J., Barminko, J., Schloss, R. S., & Yarmush, M. L. (2010). Serum starvation improves transient transfection efficiency in differentiating embryonic stem cells. Biotechnol Prog, 26(6), 1714-1723. doi:10.1002/btpr.472

Wallis, M. C., Waters, P. D., Delbridge, M. L., Kirby, P. J., Pask, A. J., Grutzner, F., . . . Graves, J. A. (2007). Sex determination in platypus and echidna: autosomal location of SOX3 confirms the absence of SRY from monotremes. Chromosome Res, 15(8), 949-959. doi:10.1007/s10577-007-1185-3

Wang, D., Kelly, B. B., Albrecht, D. E., Adams, M. E., Froehner, S. C., & Feng, G. (2007). Complete deletion of all alpha-dystrobrevin isoforms does not reveal new neuromuscular junction phenotype. Gene Expr, 14(1), 47-57.

Wang, E., Sun, S., Qiao, B., Duan, W., Huang, G., An, Y., . . . Wang, H. (2013). Identification of functional mutations in GATA4 in patients with congenital heart disease. PLoS One, 8(4), e62138. doi:10.1371/journal.pone.0062138

Wang, T., Wei, J. J., Sabatini, D. M., & Lander, E. S. (2014). Genetic screens in human cells using the CRISPR-Cas9 system. Science, 343(6166), 80-84. doi:10.1126/science.1246981

Warr, N., Carre, G. A., Siggers, P., Faleato, J. V., Brixey, R., Pope, M., . . . Greenfield, A. (2012). Gadd45gamma and Map3k4 interactions regulate mouse testis determination via p38 MAPK-mediated control of Sry expression. Dev Cell, 23(5), 1020-1031. doi:10.1016/j.devcel.2012.09.016

Warr, N., Siggers, P., Carre, G. A., Wells, S., & Greenfield, A. (2016). Genetic Analyses Reveal Functions for MAP2K3 and MAP2K6 in Mouse Testis Determination. Biol Reprod, 94(5), 103. doi:10.1095/biolreprod.115.138057

Wei, S. C., Tan, Y. Y., Weng, M. T., Lai, L. C., Hsiao, J. H., Chuang, E. Y., . . . Wong, J. M. (2014). SLCO3A1, A novel crohn's disease-associated gene, regulates nf-kappaB activity and associates with intestinal perforation. PLoS One, 9(6), e100515. doi:10.1371/journal.pone.0100515

White, S., Ohnesorg, T., Notini, A., Roeszler, K., Hewitt, J., Daggag, H., . . . Sinclair, A. (2011). Copy number variation in patients with disorders of sex development due to 46,XY gonadal dysgenesis. PLoS One, 6(3), e17793. doi:10.1371/journal.pone.0017793

Wilhelm, D., & Englert, C. (2002). The Wilms tumor suppressor WT1 regulates early gonad development by activation of Sf1. Genes Dev, 16(14), 1839-1851. doi:10.1101/gad.220102

Wilhelm, D., Hiramatsu, R., Mizusaki, H., Widjaja, L., Combes, A. N., Kanai, Y., & Koopman, P. (2007). SOX9 regulates prostaglandin D synthase gene transcription in vivo to ensure testis development. J Biol Chem, 282(14), 10553-10560. doi:10.1074/jbc.M609578200

Wilkinson, B., Chen, J. Y., Han, P., Rufner, K. M., Goularte, O. D., & Kaye, J. (2002). TOX: an HMG box protein implicated in the regulation of thymocyte selection. Nat Immunol, 3(3), 272-280. doi:10.1038/ni767

Willerton, L., Smith, R. A., Russell, D., & Mackay, S. (2004). Effects of FGF9 on embryonic Sertoli cell proliferation and testicular cord formation in the mouse. Int J Dev Biol, 48(7), 637-643. doi:10.1387/ijdb.031778lw

Wilson, M. J., Jeyasuria, P., Parker, K. L., & Koopman, P. (2005). The transcription factors steroidogenic factor-1 and SOX9 regulate expression of Vanin-1 during mouse testis development. J Biol Chem, 280(7), 5917-5923. doi:10.1074/jbc.M412806200

Wilson, R. C., & Doudna, J. A. (2013). Molecular mechanisms of RNA interference. Annu Rev Biophys, 42, 217-239. doi:10.1146/annurev-biophys-083012-130404

Yang, X., Liang, R., Liu, C., Liu, J. A., Cheung, M. P. L., Liu, X., . . . Cheung, M. (2019). SOX9 is a dose-dependent metastatic fate determinant in melanoma. J Exp Clin Cancer Res, 38(1), 17. doi:10.1186/s13046-018-0998-6

Yao, H. H., Whoriskey, W., & Capel, B. (2002). Desert Hedgehog/Patched 1 signaling specifies fetal Leydig cell fate in testis organogenesis. Genes Dev, 16(11), 1433-1440. doi:10.1101/gad.981202

Yao, K., Lu, H., Cheng, H., & Zhou, R. (2006). Mutation of siRNA results in thermodynamically unstable duplex which influences knockdown of dmrt1 by RNA interference. Front Biosci, 11, 2623-2630.

Ye, X., He, L., Ma, J., Li, Y., Zhang, M., Yang, J., . . . Wei, H. (2018). Downregulation of Glt25d1 aggravates carbon tetrachlorideinduced acute hepatic injury through activation of the TGFbeta1/Smad2 signaling pathway. Mol Med Rep, 18(4), 3611-3618. doi:10.3892/mmr.2018.9392

Zhang, X., Bolt, M., Guertin, M. J., Chen, W., Zhang, S., Cherrington, B. D., . . . Coonrod, S. A. (2012). Peptidylarginine deiminase 2-catalyzed histone H3 arginine 26 citrullination facilitates estrogen receptor alpha target gene activation. Proc Natl Acad Sci U S A, 109(33), 13331-13336. doi:10.1073/pnas.1203280109

Zhang, Y., Liu, T., Meyer, C. A., Eeckhoute, J., Johnson, D. S., Bernstein, B. E., . . . Liu, X. S. (2008). Model-based analysis of ChIP-Seq (MACS). Genome Biol, 9(9), R137. doi:10.1186/gb-2008-9-9-r137

Zhang, Z., Zheng, F., You, Y., Ma, Y., Lu, T., Yue, W., & Zhang, D. (2016). Growth arrest specific gene 7 is associated with schizophrenia and regulates neuronal migration and morphogenesis. Mol Brain, 9(1), 54. doi:10.1186/s13041-016-0238-y

Zhao, L., Svingen, T., Ng, E. T., & Koopman, P. (2015). Female-to-male sex reversal in mice caused by transgenic overexpression of Dmrt1. Development, 142(6), 1083-1088. doi:10.1242/dev.122184

Zhu, G., Warren, L., Aponte, J., Gulsvik, A., Bakke, P., Anderson, W. H., . . . International, C. G. N. I. (2007). The SERPINE2 gene is associated with chronic obstructive pulmonary disease in two large populations. Am J Respir Crit Care Med, 176(2), 167-173. doi:10.1164/rccm.200611-1723OC

Appendices

Appendix 1

Materials and General Methods:

General materials and methods are described here. Sections describing specific methods have been included in each chapter

Chemicals and reagents:

Chemical	Manufacturer
Ampicillin	Sigma Aldrich
Antibiotic-Antimyotic	Gibco
Antigen Citrate-based unmasking solution	Vector, H-3300
Butyrate	Sigma Aldrich
Dako Fluorescent Mounting Medium	Dako, Agilent Technologies
DMEM/F12 + Glutamax	Gibco
DNA grade Ethanol	Sigma Aldrich
DynabeadsTM Protein A	Invitrogen
Ethylene glycol-bis(β-aminoethylether) (EGTA)	Sigma Aldrich
Ethylenediaminetetraacetate (EDTA)	Sigma Aldrich
Fetal Bovine Serum	Gibco
Formaldehyde	Sigma Aldrich
Glycine	Sigma Aldrich
Lipofectamine 2000	Invitrogen
Na-deoxycholate	Sigma Aldrich
Optimal Cutting Temperature compound (OCT)	Tissue-Tek
Opti-MEM	Gibco
Paraformaldehyde (PFA)	Sigma Aldrich
Phosphate buffered saline (tissue culture grade)	Gibco
Proteinase K	Invitrogen
PVDF membrane	Millipore
Sodium dodecyl sulphate (SDS)	Sigma Aldrich
Sudan Black B, Fat soluble diazo dye	Abcam
TRI Reagent®	Sigma Aldrich
Tris-Hydrochloride (Tris-HCl)	Sigma Aldrich
Triton X-100	Sigma Aldrich
Tween 20	Sigma Aldrich
Versene	Gibco

X-tremeGENE 9 DNA Transfection Reagent	Sigma Aldrich
Yeast Extract	Sigma Aldrich

Kits:

Kit	Manufacturer
Dual-Luciferase Reporter Assay System	Promega
ECL Western Blotting Kit	GE Healthcare Life Sciences
Genopure Plasmid Midi Kit	Roche
Mouse On Mouse (MOM) immunodetection kit	Vector
NE-PER Kit	Pierce Biotechnology
QuantiTect Reverse Transcription Kit	Qiagen
QuantiTect SYBR® Green Lightcycler RT-PCR Kit	Qiagen

Standard buffers and solutions:

Solution	Composition
ChIP Elution Buffer	20mM Tris-HCl, pH 7.5 5mM EDTA 50mM NaCl
ChIP Lysis buffer	50mM Tris-HCl, pH 8.0 10mM EDTA 1% SDS Protease cocktail inhibitor 1mM Phenylmethylsulfonyl fluoride 20mM Butyrate
ChIP TE Buffer	10mM Tris-HCl, pH 8.0 10mM EDTA
Growth Medium	DMEM/F12 + Glutamax 10% Fetal Bovine Serum 1% Antibiotic-Antimyotic
Lysogeny Broth (LB) Agar	1.5% bactoagar added to LB medium Autoclave and add ampicillin when medium has reached 55°C

LB Medium	1% (w/v) NaCl
	1% (w/v) tryptone
	0.5% yeast extract
Phosphate Buffered Saline (PBS)	10mM Na_2HPO_4
	1.8mM KH_2PO_4
	2.7mM KCl
	137mM NaCl
	Adjust pH tp7.3 with HCl
Radioimmunoprecipitation assay (RIPA) buffer	10mM Tris-HCl, pH 7.5
	1mM EDTA
	0.5mM EGTA
	1% Triton X-100
	0.1% SDS
	0.1% Na-deoxycholate
	100mM NaCl
	Protease Inhibitor Cocktail
Tris-buffered saline with Tween 20 (TBS-T)	2.7mM KCL
	137mM NaCl
	19mM Tris base
	0.1% Tween 20
	Adjust pH to 7.4
Towbin's running buffer	25mM Tris
	192mM Glycine
	0.1% SDS
Towbin's transfer buffer	25mM Tris
	192mM Glycine
	20% (v/v) Methanol

Plasmids and siRNA:

Name	Source
pcDNA3	Clontech
pcDNA3-*SOX9*	Alankarage et al., 2016
pEF-GFP	Alankarage et al., 2016
Pgl4.10	Promega
siControl	Santa Cruz, sc-37007
siSOX9	Santa Cruz, sc-36533
siNEDD9 A	Sigma Aldrich, SASI_Hs01_00191226
siNEDD9 B	Sigma Aldrich, SASI_Hs01_00191227
Negative Control *siRNA*	Sigma Aldrich, SIC001

Antibodies and cell markers:

Antibody/cell marker	Source
4′,6-diamidino-2-phenylindole (DAPI)	Sigma Aldrich
Donkey anti-Goat Alexa Fluor 594	Thermo Fisher
Donkey anti-Mouse	Merck Millipore, AP160P
Donkey anti-Mouse Alexa Fluor 594	Thermo Fisher
Donkey anti-Rabbit Alexa Fluor 488	Thermo Fisher
Donkey anti-Rabbit Alexa Fluor 594	Thermo Fisher
Goat anti Rabbit	Dako, P0448
Goat anti-AMH	Santa Cruz, sc-6886
Mouse anti-CDH2	DSHB Hybridoma Product MNCD2
Mouse anti-NEDD9	Abcam, ab18056
Mouse anti-TBP	Santa Cruz, sc-421
Mouse anti-β Tubulin	Merck Millipore, MAB3408
Rabbit anti-Laminin	Sigma Aldrich, L9393
Rabbit anti-Phospho-histone H3	Merck Millipore, 06-570
Rabbit anti-SOX9	Merck Millipore, AB5535
Rabbit polyclonal IgG	Abcam, Ab37415

Cell lines:

Cell line	ID	Description
COS-7	ATCC CRL 1651	Monkey kidney fibroblast cell line
NT2/D1 (NTERA 2 cl. D1)	ATCC CRL-1973	Multipotent human testicular embryonic carcinoma cell line

Primers:

Name	Manufacturer
hAMH	Fwd- CCAGCGCTGTCTAGTTTGGT
	Rev- GCAGAGTGGCCTTCTCAAAG
hNEDD9	Fwd- CAAGTGCCACCTTCCTACCA
	Rev- AGACGTCCTTTTGGTATCTGGA
hRPS29	Fwd- GCACTGCTGAGAGCAAGATG
	Rev- ATAGGCAGTGCCAAGGAAGA
hSOX9	Fwd- ATCTGAAGAAGGAGAGCGAG
	Rev- TCAGAAGTCTCCAGAGCTTG

Nedd9 Promoter ChIP primers:

	Forward	Reverse
1	CGCAGGCACAGCTTTCAG	GGCACCGCAGTGCTTAAT
2	GTGGGTTGAGCCGTTTTC	CCGGGACCTTCTCGCTTT
3	ACACTAGTTAAGACAGCATTAAGCACT	ACTGACAAGCGGCTCTGC
4	GCGCTAGATGAAAGCGAGA	AATGAGGTCCGCGATCAG
5	AGCGCCTCCCTCAAGTCT	CAGGGCCTGAGCATTACC
6	GCTGATCGCGGACCTCAT	AGCAAAAAGAAGCGATCACA
7	TGCCCACCCCTAATTCTG	CAGGACGGTTCCCCACTT
8	TGACAAGAACTTGTAATGTGATCG	GGAGGACAGAGTAAGGTTCAGG
9	AAGTGGGGAACCGTCCTG	CAGTTTCTTTAAAATTTGGGTTAATCT
10	GAAAGAACAGGAAAAGGAGATACA	TGAAGGAGTTGCTAGGTCACAG
11	CACAAAAGCAGTCTGACAGTCG	CGTTTCATGTAGAGATTGTGAGG
12	TCTGACAGTCGCGCTTCC	TTTGTTCCCGGAGTTCGT
13	ATGAAACGAACTCCGGGAAC	GGAAAGAAAAAGGGACAGAGAG
14	CTCCGGGCCCCTTTTTACT	CAAACAGTCACACACACACAAA
15	TGCTGATACCTCTCTCTCTCTG	TGCAGACTGACATCGCAAA
16	TGTGTGTGTGACTGTTTGCTTTTT	GCGTGTGCTAGAGGGTTCC
17	TGCGATGTCAGTCTGCAA	GTGTGACCCGCAACTCTGA
18	ACACGCACCAGCGTTTTC	ACCCCATCCGAGAGGTCA
19	GCGACCTTCAGTGGCTTT	GAACTCAGTGGACGGTGATG

Transformation of DNA into Escherichia coli- DH5α competent cells (50μl) were thawed on ice. Cells were incubated with 10ng of plasmid DNA for 20 minutes. The cells were then heat shocked at 42°C for 45 seconds and then allowed to recover on ice for 2 minutes. 1ml of LB medium was added to the cells and they were incubated at 37°C for 1 hour with shaking at 250rpm. 100μl of bacterial culture was spread onto a LB agar plate with 100μg/ml of ampicillin to select positively transformed colonies. Plates were incubated at 37°C overnight.

Midiprep isolation of DNA plasmid- A starter culture was generated by inoculation of a single bacterial colony from a LB agar plate in 3ml of LB medium containing 100μg/ml of ampicillin and incubated for 8 hours at 37°C with shaking at 250rpm. The starter culture was then added to 100-200ml of LB medium containing 100μg/ml of ampicillin and incubated overnight at 37°C with shaking at 250rpm. Plasmid DNA was isolated using the Genopure Midi kit according to the manufacturer's instructions.

NT2/D1 cell culture- Cell lines were sub-cultured every 2-3 days when 90% confluency was reached. Cell culture media was removed by aspiration and cells were washed in PBS. After discarding PBS, cells were submerged in just enough Versene to cover the surface at 37°C for 5 minutes, followed by mechanical dissociation through a pipetteboy to ensure cells were in a single cell suspension. Cells were then diluted to 4x the volume in fresh filtered growth medium. A 1 in 4 dilution was sub-cultured into fresh, filtered growth medium in a new cell culture flask.

Appendix 2

Gene lists from RNAseq analysis

Table 1. Transcriptional profiling of genes activated by Sox9 (Amh-*Cre Sox9*^{*flox/flox*} RNAseq) and cell type enriched genes (Jameson et al., 2012; Rahmoun et al., 2017)

Sertoli cell enriched	Male germ cell enriched	Interstitial/Leydig cell enriched	Granulosa cell enriched	Female germ cell enriched
Gjb2	Uchl1	Hhip	Uchl1	Rnf208
Padi2	Utf1	Sostdc1		Cited1
Sox10	Rbm38	Olfml3		AU015836
Rnf208		Ptch1		Rtn4rl1
Sox9				Cenpv
Gm10863				Fgf13
Tesc				Nudt19
Cldn11				Dsp
Mall				
Jakmip2				
Nt5e				
Gprin3				
Cadps				
Cited1				
Col9a3				
Amh				
Sh3gl2				
Serpine2				
Erbb3				
5330417C22Rik				
2810432L12Rik				
Tmem117				
Dtna				
Trpc3				
AU015836				
Spint2				
Ptgds				
Efhd1				
Cnga1				
Rasl12				
Gstm7				
D3Bwg0562e				
Hist1h2bc				
Kcnh1				
Mapk4				
Col14a1				
Cacna2d2				
Socs2				
Dhh				
Gdnf				
Smtnl2				
Plcb2				
Slco3a1				
Rtn4rl1				
Mmd2				
Rcan1				
Rnd2				
Efhd2				
Adamts16				
Tmcc3				
Tox				
Qsox2				
Shbg				
Cbln4				
Chchd10				
Trim47				
Cenpv				
Mybl1				
Cst9				
Gstm6				
Abtb2				
Limk1				
Entpd5				
Ctsl				

Rab31 Ttyh1 Fgf13 Msi1 Eps8 Ppp1r16b Slc6a8 Fbln2 Slc7a5 Glt25d1 Ankrd13a Tacc1 Ttyh3 Myo7a Tmem185b Nudt19 Dsp Scara5 Fat1 Ctnna2 Synj2 Atp1a1 Slc45a4 Slc20a1 Gpr37 Nedd9 Pak3 Rps6ka2 Tyro3 Plod2 Arhgef10 Slc38a1 Gas7				

Table 2. Transcriptional profiling of genes repressed by Sox9 (Amh-*Cre Sox9*$^{flox/flox}$ RNAseq) and cell type enriched genes (Jameson et al., 2012; Rahmoun et al., 2017)

Sertoli cell enriched	Granulosa cell enriched	Female germ cell enriched
Ccl17 Nxf3 Ppargc1a	Akr1c14 Cacna1d Cgn Cntnap5a Dclk1 Dsc2 Gdpd2 Grik3 Mllt3 Rnf43	Jazf1

Table 3. Lists of genes created when analysing the Mouse and Bovine (MoBo) Sox9 ChIPseqs, Amh-*Cre Sox9^{flox/flox}* RNAseq (published in (Rahmoun et al., 2017)) and E13.5 Sertoli cell enriched genes (Jameson et al., 2012)

MoBo ChIP and downregulated RNAseq	Column 1 and enriched in E13.5 Sertoli cells	Column 1 and not enriched in E13.5 Sertoli cells	Mouse ChIP only, downregulated and enriched in E13.5 Sertoli cells	Bovine ChIP only, downregulated and enriched in E13.5 Sertoli cells
Mybl1	Mybl1	Sox13	Sft2d2	Ankrd56
Serpine2	Serpine2	Gja1	Smyd2	Nkx3-1
Tmem185b	Tmem185b	Col18a1	Socs2	Kif19a
Amh	Amh	Elmo1	Cenpv	Nt5e
Tmcc3	Tmcc3	Ptch1	Trim47	Gprin3
Gas7	Gas7	Basp1	Tmem30b	Lgr5
Smtnl2	Smtnl2	Aard	Nkd2	Cited1
Rtn4rl1	Rtn4rl1	Tuba1c	Gjb2	Col9a3
Rnd2	Rnd2	Olfml2a	Gdnf	Erbb3
Sox9	Sox9	Col27a1	Ank	Ptgds
Entpd5	Entpd5	Kif2c	Trib1	Gstm7
Dsp	Dsp	Col9a2	Slc38a1	D3Bwg0562e
Ctsl	Ctsl	Uchl1	Abca2	Col14a1
Tmem117	Tmem117	Lrrc8b	Qsox2	Rcan1
Sox10	Sox10	Arpc1b	Gm1337	Col2a1
Dhh	Dhh	Foxm1	Rbm38	Hhip
Dtna	Dtna	Ptpn5	Cbln4	Pgp
Mapk4	Mapk4	Mesdc1	Fabp5	Scrib
Abtb2	Abtb2	Stim1	2810432L12Rik	2900010M23Rik
Tyro3	Tyro3	Ssbp4	BC057022	Gstm6
Trpc3	Trpc3	Mmp15	Gng12	Rab31
Atp1a1	Atp1a1	Pvrl1	Mcm2	Ttyh1
Tox	Tox		Lrig1	Fgf13
Sh3gl2	Sh3gl2		Pde2a	Ppp1r16b
Efhd2	Efhd2		Utf1	Col25a1
Ankrd13a	Ankrd13a		Fat1	Sostdc1
Msi1	Msi1		Plod2	Smoc1
Limk1	Limk1			Psmd3
Ttyh3	Ttyh3			Slc20a1
Gpr37	Gpr37			Nedd9
Spint2	Spint2			Rps6ka2
Nudt19	Nudt19			Ucp2
Slco3a1	Slco3a1			Fkbp1a
Arhgef10	Arhgef10			
Tacc1	Tacc1			
Glt25d1	Glt25d1			
Slc7a5	Slc7a5			
Sox13				
Gja1				
Col18a1				
Elmo1				
Ptch1				
Basp1				
Aard				
Tuba1c				
Olfml2a				
Col27a1				
Kif2c				
Col9a2				
Uchl1				
Lrrc8b				
Arpc1b				
Foxm1				
Ptpn5				
Mesdc1				
Stim1				
Ssbp4				
Mmp15				
Pvrl1				

Appendix 3

Development of a new model of human Sertoli cell function

Introduction

Chapter 3 of this thesis has addressed a key challenge in assessing candidate DSD genes for their cellular function in the development of the testis by developing methods of assaying Sertoli cell function. In Chapter 3, *SOX9* was knocked down and changes to Sertoli cell functions were assessed. In Chapter 4, this analytical method was also applied to a candidate SOX9 target gene, *NEDD9*. This successfully predicted a Sertoli cell function, for which a corresponding phenotype was found in the embryonic testis of *Nedd9* knockout mouse gonads.

Whilst providing robust results, the current use of NT2/D1 cells in these assays has its caveats, mainly stemming from the use of short interfering RNA (siRNA) to knockdown the gene of interest. RNA interference is an extensively used approach for reverse genetics, and until recently was undoubtedly the most extensively used approach (Boettcher & McManus, 2015). The use of siRNA relies on the ability of the designed nucleotide to hijack the cells RNA interference machinery and post-transcriptionally target mRNA for degradation. A great advantage of the use of siRNA is that this silencing machinery is present in almost every mammalian cell type so, with a simple transfection a change in transcripts present can be rapidly observed (Wilson & Doudna, 2013). Manipulation with siRNA results in a transient knockdown meaning that gene expression will not be completely abolished, and the effects are not permeant. This is a safe and rapid method of reducing gene expression. However, these features also mean that transfection and siRNA can skew observed phenotypic results in repeat experiments. Additionally, the reduction achieved with siRNA may not be physiologically relevant for enough to elicit a clear cell behavioural change. Furthermore, the RNA interference machinery is mostly found in the cytoplasm meaning that long non-coding RNAs cannot be targeted by this method (Bassett et al., 2014).

Clustered Regularly Interspaced Short Palindromic Repeats (CRISPR) provides a solution to these problems. This relies on the use of a CRISPR associated protein, the most common being Cas9, which is a programmable DNA nuclease (Boettcher & McManus, 2015). Thus, with a properly designed single chimeric guide RNA (sgRNA), Cas9 can be programmed to edit the genome and completely knockout a gene of interest. Unless the gene is essential for the cell, thus causing death with complete ablation, this will exacerbate any phenotypes relative to siRNA knockdown. By creating a stable Cas9 expressing NT2/D1 cell line, the process of CRISPR the speed at which gene editing can be completed can be sped up relative to using a wildtype NT2/D1 cell line. This means that multiple sgRNAs can be screen for

efficiency at the same time using cells from a homogenous origin. It is worth noting however that this approach is also not without its caveats. Firstly, evidence is emerging of off target, long range deletions using CRISPR. Functionally these may have an effect on the cell line created, demanding the need for screening with multiple sgRNAs (Kosicki, Tomberg, & Bradley, 2018). Secondly, this approach is not totally efficient as every copy of the gene needs to be successfully edited in order to achieve homozygous disruption (Ran et al., 2013). Again, this demands the need for screening of several clonal lines. Furthermore, this process takes a lot longer than siRNA knockdown with maximum gene editing observed after 5 to 8 days (Wang, Wei, Sabatini, & Lander, 2014). Therefore, by having both models available, the appropriate direction can be taken given the gene of interest.

Thus, the following experiments aimed to create a stable Cas9 expressing cell line. A proof-of-concept experiment is also planned where the intent is to knockout *SOX9* and compare phenotypic and functional changes with the results observed in Chapter 3 of this thesis.

Methods

All experiments conducted in this appendix have biosafety approval from the Monash University Ethics and Compliance Committee, Project 12177. All viral vectors have been supplied by MHTP Functional Genomics Platform and experiments were undertaken with kind advice of A/Prof. Joseph Rosenbluh

Antibiotic Sensitivity test- NT2/D1 Blasticidin (Gibco #A111-38.03) and Puromycin (Gibco #A111-39.03) sensitivity was tested by culturing wildtype cells as described in (Knower et al., 2007) with a gradient of antibiotic concentrations for 8 and 4 days respectively. Specifically, NT2/D1 cells were seeded in a 12 well plate at a density of 1.3×10^5 cells per well. After 24 hours, the cells were gently washed with 37°C PBS and the media was replaced with fresh culture media and blasticidin or puromycin. Blasticidin or puromycin concentrations ranged from 0-10µg/ml. Cell death was monitored daily, with media and antibiotics replaced every 48 hours. Antibiotics were always prepared fresh from a 10mg/ml stocked stored at -20°C. Optimal concentration was determined when complete cell death was observed after 6 days for blasticidin and 2 days for puromycin.

Virus production- Cas9 expressing virus and validation virus was generated by MHTP Functional Genomics Platform. Future viruses carrying sgRNA will be produced by Harley lab using the following guidelines. HEK293T cells at a low passage were transfected using standard transfection protocols (Knower et al., 2007) with psPAX2 plasmid, pMD2.g plasmid and a transfer plasmid (lentiGuide-puro, www.addgene.org) encoding the donor nucleic acid of interest. Media is collected after 24 and 48 hours, pooled and used in transduction.

Spinfection- In a 12 well plate, 1.3×10^5 NT2/D1 cells were seeded in 1ml of media per well, 2 wells in total. 1000µl of virus was added to well 1 and the equivalent volume of media to well 2. The plate was then centrifuged at 1070g for 30 minutes at room temperature before being placed in an incubator at 37°C. 24 hours post transfection, medium was replaced in both wells with 2ml of normal growth medium heated to 37°C with 0.6µg/ml of blastocidin. Cell death was monitored daily, with media and antibiotics replaced every 48 hours. When all cells in the control well were dead (6 days post transduction) the surviving cells in the infected well were considered transduced. Cells were then expanded and moved into larger vessels with blasticidin maintained in medium at 0.6µg/ml.

Testing of Cas9 activity- In a 12 well plate, 1.3×10^5 NT2/D1-Cas9 cells were seeded in 1ml of media plus 0.6g/ml blastocidin per well, 2 wells in total. In a third well, 1.3×10^5 wildtype NT2/D1 cells were seeded in 1 ml of media only. 1000µl of BRD011 virus (a construct driving co-expression of GFP and a guide which targets the GFP sequence) was added to well 1 (NT2/D1-Cas9) and well 3 (wildtype NT2/D1), and the equivalent volume of media to well 2 (NT2/D1-Cas9). As per the protocol above the plate containing the cells was then centrifuged at 1070g for 30 minutes at room temperature before being placed in an incubator at 37°C. 24 hours post transfection, medium was replaced in both wells with 2ml of normal growth medium (plus 0.6µg/ml blasticidin in wells 1 and 2) heated to 37°C plus 1µg/ml of puromycin. GFP expression and cell death was monitored daily, with media and antibiotics replaced every 48 hours. When all cells in the control well 2 were dead (2 days post transduction) the surviving cells in the infected well were considered transduced. Cells were then expanded and moved into larger vessels with blasticidin maintained in medium at 0.6µg/ml.

sgRNA design- sgRNAs were designed using the Broad Institute sgRNA design tool (https://portals.broadinstitute.org/gpp/public/). Guides were designed for CRISPRko using the SpyoCas9 (NGG) enzyme using the Human GRCh38 genome and sequence of *SOX9*. The top 5 designed sgRNA sequences, as defined using the sgRNA design tool were selected for synthesis. The following published AAVS1 guides were ordered to be synthesised as to use as a control: ATCCTGTCCCTAGTGGCCC (Maggio et al., 2014), GGGGCCACTAGGGACAGGAT (Mali et al., 2013), GGGGCCACTAGGGACAGGAT (Wang et al., 2014).

Results

Active Cas9-expressing NT2/D1 cells

NT2/D1 cells were infected with a virus co-expressing Cas9 and blasticidin resistance. Cells which survived this antibiotic selection were considered Cas9 positive but confirmation of Cas9 activity was still required. Cas9 activity was verified by infecting cells with a construct driving

co-expression of GFP and a sgRNA which targets the GFP sequence. Thus, if the Cas9 protein is active in the NT2/D1 cells, GFP expression will be seen initially and then will be lost. **Figure 1** demonstrates that 1 day post infection with the GFP construct, GFP positive cells are seen in both the wildtype NT2/D1 cells and the NT2/D1-Cas9 cells. As a negative control, NT2/D1-Cas9 cells not infected with the GFP virus are also shown. After 2 days, GFP expression is reduced in the NT2/D1-Cas9 cells while the expression increased in the wildtype NT2/D1 cells. Here, expression is seen as both concentrated patches of green and as a speckled lawn. At 2 days post infection, all negative control cells (NT2/D1-Cas9) are dead due to being grown in puromycin. By 4 days post infection, GFP expression is lost from the NT2/D1-Cas9 cells and is further increased in the wildtype NT2/D1 cells. At day 4, the cells with puromycin resistance are overgrowing resulting in loss of viability. Thus, this experiment demonstrates that NT2/D1 cells expressing stable Cas9 have been produced.
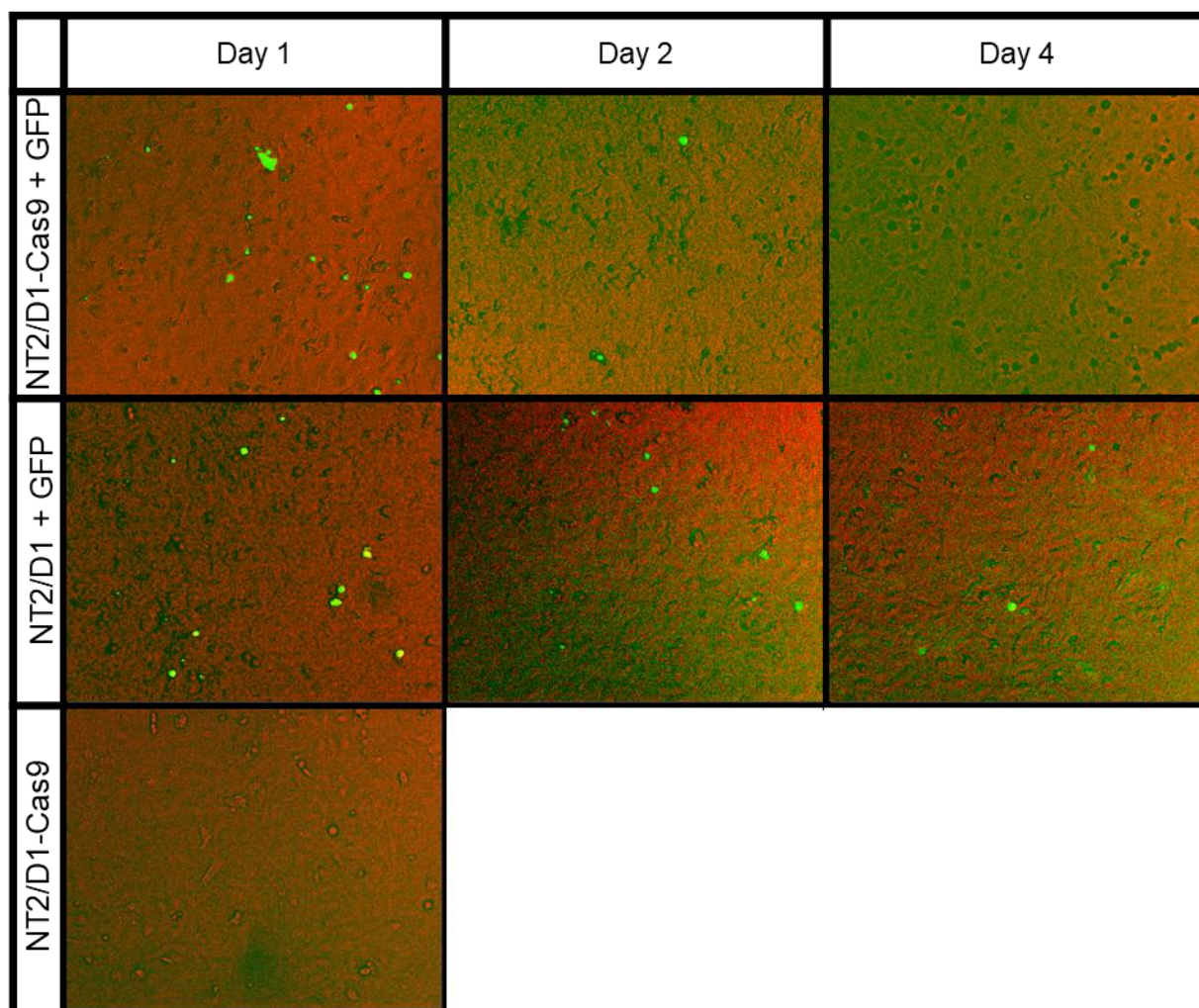
Figure 1 Active Cas9-expressing NT2/D1 cells. Cells were photographed 1, 2 and 4 days post-infection with GFP and corresponding sgRNA construct. NT2/D1-Cas9 refers to cells which have been infected with a Cas9 expressing construct and survived selection using basticidin resistance. +GFP refers to cells which have been infected with the GFP and corresponding sgRNA construct. The negative control, NT2/D1-Cas9 was only photographed for 1 day as all cells were dead by day 2.

Following the production and initial validation of these cells an unforeseeable, catastrophic event resulted in the destruction of the stocks of NT2/D1-Cas9 cells. Despite multiple attempts, they were unable to be recovered. Subsequent experiments designed to knockout *SOX9* therefore could not be completed in the scope of this thesis. These experiments are being repeated by other Harley lab members using the protocols detailed above and the sgRNAs designed in **Table 1**.

Table 1. sgRNAs designed to knockout *SOX9*

sgRNA Cut Position	Orientation	sgRNA Sequence	PAM Sequence	Exon Number	Target Cut Length	On-Target Efficacy Score
72123659	antisense	ACGTCGCGGAAGTCGATAGG	GGG	3	802	0.6528
72122819	antisense	TTCACCGACTTCCTCCGCCG	CGG	2	532	0.663
72121651	sense	CAAAGGCTACGACTGGACGC	TGG	1	260	0.6256
72121481	sense	ACCATGTCCGAGGACTCCGC	GGG	1	90	0.5906
72122962	antisense	ACTCACCCGAGTGCTCGCCG	GGG	2	675	0.6141

Appendix 4

Publications During Enrolment

Contents lists available at ScienceDirect

The International Journal of Biochemistry & Cell Biology

Molecules in focus

SOX9: A genomic view of tissue specific expression and action

Aleisha Symon [a,b], Vincent Harley [a,b,*]

[a] Molecular Genetics and Development Laboratory, Hudson Institute of Medical Research, Melbourne, Australia
[b] Department of Anatomy and Developmental Biology, Monash University, Melbourne, Australia

ABSTRACT

The SOX9 transcription factor controls the differentiation of many cell types among vertebrates. The *SOX9* gene locus is large and complex and contains various tissue-specific enhancers. Individual enhancers direct specific expression of *SOX9* in chondrocytes, Sertoli cells and cranial neural crest cells. Human *SOX9* mutations can lead to either the complete Campomelic Dysplasia syndrome, or isolated clinical features, depending upon whether the mutation occurs in the coding region or in enhancer regions. Chromatin Immunoprecipitation has helped to define SOX9 control of target gene expression at the genome wide level in hair follicle stem cells and in chondrocytes where SOX9 binds at super-enhancers. SOX9 binding proximal to promoters controls basal cell activity whereas cell type specificity is directed from distal enhancers.

© 2017 Elsevier Ltd. All rights reserved.

1. Introduction

SOX9 belongs to the family of S̲R̲Y̲-related high-mobility-group b̲o̲x̲ (SOX) transcription factors that mediate cell fate by activating genes that maintain pluripotency, direct cell lineage differentiation, and sustain adult tissue homeostasis. Human *SOX9* gene mutations cause Campomelic Dysplasia (CD), a severe skeletal malformation syndrome where two thirds of chromosomally XY patients develop as females due to 46 XY, gonadal dysgenesis (Wagner et al., 1994). SOX9 is crucial not only for bone and testes development but also for other somatic tissues such as hair follicles and heart valves (Kadaja et al., 2014; Garside et al., 2015). This review will focus on the tissue-specific, versatile control of both *SOX9* expression and protein function in cell lineage differentiation.

2. *SOX9* gene structure and tissue-specific enhancers

In humans, *SOX9* lies on chromosome 17 in a 3 Mb region devoid of other protein-coding genes and the regulatory region controlling its expression is large and complex (Fig. 1). Human mutations in the coding region of *SOX9* or in the regulatory region results in CD, or aspects of the CD syndrome, such as isolated craniofacial anomalies or testicular dysgenesis. Analysis of patients with varying characteristics of CD has provided insight into the regions which govern

SOX9 expression in a variety of contexts (Gordon et al., 2009). The position of the chromosome breakpoint can dictate the phenotype associated with the disease. For example, copy number variations between 50 and 350 kb upstream of *SOX9* result in bowing of the long bones (Campomelia) (Fig. 1a), and those further upstream result in mild to no bowing (Acampomelia) (Bagheri-Fam et al., 2012). Transgenic reporter studies in mice have also demonstrated that discrete enhancers control *SOX9* expression in different tissues (Fig. 1b). However, the human counterparts of mouse enhancers are not always active in mice. For example, expression of *SOX9* in the mouse testes is controlled in part by a 3.2 kb enhancer located 13 kb upstream of the transcription start site called *TES* (testis-specific enhancer) (Sekido and Lovell-Badge, 2008; Gonen et al., 2017). In transgenic mice, the human *TES* sequence fails to direct testis-specific expression. Despite many human 46, XY gonadal dysgenesis cases being investigated, the human *SOX9* testis enhancer regions remain elusive.

Repression of *SOX9* gene expression is also essential for the function and development of tissues including hair follicles, bone and ovaries (Xu et al., 2015; Uhlenhaut et al., 2009; Hattori et al., 2010). In hair follicles, SOX9 is required to specify stem cells allowing for cyclical hair growth. Repression of *SOX9* by Wnt/β-catenin signalling allows for the initiation of hair follicle growth. Conditional inactivation of β-catenin in epithelial cells led to expanded SOX9 expression in hair follicles and defective hair follicle development (Xu et al., 2015). During bone formation, *SOX9* is expressed in proliferating chondrocytes but disappears from the hypertrophic chondrocytes (Hattori et al., 2010). Misexpression of SOX9 in the hypertrophic chondrocytes in transgenic mice perturbed bone
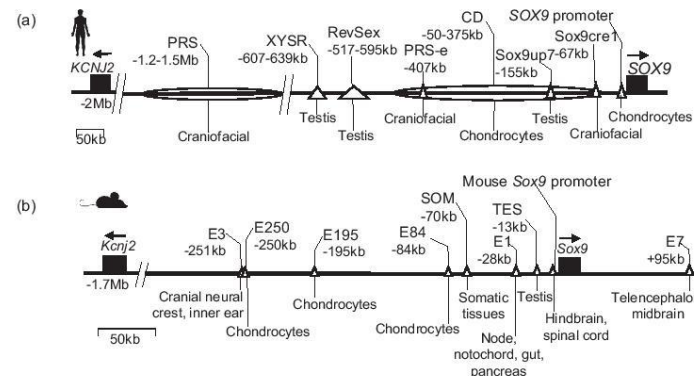
19

Fig. 1. SOX9 gene structure. All genomic locations are shown as distances from the transcription start site of *SOX9*. Descriptions on the under-side of the DNA detail which tissues the enhancer/region is controlling. (a) Schematic representation of the 2 Mb region upstream of the human *SOX9* gene. The *SOX9* regulatory region contains enhancers for *SOX9* expression in a variety of tissues. The position of enhancers (triangles) and regions mutated in aspects of Campomelic Dysplasia (ovals) identified from patient DNA analysis, such as those m| with Pierre-Robin Syndrome (PRS, PRS-e, Sox9cre1 (Benko et al., 2009; Gordon et al., 2014; Jakobsen et al., 2007)), Disorders of Sex Development (XYSR, RevSex (Kim et al., 2015; Hyon et al., 2015)) or Campomelia (CD, SOX9 Promoter (Yao et al., 2015)) are indicated. Sox9up7 was identified from bioinformatic analysis followed by luciferase assay for validation (Ohnesorg et al., 2016). (b) Schematic representation of the 1.7 Mb region upstream and 1 kb region downstream of the mouse *SOX9* gene. Shown are regulatory regions identified and validated using both mutational analyses and transgenic reporter lines to track enhancer activity. E1, E3, E7, Mouse *SOX9* promoter, E84, E195 and E250 activity was identified using *LacZ* reporter lines where the enhancers direct expression in discrete tissues (Yao et al., 2015; Bagheri-Fam et al., 2006). SOM regulates SOX9 expression in a number somatic tissues (pancreas, lung, kidney, salivary gland, gut and liver). Identified through both a *LacZ* transgenic reporter and mouse knockout studies (Mead et al., 2013). *TES*, the testis specific enhancer of *SOX9* expression was discovered by systematic deletions in the 5′ regulatory region of *SOX9* using reporter transgenic mice (Sekido and Lovell-Badge, 2008).

Fig. 2. SOX9 protein structure. The dimerisation domain (DIM) immediately precedes the HMG box. The proline, glutamine, alanine (PQA) rich region and proline, glutamine, serine (PQS) rich region are required for transactivation. Phosphorylation of Serine residues (Ser) facilitate sumoylation and lysine (Lys) residues targets SOX9 for both sumoylation and ubiquitination. First and last amino acid numbers of domains are shown in black (Harley et al., 2003).

vascular invasion, bone marrow formation and endochondral ossification. In the ovaries, suppression of *SOX9* is essential for the differentiation of the bipotential gonad into an ovary rather than into a testis. A direct genomic mechanism has been described whereby FOXL2 acts synergistically with Estrogen Receptor Alpha to repress *SOX9* through binding to *TES* (Uhlenhaut et al., 2009). In the absence of FOXL2 in postnatal mouse ovaries, the female granulosa cells transdifferentiate into male Sertoli cells.

3. General properties of SOX9 protein

The SOX9 protein is comprised of 509 amino acids and four domains; a high-mobility-group box, a dimerization domain and two transactivation domains, one rich in prolines/glutamines/alanines (PQA) and the other rich in prolines/glutamines/serines (PQS) (Fig. 2). The defining feature of the SOX proteins is the highly conserved HMG domain, a DNA binding region which recognises and bends DNA at specific sequences to alter target gene expression (SOX9 motif is AGAACAATGG (Mertin et al., 1999)). SOX9 is a member of the SOXE group (along with SOX8 and SOX10 (Bowles et al., 2000)). The SOXE proteins can form both homo- and hetero-dimers (such as SOX9-SOX9 or SOX9-SOX8. One current model suggests that dimerization is achieved through co-operative binding between the dimerization

domain of one SOXE protein and the HMG box of its partner SOXE protein (Huang et al., 2015). Analysis of DNA binding motifs from SOX9 Chromatin Immunoprecipitation followed by Next Generation Sequencing (ChIPseq) on mouse chondrocytes and from DNase Hypersensitivity arrays (which reveal open chromatin, likely subject to active regulation) in melanoma cells, identified a palindromic SOXE motif separated by 3–5 bases (Huang et al., 2015). However, these sequences were not identified in SOX9 ChIPseq of hair follicles or DNase hypersensitive regions from 57 other human cell lines from the Encyclopedia of DNA Elements (ENCODE) project. This strongly suggests that gene regulation through SOXE dimers is cell-type specific (Huang et al., 2015). Cell specific dimerization is also revealed through human *SOX9* mutations. Mutation in the dimerization domain of *SOX9* results in CD without sex reversal suggesting that Sertoli cell function of SOX9 requires SOX9 as monomers, whereas chondrocyte function requires SOX9 as dimers (SOX9 role in the testis – see Section 4.3) (Bernard et al., 2003).

SOX9 is subject to post translational modifications which alter its nuclear import (phosphorylation and acetylation) and its rate of degradation (ubiquitination and sumoylation) (Sim et al., 2008). For example, Bar Oz et al. proposed a mechanism in chondrocytes by which acetylation regulates SOX9 nuclear import (Bar Oz et al., 2016). TAT Interactive Protein (TIP60) acetylates SOX9 at Lysine 61, 253 and 398 whereas Sirtuin 1 can deacetylate these residues thereby inhibiting TIP60 activity. When SOX9 is hypo-acetylated, it can interact with importin β to facilitate SOX9 nuclear entry and increase target gene expression.

4. SOX9 control of target gene expression in multiple cell types

Evidence is emerging that SOX9 regulates some of its target genes through regions of the genome containing large clusters of transcriptional enhancers called super-enhancers (Whyte et al., 2013). These regions are abundant in Histone H3 acetylated at

lysine 27 (H3K27ac), a modification which prevents repression of the enhancer by methylation. The regions are also abundant in Histone H3 with monomethylation of lysine 4 (H3K4Me1) and Mediator complex, both of which are involved in the initiation of transcription (Adam et al., 2015).

In many cell types SOX9 positively regulates its own transcription. An enhancer region called *SOM* (activator of *SOX9* in somatic tissues), which lies 70 kb upstream of the *SOX9* transcription start site, is involved in *SOX9* auto-regulation in many somatic tissues during mouse development including the pancreas, lung, kidney, salivary gland, gut and liver (Fig. 1b) (Mead et al., 2013). Mutation of *SOM* in mice results in reduced *SOX9* mRNA by 18–37% in somatic tissues during embryonic and early post-natal development. SOX9 ChIP and electrophoretic mobility shift assay showed that SOX9 directly binds and auto-regulates *SOM* as a homodimer. *SOX9* expression in embryonic testis is auto-regulated by another enhancer known as *TES* (testis enhancer of *SOX9* – see Section 2) (Sekido and Lovell-Badge, 2008; Gonen et al., 2017). *SOX9* expression is initiated by the male-specific factor SRY (Sex determining region of the Y chromosome). SRY synergises with the nuclear receptor/transcription factor SF1 (encoded by the gene *NR5A1*) to up-regulate *SOX9* transcription. SOX9 protein binding as a monomer then takes the place of SRY and synergises with SF1 to maintain high levels of SOX9 in Sertoli cells through an auto-regulatory loop (Sekido and Lovell-Badge, 2008). Similar to *SOM*, when *TES* is deleted using a ubiquitous Cre in mice, *SOX9* mRNA was reduced to 44% of wild type level indicating that while it makes a major contribution to overall *SOX9* expression, it does not act alone (Gonen et al., 2017).

To further our understanding of SOX9 function in individual cell types, targeted knockout mice have been generated using the Cre-Lox system, circumventing the embryonic lethality of the complete *SOX9* knockout by day 11.5 (E11.5) (Barrionuevo et al., 2009; Lavery et al., 2011). Transcriptomic analyses comparing wild type and SOX9 null tissue has generated pathways and identified genes responsive to SOX9. These datasets are powerful, particularly when combined with ChIP-seq of the appropriate wild type tissue to identify direct target genes of SOX9. This approach has been successfully applied to chondrocytes, hair follicle stem cells, Sertoli cells and endocardial cushion cells (Kadaja et al., 2014; Oh et al., 2014; Ohba et al., 2015).

4.1. Chondrocytes

In chondrogenesis SOX9 regulates the formation of the endochondral skeleton. The first description of the critical function of SOX9 in chondrogenesis was in 1999 when chimeric mouse embryos were generated with SOX9 knocked out. *SOX9*-null cells were autonomously excluded from chondrocytes undergoing mesenchymal condensation, a critical prerequisite of chondrogenesis. Further to this, teratomas derived from *SOX9* knockout cells failed to form chondrocytes (Bi et al., 1999). Knocking out *SOX9* expression before mesenchymal condensation results in an absence of bone and cartilage. *SOX9* inactivation after mesenchymal condensation causes mice to develop severe chondroplasia due to a complete lack of cartilage, indicating that it is necessary for chondrogenesis at multiple steps (Akiyama et al., 2002).

Probing by ChIPseq revealed that regions upstream of key chondrocyte genes contain peaks of H3K27ac, a characteristic of super-enhancers. Expression of the genes associated with these super-enhancers was significantly higher than those associated with typical enhancers (Ohba et al., 2015). Two other SOX proteins, SOX5 and SOX6 are also necessary for chondrocyte differentiation. SOX5 and SOX6 cooperate with SOX9 at super-enhancers to regulate thousands of target genes (Liu and Lefebvre, 2015). Expression analysis of new-born SOX9 null mouse ribs, indicated that total gene expression was reduced 8–10-fold (Oh et al., 2014). Yet 66% of the downregulated genes showed only a 2-fold reduction in expression indicating that SOX9 might be co-operating with other transcription factors at enhancers to achieve sufficient gene transcription in these cells. In contrast, many of the strongly down-regulated genes were required for extra cellular matrix such as the collagens, a key product of chondrocytes. Over 50% of the genes downregulated in the absence of *SOX9* expression were normally bound by SOX9 as indicated by ChIPseq analysis, showing that at enhancer regions, regulation by SOX9 is largely through direct chromatin contact.

In another study, ChIPseq in new born mouse chondrocytes revealed around 27,000 sites in the genome where SOX9 is binding (Ohba et al., 2015). Analysis of the motifs for SOX9 binding at proximal versus distal enhancers showed that where *SOX9* binds to proximal enhancers, the binding motif is not well conserved. In contrast, where *SOX9* is bound to distal enhancers the consensus binding motifs are well conserved and were often dimeric SOX sites, separated by 4 nucleotides. Analysis of the types of genes downstream of these distinct classes of binding motif led the authors to suggest that SOX9 regulates gene expression by two distinct modes. SOX9 can regulate the basal transcriptional activities of the cell (chondrocyte) indirectly at proximal enhancers, possibly by associating with the proximal basal transcription complex of genes, or can bind directly to DNA as a dimer at distal enhancers to activate the expression of chondrocyte specific genes (Ohba et al., 2015).

4.2. Hair follicle stem cells

SOX9 is expressed in a population of outer root sheath cells where it maintains the stem cell population in hair follicles. Mice with *SOX9* ablated in the hair follicles lack the ability to recover their coat upon loss of hair (Kadaja et al., 2014). Instead of maintaining stem-ness, the outer root sheath cells differentiate down the epidermal lineage. Probing super-enhancers using ChIP revealed that it is likely SOX9 not only controls super-enhancer activity but is also able to initiate binding at super-enhancers and induce H3K27acetylation at regions which were previously silenced (Adam et al., 2015). In hair follicle cells where *SOX9* was ablated, expression of 193 genes was downregulated of which 38% were hair follicle stem cell specific genes. This suggested that SOX9 is essential to establishing the stem cell niche (Kadaja et al., 2014). Further to this, ChIPseq data showed that 33% of the genes downregulated in the knockout were also bound by SOX9, versus 17% of those upregulated. This suggests that SOX9 control of the expression of hair follicle stem cell genes is largely direct and positive, as it is in chondrocytes. Notably, unbiased motif analysis of these ChIPseq peaks showed that there was low sequence specificity for SOX9 binding, and that the SOX9 consensus sequence identified for binding *in vitro* was not enriched. Weak specificity is emerging as a feature of SOX9 target gene regulation; perhaps because sub-optimal binding allows for partners and modifiers to co-operatively bind with SOX9 at super-enhancers and influence the dynamics of target gene expression.

4.3. Sertoli cells

Sertoli cells are the supporting cells of the male gonad which drive the differentiation of the other cell types of the testis. In the mammalian embryo, chromosomally XX mice carrying a *SOX9* transgene expressed in the gonads develop as males, as do XX humans with *SOX9* duplications. This indicates that in the chromosome context of a gene duplication, the likely *SOX9* overexpression is sufficient to direct the formation of the testis in the absence of a Y chromosome (Vidal et al., 2001; Huang et al., 1999). In males, SOX9 directs the differentiation of Sertoli cells, and in humans XY sex

reversal arises from a range of SOX9 mutations. These include deletions encompassing the SOX9 open reading frame, certain missense mutations, as well as long range deletions 609–640 kb upstream of the SOX9 transcription start site that remove putative testis-specific enhancers. (Wagner et al., 1994; Morais da Silva et al., 1996; Barrionuevo et al., 2006; Kim et al., 2015). In humans, heterozygous SOX9 mutations cause CD syndrome with associated sex reversal in 75% of XY cases. In mice this is not the case where gonad development proceeds normally with 50% of wild type SOX9 mRNA (Wagner et al., 1994; Kim et al., 2015). It is not until SOX9 mRNA levels fall below 23% of wild type levels that the first phenotypic and molecular signs of sex reversal are observed (Gonen et al., 2017). As SOX9 null mice die at the onset of testis formation (E11.5), conditional knockouts have been used to investigate its testicular role. SOX9 was conditionally inactivated in the primordial gonad using Cytokeratin 19-Cre/SOX9 flox mice. SOX9 null embryonic XY gonads were completely sex reversed, and developed into ovaries (Barrionuevo et al., 2006). SOX9 has also been knocked out in Sertoli cells after sex determination using Amh-Cre mice (Barrionuevo et al., 2009). In this model Sertoli cells form normally and SOX9 protein is detected at E12.5 but only a few Sertoli cells remain SOX9-positive by E13.5. Testis development in these mice is normal however they develop sterility at 5–6 months of age indicating that SOX9 plays important roles in both the differentiation of the testis and the maintenance of testis function. When these mice are crossed onto a SOX8 null background, inactivation of SOX9 after sex determination leads to a more severe phenotype, the reprogramming of Sertoli cells into their female counterpart, granulosa cells. This shows that SOX8, another SOXE protein can compensate for the loss of SOX9. When both are present they may work together to regulate genes critical in testis development. ChIP analysis with microarray (ChIP-on-Chip) after sex determination (E12.5) identified the promoters of 1900 genes bound by SOX9 in regions 2 kb proximal to the transcription start site (Li et al., 2014). A small number of these genes have been validated as having testicular functions related to SOX9. Soon after the expression of SOX9 is upregulated, two additional regulatory loops maintain SOX9 expression levels via Prostaglandin D2 and FGF9 (Colvin et al., 2001; Moniot et al., 2009). Another SOX9 target gene, Anti-Mullerian Hormone is necessary for the regression of female reproductive structures and Amh mutant mice retain these tracts (Behringer et al., 1994; Arango et al., 1999). Mutation of SOX9 target genes, such as Prostaglandin D Synthase and Fibroblast Growth Factor 9 results in male to female sex reversal, but more targets with an essential role remain to be discovered (Colvin et al., 2001; Moniot et al., 2009).

4.4. Endocardial cushion cells

During embryonic development, the heart valves arise from a precursor population of endocardial cushion cells which express SOX9, and expression persists in endocardial cushion cells in later stages of development. Conditional inactivation of SOX9 using a Tie2-cre resulted in the loss of SOX9 from developing hearts (Garside et al., 2015; Lincoln et al., 2007). Mice die between E11.5 and E14.5 due to defective heart valve maturation suggesting that SOX9 plays an important role in the differentiation, patterning and homeostasis of heart valves (Lincoln et al., 2007; Akiyama et al., 2004). Here, SOX9 upregulates the expression of extra cellular matrix genes, similar to chondrocytes (Garside et al., 2015). A study investigating the differences between chondrocytes and heart valves at E12.5, found that 2453 genes are bound by SOX9 in heart valves, fewer than half of that in the limb buds at the same stage. Of these heart valve genes, 1825 were specific to heart valves, including transcription factors known to have a role in heart development, such as SOX4. This indicates that SOX9 has many tissue-specific roles, in addition to the regulation of basal cell activ-

ities. Moreover, the tissue-specific context affects the nature of SOX9 binding. SOX9 in heart valves binds primarily as a monomer to its target genes, in contrast to SOX9 in chondrocytes where it binds primarily as a dimmer (Garside et al., 2015).

5. Conclusion

From only a small number of tissues are we beginning to understand the complex regulation and action of SOX9 at the genomic level. We have little information on tissues such as the pancreas where SOX9 plays essential roles in the differentiation of multiple cell types (Kopp et al., 2011). Given the complexity and size of the 2 Mb upstream regulatory region of SOX9, many more enhancers will be uncovered. In these unexplored tissues, the cell-specific environment will likely dictate novel regulatory modules upstream of SOX9, and the transcriptional complexes involving SOX9, controlling target gene expression downstream.

References

Adam, R.C., et al., 2015. Pioneer factors govern super-enhancer dynamics in stem cell plasticity and lineage choice. Nature 521 (7552), 366–370.

Akiyama, H., et al., 2002. The transcription factor Sox9 has essential roles in successive steps of the chondrocyte differentiation pathway and is required for expression of Sox5 and Sox6. Genes Dev. 16 (21), 2813–2828.

Akiyama, H., et al., 2004. Essential role of Sox9 in the pathway that controls formation of cardiac valves and septa. Proc. Natl. Acad. Sci. U.S.A. 101 (17), 6502–6507.

Arango, N.A., Lovell-Badge, R., Behringer, R.R., 1999. Targeted mutagenesis of the endogenous mouse Mis gene promoter: in vivo definition of genetic pathways of vertebrate sexual development. Cell 99 (4), 409–419.

Bagheri-Fam, S., et al., 2006. Long-range upstream and downstream enhancers control distinct subsets of the complex spatiotemporal Sox9 expression pattern. Dev. Biol. 291 (2), 382–397.

Bagheri-Fam, S., et al., 2012. Sox9 gene regulation and the loss of the XY/XX sex-determining mechanism in the mole vole Ellobius lutescens. Chromosome Res. 20 (1), 191–199.

Bar Oz, M., et al., 2016. Acetylation reduces SOX9 nuclear entry and ACAN gene transactivation in human chondrocytes. Aging Cell 15 (3), 499–508.

Barrionuevo, F., et al., 2006. Homozygous inactivation of Sox9 causes complete XY sex reversal in mice. Biol. Reprod. 74 (1), 195–201.

Barrionuevo, F., et al., 2009. Testis cord differentiation after the sex determination stage is independent of Sox9 but fails in the combined absence of Sox9 and Sox8. Dev. Biol. 327 (2), 301–312.

Behringer, R.R., Finegold, M.J., Cate, R.L., 1994. Mullerian-inhibiting substance function during mammalian sexual development. Cell 79 (3), 415–425.

Benko, S., et al., 2009. Highly conserved non-coding elements on either side of SOX9 associated with Pierre Robin sequence. Nat. Genet. 41 (3), 359–364.

Bernard, P., et al., 2003. Dimerization of SOX9 is required for chondrogenesis, but not for sex determination. Hum. Mol. Genet. 12 (14), 1755–1765.

Bi, W., et al., 1999. Sox9 is required for cartilage formation. Nat. Genet. 22 (1), 85–89.

Bowles, J., Schepers, G., Koopman, P., 2000. Phylogeny of the SOX family of developmental transcription factors based on sequence and structural indicators. Dev. Biol. 227 (2), 239–255.

Colvin, J.S., et al., 2001. Male-to-female sex reversal in mice lacking fibroblast growth factor 9. Cell 104 (6), 875–889.

Garside, V.C., et al., 2015. SOX9 modulates the expression of key transcription factors required for heart valve development. Development 142 (24), 4340–4350.

Gonen, N., et al., 2017. Correction: normal levels of Sox9 expression in the developing mouse testis depend on the TES/TESCO enhancer, but this does not act alone. PLoS Genet. 13 (2), pe1006584.

Gordon, C.T., et al., 2009. Long-range regulation at the SOX9 locus in development and disease. J. Med. Genet. 46 (10), 649–656.

Gordon, C.T., et al., 2014. Identification of novel craniofacial regulatory domains located far upstream of SOX9 and disrupted in Pierre Robin sequence. Hum. Mutat. 35 (8), 1011–1020.

Harley, V.R., Clarkson, M.J., Argentaro, A., 2003. The molecular action and regulation of the testis-determining factors. SRY (sex-determining region on the Y chromosome) and SOX9 [SRY-related high-mobility group (HMG) box 9]. Endocr. Rev. 24 (4), 466–487.

Hattori, T., et al., 2010. SOX9 is a major negative regulator of cartilage vascularization, bone marrow formation and endochondral ossification. Development 137 (6), 901–911.

Huang, B., et al., 1999. Autosomal XX sex reversal caused by duplication of SOX9. Am. J. Med. Genet. 87 (4), 349–353.

Huang, Y.H., et al., 2015. SOXE transcription factors form selective dimers on non-compact DNA motifs through multifaceted interactions between dimerization and high-mobility group domains. Sci. Rep. 5, 10398.

Hyon, C., et al., 2015. Refining the regulatory region upstream of SOX9 associated with 46. XX testicular disorders of Sex Development (DSD). Am. J. Med. Genet. A 167A (8), 1851–1858.

Jakobsen, L.P., et al., 2007. Pierre Robin sequence may be caused by dysregulation of SOX9 and KCNJ2. J. Med. Genet. 44 (6), 381–386.

Kadaja, M., et al., 2014. SOX9: a stem cell transcriptional regulator of secreted niche signaling factors. Genes Dev. 28 (4), 328–341.

Kim, G.J., et al., 2015. Copy number variation of two separate regulatory regions upstream of SOX9 causes isolated 46,XY or 46. XX disorder of sex development. J. Med. Genet. 52 (4), 240–247.

Kopp, J.L., et al., 2011. Sox9+ ductal cells are multipotent progenitors throughout development but do not produce new endocrine cells in the normal or injured adult pancreas. Development 138 (4), 653–665.

Lavery, R., et al., 2011. XY Sox9 embryonic loss-of-function mouse mutants show complete sex reversal and produce partially fertile XY oocytes. Dev. Biol. 354 (1), 111–122.

Li, Y., Zheng, M., Lau, Y.F., 2014. The sex-determining factors SRY and SOX9 regulate similar target genes and promote testis cord formation during testicular differentiation. Cell Rep. 8 (3), 723–733.

Lincoln, J., et al., 2007. Sox9 is required for precursor cell expansion and extracellular matrix organization during mouse heart valve development. Dev. Biol. 305 (1), 120–132.

Liu, C.F., Lefebvre, V., 2015. The transcription factors SOX9 and SOX5/SOX6 cooperate genome-wide through super-enhancers to drive chondrogenesis. Nucleic Acids Res. 43 (17), 8183–8203.

Mead, T.J., et al., 2013. A far-upstream (−70 kb) enhancer mediates Sox9 auto-regulation in somatic tissues during development and adult regeneration. Nucleic Acids Res. 41 (8), 4459–4469.

Mertin, S., McDowall, S.G., Harley, V.R., 1999. The DNA-binding specificity of SOX9 and other SOX proteins. Nucleic Acids Res. 27 (5), 1359–1364.

Moniot, B., et al., 2009. The PGD2 pathway, independently of FGF9, amplifies SOX9 activity in Sertoli cells during male sexual differentiation. Development 136 (11), 1813–1821.

Morais da Silva, S., et al., 1996. Sox9 expression during gonadal development implies a conserved role for the gene in testis differentiation in mammals and birds. Nat. Genet. 14 (1), 62–68.

Oh, C.D., et al., 2014. SOX9 regulates multiple genes in chondrocytes, including genes encoding ECM proteins, ECM modification enzymes, receptors, and transporters. PLoS ONE 9 (9), pe107577.

Ohba, S., et al., 2015. Distinct transcriptional programs underlie Sox9 regulation of the mammalian chondrocyte. Cell Rep. 12 (2), 229–243.

Ohnesorg, T., et al., 2016. Using ROADMAP data to identify enhancers associated with disorders of sex development. Sex Dev. 10 (2), 59–65.

Sekido, R., Lovell-Badge, R., 2008. Sex determination involves synergistic action of SRY and SF1 on a specific Sox9 enhancer. Nature 453 (7197), 930–934.

Sim, H., Argentaro, A., Harley, V.R., 2008. Boys, girls and shuttling of SRY and SOX9. Trends Endocrinol. Metab. 19 (6), 213–222.

Uhlenhaut, N.H., et al., 2009. Somatic sex reprogramming of adult ovaries to testes by FOXL2 ablation. Cell 139 (6), 1130–1142.

Vidal, V.P., et al., 2001. Sox9 induces testis development in XX transgenic mice. Nat. Genet. 28 (3), 216–217.

Wagner, T., et al., 1994. Autosomal sex reversal and campomelic dysplasia are caused by mutations in and around the SRY-related gene SOX9. Cell 79 (6), 1111–1120.

Whyte, W.A., et al., 2013. Master transcription factors and mediator establish super-enhancers at key cell identity genes. Cell 153 (2), 307–319.

Xu, Z., et al., 2015. Embryonic attenuated Wnt/beta-catenin signaling defines niche location and long-term stem cell fate in hair follicle. Elife 4.

Yao, B., et al., 2015. The SOX9 upstream region prone to chromosomal aberrations causing campomelic dysplasia contains multiple cartilage enhancers. Nucleic Acids Res. 43 (11), 5394–5408.

Biology of Sex Differences

Identification of novel candidate genes for 46,XY disorders of sex development (DSD) using a C57BL/6J-Y^{POS} mouse model

Hayk Barseghyan[1,2], Aleisha Symon[4], Mariam Zadikyan[2], Miguel Almalvez[1,2], Eva E. Segura[2], Ascia Eskin[2], Matthew S. Bramble[1,2], Valerie A. Arboleda[2], Ruth Baxter[2], Stanley F. Nelson[2], Emmanuèle C. Délot[1,2,3], Vincent Harley[4†] and Eric Vilain[1,2,3*†]

Abstract

Background: Disorders of sex development (DSD) have an estimated frequency of 0.5% of live births encompassing a variety of urogenital anomalies ranging from mild hypospadias to a discrepancy between sex chromosomes and external genitalia. In order to identify the underlying genetic etiology, we had performed exome sequencing in a subset of DSD cases with 46,XY karyotype and were able to identify the causative genetic variant in 35% of cases. While the genetic etiology was not ascertained in more than half of the cases, a large number of variants of unknown clinical significance (VUS) were identified in those exomes.

Methods: To investigate the relevance of these VUS in regards to the patient's phenotype, we utilized a mouse model in which the presence of a Y chromosome from the *poschiavinus* strain (Y^{POS}) on a C57BL/6J (B6) background results in XY undervirilization and sex reversal, a phenotype characteristic to a large subset of human 46,XY DSD cases. We assessed gene expression differences between B6-Y^{B6} and undervirilized B6-Y^{POS} gonads at E11.5 and identified 515 differentially expressed genes (308 underexpressed and 207 overexpressed in B6-Y^{POS} males).

Results: We identified 15 novel candidate genes potentially involved in 46,XY DSD pathogenesis by filtering the list of human VUS-carrying genes provided by exome sequencing with the list of differentially expressed genes from B6-Y^{POS} mouse model. Additionally, we identified that 7 of the 15 candidate genes were significantly underexpressed in the XY gonads of mice with suppressed *Sox9* expression in Sertoli cells suggesting that some of the candidate genes may be downstream of a well-known sex determining gene, *Sox9*.

Conclusion: The use of a DSD-specific animal model improves variant interpretation by correlating human sequence variants with transcriptome variation.

Keywords: Disorders of sex development, 46,XY DSD, Undervirilization, C57BL/6J mouse, RNA-Seq, Exome, Gonadal dysgenesis

* Correspondence: evilain@childrensnational.org
†Equal contributors
[1]Center for Genetic Medicine Research, Children's Research Institute,
Children's National Health System, Washington, DC 20010, USA
[2]Department of Human Genetics, David Geffen School of Medicine,
University of California, Los Angeles, CA 90095, USA
Full list of author information is available at the end of the article

Background

Human sex development is dictated by the inheritance of either an X or Y chromosome from the father to offspring. The male sex determination step starts with the expression of a Y-chromosome-encoded transcription factor *SRY* (sex-determining region Y) in the bipotential gonad, initiating a cascade of molecular and cellular events leading to testicular organogenesis [1]. In the absence of the Y chromosome, female-specific pathways are initiated for proper ovarian development [2]. Sex differentiation then occurs, mostly under the influence of testicular (e.g., testosterone, AMH) or ovarian (e.g., estradiol) hormones or transcription factors (e.g., *COUP-TFII*) that further differentiate the body into typical male or female structures, including both internal and external genitalia [3, 4]. Anomalies in hormonal exposure and/or gene mutations disrupting sex development pathways lead to disorders of sex development (DSD) [5–7], defined as "congenital conditions in which development of chromosomal, gonadal, or anatomic sex is atypical" [8]. The umbrella term DSD encompasses conditions ranging from mild hypospadias (abnormal location of the meatus) to discrepancy between sex chromosomes and external genital phenotype (formerly known as sex reversal, either complete or with ambiguous genitalia). DSDs are estimated to affect up to 0.5% of the population [9]. The birth of a child with a DSD may be highly stressful for families, bringing uncertainty in regard to the child's future psychosexual development and clinical management [8, 10, 11].

At present, a specific molecular diagnosis is identified at variable rates in different DSD conditions, and gonadal dysgenesis cases are arguably the most difficult to diagnose. The majority (80–90%) of isolated 46,XX testicular DSD are explained by *SRY* translocations, but only a minority (~ 10%) of ovotesticular DSD in 46,XX individuals are [12]. Copy number variants of the *SOX9* and *SOX3* gene regions are a well-established etiology but only explain a few cases [12]. More recently, a single nucleotide variant in *NR5A1* (nuclear receptor subfamily 5 group A member 1) gene resulting in p.Arg92Trp amino acid change has been associated with 46,XX testicular (and ovotesticular) DSD [13, 14]. The majority of cases of ovarian dysgenesis occur in individuals with an abnormal sex chromosome complement, most commonly 45,X (Turner syndrome), but the advent of next-generation sequencing has recently identified many autosomal genes implicated in determination and maintenance of the ovarian fate. They affect various processes, in particular DNA repair, replication, and stability, but explain a minority of cases [15, 16]. Among 46,XY DSD cases with gonadal dysgenesis, about 15% each are due to *SRY*, *NR5A1*, and *MAP3K1* (mitogen-activated protein kinase kinase kinase 1), and rare cases have been attributed to mutations in other genes such as *SOX9* (SRY-box9), *NR0B1* (nuclear receptor subfamily 0 group B member 1), or *FGFR2* (fibroblast growth factor receptor 2) [17, 18].

Nevertheless, collectively, the genetic etiology is still not identified in greater than 50% of DSD patients, suggesting the existence of a number of unknown sex-determining genes. We endeavored to identify novel candidate genes for 46,XY gonadal dysgenesis.

Next-generation sequencing has become instrumental in DSD diagnosis, including clinical exome sequencing and gene panels [17, 19–21] with high diagnostic rates reported for known DSD genes. In a cohort of 46,XY DSD patients, we established a diagnosis in approximately 1/3 of cases [22], similar to rates for other rare disorders [23, 24]. Another 15% of the exomes in the cohort contained variants of unknown significance (VUS) in known DSD genes that could not be validated as pathogenic but were reported to the referring clinicians to orient further endocrine or imaging testing toward a definitive diagnosis (the variants were termed as "actionable VUS"). Half of the cases from our cohort remained undiagnosed but contained hundreds of VUS that provide an opportunity for identification of novel etiologies for DSD. Here, we utilize an animal model of DSD with gonadal dysgenesis and undervirilization [25, 26] to identify a group of genes that were misexpressed during disrupted testis development. This list was cross-referenced with the list of VUS from 46,XY DSD patients to predict which VUS might be causative in cases where exome sequencing did not result in a definitive diagnosis. We show that the identified 15 novel candidate genes contain a VUS identified in 46,XY DSD cases and are expressed at the time of sex development in a sex-differential manner. In addition, we show that the expression of many of these genes in the developing male gonads is dependent on the known sex-determining gene *Sox9*.

Methods

Exome sequencing and analysis

DNA was isolated from peripheral blood using Gentra Puregene Blood Kit (Qiagen, USA) or saliva collected using ORAgene ORG-500 (DNAgenoteck, Canada). Sequencing libraries and exome capture was done for each sample following manufacturer's protocols for SureSelect All Exon 50 Mb capture kit (Agilent Technologies) and Nextera Rapid Capture (Illumina, USA). Sequencing was performed on an Illumina HiSeq2500 as 50-100 bp paired-end run at the UCLA Clinical Genomics Center.

The sequence reads, FASTQ files, were aligned to the human reference genome (GRCh37/hg19 Feb. 2009 assembly) using BWA (Burrows-Wheeler Alignment tool) [27] and Novoalign (novocraft.com). The output BAM files were sorted and merged, and PCR duplicates were removed using Picard. INDEL (insertion and deletion) realignment and recalibration was performed using Genome Analysis Tool Kit (GATK) (broadinstitute.org). Both single-nucleotide variants (SNVs) and small INDELs were called within the Ensembl coding exonic intervals ± 2 bp using

GATK's Unified Genotyper, then recalibrated and filtered using GATK variant-quality score recalibration and variant filtration tools. All high-quality variants were annotated using SNP&Variation Suite and VarSeq—variant filtration and annotation software (Golden Helix, USA). All variants were filtered by a minor allele frequency (MAF) of < 1% and intersected with the DSD gene list to identify mutations in known DSD genes. The list is comprised of a primary gene list of well-annotated genes involved in sex determination and differentiation [17], as well as a secondary list of genes that are more loosely associated with sex development, e.g., their OMIM (Online Mendelian Inheritance of Man) description contains sex development keywords.

The variants identified by exome sequencing were classified into causative or likely causative variants following the recommendations of the American College of Medical Genetics and Genomics [28]. All other variants with minor allele frequency below 1% were classified as variants of unknown significance (VUS). To assess previously unreported missense variants, we used two in silico algorithms SIFT [29] and PolyPhen [30] to predict the pathogenicity of a missense variant based on conservation of the amino acid across species, the physical characteristics of the altered amino acid, and the possible impact on protein structure and function. All variants with low quality scores were validated by Sanger sequencing [31].

Animal care and dissections

The C57BL/6J and C57BL/6J-Y^{POS} animals were housed at the UCLA Animal Care Facility following the guidelines of the University of California, Los Angeles, Division of Laboratory Animal Medicine. All experiments were approved by the Institutional Animal Care and Research Committees of UCLA. Wild-type C57BL/6J males and females used for breeding were purchased from the Jackson Laboratory (Bar Harbor, USA), which is fully accredited by the American Association for Accreditation of Laboratory Animal Care.

We have previously identified a 1.5-Mb congenic region on chromosome 11 that confers 80% protection from B6-Y^{POS} sex reversal in the heterozygous state (B6-110h-Y^{POS}) and complete protection in the homozygous state (B6-110H-Y^{POS}) [25]. This protective region allows for continual maintenance of subfertile *poschiavinus* male mice as a breeding colony, with an option of generating unprotected B6-Y^{POS} males by mating heterozygous B6-110h-Y^{POS} males with wild-type (WT) B6 females. Overnight mating was performed using either the wild-type (WT) B6 or B6-110h-Y^{POS} (protected from sex reversal) males and WT B6 females. Dissections were performed at E11.5; the gonads were separated from the mesonephros and placed in RNA stabilizing solution RNA*later* (Ambion). DNA was extracted from the rest of the embryos for genotyping.

Chromosomal sex was determined using a single primer pair for X-linked *Smc*-x gene (330 bp) and the Y-linked *Smc*-y gene (301 bp) (forward: 5′CCGCTGCCAAATTCTTTGG3′; reverse: 5′TGAAGCTTTTGGCTTTGAG3′). The presence of the Y^{POS} chromosome was determined by a SNP between Y^{B6} and Y^{POS} Sry gene using the primer sets 5′TGAATGC ATTTATGGTGTGGTC3′; 5′AGCTTTGCTGGTTTTTG-GAGTA3′. Immomix Red (Bioline, UK). Presence or absence of the 110 h protective region in B6-Y^{POS} males was checked by Sanger sequencing of two regions 11-10 and 11-11 containing SNP rs27019103 (5′AAAGTGTGCTTCC-CAGGAGA3′; 5′CCTCTCCCTCAACCCCTAAG3′) and SNP rs28240850 (5′CCACAGCTGGAGGTAGGGTA3′; 5′CCTAAGATGCCATGGGAAGA3′) respectively [25].

Total RNA was isolated from combined embryonic gonadal tissue (50–70 gonads per group) using Qiagen RNeasy Kit (Qiagen) following manufacturer's guidelines. RNA quality was assessed by Agilent 2100 Bioanalyzer (Agilent Technologies). All samples were required to have RNA integrity scores (RIN) greater than 8.

Experiments on *AmhCre Sox9floxflox* mice were carried out in strict adherence with the recommendations in the Australian code of practice for the care and use of animals for scientific purposes from the National Health and Medical Research Council.

E13.5 gonads were separated from the mesonephros and total RNA was isolated using the RNeasy Kit (Qiagen), as described in Rahmoun et al. [32]. Embryos were genotyped, and the RNA from the six gonads was pooled into wild-type XY, XX, or XY *AmhCre Sox9floxflox* (*Sox9* knockout). This was repeated in three biological replicates; protocols are detailed in Rahmoun et al. [32].

RNA sequencing and expression analysis

RNA from each sample was submitted to the UCLA Neuroscience Genomic Core (UNGC) for library preparation and sequencing. Library preparation was performed using TruSeq Stranded Total RNA kit (Illumina) with Poly-A selection following manufacturer's guidelines. Sequencing was performed on HiSeq 2500 (Illumina) with 69 bp paired-end run on a rapid flowcell capable of generating 150 M reads per lane. Four samples were multiplexed and sequenced over two rapid lanes with each sample receiving approximately 75 million reads with > 85% map rate.

The generated sequencing reads were aligned to the mouse genome, version mm10 with STAR [33]. Transcript abundance was assessed by Cufflinks (v2.1.1) [34], using a GTF file based on Ensembl mouse NCBI37. Differential expression analysis was based on fold change differences greater than 1.5 between the groups being compared. Differentially expressed genes were split into two categories: underexpressed and overexpressed in B6-Y^{POS} males. Both categories were separately subjected to pathway enrichment analysis using Gene Ontology Consortium [35].

To analyze the RNA from *AmhCre Sox9floxflox* XY gonads and wild-type XY and XX gonads, libraries were generated using the NuGEN Mondrian Technology and SPIA amplification methodology, and the data was processed and aligned to the mouse genome (Ensembl version 38.77) as described by Rahmoun et al. [32]. To eliminate composition biases, the trimmed mean of *M* values (TMM) method was used for normalization between the samples [36]. The adjusted *P* value of 0.05 was used to assess which genes were differentially expressed between XY and *AmhCre Sox9floxflox* XY (*Sox9* KO). Graphs of gene expression were made using GraphPad Prism.

Quantitative PCR

Reverse transcription of RNA to cDNA was performed using Tetro cDNA Synthesis Kit (Bioline, UK) following manufacturer's protocol. The primer sequences used are detailed in Additional file 1: Table S1. Primers were designed using autoprime software (autoprime.de) and spanned exon-exon junctions for optimal RNA quantification. cDNA was quantified using QuBit HS (Invitrogen) for double-stranded DNA, and a total of 3 ng of cDNA was used per sample for amplification. qPCR was carried out in duplicates using SensiFAST™ SYBR No-ROX Kit (Bioline, UK) by DNA Engine Opticon® 2 real-time PCR detection system (BioRad, USA). Reaction conditions were as follows: 95 °C for 10 min, then 40 cycles of 95 °C for 15 s, 60–64 °C (see Additional file 1: Table S1) for 10 s, and 72 °C for 15 s. Data was analyzed via Opticon Monitor Software (BioRad). Standard curves were generated from a mix of cDNA of all tested samples with five iterations of 1:4 dilutions. Average cycle threshold values (Ct) for each gene/sample were determined based on two replicates. Complementary DNA amounts were estimated based on Ct values and linear equation $y = mx + b$ (where y is the Ct value, m is the slope, x is the cDNA amount, and b is the intercept).

Immunohistochemistry

Fbln2 expression in the embryonic gonads at E12.5 was assessed using immunohistochemistry following the experimental design of Wilhelm et al. [37], using the anti-*Fbln2* rabbit polyclonal, sc-30176 (Santa Cruz Biotechnology) antibody. Topro (Invitrogen) was used to counterstain nuclei. All images were taken on a Zeiss LSM 510 Meta confocal microscope.

For the assessment of Sox9 and laminin expression in wild-type and *AmhCre Sox9 floxflox* gonads at E13.5, embryos were fixed overnight in 4% paraformaldehyde (PFA) at 4 °C, then washed three times in 1× PBS. The embryos were processed and embedded into paraffin, cut at 5 μm, and mounted onto slides. The slides were baked at 60 °C (30 min), deparaffinized using three washes of xylene, and hydrated using three washes of 100% ethanol, then distilled water and 1× PBS. Antigen retrieval was performed by microwaving slides (on high) in 10 mM sodium citrate (pH = 6.0) for 20 min. Sections were then blocked for 30 min with 5% normal donkey serum, and stained overnight at 4 ° C with primary antibodies for anti-Sox9 rabbit polyclonal (1:400) and anti-Laminin rabbit polyclonal (1:100). Sections were washed three times in 1× PBS with 0.1% Tween20 (1× PBST) and incubated with the fluorescent-conjugated secondary antibodies, Donkey anti-rabbit AlexaFluor488 (Thermo Fisher, 1 μg/mL), for 1 h at room temp. Sections were washed three times in 1× PBST, then incubated in 0.1% Sudan Black in 70% EtOH for 5 min to quench background autofluorescence. Lastly, sections were washed three times in 1× PBST, counterstained using DAPI, then washed three times in 1× PBS and mounted using Dako Fluorescent Mounting Medium (Dako). Sections were imaged using fluorescence microscopy (Olympus Corp).

Results

46,XY DSD cases with uninformative exome sequencing

As previously described, we have performed exome sequencing on a cohort of 40 individuals diagnosed with 46,XY DSD [22]. To identify the disease-causing mutations, a DSD-specific gene list (published elsewhere [17]) was used for variant filtration. Exome sequencing was not able to identify the genetic diagnosis in > 50% of cases. To address this issue, we compiled a cohort of 32 DSD cases with uninformative exome and 46,XY karyotype for further investigation (Table 1) (this new cohort includes 21 unresolved cases from [22] and additional 11 cases with uninformative exomes enrolled since). As evident from Table 1, the range of associated clinical features was wide, which is a typical characteristic of DSD presentation. Patients could be grouped into four categories based on the appearance of the external genitalia and gonadal development: (1) 46,XY women with gonadal dysgenesis (GD), when gonadal phenotype had been ascertained by the clinical team; (2) 46,XY females; (3) 46,XY with ambiguous genitalia (and unknown sex of rearing at the time of enrollment); and (4) 46,XY males, with hypogonadism.

C57BL/6J-Y *poschiavinus* mice as a model for 46,XY gonadal dysgenesis

In cases where no pathogenic variant was found by exome sequencing, we identified many VUS outside of the DSD clinical gene list. To investigate the relevance of these VUS in regard to patients' phenotype, we utilized a powerful mouse model for studying undervirilization in human 46,XY individuals. In this model, the presence of a Y chromosome originating from a *M. domesticus poschiavinus* strain (Y^{POS}) on a C57BL/6J (B6) background (B6-Y^{POS}), an inbred laboratory strain that normally carries a *M. musculus* Y chromosome, results in disrupted testicular development and female genital phenotype [38].

174

Table 1 Cohort of 46,XY DSD cases with uninformative exome sequencing

Patient ID	Category	DSD category	Clinical features
RDSD002	1	46,XY female, CGD	–
RDSD003	1	46,XY female, PGD	No uterus; Fallopian tubes present; short vagina; very low T and undetectable estradiol; gonads not found
RDSD004	1	46,XY female, GD	–
RDSD006	2	46,XY female	Amelia (missing limbs)
RDSD007	1	46,XY female, GD	Adrenal rests
RDSD010	2	46,XY female	Clitoromegaly
RDSD011	2	46,XY female	Short stature
RDSD012	2	46,XY female	Kidney disease; possible Denys-Drash syndrome
RDSD013	1	46,XY female, CGD	Normal uterus and Fallopian tubes; streak gonads
RDSD018	3	46,XY ambiguous genitalia	Partial fusion of labioscrotal folds; small phallus; penoscrotal hypospadias
RDSD020	3	46,XY ambiguous genitalia	Developmental delay; agenesis of corpus callosum
RDSD021	3	46,XY ambiguous genitalia	Adrenal hypoplasia congenita; dysmorphic features
RDSD022	3	46,XY ambiguous genitalia	Microcephaly; intestinal dysmotility; optic nerve hypoplasia
RDSD025	4	46,XY male, micropenis/cryptochidism	Severe growth and developmental retardation; testes not seen by ultrasound
CDSD029	4	46,XY male, hypospadias	–
CDSD030	2	46,XY female	Large clitoris; no uterus or vaginal opening; inguinal testes
CDSD031	3	46,XY ambiguous genitalia, CGD	Abdominal gonads with no oocytes; no seminiferous tubules; no clitoromegaly; posterior fusion of labia; urogenital sinus
CDSD032	2	46,XY female	Inguinal testes w/ immature seminiferous tubules; no uterus or Fallopian tubes; deafness; impaired cognition
CDSD034	3	46,XY ambiguous genitalia	Undescended testes; bifid scrotum; hypospadias
CDSD036	3	46,XY ambiguous genitalia	Bilateral descended testes; midshaft hypospadias; chordee
CDSD039	4	46,XY male, micropenis	No uterus or ovaries per ultrasound; ambiguous genitalia; undervirilization
RDSD041	2	46,XY female	Complete androgen insensitivity syndrome
RDSD042	4	46,XY male, hypospadias	–
RDSD043	1	46,XY female, GD	–
RDSD044	4	46,XY male, anorchia	Congenital bilateral anorchia; fully formed scrotum; definite penis (mildly shortened); no hypospadias; responsive to testosterone
RDSD045	4	46,XY male, hypospadias/cryptorchidism	Azoospermia; high T levels
RDSD046	2	46,XY female	Multiple congenital anomalies; no uterus; abdominal gonads—testes
RDSD047	4	46,XY male, microphallus	Hypogonadism; hypospadias
RDSD048	4	46,XY male, micropenis	–
RDSD049	4	46,XY male, hypospadias	–
CDSD050	4	46,XY male, hypospadias	Chordee; bifid scrotum; cryptorchidism
CDSD051	2	46,XY female	Growth delay; short stature

Anatomical description follows the standardized nomenclature in Hennekam et al. [55], except when only historical description was available in patient's file. Patient IDs refer to cases enrolled for research purposes (RDSD) or enrolled through the UCLA clinical genomic center (CDSD). Numbering is not consecutive to maintain consistency with the numbering in Baxter et al. [22] for patients who are in both cohorts
CGD/PGD complete/partial gonadal dysgenesis

175

B6-Y^{POS} males (Fig. 1b; Additional file 2: Table S2). To validate the integrity of the method and make sure that the correct tissue was dissected at the correct embryonic stages, we first looked at the expression levels of two important genes involved in testicular development, *Sry* and *Sox9*. High *Sry* and low *Sox9* expression levels in B6-Y^{POS} males indicated the correct timing of embryonic development (Fig. 1c), expression of which coincided with a previous publication [41]. Second, we verified which genes in our DSD gene list used for exome variant filtering were present in the B6-Y^{B6}/B6-Y^{POS} differentially expressed gene list. The comparison of the two lists revealed that 21 genes were in common: 15 underexpressed and 6 overexpressed (Additional file 2: Table S2). In our previous cohort [22], out of these 21 genes, 3 (*HSD17B3* (hydroxysteroid 17-beta dehydrogenase 3), *STAR* (steroidogenic acute regulatory protein), *FGFR2*) contained a pathogenic variant identified by exome sequencing, explaining a total of 5 cases, and 2 (*DHH* (desert hedgehog), *MAMLD1* (mastermind-like domain-containing 1)) contained a variant that was reported to the clinician to orient further endocrine or imaging testing toward a definitive diagnosis. Cumulatively, these findings indicate that the gene expression analyses were carried out in a correct tissue type, at the correct developmental time point, and that the differentially expressed genes between B6-Y^{B6} and B6-Y^{POS} males may potentially be important in sex development.

Filtering of VUS in 46,XY DSD cases using the B6-Y^{POS} gene list

On average, exome sequencing identifies ~ 21,000 variants per single case [23]. Since DSDs are rare conditions, all variants identified in exome with a minor allele frequency (MAF) of more than 1% in the population were excluded. The variants remaining after the MAF cutoff were classified as variants of unknown significance. The number of genes with a VUS in each case ranged from 30 to 1100 with an average of approximately 730 genes per case. The gene list generated via expression studies in B6-Y^{B6}/B6-Y^{POS} mice, consisting of 515 genes, was used to filter the list of VUS-containing human genes identified by exome sequencing. The comparison of two lists identified 305 (189 underexpressed and 116 overexpressed in B6-Y^{POS}) genes that were both differentially expressed in B6-Y^{POS} males and contained a VUS in the 46,XY DSD cohort with an uninformative exome (Fig. 1b).

All these genes are known to be expressed in the developing gonad at the time of sex determination (e.g., the method used to identify these genes intrinsically already ensures that all those genes are expressed in the relevant tissue (gonad) at the relevant developmental time). In order to increase the probability of identifying relevant candidate genes involved in 46,XY DSD pathogenesis, we further queried if the differentially expressed genes from the mouse model (all 515 genes) were involved in any known biological processes. Gene Ontology Consortium (GOC) [42] enrichment analysis confirmed that genes underexpressed in B6-Y^{POS} males were indeed enriched in biological processes known to control multicellular organism and anatomical structure development, including male reproductive development (Additional file 3: Table S3). Understanding the relevance of the genes that were overexpressed in B6-Y^{POS} males was less straightforward. These genes were enriched in only two biological processes: response to extracellular stimulus and epithelial cell differentiation. Both of these categories had a high *P* value indicating that many genes in the overexpressed category are not associated with any known biological processes at this time. In addition, all of the pathogenic variants identified in our previous 46,XY DSD cohort [22] were in the underexpressed category of genes, indicating that they need to be expressed at higher levels in the developing gonad for proper testicular formation.
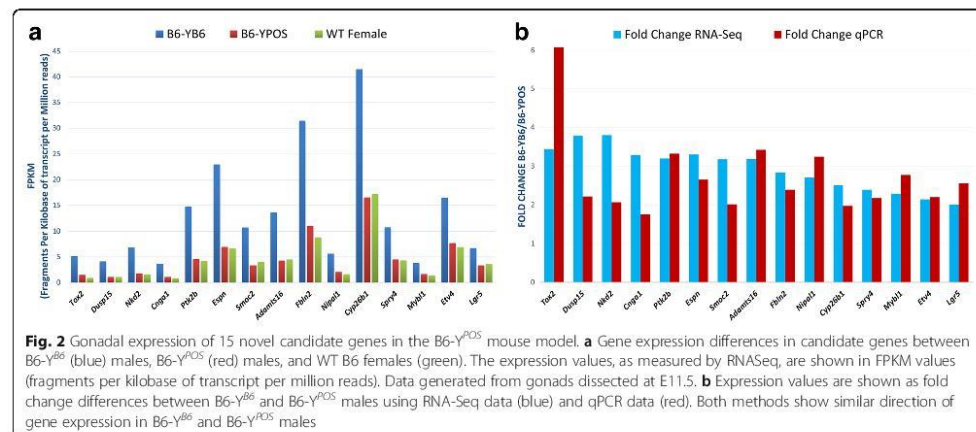
Based on these findings, we focused on variants identified in genes underexpressed in B6-Y^{POS} males whose higher expression in WT males correlated with normal male sex development. To choose a fold change cutoff, we looked at fold change differences in expression between B6-Y^{B6} and B6-Y^{POS} males for genes present in our clinical primary gene list. We found that the majority of the genes have an expression that is 2-fold higher in WT males compared to B6-Y^{POS} males (Fig. 1d). To make the analysis more stringent and improve the confidence of identifying true candidate genes involved in male sex development, we therefore increased the fold change cutoff in expression between the B6-Y^{B6} and B6-Y^{POS} males from 1.5 to 2. This change decreased the number of underexpressed genes from 189 to 53. Additional filtering was performed based on variant frequency (variants with MAF close to or below 0.1%), amino acid conservation (variants in highly conserved residues across multiple species were given preference), number of variants contained in a gene across the cohort, in silico predictions for pathogenicity (preference was given to the variants predicted to be deleterious or damaging), availability of literature (some weight was given to genes with known functions), and gonadal cell-specific expressivity using GenitoUrinary Developmental Molecular Anatomy Project (GUDMAP) data [43] (preference was given to genes expressed in male-typical cells).

Using the abovementioned filtering criteria, we identified 15 novel candidate sex developmental genes, variants in which may be involved in 46,XY DSD pathogenesis. The list of VUS identified in the 46,XY cohort is shown in Table 2. The relative expressions of these genes in B6-Y^{B6}, B6-Y^{POS}, and WT females are shown in Fig. 2a. The expression changes of all 15 genes were confirmed using quantitative real-time PCR (Fig. 2b).

Table 2 List of VUS in candidate genes found in the cohort of 32 46,XY DSD patients

Gene	DSD case ID	Zygosity	HGVSc	HGVSp	MAF gnomAD (%)
TOX2	RDSD021	Het	c.319G>A	p.Gly107Ser	0
	CDSD036	Cmpd Het	c.448A>G	p.Met150Val	0
	CDSD036	Cmpd Het	c.1201C>G	p.Pro401Ala	0
	CDSD036	Cmpd Het	c.1122_1124dupGCC	p.Pro376dup	0
DUSP15	RDSD020	Het	c.563G>C	p.Arg188Pro	0.002
NKD2	RDSD003	Het	c.1151G>A	p.Arg384Gln	0.001
CNGA1	CDSD030	Het	c.1478G>A	p.Arg493Gln	0.09
	RDSD022	Het	c.398G>T	p.Gly133Val	0.03
PTK2B	RDSD011	Het	c.1799G>A	p.Arg600Gln	0.0008
ESPN	RDSD044	Het	c.2230G>A	p.Asp744Asn	0.02
SMOC2	CDSD030	Het	c.1276G>A	p.Val426Met	0.3
ADAMTS16	RDSD013	Het	c.2200G>A	p.Val734Ile	0.8
	RDSD002	Het	c.298C>T	p.Arg100Trp	0.1
	RDSD022	Het	c.1405T>G	p.Phe469Val	0.02
FBLN2	CDSD030	Het	c.1486G>A	p.Ala496Thr	0.033
	CDSD029	Het	c.3605C>G	p.Ala1202Gly	0.004
NIPAL1	RDSD003	Het	c.1207A>G	p.Thr403Ala	0.1
	CDSD031	Het	c.31G>A	p.Glu11Lys	0
CYP26B1	CDSD032	Het	c.805C>G	p.Leu269Val	0.008
SPRY4	CDSD039	Het	c.446C>G	p.Pro149Arg	0.0004
MYBL1	RDSD004	Het	c.754T>A	p.Phe252Ile	0.05
	CDSD029	Het	c.1832G>C	p.Ser611Thr	0.0008
	RDSD049	Het	c.936T>A	p.Asn312Lys	0.03
ETV4	RDSD006	Het	c.523C>A	p.His175Asn	0.1
LGR5	RDSD007	Het	c.1834G>A	p.Val612Met	0.004
	RDSD020	Het	c.2341C>G	p.Pro781Ala	0.8
	RDSD048	Het	c.2537C>A	p.Thr846Asn	0

Het heterozygous, *Cmpd het* compound heterozygous, *HGVSc* Human Genome Variation Society coding sequence location, *HGVSp* Human Genome Variation Society protein sequence location, *MAF* minor allele frequency, *gnomAD* genome Aggregation Database

Fig. 2 Gonadal expression of 15 novel candidate genes in the B6-Y^{POS} mouse model. **a** Gene expression differences in candidate genes between B6-Y^{B6} (blue) males, B6-Y^{POS} (red) males, and WT B6 females (green). The expression values, as measured by RNASeq, are shown in FPKM values (fragments per kilobase of transcript per million reads). Data generated from gonads dissected at E11.5. **b** Expression values are shown as fold change differences between B6-Y^{B6} and B6-Y^{POS} males using RNA-Seq data (blue) and qPCR data (red). Both methods show similar direction of gene expression in B6-Y^{B6} and B6-Y^{POS} males

Expression of the novel candidate genes is *Sox9*-dependent
The time point chosen for our gene expression analysis was such that the *Sry* gene expression was similar between B6-Y^{B6} and B6-Y^{POS} males. At that time, the downstream target of *Sry, Sox9* was significantly decreased in B6-Y^{POS} males (Fig. 1c), as previously described [41]. In order to identify if *Sox9* had any effect on expression of the candidate genes, we used the *Amh-Cre Sox9flox/flox* mouse model where *Sox9* expression is suppressed in Sertoli cells [44]. By E13.5, Sox9 protein is completely absent (Fig. 3a), and these mice show postnatal fertility defects [44]. Earlier *Sox9* knockout models result in complete sex reversal (XY with ovaries) [45, 46] or embryonic lethality [47]; neither situation sheds light on *Sox9* target genes during sex determination. The *Amh-Cre Sox9flox/flox* mouse model allows the examination of *Sox9* loss in an intact Sertoli cell environment.
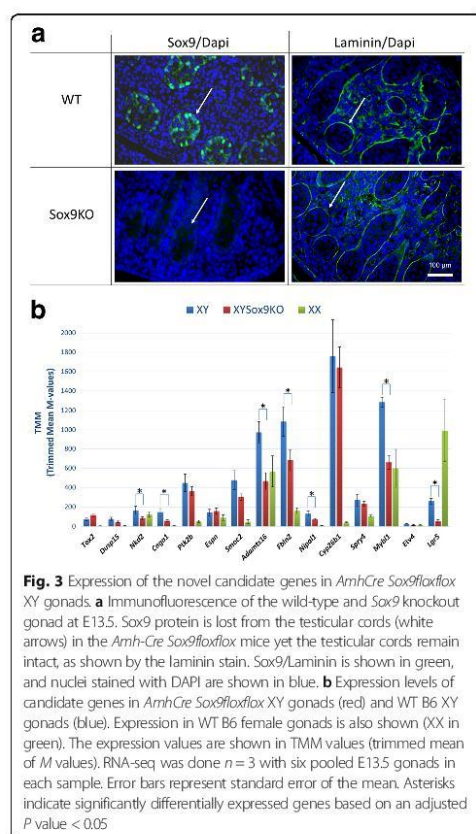
Performing gene expression analysis via RNA sequencing in mice with suppressed *Sox9* expression showed that 13 of
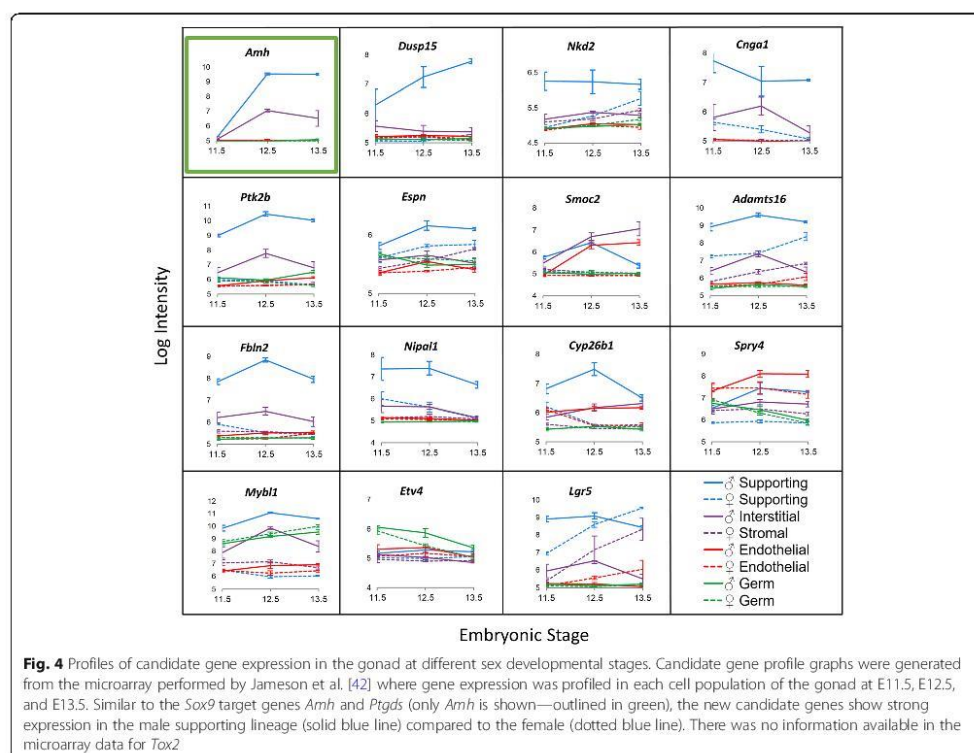

Fig. 3 Expression of the novel candidate genes in *AmhCre Sox9floxflox* XY gonads. **a** Immunofluorescence of the wild-type and *Sox9* knockout gonad at E13.5. Sox9 protein is lost from the testicular cords (white arrows) in the *Amh-Cre Sox9floxflox* mice yet the testicular cords remain intact, as shown by the laminin stain. Sox9/Laminin is shown in green, and nuclei stained with DAPI are shown in blue. **b** Expression levels of candidate genes in *AmhCre Sox9floxflox* XY gonads (red) and WT B6 XY gonads (blue). Expression in WT B6 female gonads is also shown (XX in green). The expression values are shown in TMM values (trimmed mean of *M* values). RNA-seq was done *n* = 3 with six pooled E13.5 gonads in each sample. Error bars represent standard error of the mean. Asterisks indicate significantly differentially expressed genes based on an adjusted *P* value < 0.05

the novel candidate genes for 46,XY DSD underexpressed in B6-Y^{POS} males, were also underexpressed in *Sox9* knockout male gonads with 7 being significantly different (Fig. 3b). This finding suggests that *Sox9* may be upstream of some of the novel candidate genes for 46,XY DSD. In addition, the profiles of gonadal gene expressions from GUDMAP reveal that in almost all cases, the patterns of gene expression are similar to bona fide target genes of *Sox9* such as *Amh* (anti-Müllerian hormone) and *Ptgds* (prostaglandin D2 synthase) [42, 48, 49]. The target gene expression is higher in the male supporting cells (Sertoli) than in the female supporting cells (granulosa) (Fig. 4). The rest of the genes may be regulated by other transcription factors such as *Nr5a1*, which is a known regulator of *Cyp26b1* (cytochrome P450 family 26 subfamily B member 1) [50]. Collectively, our results show that variants in the candidate genes such as the ones we have identified in the 46,XY DSD cases (Table 2) may be responsible for the patient's phenotype.

Discussion
The use of the undervirilized B6-Y^{POS} mice as a model for 46,XY DSD in humans provides valuable screening information toward the identification of novel genes involved in male sex development, mutations in which could lead to anomalies in gonadal development in 46,XY patients with DSD. All of the identified candidate genes are expressed in the developing mouse gonad at the relevant time for sex determination and, as we have shown (Fig. 3a, b), the expression of many of these genes may be *Sox9*-dependent. However, when studying complex disorders such as DSD, it is important to note that even though the mouse models used here are extremely beneficial for identification of the underlying genetic cause in humans, they still do not provide the full spectrum of gene expression/interactions that occur during human sex development.

Mutations in the novel candidate genes identified via the Y^{POS} mouse model are likely to be causative. For example, one of the candidate genes *Adamts16* (A disintegrin and metalloproteinase with thrombospondin type 1 motif, 16) has been shown to be co-expressed with the known DSD gene *Wt1* (Wilms tumor 1) in embryonic gonads, adult testes, and spermatids [38]. Moreover, targeted disruption of *Adamts16* in rats results in cryptorchidism and sterility [51]. In our 46,XY DSD cohort, we identified three heterozygous variants in this gene (Table 2). Patients RDSD013 and RDSD002, both 46,XY women with complete gonadal dysgenesis, had a missense variant leading to amino acid change at positions p.Val734Ile and p.Arg100Trp respectively. These changes were located in the propeptide or cysteine-rich domain of the ADAMTS16 protein and may prevent expression or proper folding of the protein. The third missense variant (p.Phe469Val) in patient RDSD022 (46,XY, with ambiguous genitalia) was located in the

Fig. 4 Profiles of candidate gene expression in the gonad at different sex developmental stages. Candidate gene profile graphs were generated from the microarray performed by Jameson et al. [42] where gene expression was profiled in each cell population of the gonad at E11.5, E12.5, and E13.5. Similar to the *Sox9* target genes *Amh* and *Ptgds* (only *Amh* is shown—outlined in green), the new candidate genes show strong expression in the male supporting lineage (solid blue line) compared to the female (dotted blue line). There was no information available in the microarray data for *Tox2*

peptidase domain of the protein and predicted damaging by in silico tools suggesting a possible impairment of the enzymatic function of ADAMTS16.

We have also identified two rare variants (p.Ala496Thr; p.Ala1202Gly) in the *FBLN2* (fibulin 2) gene in two cases with different phenotypes: 46,XY female with inguinal testes/ enlarged clitoris and 46,XY male with hypospadias. Additional rare *FBLN2* variants were present in six other unrelated cases with previously identified genetic diagnosis (i.e., each with a pathogenic variant identified in a known DSD gene). This suggest that variants in *FBLN2* are overrepresented in DSD population and may act as modifiers of the phenotype. We (Fig. 5) and others [52] show that *Fbln2* is expressed in a sexually dimorphic pattern in the developing gonad. Immunohistochemical staining at E12.5 indicated that WT B6 females have virtually no Fbln2 expression in the developing ovaries (Fig. 5, left panel), whereas WT B6 males (right panel) have very high expression in the developing testes suggesting an important role of Fbln2 in sexual dimorphism. *FBLN2* has been proposed as a candidate gene for 46,XY DSD in an unpublished meeting abstract (K. MacElreavey, personal communication).

We identified a single variant, predicted to be damaging by in silico tools, in the *SPRY4* (sprouty RTK signaling antagonist 4) gene in a 46,XY male patient (CDSD039) with hypogonadism. *SPRY4* variants have been found in a cohort of patients presenting with hypogonadotropic hypogonadism with or without anosmia (HH17, OMIM #615266) [53]. These genes are believed to be functioning in an oligogenic model, with variants in several genes possibly needed for phenotypic expression. Variants in *SPRY4* have been found in association with variants in *FGFR1* (fibroblast growth factor receptor 1) (HH2, OMIM #147950) and *DUSP6* (dual specificity phosphatase 6) (HH19, OMIM #615269), the two other FGF signaling pathway components. An *FGFR2* missense mutation was reported in a 46,XY female DSD patient, for which a corresponding mouse model showed partial sex reversal with reduced *Spry4* (2-fold) and *Dusp6* expression (> 2-fold) [54]. We did not identify *FGFR1* or *DUSP6* variants in the exome of patient CDSD039 (which would have been diagnostic for this patient). However, *DUSP6* is present in the differentially expressed gene list (underexpressed in B6-Y^POS with a
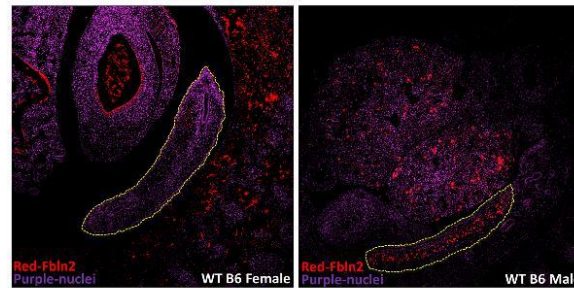
Fig. 5 Fbln2 protein expression in WT B6 females and males at E12.5 by immunohistochemistry. Section of WT B6 female and male embryos at E12.5 stained for Fbln2 (red) and cell nuclei (purple). Fbln2 is expressed in a sexually dimorphic pattern as no expression is present in WT B6 female (left), whereas the expression in WT B6 male is high. The gonads are encircled by yellow dashed lines

fold change of 1.7) and another gene coding for a dual-specificity phosphatase, *DUSP15* (dual specificity phosphatase 15), is in our final candidate gene list, with under-expression in B6-Y^{POS} (fold change > 2) and contains a VUS in one patient.

Conclusions

Exome sequencing provides high-throughput genetic diagnostic capability that has become the core of modern clinical genetics. However, many variants identified by whole exome sequencing are uninterpretable clinically. The C57/BL6J-Y^{POS} model narrows the interpretive gap by correlating human sequence variants with transcriptome variation. This approach allowed the identification of 15 novel candidate genes for human 46,XY DSD.

Additional files

Additional file 1: Table S1. Primer sets used for quantitative PCR validation. (DOCX 12 kb)

Additional file 2: Table S2. Genes differentially expressed between B6-Y^{B6} and B6-Y^{POS} males. All 515 differentially expressed genes (column 1) either underexpressed or overexpressed (column 3) in B6-Y^{POS} males with corresponding fold change difference (column 2) are shown. The table also contains the DSD-specific gene list used to filter exome variants (column 4) as well as which genes are common between two lists (column 5). (XLSX 30 kb)

Additional file 3: Table S3. Biological processes in which differentially expressed genes are involved. The list of 515 genes found to be differentially expressed between B6-Y^{POS} and WT male embryonic gonads was analyzed using the Gene Ontology Consortium functional annotation software. The categories of Gene Ontology biological processes are shown in column 1. *P* value (column 5) is defined as the probability of seeing the indicated number of genes from the custom list (column 4) in the GO term gene list (column 3), given the total number of annotated genes in the whole genome. (DOCX 12 kb)

Availability of data and materials

Data generated or analyzed during this study are partially included in this published article. The datasets generated and/or analyzed during the current study are available from the corresponding author on a reasonable request.

Authors' contributions

HB designed the study; acquired, analyzed, and interpreted the data; and prepared the manuscript. AS, MZ, MA, ES, AS, MSB, VAA, and RB acquired, analyzed, and interpreted the data. AS, ED, VH, and EV aided in the experimental design, data analysis, and manuscript preparation. SFN, ED, VH, and EV provided senior oversight for the design, analysis, and interpretation. All authors indicated the approval for publication.

Ethics approval and consent to participate

Research involving human subjects, human material, and human data have been performed in accordance with protocols (IRB# 11-001491; IRB# 11-001775) approved by the UCLA Institutional Review Board. Experimental studies involving animals, animal tissues, and data have been performed in accordance with approved protocol (ARC# 2000-088-51A) by UCLA Chancellor's Animal Research Committee as well as Animal Ethics Committee of Southern Health (Clayton, Australia, ethics number MMCB/2009/30).

Consent for publication

Participants have consented by approved IRB protocol to share their de-identified data.

Competing interests

The authors declare that they have no competing interests.

Publisher's Note

Springer Nature remains neutral with regard to jurisdictional claims in published maps and institutional affiliations.

Author details
[1]Center for Genetic Medicine Research, Children's Research Institute, Children's National Health System, Washington, DC 20010, USA. [2]Department of Human Genetics, David Geffen School of Medicine, University of California, Los Angeles, CA 90095, USA. [3]Department of Pediatrics, David Geffen School of Medicine, University of California, Los Angeles, CA 90095, USA. [4]Department of Brain and Gender, Hudson Institute of Medical Research, Clayton, VIC 3168, Australia.

References
1. Koopman P, Sinclair A, Lovell-Badge R. Of sex and determination: marking 25 years of Randy, the sex-reversed mouse. Development. 2016;143(10):1633–7.
2. Eggers S, Ohnesorg T, Sinclair A. Genetic regulation of mammalian gonad development. Nat Rev Endocrinol. 2014;10(11):673–83.
3. Ahmed SF, Hughes IA. The genetics of male undermasculinization. Clin Endocrinol. 2002;56(1):1–18.
4. Zhao F, Franco HL, Rodriguez KF, Brown PR, Tsai MJ, Tsai SY, et al. Elimination of the male reproductive tract in the female embryo is promoted by COUP-TFII in mice. Science. 2017;357(6352):717–20.
5. Arboleda VA, Fleming AA, Vilain E. Disorders of sex development. In: Weiss RE, Refetoff S, editors. Genetic diagnosis of endocrine disorders. London: Academic Press; 2010. p. 227–43.
6. Délot E, Vilain E. Disorders of sex development. In: Strauss JF, Barbieri RL, Gargiulo AR, editors. Yen & Jaffe's reproductive endocrinology. Philadelphia: Elsevier; 2019.
7. Ono M, Harley VR. Disorders of sex development: new genes, new concepts. Nat Rev Endocrinol. 2013;9(2):79–91.
8. Lee PA, Houk CP, Ahmed SF, Hughes IA. Consensus statement on management of intersex disorders. International Consensus Conference on Intersex. Pediatrics. 2006;118(2):e488–500.
9. Lee PA, Nordenstrom A, Houk CP, Ahmed SF, Auchus R, Baratz A, et al. Global disorders of sex development update since 2006: perceptions, approach and care. Horm Res Paediatr. 2016;85(3):158–80.
10. Sandberg DE, Gardner M, Cohen-Kettenis PT. Psychological aspects of the treatment of patients with disorders of sex development. Semin Reprod Med. 2012;30(5):443–52.
11. Warne GL. Long-term outcome of disorders of sex development. Sex Dev. 2008;2(4–5):268–77.
12. Delot EC, Vilain EJ. Nonsyndromic 46,XX testicular disorders of sex development. In: Pagon RA, et al, editors. GeneReviews(R). Seattle; 1993.
13. Baetens D, Stoop H, Peelman F, Todeschini AL, Rosseel T, Coppieters F, et al. NR5A1 is a novel disease gene for 46,XX testicular and ovotesticular disorders of sex development. Genet Med. 2017;19(4):367–76.
14. Bashamboo A, Donohoue PA, Vilain E, Rojo S, Calvel P, Seneviratne SN, et al. A recurrent p.Arg92Trp variant in steroidogenic factor-1 (NR5A1) can act as a molecular switch in human sex development. Hum Mol Genet. 2016;25(23):5286.
15. Chapman C, Cree L, Shelling AN. The genetics of premature ovarian failure: current perspectives. Int J Womens Health. 2015;7:799–810.
16. Caburet S, Arboleda VA, Llano E, Overbeek PA, Barbero JL, Oka K, et al. Mutant cohesin in premature ovarian failure. N Engl J Med. 2014;370(10):943–9.
17. Barseghyan H, Delot E, Vilain E. New genomic technologies: an aid for diagnosis of disorders of sex development. Horm Metab Res. 2015;47(5):312–20.
18. Granados A, Alaniz VI, Mohnach L, Barseghyan H, Vilain E, Ostrer H, et al. MAP3K1-related gonadal dysgenesis: six new cases and review of the literature. Am J Med Genet C Semin Med Genet. 2017;175(2):253–9.
19. Delot EC, Papp JC, DSD-TRN Genetics Workgroup, Sandberg DE, Vilain E. Genetics of disorders of sex development: the DSD-TRN experience. Endocrinol Metab Clin N Am. 2017;46(2):519–37.
20. Eggers S, Sadedin S, van den Bergen JA, Robevska G, Ohnesorg T, Hewitt J, et al. Disorders of sex development: insights from targeted gene sequencing of a large international patient cohort. Genome Biol. 2016;17(1):243.
21. Kim JH, Kang E, Heo SH, Kim GH, Jang JH, Cho EH, et al. Diagnostic yield of targeted gene panel sequencing to identify the genetic etiology of disorders of sex development. Mol Cell Endocrinol. 2017;444:19–25.
22. Baxter RM, Arboleda VA, Lee H, Barseghyan H, Adam MP, Fechner PY, et al. Exome sequencing for the diagnosis of 46,XY disorders of sex development. J Clin Endocrinol Metab. 2015;100(2):E333–44.
23. Lee H, Deignan JL, Dorrani N, Strom SP, Kantarci S, Quintero-Rivera F, et al. Clinical exome sequencing for genetic identification of rare Mendelian disorders. JAMA. 2014;312(18):1880–7.
24. Yang Y, Muzny DM, Reid JG, Bainbridge MN, Willis A, Ward PA, et al. Clinical whole-exome sequencing for the diagnosis of mendelian disorders. N Engl J Med. 2013;369(16):1502–11.
25. Arboleda VA, Fleming A, Barseghyan H, Delot E, Sinsheimer JS, Vilain E. Regulation of sex determination in mice by a non-coding genomic region. Genetics. 2014;197(3):885–97.
26. Umemura Y, Miyamoto R, Hashimoto R, Kinoshita K, Omotehara T, Nagahara D, et al. Ontogenic and morphological study of gonadal formation in genetically-modified sex reversal XY(POS) mice. J Vet Med Sci. 2016;77(12):1587–98.
27. Li H, Durbin R. Fast and accurate long-read alignment with burrows-wheeler transform. Bioinformatics. 2010;26(5):589–95.
28. Rehm HL, Bale SJ, Bayrak-Toydemir P, Berg JS, Brown KK, Deignan JL, et al. ACMG clinical laboratory standards for next-generation sequencing. Genet Med. 2013;15(9):733–47.
29. Kumar P, Henikoff S, Ng PC. Predicting the effects of coding non-synonymous variants on protein function using the SIFT algorithm. Nat Protoc. 2009;4(7):1073–81.
30. Adzhubei IA, Schmidt S, Peshkin L, Ramensky VE, Gerasimova A, Bork P, et al. A method and server for predicting damaging missense mutations. Nat Methods. 2010;7(4):248–9.
31. Strom SP, Lee H, Das K, Vilain E, Nelson SF, Grody WW, et al. Assessing the necessity of confirmatory testing for exome-sequencing results in a clinical molecular diagnostic laboratory. Genet Med. 2014;16(7):510–5.
32. Rahmoun M, Lavery R, Laurent-Chaballier S, Bellora N, Philip GK, Rossitto M, et al. In mammalian foetal testes, SOX9 regulates expression of its target genes by binding to genomic regions with conserved signatures. Nucleic Acids Res. 2017;45(12):7191–211.
33. Dobin A, Davis CA, Schlesinger F, Drenkow J, Zaleski C, Jha S, et al. STAR: ultrafast universal RNA-seq aligner. Bioinformatics. 2013;29(1):15–21.
34. Trapnell C, Williams BA, Pertea G, Mortazavi A, Kwan G, van Baren MJ, et al. Transcript assembly and quantification by RNA-Seq reveals unannotated transcripts and isoform switching during cell differentiation. Nat Biotechnol. 2010;28(5):511–5.
35. The Gene Ontology, C. Expansion of the Gene Ontology knowledgebase and resources. Nucleic Acids Res. 2017;45(D1):D331–8.
36. Robinson MD, Oshlack A. A scaling normalization method for differential expression analysis of RNA-seq data. Genome Biol. 2010;11(3):R25.
37. Wilhelm D, Washburn LL, Truong V, Fellous M, Eicher EM, Koopman P. Antagonism of the testis- and ovary-determining pathways during ovotestis development in mice. Mech Dev. 2009;126(5–6):324–36.
38. Eicher EM, Washburn LL, Whitney JB 3rd, Morrow KE. Mus poschiavinus Y chromosome in the C57BL/6J murine genome causes sex reversal. Science. 1982;217(4559):535–7.
39. Bullejos M, Koopman P. Spatially dynamic expression of Sry in mouse genital ridges. Dev Dyn. 2001;221(2):201–5.
40. Kobayashi A, Chang H, Chaboissier MC, Schedl A, Behringer RR. Sox9 in testis determination. Ann N Y Acad Sci. 2005;1061:9–17.
41. Bullejos M, Koopman P. Delayed Sry and Sox9 expression in developing mouse gonads underlies B6-Y(DOM) sex reversal. Dev Biol. 2005;278(2):473–81.
42. Jameson SA, Natarajan A, Cool J, DeFalco T, Maatouk DM, Mork L, et al. Temporal transcriptional profiling of somatic and germ cells reveals biased lineage priming of sexual fate in the fetal mouse gonad. PLoS Genet. 2012; 8(3):e1002575.
43. Harding SD, Armit C, Armstrong J, Brennan J, Cheng Y, Haggarty B, et al. The GUDMAP database—an online resource for genitourinary research. Development. 2011;138(13):2845–53.
44. Barrionuevo F, Georg I, Scherthan H, Lecureuil C, Guillou F, Wegner M, et al. Testis cord differentiation after the sex determination stage is independent of Sox9 but fails in the combined absence of Sox9 and Sox8. Dev Biol. 2009; 327(2):301–12.
45. Barrionuevo F, Bagheri-Fam S, Klattig J, Kist R, Taketo MM, Englert C, et al. Homozygous inactivation of Sox9 causes complete XY sex reversal in mice. Biol Reprod. 2006;74(1):195–201.
46. Lavery R, Lardenois A, Ranc-Jianmotamedi F, Pauper E, Gregoire EP, Vigier C, et al. XY Sox9 embryonic loss-of-function mouse mutants show complete sex reversal and produce partially fertile XY oocytes. Dev Biol. 2011;354(1):111–22.
47. Bi W, Huang W, Whitworth DJ, Deng JM, Zhang Z, Behringer RR, et al. Haploinsufficiency of Sox9 results in defective cartilage primordia and premature skeletal mineralization. Proc Natl Acad Sci U S A. 2001;98(12):6698–703.

Barseghyan *et al. Biology of Sex Differences* (2018) 9:8

Page 13 of 13

48. Behringer RR, Finegold MJ, Cate RL. Müllerian-inhibiting substance function during mammalian sexual development. Cell. 1994;79(3):415–25.
49. Moniot B, Declosmenil F, Barrionuevo F, Scherer G, Aritake K, Malki S, et al. The PGD2 pathway, independently of FGF9, amplifies SOX9 activity in Sertoli cells during male sexual differentiation. Development. 2009;136(11):1813–21.
50. Kashimada K, Svingen T, Feng CW, Pelosi E, Bagheri-Fam S, Harley VR, et al. Antagonistic regulation of Cyp26b1 by transcription factors SOX9/SF1 and FOXL2 during gonadal development in mice. FASEB J. 2011;25(10):3561–9.
51. Abdul-Majeed S, Mell B, Nauli SM, Joe B. Cryptorchidism and infertility in rats with targeted disruption of the Adamts16 locus. PLoS One. 2014;9(7):e100967.
52. Bouma GJ, Hudson QJ, Washburn LL, Eicher EM. New candidate genes identified for controlling mouse gonadal sex determination and the early stages of granulosa and Sertoli cell differentiation. Biol Reprod. 2010;82(2):380–9.
53. Miraoui H, Dwyer AA, Sykiotis GP, Plummer L, Chung W, Feng B, et al. Mutations in FGF17, IL17RD, DUSP6, SPRY4, and FLRT3 are identified in individuals with congenital hypogonadotropic hypogonadism. Am J Hum Genet. 2013;92(5):725–43.
54. Bagheri-Fam S, Ono M, Li L, Zhao L, Ryan J, Lai R, et al. FGFR2 mutation in 46,XY sex reversal with craniosynostosis. Hum Mol Genet. 2015;24(23):6699–710.
55. Hennekam RC, Allanson JE, Biesecker LG, Carey JC, Opitz JM, Vilain E. Elements of morphology: standard terminology for the external genitalia. Am J Med Genet A. 2013;161A(6):1238–63.

This inherited phenomenon has been extensively studied in the B6-Y^{POS} animals. The failure to develop testes stems from the inability of the *Sry^{POS}* gene to initiate normal testicular development when B6 autosomal and/or X-linked factors are present. Virtually all B6-Y^{POS} animals develop some ovarian tissue; half develop exclusively ovarian tissue, classified as completely sex-reversed; and the remainder develop both ovarian and testicular tissue, classified as partially sex-reversed (gonad morphology shown in Fig. 1a). The B6-Y^{POS} mice represent a good model for studying 46,XY DSD with gonadal dysgenesis because of the overlap of the major phenotypic features that are present in both humans and mice such as normal physical appearance without clinical findings including major organs other than the reproductive system, normal karyotype, external genitalia that range from ambiguous to typical female-like, internal genitalia ranging from absent Müllerian structures to presence of a uterus, and abnormal gonadal development characterized as dysgenetic testes, streak, or ovotestes.
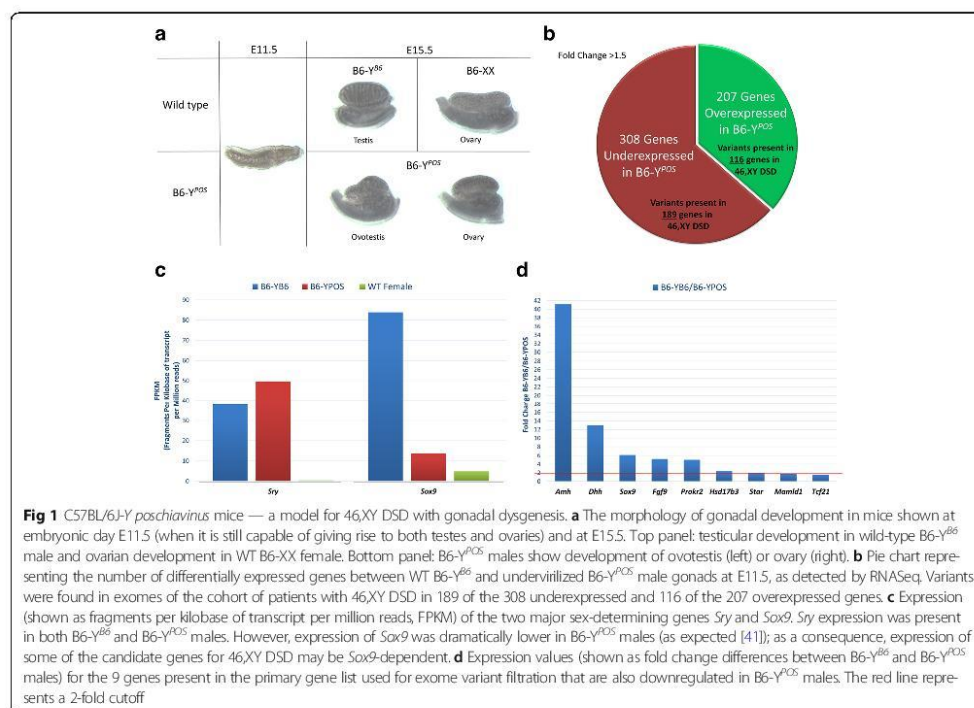
In the embryonic mouse gonad, *Sry* is normally expressed in a dynamic wave (central to distal) between E10.5 and E12.5 in the XY genital ridge, with peak *Sry* expression occurring in normal XY^{B6} genital ridges at ~E11.5, i.e., at the 16–18 tail somite stage of development, which is followed by the upregulation of *Sox9* [39, 40]. In contrast, expression of the *Sry^{POS}* gene peaks 10 to 14 h later in the genital ridges of B6-Y^{POS} fetuses [41]. We hypothesized that abnormal gonadal expression of specific genes in B6-Y^{POS} males, after the surge of *Sry* during gonadal development, would correlate with the genes in which VUS were identified in 46,XY DSD patients by exome sequencing.

Gene expression differences between B6-Y^{B6} and of B6-Y^{POS} males

Since all of the 46,XY DSD patients in the cohort carried a functional *SRY* gene, it was important to perform gene expression analysis in the animal model after the peak of *Sry* expression for optimal comparability. To achieve this, gonadal tissue from WT B6-Y^{B6} and undervirilized B6-Y^{POS} males at embryonic day E11.5, specifically at 21 tail somites (a time point when the surge of *Sry* gene was complete in both B6-Y^{B6} and B6-Y^{POS} males), was collected to perform RNA sequencing for assessment of differential gene expression.

Using this method, we identified 515 genes that were differentially expressed between B6-Y^{B6} and B6-Y^{POS} males with a fold change greater than 1.5. Out of these 515 genes, 308 were underexpressed and 207 were overexpressed in

Fig 1 C57BL/6J-Y *poschiavinus* mice — a model for 46,XY DSD with gonadal dysgenesis. **a** The morphology of gonadal development in mice shown at embryonic day E11.5 (when it is still capable of giving rise to both testes and ovaries) and at E15.5. Top panel: testicular development in wild-type B6-Y^{B6} male and ovarian development in WT B6-XX female. Bottom panel: B6-Y^{POS} males show development of ovotestis (left) or ovary (right). **b** Pie chart representing the number of differentially expressed genes between WT B6-Y^{B6} and undervirilized B6-Y^{POS} male gonads at E11.5, as detected by RNASeq. Variants were found in exomes of the cohort of patients with 46,XY DSD in 189 of the 308 underexpressed and 116 of the 207 overexpressed genes. **c** Expression (shown as fragments per kilobase of transcript per million reads, FPKM) of the two major sex-determining genes *Sry* and *Sox9*. *Sry* expression was present in both B6-Y^{B6} and B6-Y^{POS} males. However, expression of *Sox9* was dramatically lower in B6-Y^{POS} males (as expected [41]); as a consequence, expression of some of the candidate genes for 46,XY DSD may be *Sox9*-dependent. **d** Expression values (shown as fold change differences between B6-Y^{B6} and B6-Y^{POS} males) for the 9 genes present in the primary gene list used for exome variant filtration that are also downregulated in B6-Y^{POS} males. The red line represents a 2-fold cutoff

183

In mammalian foetal testes, SOX9 regulates expression of its target genes by binding to genomic regions with conserved signatures

Massilva Rahmoun[1,†], **Rowena Lavery**[2,†], **Sabine Laurent-Chaballier**[3,‡], **Nicolas Bellora**[4,‡], **Gayle K. Philip**[5,‡], **Moïra Rossitto**[1], **Aleisha Symon**[2], **Eric Pailhoux**[6], **Florence Cammas**[3], **Jessica Chung**[5], **Stefan Bagheri-Fam**[2], **Mark Murphy**[7], **Vivian Bardwell**[7], **David Zarkower**[7], **Brigitte Boizet-Bonhoure**[1], **Philippe Clair**[8], **Vincent R. Harley**[2,*,§] **and Francis Poulat**[1,*,§]

[1]Institute of Human Genetics, CNRS-University of Montpellier UMR9002, 34396 Montpellier cedex 5, France, [2]The Hudson Institute of Medical Research and Department of Anatomy, Monash University, Melbourne, Australia, [3]Institut de Recherche en Cancérologie de Montpellier, IRCM, INSERM U1194, Université de Montpellier, Institut régional du Cancer de Montpellier, Montpellier F-34298, France, [4]Instituto Andino Patagónico de Tecnologías Biológicas y Geoambientales (IPATEC), Universidad Nacional del Comahue - CONICET, Bariloche, Argentina, [5]VLSCI, LAB-14, 700 Swanston Street, Carlton 3053, Victoria, Australia, [6]INRA Biologie du Développement et Reproduction, Domaine de Vilvert, 78352 Jouy-en-Josas Cedex, France, [7]Department of Genetics, Cell Biology and Development, University of Minnesota, 6-160 Jackson hall, 321 Church St, SE, Minneapolis, MN 55455, USA and [8]University of Montpellier, Montpellier GenomiX, bat 24, Place Eugène Bataillon, 34095 Montpellier cedex 5, France

ABSTRACT

In mammalian embryonic gonads, SOX9 is required for the determination of Sertoli cells that orchestrate testis morphogenesis. To identify genetic networks directly regulated by SOX9, we combined analysis of SOX9-bound chromatin regions from murine and bovine foetal testes with sequencing of RNA samples from mouse testes lacking *Sox9*. We found that SOX9 controls a conserved genetic programme that involves most of the sex-determining genes. In foetal testes, SOX9 modulates both transcription and directly or indirectly sex-specific differential splicing of its target genes through binding to genomic regions with sequence motifs that are conserved among mammals and that we called 'Sertoli Cell Signature' (SCS). The SCS is characterized by a precise organization of binding motifs for the Sertoli cell reprogramming factors SOX9, GATA4 and DMRT1. As SOX9 biological role in mammalian gonads is to determine Sertoli cells, we correlated this genomic signature with the presence of SOX9 on chromatin in foetal testes, therefore equating this signature to a

genomic bar code of the fate of foetal Sertoli cells. Starting from the hypothesis that nuclear factors that bind to genomic regions with SCS could functionally interact with SOX9, we identified TRIM28 as a new SOX9 partner in foetal testes.

INTRODUCTION

Sex determination in mammals provides an ideal *in vivo* model to study cell fate regulation by transcription factors. Indeed, embryonic gonads originate from a bipotential primordium (the genital ridge) that can differentiate into testis or ovary via the action of distinct transcription factors. In the mouse embryo, sex determination occurs between embryonic day (E) 10.5 and E12.5 (1) by differentiation of progenitors into a specific cell population (the supporting cells) within the genital ridge. Supporting cells organize the embryonic gonads morphologically and induce sex determination in the germinal lineage. In males, differentiation of supporting cells, also known as Sertoli cells, is driven by the expression of the Y chromosome gene *Sry* that activates the autosomal gene *Sox9* (2), a SOX E group family member. In the absence of *Sry* in females, progenitors differentiate into granulosa cells, the female supporting cell lineage. Genetic experiments have demonstrated that *Sox9*

*To whom correspondence should be addressed. Tel: +33 4 34 35 99 40; Fax: +33 4 34 35 99 01; Email: francis.poulat@igh.cnrs.fr
Correspondence may also be addressed to Vincent R Harley. Email: vincent.harley@hudson.org.au
†These authors contributed equally to this work as first authors.
‡These authors contributed equally to this work as second authors.
§These authors contributed equally to this work as last authors.

is the essential direct target gene of SRY ([3]) and the central effector of the male pathway. Heterozygous missense or nonsense *SOX9* mutations in 46, XY human patients cause Disorders of Sex Development (DSD) and induce a highly penetrant (75%) male-to-female sex-reversal phenotype as well as campomelic dysplasia ([4]). Similarly, targeted disruption of *Sox9* in mouse embryonic testes leads to their development into ovaries ([5,6]). Conversely, *SOX9* duplication in XX patients ([7]) or ectopic expression of *Sox9* in mouse embryonic XX gonads induces testis formation ([8,9]). Upon *Sox9* activation in mouse embryonic gonads, *Sox8* and *Sox10*, the two other SOX E group members, are also induced and either gene can replace *Sox9* function and masculinize the gonad ([10,11]).

Four other transcription factors are required for Sertoli cell differentiation: DMRT1, GATA4, WT1 and SF1 (also known as NR5A1). Like for SOX9, alterations or point mutations in the genes encoding these factors have been detected in XY individuals with DSD (([12]) and reviewed by ([13])) and ablation of each of these genes affects testis development in the mouse ([14–17]). Together, DMRT1, GATA4, WT1, SF1 and SOX9 induce direct reprogramming of mouse embryonic fibroblasts into functional embryonic Sertoli-like cells, thereby defining the transcription factor module required for the Sertoli cell fate ([18]). However, *Sox9* is the only one with male-specific expression and induces female-to-male sex reversal when ectopically expressed in XX human and mouse gonads ([7–9]), while *Dmrt1*, *Gata4*, *Wt1* and *Sf1* are expressed in both male and female progenitors. By contrast, *Dmrt1* overexpression in female embryonic gonads induces incomplete Sertoli differentiation without testis cords formation ([19]), while *Dmrt1* expression at a physiological level cannot induce the male pathway in XX embryonic gonads ([20]). Taken together, genetic, transcriptomic and direct reprogramming experiments suggest that the fate choice towards Sertoli cells is controlled by SOX9 and its set of target genes. This implies that the differentiation of supporting cell progenitors into male-specific Sertoli cells or female-specific granulosa cells is controlled by SOX9 presence or absence.

In the present study, to better understand the mechanisms underlying SOX9 role in foetal Sertoli cell differentiation, we used chromatin immunoprecipitation followed by sequencing (ChIP-seq) of samples from foetal testes of two distant mammals (mouse and cattle). We found that SOX9 binds to 4293 genes in common between the mouse and bovine genomes. Most of these genes are already known to be involved in sex determination. Moreover, transcriptomic (RNA-seq) analysis of foetal testes from *Sox9* knockout mice showed that SOX9 not only regulates transcription of its target genes directly, but also influences their RNA splicing.

Finally, analysis of the ChIP-seq data from these two distant mammals allowed the identification of genomic DNA motifs that characterize genes bound by SOX9 in differentiated Sertoli cells from foetal testes. This 'Sertoli cell signature' (SCS) is conserved among mammals and is characterized by the organized clustering of SOX9, GATA4 and DMRT1 binding sites. At the chromatin level, we observed that DMRT1 and GATA4 can be co-localized with SOX9 on its target genes. *In silico* prediction of SCS iden-

tified a potential link between SOX9 and the nuclear factor TRIM28 (TIF1ß or KAP1). We confirmed this prediction experimentally by showing the physical interaction between SOX9 and TRIM28 in foetal testes, their co-localization on the foetal testis chromatin and their potential functional interaction in transcriptional regulation.

MATERIALS AND METHODS

Cells and animals

NT_2D_1 cells were obtained from the American Type Culture Collection (ATCC) and cultivated in DMEM/F12 medium with Glutamax (Life Technologies) supplemented with 10% foetal bovine serum (Life Technologies). Animal care and handling (mouse foetal gonads used for ChIP-seq) were according to the 'Réseau des Animaleries de Montpellier' (RAM). For the foetal gonads from wild type and $Sox9^{\Delta/\Delta}$ animals (RNAseq), all procedures involving mice were approved by the Animal Ethics Committee of Monash University, Australia. Experiments on bovine foetuses reported in this work were performed in agreement with the ethical guidelines of the French National Institute for Agricultural Research (INRA). Foetuses were produced by artificial insemination of Holstein females with semen of Holstein males (day 0) and collected at E90 at the INRA slaughterhouse (France). The protocol (no. 12/046) was approved by the local ethics committee (COMETHEA) and Eric Pailhoux is the recipient of an official authorization for animal experimentation (no. B91-649).

Tissue fixation and ChIP-seq analysis

Micro-dissected gonads were separated from the mesonephros of E13.5 (mouse) or E90 (bovine) embryos, snap-frozen and stored at −80°C. Frozen gonads were crushed in liquid nitrogen using a mortar. Powdered tissue samples were immediately fixed with PBS containing 2 mM of disuccinimidyl glutarate (DSG) (Pierce ref 20693) for 30 min as described previously ([21]). After three washes with PBS, samples were fixed in PBS/1% formaldehyde at room temperature for 30 min. Protein A coupled to Dynabeads magnetic beads (Life Technologies) was pre-incubated at 4°C with saturating buffer [1 mg/ml BSA, 0.2 mg/ml glycogen (Roche), 1 mg/ml yeast tRNA (Roche) in 1× PBS] for 1 h. Beads were then incubated at 4°C with 2 μg of purified home-made rabbit polyclonal anti-SOX9 IgG antibody ([22]) in 50 μl of PBS/0.02% Tween for 4 h. After washing, antibody-bound beads were used for immunoprecipitation (IP) of 20 μg of sonicated chromatin overnight. IP and washing buffers were as described ([2]). Unbound sonicated DNA was sequenced as input. Six independent IPs were pooled in two samples (three IPs/each) and used for construction of two independent ChIP-seq libraries that were sequenced at the BGI facility (BGI Shentzen, China). ChIP-seq reads were aligned to the mouse genome using SOAP2.21 (mm9, build 37) or to the bovine genome (Bostau6, UMD3.1). For peak calling, as the number of reads in the inputs was twice that in the ChIP-seq experiments, 20 million reads were randomly sampled from each input, using a homemade script that respects the proportion of reads per chromosome of the initial input.

With this method, 10 input samples were generated for each ChIP-seq analysis that were used for ten rounds of peak calling with the MACS software (1.4) (23) (bw = 250, mfold = 10 and P value = 1e−5). Peaks common to the 10 operations with FDR<0.05 were kept for further analysis. Peaks were assigned to neighbouring genes using the PAVIS annotation tool (http://manticore.niehs.nih.gov/pavis2/) with the UCSC annotation for mouse mm9 and the Ensembl annotation UMD3.1r82 for bovine Bostau6. For annotation of the bovine peaks using the mouse genome as reference, bovine coordinates were translated to mouse mm9 coordinates, as previously described (24), using the UCSC LiftOver tool. Coordinates translated to mm9 where then annotated using PAVIS. The correspondence of orthologous genes between mouse and bovine were analyzed using BIOMART (http://www.ensembl.org/biomart/martview/5761d5751336b65a1461f18d849facfe). Pathway analysis was performed using the MetaCore™ GeneGo software to map genes to a global database of known networks (https://portal.genego.com/). The top 50 enriched ($P < 0.05$) pathway networks were analyzed from genes associated to the mouse and bovine SOX9 ChIP-seq peaks.

ChIP-qPCR and sequential ChIP-qPCR

Experiments were carried out with the same protocol as for ChIP-seq. The anti-DMRT1 antibody was described previously (25); the anti-GATA4 antibody and control IgG were purchased from Santa-Cruz Biotech, Heidelberg, Germany (Sc-1237and sc-66830, respectively). For sequential ChIP, the rabbit-anti SOX9 antibody was cross-linked to protein A prior to immunoprecipitation in order to prevent its dissociation from protein A magnetic beads. After incubation of the antibody with protein A Dynabeads, beads were washed with 0.2 M sodium borate pH 9.0 and incubated in the same buffer in the presence of 20 mM dimethylpimelimidate (DMP, Pierce ref 21666) at room temperature for 45 min. Beads were then washed and incubated at RT with 0.2 M ethanolamine pH 8.0 for 1 h, washed three times with 0.58% (v/v) acetic acid/150 mM NaCl and then three times with PBS. In each experiment, the equivalent of 2 μg of coupled antibody was used. Chromatin was eluted from antibodies after immunoprecipitation with 10 mM Tris pH 8, 1 mM EDTA, 2% SDS, 15 mM DTT at 37°C for 1 h. Supernatants were diluted 1:20 in 50 mM Tris pH8, 150 mM NaCl, 2 mM EDTA, 1% Triton X100 and processed for the second immunoprecipitation as before.

After de-crosslinking, DNA was purified with the MinElute PCR Purification Kit (QIAGEN GmbH, D-40725 Germany, ref 28004). Quantitative PCR was performed with the SYBR Select Master Mix (Applied Biosystems ref 4472908) and a LightCycler 480 apparatus (Roche). Primer sequences are listed in Supplementary Table S9 of the Additional Methods.

Embryonic tissue collection and RNA preparation

Micro-dissected gonads were separated from the mesonephros of E13.5 embryos, snap-frozen and stored at −80°C. Amh-*Cre; Sox9^{flox/flox}* mice were obtained as described previously (26). All animal work was approved by Monash Medical Centre Animal Ethics (MMCB/2012/23). RNA was extracted using the RNeasy Kit (QIAGEN GmbH, Germany). The developmental stage and phenotype of each embryo was visually analyzed and recorded. A tail piece was collected for genotyping and genetic sex was determined as previously described (27). Each RNA sample (Amh-*Cre; Sox9^{flox/flox}* XY and wild type *Sox9^{flox/flox}* XX) consisted of a minimum of six pooled gonads for each genotype. An equal number of age-matched mouse gonads for each genotype was collected and divided in two additional groups to provide three biological replicates for each RNA-seq analysis. RNA quality was assessed by measuring the optical density at 230, 260 and 280 nm using a ND-1000 Spectrophotometer (Nanodrop, Wilmington, DE, USA) and by evaluating their integrity using the Agilent 2100 BioAnalyzer (Agilent Technologies, Santa Clara, CA, USA). RNA samples with a RIN value of ≥7.5 were used to generate cDNA libraries for sequencing. Typically, 800 ng of high quality total RNA was obtained from six pooled Amh-*Cre; Sox9^{flox/flox}* gonads.

RNA-seq library preparation, sequencing and analysis

Libraries were generated using the NuGEN Mondrian Technology and the SPIA amplification methodology that specifically selects and linearly reverse transcribes non-ribosomal RNA. 6pM of bar-coded libraries per lane were sequenced using the Illumina HiSeq1500 and paired-end RNA sequencing chemistry (150nt read lengths at 50 million reads per sample). All datasets were processed with the RNA-seq pipeline (http://dx.doi.org/10.5281/zenodo.47479) as follows. Sequencing reads were quality-filtered and adapters were removed using *Trimmomatic* (version 0.30) (28). Reads shorter than 36 bp were discarded from subsequent analyses and the remaining trimmed reads were mapped to the *Mus musculus* genome (Ensembl version 38.77) using *Tophat2* (version 2.0.8) (29). *HTSeq-count* (version 0.6.1p1) (30) was used to count the reads overlapping with genes using the union overlap resolution mode. A statistical analysis of the count data was then performed using '*voom*'(31) from the '*limma*' (version 3.24.0) (32) *R* package to assess the differential expression between the different experimental conditions (KO versus XX, KO versus XY, and XX versus XY). Specifically, filtering was performed to include only genes the expression of which in counts-per-million (CPM) was greater than 1 in at least two samples. To eliminate composition biases between libraries, the Trimmed Mean of *M*-values (TMM) method was used to calculate normalization factors between samples (33). The *voomWithQualityWeights* function (34), which combines observational-level and sample-specific weights, was used in the subsequent linear modelling to down-weight more variable samples (35). Differentially expressed genes were examined with an adjusted p value cut-off of 0.05.

For alternative splicing analysis, RNA-seq datasets were analyzed independently as follows. Paired-end raw reads were cleaned of sequencing contaminants with Scythe (https://github.com/vsbuffalo/scythe.) and quality trimmed with Sickle (https://github.com/najoshi/sickle) to keep only

reads with a minimum length of 21nt. Mouse genomic sequences (mm10) and annotations (Ensembl 75) were retrieved from the UCSC genome browser. Alignments to the mouse genome were performed with STAR v2.4.1c (36) and quantification of Ensembl isoforms with Salmon v0.3.0 (http://biorxiv.org/content/early/2015/10/03/021592). Both programs ran with default read-matching parameters. Differential expression was calculated between pairs of conditions using one-way ANOVA and *t*-tests on square-root transformed TPM data of the three replicates (37). MISO (38) was used for alternative splicing analysis and results were gathered with the following parameters: –num-inc 0 –num-exc 0 –num-sum-inc-exc 5 –delta-psi 0.20 –bayes-factor 1. SOX9 ChIP-seq peaks were translated from the mm9 genome assembly to mm10 using LiftOver for correspondence of splicing events with ChIP-seq peaks.

Motifs analyses

Detailed in supplemental methods.

Cell culture, generation of tet-SOX9 cell lines and gene expression analysis by RT-qPCR

NT_2D_1 and HEK293T cells were cultured as previously described (39,40). For generation of lentiviral vectors, the human SOX9 open reading frame was cloned in a modified version of the pTRIPZ vector (Open Biosystems) to introduce a HA-tag in the SOX9 N-terminus. Viral particles were produced at the vectorology facility (PVM, Plateforme de Vectorologie de Montpellier). After infection with the pTRIPZ-SOX9 plasmid, NT_2D_1 and HEK293T cells were grown in the presence of 1 µg/ml puromycin (Invitrogen). SOX9 expression was inducted by addition of 2 µg/ml tetracycline (Sigma) for 16 h. Tet-SOX9-HEK293 cells were transfected with empty plasmid or pCX-Flag-mTRIM28 using Lipofectamine® 2000 (Invitrogen) following the manufacturer's protocol. Total RNA was isolated using the TRIzol® reagent (Life Technologies) and the DNA-free Kit (Invitrogen). Total RNA was reverse transcribed with SuperScript® IV (Invitrogen) and quantitative PCR performed as described in the ChIP-qPCR chapter. Primer sequences are listed in Supplementary Table S8 of Additional Methods.

Gel mobility shift assay

Proteins were produced using TNT™ Quick Coupled /Translation System (Promega) according to the manufacturer's instructions. Probe annealing and experiments were carried out as described before (41) for mouse DMRT1 and with some modifications for GATA4 and SOX9. For SOX9 binding assay, the non-specific competitor dI-dC was replaced by poly(dG-dC) (GE Healthcare). Mouse GATA4 was *in vitro* translated using as template the pCS2⁺mGATA4 plasmid, a generous gift from Dr Sergei Tevosian.

For Figure 4, the top strand probes were:

Lats2: 5′-ggCCGAGCGGGACATTCGCTACATTG TTGGCATTCCACGGGCG-3′

Lmo4: 5′-ggCATCTCCCATTATTGTTCCAAATCTC ATTTCATTTTGAA-3′

Mrpl45: 5′-ggGTTTTTTTCACCGATTGTAAATAA GGTGTAACAATGTGTTAAGGAACCAGGA-3′

DMRT1 BS (12): 5′-ggGGGAGATTTGATACATTG TTACTTTATGG-3′

GATA4 BS (42): 5′-ggGGGGCTTTGGTCTCAGCT TATCAAACTGCCCTG-3′

SOX9 BS (43): 5′-ggGTTGACAGAACAATGGCTGC TAGA-3′

The 'g' nucleotides at C-terminus were added for probe labelling with Klenow DNA polymerase and α [³²P]-dCTP

Immunoprecipitation using NT_2D_1 cell and embryonic gonad tissue extracts

Co-immunoprecipitation using NT_2D_1 cell extracts was performed as previously described (39) with 2 µg of purified rabbit antibodies against the N- (44) or C-terminal (22) regions of SOX9. For immunoprecipitations using male and female E13.5 gonad tissues, nuclear extracts were prepared with the Nuclear Extract Kit (Active Motifs, La Hulpe, Belgium). Nuclear extracts corresponding to 30 pairs of gonads were diluted in lysis buffer in the same conditions as for NT_2D_1 cells. After extensive washes (wash buffer: 150 mM NaCl, 50 mM Tris pH 7.5, 2 mM EDTA, 1% NP40), immune complexes were analyzed by western blotting using a monoclonal antibody against mouse TRIM28 (45). As control, 5% of immunoprecipitated supernatant was used for western blotting with a control IgG antibody (Santa-Cruz Biotech, Heidelberg, Germany).

Immunostaining and antibodies

Gonads were dissected from staged embryos, fixed in 4% paraformaldehyde and paraffin-embedded. Expression of SOX9, TRIM28 and DMRT1 was assessed by incubating 5-µm sections with a rabbit polyclonal anti-SOX9 (1:300) (22), a mouse monoclonal anti-TRIM28 (1:2000) (46) and a goat polyclonal anti-DMRT1 (1:25) antibody (Santa Cruz Cat. No. sc-104885) at 4°C overnight, followed by the appropriate secondary antibodies (1/800) (Alexa-Ig, Molecular Probe). Nuclei were stained with DAPI (Sigma). Images were captured with a Zeiss Axioimager Apotome microscope or a DeltaVision OMX microscope.

In vitro pull-down assay

The bacterially expressed GST-mTRIM28 fusion protein was produced and purified as previously described (40). The open reading frame of human SOX9 was cloned in the pet28a vector (Novagen) and the histidine-tagged protein (6xHis-SOX9) was bacterially expressed and purified as previously described (47). For *in vitro* interaction, purified GST-TRIM28 or GST alone was incubated with 6xHis-SOX9 in 150 mM NaCl, 50 mM Tris pH 7.5, 0.5 mM DTT and 0.5% NP40 supplemented with 1 mg/ml of BSA (Sigma) at room temperature for 20 min. Protein complexes were captured using glutathione–agarose beads (Sigma). After extensive washes, proteins were analyzed by western blotting with the previously described anti-SOX9 and -TRIM28 antibodies.

187

Availability of data and computer programs

Datasets generated for this manuscript are accessible at GEO (http://www.ncbi.nlm.nih.gov/geo/) with the accession number GSE81490. Computer programs, source codes and scripts are freely available at GitHub (https://github.com/fpoulat/SCS-motifs-scanning)

RESULTS

Most genes interacting with SOX9 contribute to Sertoli cell determination in foetal testis

ChIP-seq experiments were performed using chromatin from E13.5 mouse and E90 bovine foetal testes. In both species, this represents the stage of testis development when Sertoli cells differentiate. The specificity of the homemade anti-rabbit SOX9 antibody used for ChIP was demonstrated by the finding that the antibody recognized only chromatin from male, but not female E13.5 gonads in a slot-blot experiment (Supplementary Figure S1).

ChIP-seq experiments gave 6419 (mouse) and 11 988 (bovine foetal testis) peaks with FDR<0.05 (Supplementary Table S1: Sheets 'ChIP-seq mouse mm9' and 'ChIP-seq bovine Bostau6'). To overcome the problem of limited gene annotations in the *Bos taurus* genome (BosTau6), bovine peaks were attributed either by direct annotation using the bovine genome assembly (BosTau6, Ensembl UMD3.1) (Supplementary Table S1: Sheet 'ChIP-seq bovine Bostau6'), or by translating the BosTau6 genomic coordinates of the bovine ChIP-seq peaks to the mouse genome assembly mm9 using the LiftOver tool from UCSC (Supplementary Table S1: Sheet 'ChIP-seq bovine liftover mm9'). The 6419 ChIP-seq peaks from the mouse samples were assigned to 5844 genes and the 11 988 peaks from bovine samples were assigned to 8229 genes by direct annotation using the bovine genome and to 8957 genes using LiftOver from BosTau6 to mm9. Among the mouse peaks, 70% were preferentially located within the gene body [5′ untranslated regions (UTRs): 19%. 3′ UTRs: 1%. exons: 15%; introns: 35%] and 30% were outside [24% upstream the Transcription Start Site (TSS) and 6% downstream the Transcription End Site (TES)] (Figure 1A, left panel). Conversely, direct annotation using the BosTau6 genome assembly indicated that 62% of bovine peaks were outside the gene body (48% upstream of the TSS and 14% downstream of the TES) (Figure 1A, middle panel). However, when using the mouse genome as reference after translation of the bovine coordinates, the bovine and mouse peak distributions were comparable (Figure 1A, right panel).

Cross-species comparison (24) of the regions bound by SOX9 in bovine and mouse foetal testes, identified 4293 peaks that were common to both ChIP-seq datasets, 75% of which (3236 peaks) overlapped by >500 bp (Figure 1B). From these 4293 peaks, 3849 neighboring genes were annotated that showed strict orthology using Biomart. This suggests that SOX9 binds to and regulate a similar core set of genes in two evolutionarily distant mammals. Some of these genes (for instance, *Col27a1/COL27A1* (48), *Fgf9/FGF9* (49) and *Sox10/SOX10* (10)) displayed striking similarity of peak location in the mouse and bovine ChIP-seq datasets.

Conversely, the peak profile of *Lmo4/LMO4* (50) was relatively different between species.

Gene Ontology (GO) term enrichment analysis (Supplementary Table S1: Sheets GO) of genes bound by SOX9 showed that the male sex differentiation pathway was enriched in the mouse ($P = 3.454 \times 10^{-7}$), bovine ($P = 2.972 \times 10^{-7}$) and the combined mouse and bovine gene sets ($P = 3.811 \times 10^{-6}$). Moreover, other enriched pathways, such as FGF, NOTCH, Hedgehog and WNT signalling cascades, also contribute to male sex determination and gonad function.

Most genes that have been involved in mammalian gonad determination and differentiation by genetic or functional studies were identified here as SOX9 targets (Table 1). This included genes with early roles, such as *Sry* activation (*Kdm3a* (51), *Gadd45g* (52), *Gata4* (53) and *Cbx2* (54)), and genes acting downstream of SOX9 (*Tcf21* (55), *Sox10* (10), *Fgf9* (56), *Dhh* (57), *Hhat* (58) and *Amh* (59)). Some genes were bound by SOX9 in the mouse, but not in cattle (*Ctnnb1, Cited2, Dmrt1, Hhat, Notch1, Pdgfa* and *Wnt4*), or *vice-versa* (*CYP26B1, PTGDS, SOX8*), suggesting a divergent regulation between species, or SOX9 redundancy with other SOX E group factors (SOX8 and 10) (10,60). SOX9 also bound to genes involved in the female programme of sex determination, such as *Wnt4* (61), *Fst, Bmp2* (62) and *FoxL2* (63), suggesting that it could negatively regulate their transcription in Sertoli cells.

Transcriptional regulation by SOX9 in foetal testis at E13.5

Comparison of the mouse SOX9 ChIP-seq dataset with previously published transcriptomic datasets from male and female supporting cell lineages (Sertoli and granulosa cells, respectively) in mouse E13.5 gonads (64) enabled us to identify candidate genes that could be up- or down-regulated by SOX9 cell autonomously at this stage. Specifically, 38% (557 out of 1451) of genes that were upregulated and 44% (539 out of 1225) of genes that were repressed in Sertoli cells compared with granulosa cells at E13.5 were bound by SOX9 (Figure 2A; see also Supplementary Table S1: Sheet 'ChIP-seq mouse mm9').

Then, to better understand SOX9 transcriptional function in foetal mouse testes, we analysed by RNA-seq the transcriptome of E13.5 gonads in which SOX9 was present or not. *Sox9* conditional knock-out in differentiating Sertoli cells was performed soon after testis commitment by crossing mice carrying the *Sox9* allele (*Sox9^flox^*) (65) with mice in which the Cre recombinase was controlled by the *Amh* gene promoter (66). In this context, a mild phenotype is observed and the effect on E13.5 gonad transcriptome can be essentially attributed to transcriptional mis-regulation in Sertoli cells due to *Sox9* loss (67). *Sox9* mRNA quantification in the RNA-seq datasets obtained using E13.5 wild type (WT) XY and XX gonads and XY mutant gonads (subsequently named XY *Sox9^Δ/Δ^* or KO in figures) showed that *Sox9* transcript levels were comparable in *Sox9^Δ/Δ^* XY and XX gonads (Supplementary Figure S2A), as previously reported (67).

Detailed analysis of the *Sox9^Δ/Δ^* testis transcriptome showed the downregulation of 240 mRNAs and the upregulation of 107 transcripts compared with WT XY testes
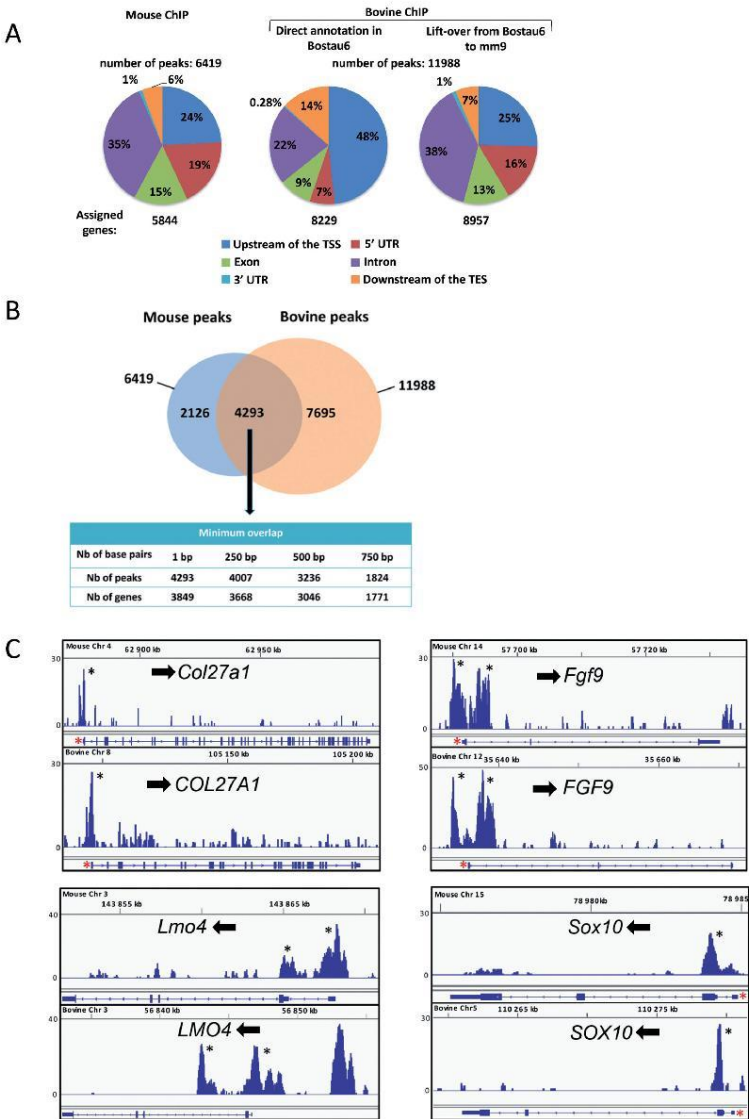
Figure 1. SOX9 peaks in mouse and bovine foetal testes. (**A**) Distribution of SOX9 peaks relative to neighbouring genes and gene components: upstream of the transcription start site (TSS), 5′ untranslated region (5′ UTR), exon, intron, 3′ untranslated region (3′ UTR) and downstream of the transcription end site (TES). For the bovine ChIP-seq dataset, annotations were made directly using the BosTau6 genome assembly (Ensembl UMD3.1) (middle pie-chart) or indirectly using LiftOver and the mouse genome (mm9) as the reference genome (right pie chart). (**B**) Venn diagram showing that SOX9 binds to 4293 orthologous mouse and bovine foetal testis regions. Bottom table: number of overlapping peaks (and of the respective genes) in the mouse and bovine ChIP-seq datasets (overlaps from 1 base pair (bp) to 750 bp). (**C**) Examples of peak position conservation in the mouse and bovine ChIP-seq datasets. For each gene, the upper panel represents the mouse gene and the lower panel the bovine gene. The input background was subtracted using IGV. Binding peaks called by MACS are indicated by asterisks. As in the BosTau6 genome assembly the TSS of bovine *FGF9* are missing, they were determined using LiftOver with mm9 and added by hand using IGV. Black arrows, direction of transcription; red stars, transcription start sites.

189
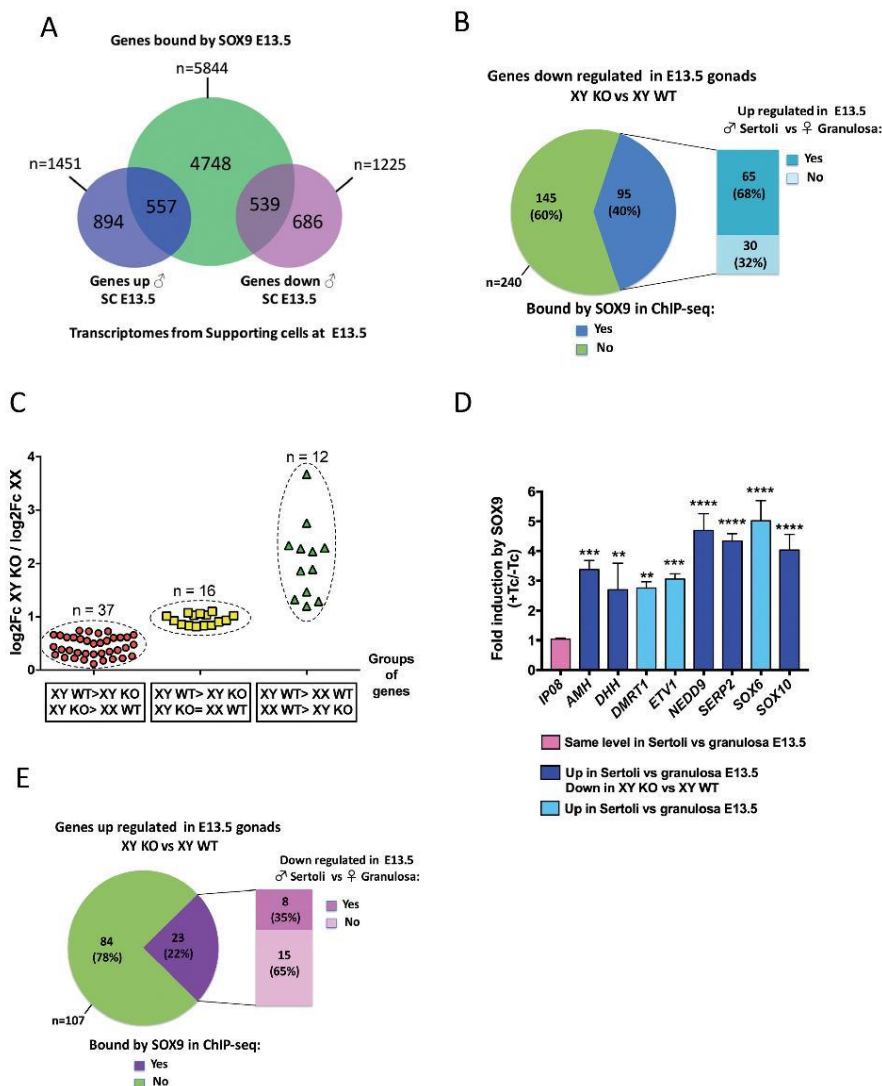
Figure 2. SOX9 role in the expression of its target genes in foetal testis (**A**) Venn diagram showing the association between mouse SOX9-bound genes (ChIP-seq dataset) and genes that are differentially expressed in E13.5 Sertoli and granulosa cells. Genes up or down: genes that are upregulated or downregulated in E13.5 male and female supporting cells (SC) (64). (**B**) Pie chart showing the classification of genes that are downregulated in $Sox9^{\Delta/\Delta}$ XY (XY KO) versus wild type XY (XY WT) gonads in genes bound or not by SOX9 (mouse ChIP-seq dataset). Among the 95 SOX9-bound genes, 68% were upregulated at E13.5 in wild type Sertoli versus granulosa cells (64). (**C**) The ratio between the log2 fold change (FC) of XY KO versus XY WT and the log2FC of XX WT versus XY WT allowed classifying the differentially regulated genes in three groups according to their levels of expression in the XY WT, XY KO and XX WT RNA-seq datasets. (**D**) RT-qPCR analysis of SOX9-mediated induction of gene expression in tet-SOX9-NT$_2$D$_1$ cells upon addition of tetracycline (Tc). Results are shown as the mean ± SD ($n = 3$); ****$P < 0.0001$; ***$P < 0.001$; **$P < 0.01$ compared with cells without tetracycline (ANOVA with the Geisser–Greenhouse correction for multiple comparisons). (**E**) Pie chart showing the classification of genes that are upregulated in XY $Sox9^{\Delta/\Delta}$ testis versus XY WT in genes bound or not by SOX9 (mouse ChIP-seq dataset). Only 8% of these SOX9-bound genes are down-regulated at E13.5 in wild type Sertoli (35%) versus granulosa cells (64).

190

Table 1. Most genes that have been involved in mammalian gonad determination and differentiation are SOX9 targets in mouse and cattle

Genes (Mouse/Bovine)	Nb of peaks in mouse	Nb of peaks in bovine	Bovine peaks orthologous to mouse peaks
Amh/AMH	1	1	0/1
Atrx/ATRX	1	1	1/1
Bmp2/BMP2	1	2	1/2
Cbx2/CBX2	1	1	1/1
Cited2/CITED2	1	0	-
Ctnnb1/CTNNB1 (β Catenin)	1	0	-
Cyp26b1/CYP26B1	0	3	-
Dhh/DHH	1	1	0/1
Dmrt1/DMRT1	1	0	-
Emx2/EMX2	1	3	1/3
Fgf9/FGF9	2	3	2/3
Fgfr2/FGFR2	1	1	0/1
FoxL2/FOXL2	2	2	0/1
Fst/FST	4	1	1/1
Gadd45g/GADD45G	1	1	1/1
Gata4/GATA4	3	3	1/3
Hhat/HHAT	1	1	0/1
Igf1r/IGF1R	1	3	0/3
Insr/INSR	1	2	1/2
Kdm3a/KDM3A (Jmjd1a/JMJD1A)	1	1	0/1
Lhx9/LHX9	2	5	3/5
Lmo4/LMO4	2	3	2/3
Map3K4/MAP3K4	0	0	-
Notch1/NOTCH1	1	0	-
Notch2/NOTCH2	1	1	0/1
Notch3/NOTCH3	0	2	-
Nr0b1/NR0B1(Dax1/DAX1)	1	1	1/1
Nr5a1/NR5A1 (Sf-1/SF-1)	2	1	0/1
Pdgfa/PDGFA	2	0	-
Ptgds/PTGDS	0	1	-
Rspo1/RSPO1	0	0	-
Six1/SIX1	1	2	1/1
Six4/SIX4	1	1	0/1
Sox8/SOX8	0	1	-
Sox9/SOX9	2	3	2/3
Sox10/SOX10	1	1	1/1
Sry/SRY	0	0	-
Tcf21/TCF21 (Pod1)	1	4	0/4
Wnt4/WNT4	1	0	-
Wt1/WT1	1	2	0/2
Wwox/WWOX	1	4	0/4
Zfpm2/ZFPM2(Fog2/FOG2)	1	5	2/5

The number of peaks per gene are shown in both species. For each gene is shown the number of bovine peaks having orthologous corresponding peaks in mouse.

(Supplementary Table S2: Sheet 'KO versus WT XY, adjusted $P < 0.05$'). Among the downregulated genes, 40% (95/240) were bound (based on our ChIP-seq experiment results) and presumably activated by SOX9 (Figure 2B and Supplementary Table S2: Sheet 'summary'). Therefore, the 240 genes downregulated in $Sox9^{\Delta/\Delta}$ testes were highly enriched in SOX9-bound genes (χ^2 test with Yates correction: $P < 0.0001$). Moreover, most of the SOX9-bound, downregulated genes (65 out of 95) were normally more strongly expressed at E13.5 in Sertoli cells than in granulosa cells (their female counterpart) (64) (see also http://www.ncbi.nlm.nih.gov/sites/GDSbrowser?acc=GDS3995) (Figure 2B and Supplementary Table S2: Sheet 'summary'). This makes of them strong candidates for positive and direct transcriptional regulation by SOX9. Comparison of the expression level of these 65 genes in the WT XY, $Sox9^{\Delta/\Delta}$ XY and WT XX gonad datasets allowed their classification into three groups. The first group represented genes whose expression in the XY mutant was intermediate between WT XY

and XX gonads (Figure 2C, red circles), suggesting that in the absence of SOX9, these genes are still partially active. This group included genes with an important role in sexual differentiation, such as *Amh* (encoding anti-Müllerian hormone) (68), *Sox10* (10) or *Dhh* (69) (Supplementary Figure S2B, upper panels). The second group (Figure 2C, yellow squares) included genes that were similarly expressed in XY $Sox9^{\Delta/\Delta}$ and WT XX gonads (e.g. *Rnd2*, *Mybl1* or *Gjb2*) (Supplementary Figure S2B, middle panels). This indicates that SOX9 regulates only the male-specific expression of these genes. The third group of genes displayed lower expression in XY $Sox9^{\Delta/\Delta}$ than in WT XX gonads (Figure 2C, green triangles and Supplementary Figure S2B, lower panels), suggesting that in E13.5 WT XX gonads, these genes are regulated by factors that are absent in XY $Sox9^{\Delta/\Delta}$ testes.

The finding that some SOX9-bound genes that were upregulated in E13.5 Sertoli cells (Figure 2A) were not downregulated in XY $Sox9^{\Delta/\Delta}$ gonads could be explained by

functional redundancy between SOX9 and SOX8. To verify that SOX9 could activate these genes, we used NT_2D_1 cells, a human cell line that displays some characteristics of Sertoli cells (70), to generate a line in which HA-tagged SOX9 expression can be induced by tetracycline (tet-SOX9-NT_2D_1 cells) (Supplementary Figure S2D shows the strong tetracycline-dependent expression of HA-tagged SOX9). We then used RT-qPCR analysis of tet-SOX9-NT_2D_1 cells before and after SOX9 induction to quantify the transcripts of genes that were bound by SOX9 in our ChIP-seq experiments (Figure 2D). Genes bound by SOX9 that were upregulated in E13.5 Sertoli cells and downregulated in E13.5 XY $Sox9^{\Delta/\Delta}$ testes (strong criteria to consider them as activated by SOX9 in Sertoli cells) were also upregulated upon induction of SOX9 by tetracycline (*AMH, DHH, NEDD9, SERP2, SOX10*) (dark blue bars in Figure 2D). Moreover, the expression of genes identified as SOX9 targets that were only upregulated in E13.5 Sertoli cells (light blue bars: *DMRT1, ETV1, SOX6*) also was increased by SOX9 expression in tet-SOX9-NT_2D_1 cells. As control, *IP08,* a SOX9-bound gene but without sexually dimorphic expression in the supporting lineage, was not upregulated by SOX9 induction in tet-SOX9-NT_2D_1 cells. These findings indicate that in foetal testes, SOX9 can bind to and upregulate the expression of genes that are only expressed in male supporting cells (i.e. Sertoli cells).

Finally, the finding that 107 genes were upregulated in KO XY gonads compared with WT XY gonads suggested that SOX9 could repress them in normal foetal testis, directly or indirectly. However, only 22% (23/107) of these genes (χ^2 test with Yates correction, $P = 0.94$) were bound by SOX9 and only eight were also upregulated in E13.5 female supporting cells compared with male supporting cells (Figure 2E and Supplementary Figure S2C). This suggests that genes repressed by SOX9 are less likely to be bound by SOX9 than genes activated by SOX9.

Role of SOX9 in RNA processing in foetal testis

SOX proteins could have a role in splicing regulation (71) and a direct link between SOX9 and the RNA processing of *Col2a1* (one of the SOX9 targets identified in our bovine ChIP-seq experiment) was demonstrated in chondrocytes (72). Therefore, we used our RNA-seq dataset to investigate SOX9 role in splicing of its target genes in foetal testis. Splicing of 154 mRNAs, of which 70 (45%) were bound by SOX9, was quantitatively different in $Sox9^{\Delta/\Delta}$ XY and WT XY testes (Figure 3A). All five classes of known alternative splicing events (73) were affected by SOX9 absence: exon cassette (also known as exon skipping), intron retention, alternative 3′ acceptor site, alternative 5′ donor site and mutually exclusive exons. Quantitative analysis of the WT XY and $Sox9^{\Delta/\Delta}$ XY RNA-seq datasets allowed calculating the Percent-Spliced-In (PSI) index that indicates the splicing efficiency for transcripts and can range from +1 (totally include) to –1 (totally exclude). The PSI values for transcripts of genes bound by SOX9 indicated that splicing efficiency differed between the WT XY and $Sox9^{\Delta/\Delta}$ XY datasets (Figure 3A; for details see Supplementary Table S3: Sheet 'XY WT versus XY KO'). Specifically, SOX9 absence affected the splicing of genes with important roles in sex

determination and differentiation, such as *Atrx* (74), *Fgfr2* (75) and *Gadd45g* (52). Importantly, in 20 of the 70 differentially spliced genes bound by SOX9 (28%), SOX9 peaks overlapped with the exon/intron boundary involved in the splicing events (gene names underlined in Figure 3A, and examples in Figure 3B). Analysis of somatic and germ cell-specific transcriptomic datasets from foetal male and female mouse gonads (64) showed that the expression of SOX9-bound genes with alternatively spliced transcripts was not particularly sex- or cell-specific (not shown). This suggests that SOX9 may regulate some discrete molecular mechanisms that require finer transcriptomic analyses to be revealed.

We next investigated SOX9 mediated sex-specific splicing by searching for common splicing events between WT XY and $Sox9^{\Delta/\Delta}$ XY and between WT XY and WT XX datasets. Compared with WT XY gonads, several transcripts showed differential splicing events that involved the same exons in $Sox9^{\Delta/\Delta}$ XY and WT XX gonads (Figure 3C). Their respective PSI values were always in a similar range when comparing WT XY with $Sox9^{\Delta/\Delta}$ XY or WT XX gonads (Supplementary Table S3: Sheets 'XY WT versus XY KO' and 'XY WT versus XX WT'). This indicates that splicing of these exons is similar in $Sox9^{\Delta/\Delta}$ XY and WT XX gonads. We conclude that SOX9 regulates male-specific splicing of several of its target genes.
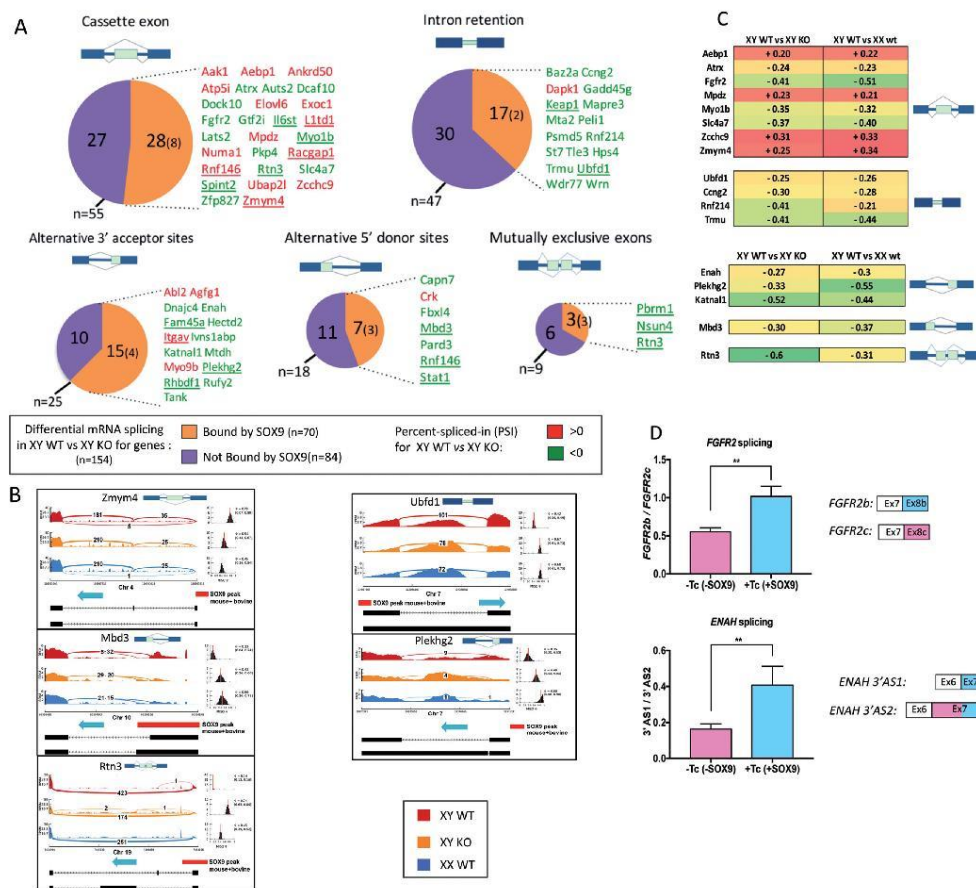
In all cases, these splicing events will modify the resulting protein sequences. Moreover, intron retention can also modify the intrinsic level of the translated proteins. For instance, in XX WT and $Sox9^{\Delta/\Delta}$ XY, retention of the second intron of the *Ubfd1* gene leads to the disruption of the open reading frame and to a shorter truncated protein of 204 amino acids instead of full length 368 amino acids UBFD1 (Figure 3B, panel Ubfd1). Moreover, at the transcriptional level, published transcriptomic datasets (64) and our RNA-seq data showed no variation in *Ubfd1* gene expression between male and female gonads, suggesting that SOX9 could control the protein level of active UBFD1 via a discrete splicing mechanism that does not affect the transcript level. Similarly, the second intron of *Gadd45g*, which has a role in sex-determination (52,76), was retained in $Sox9^{\Delta/\Delta}$ XY testes, leading to a shorter truncated protein of 52 amino acids instead of full length GADD45g (159 amino acids in length). As for the *Ubfd1* transcript, *Gadd45g* mRNA level at E13.5 was not significantly different between male and female E13.5 gonads (64).

Supporting these findings on splicing, we observed that induction of SOX9 expression in tet-SOX9-NT_2D_1 cells modified the ratio of splicing events for *FGFR2* and *ENAH* transcripts as observed in $Sox9^{\Delta/\Delta}$ XY / WT XY mouse foetal gonads (Figure 3D).

SOX9-bound genomic regions in foetal testes are enriched in binding motifs for three Sertoli cell differentiation/reprogramming factors

Our ChIP-seq analysis using chromatin from mouse and bovine foetal testes identified several regions (4293 peaks) that were bound by SOX9 in both species (Figure 1B). As DMRT1, GATA4, WT1, SF1 and SOX9 can reprogram embryonic fibroblasts into embryonic Sertoli cells (18), we

Figure 3. Analysis of differential splicing events in Sox9$^{\Delta/\Delta}$ XY gonads. (**A**) Pie charts for each of the splicing events deregulated in KO XY gonads compared with WT XY gonads. Transcripts of SOX9-bound genes (orange area) are listed in green when their Percent-Spliced-In (PSI) index is negative and in red when the PSI index is positive. For a splicing event in a given condition, PSI is between 0 (splicing event totally excluded) and 1 (splicing event totally included). The PSI values reported here correspond to the PSI value difference between genotypes. Underlined names represent genes where SOX9-bound peaks overlapped with the exons/introns involved in the splicing event; their total number is indicated between brackets in the relevant pie-chart. (**B**) Sashimi plots showing examples of the splicing events altered in *Sox9*$^{\Delta/\Delta}$ testes and described in Figure 3A, obtained from RNA-seq datasets. These transcripts correspond to genes that are bound by SOX9 in mouse *or* mouse and cattle, with ChIP-seq peaks in the vicinity of regions of splicing events (genes underlined in Figure 3A). Red bars, position of SOX9 peaks; blue arrows, direction of transcription. For each genotype (WT XY, KO XY and WT XX gonads), the quantification of the PSI value (Ψ) with 95% confidence intervals (histograms on the on right side of each panel) obtained using MISO are reported. Values reported on Sashimi plots correspond to the number of sequencing reads per splice junction. (**C**) Comparison of transcripts displaying differential splicing in WT XY versus KO XY gonads and in WT XY versus WT XX gonads. The table lists transcripts with the same differential splicing in the two situations. The color scale goes from red (inclusion of the splicing event; PSI>0) to green (exclusion of the splicing event; PSI<0). (**D**) RT-qPCR analysis of *FGFR2* and *ENAH* transcript splicing ratio using mRNA samples from tet-SOX9-NT$_2$D$_1$ cells in which SOX9 expression was induced (+Tc) or not (–Tc). Data are the mean ± SD (*n* = 3); *******P* < 0.01 compared with the –Tc condition (Student's *t* test).

193

asked whether conserved binding motifs for these factors could be present in the vicinity of the identified SOX9 binding sites. Therefore, we developed a normalization bioinformatics method to detect sequences enriched in known consensus DNA motifs (41,43,77–79) recognized by the five Sertoli cell differentiation factors in the mouse and bovine SOX9 ChIP-seq datasets. The motif enrichment fold was the ratio of the number of binding motifs found in the ChIP-seq datasets versus the number found in the corresponding scrambled sequences (30 sets). The mouse and bovine ChIP-seq datasets were similarly enriched in DNA-binding motifs for SOX9, DMRT1 and GATA4 (i.e. the ratio ChIP/scrambled was >1) (Figure 4A, red and orange bars, left histogram) compared with unrelated genomic regions (blue bars). Conversely, SF1 motifs were not enriched and WT1 motifs were non-specifically enriched in the ChIP-seq datasets as well as in the unrelated genomic regions. As a control, binding motifs of transcription factors not related to Sertoli cell differentiation were not enriched in the two ChIP-seq datasets (Figure 4A, right histogram). SOX9/DMRT1/GATA4 binding motif enrichment was neither due to repetitive sequences (Supplementary Figure S3A) nor dependent on the position of the peaks relative to the gene body (Supplementary Figure S3B). Thus, SOX9 target sequences are enriched in binding motifs for SOX9, GATA4 and DMRT1. The same motif enrichment was also found in the orthologous regions of twelve other mammal genomes (Supplementary Figure S3C), suggesting that this genomic feature is conserved among mammals.

To determine whether this global motif enrichment reflected a situation existing at each genomic fragment bound by SOX9, we investigated the co-occurrence of SOX9, GATA4, DMRT1, SF1 and WT1 binding motifs in both SOX9 ChIP-seq datasets. The number of occurrences of DNA motifs for the five Sertoli cell differentiation/reprogramming factors was plotted against each other to assess whether a linear correlation existed between motifs (examples of scatterplots with Pearson correlation coefficients, PCC, are presented in Supplementary Figure S3D). The PCC obtained for the ChIP-seq datasets and control scrambled sequences showed a strong correlation (PCC between 0.7 and 0.9) among SOX9, GATA4 and DMRT1 motifs in both mouse and bovine ChIP-seq datasets (Figure 4B). By contrast, SF1 motifs were poorly represented (Figure 4B and Supplementary Figure S3D; PCC: 0.30–0.37) and WT1 motifs showed almost no correlation with the other four motifs. No correlation was observed between SOX9 motifs and TF motifs (negative control) and for any combination with the corresponding scrambled sequences. The co-occurrence of SOX9, GATA4 and DMRT1 DNA-binding motifs was also observed in the orthologous regions of SOX9 ChIP-seq datasets from the twelve mammalian genomes (Figure 4C). This indicates that the association of SOX9, GATA4 and DMRT1 DNA-binding motifs in these genomic regions is conserved among mammals. Compilation of the three motifs enriched in both ChIP-seq datasets showed that they were highly similar in rodent and bovine species (Supplementary Figure S3E), but displayed a milder selectivity than the consensus motifs obtained by *in vitro* selection for SOX9 (43), GATA4 (77) and DMRT1 (41).

Characterization of a Sertoli cell signature (SCS) in SOX9 genomic targets in foetal testis

To determine whether this SOX9, GATA4 and DMRT1 DNA-binding motif enrichment at SOX9-bound genomic regions was unique to foetal Sertoli cells, we analysed SOX9, GATA4 and DMRT1 binding motif enrichment in randomly selected ChIP-seq datasets for 13 transcription factors and eight SOX factors expressed in various tissue and cell types (http://www.ncbi.nlm.nih.gov/geo/). Compared with the mouse SOX9 ChIP-seq foetal testis dataset, we did not detect any motif enrichment in ChIP-seq datasets for the unrelated transcription factors (Figure 4D) and other SOX factors (Figure 4E).

Analysis of SOX9 ChIP-seq datasets from seven other mouse tissues highlighted a slight SOX9/DMRT1/GATA4 binding motif enrichment in rib chondrocytes (80), atrioventricular canal (AVC), limb (81) and hair follicle stem cells (HF-SCs) (82) (Figure 4F, blue bars). This enrichment was similar to the one observed for other transcription factors and SOX factors. On the other hand, in mouse basal cell carcinoma (BCC) (83) and human colorectal cancer cells (84), SOX9/DMRT1/GATA4 binding motif enrichment was comparable to the one observed in foetal testis, but for the DMRT1 motif (Figure 4F, green bars). After conversion of the coordinates of the relevant human regions to the mouse orthologous regions, we found an important peak overlap between our SOX9 ChIP-seq testis datasets and the colorectal cancer cell and BCC datasets, but not with the rib chondrocyte, limb, AVC and HF-SC SOX9 ChIP-seq datasets (Supplementary Figure S4). This shows that, at least in these two cancer types, SOX9 binds to regions with genomic features very similar to those observed in differentiated foetal Sertoli cells.

We named this genomic feature the 'Sertoli Cell Signature' (SCS) because we detected enrichment for SOX9/DMRT1/GATA4 binding motifs specifically in genomic regions bound by SOX9 in Sertoli cells from foetal testis.

Binding motifs in the SCS are clustered and organized

We then asked whether the SOX9/DMRT1/GATA4 binding motifs were organized within ChIP-seq peaks. In most of the cases, adjacent binding motifs were separated by less than 50 bp both in the mouse and bovine ChIP-seq datasets, indicating that they clustered together (Supplementary Figure S5A). By analyzing nucleotide spacing between motifs in both murine and bovine datasets (Supplementary Figure S5B) we observed that the distance between adjacent motifs was lower than ten nucleotides and remarkably conserved from mouse to cattle in term of distance and orientation. For instance, SOX9 motifs were preferentially on the same strand and separated by one or three nucleotides. Altogether, our results show that SOX9/DMRT1/GATA4 motifs are strongly clustered in both species. To confirm this, the distance of each motif relative to the nearby TSS was measured in peaks positioned
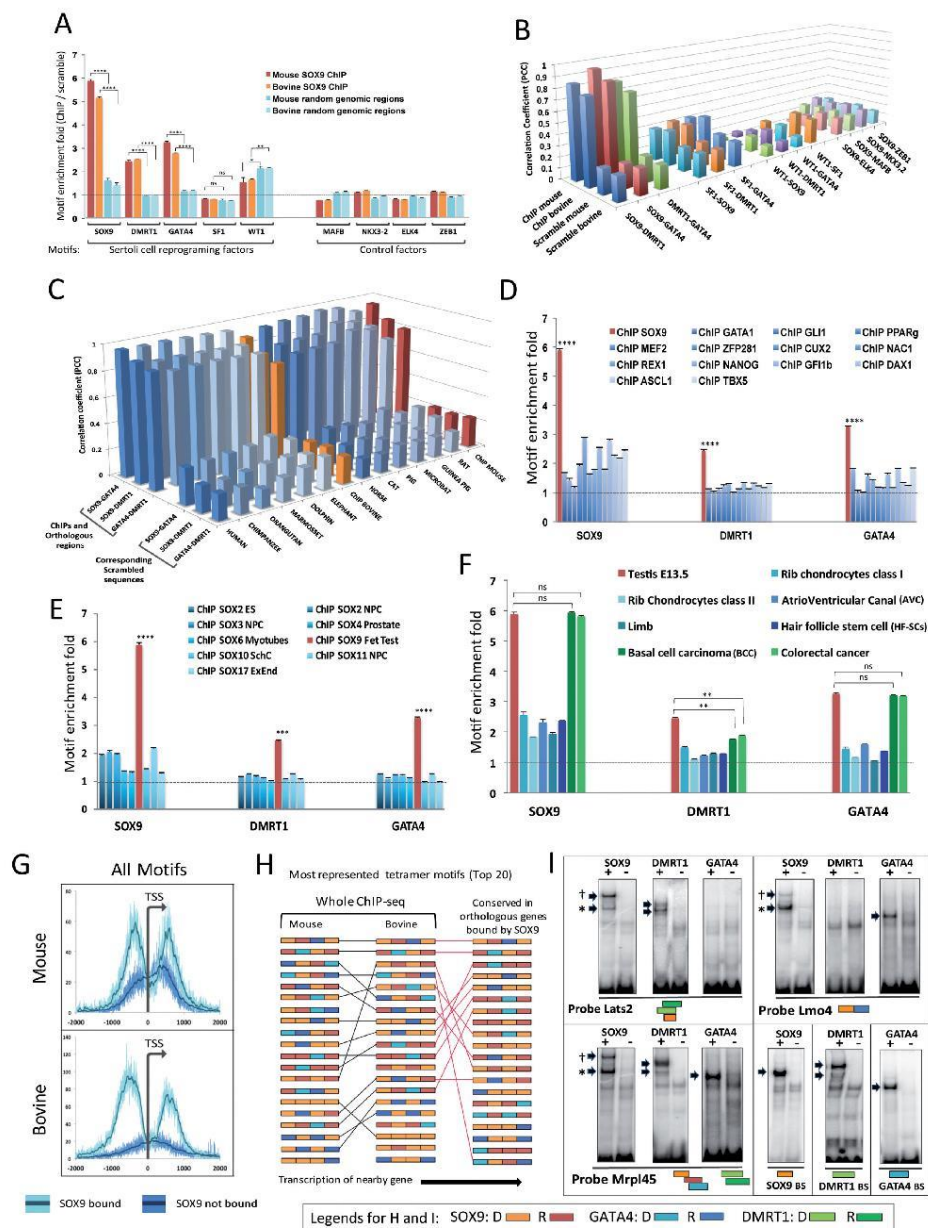
Figure 4. In foetal testis, SOX9 binds to genomic regions enriched in SOX9, DMRT1 and GATA4 binding motifs. (**A**) Global enrichment of binding motifs for the five Sertoli cell differentiation/reprograming factors (SOX9, GATA4, DMRT1, SF1 and WT1) and four unrelated transcription factors (control factors) in the mouse and bovine SOX9 ChIP-seq datasets (red and orange bars). Randomly selected mouse and bovine genomic regions (blue

near the TSS (i.e. from –1 kb to +1 kb around the TSS). The distribution of the three binding motifs analysed together (Figure 4G) or separately (Supplementary Figure S5C) followed a bimodal pattern around the TSS of both mouse and bovine SOX9 target genes, but not of unrelated genes (not bound by SOX9). This shows that in the mouse and cattle, SOX9/DMRT1/GATA4 binding motifs cluster and that for peaks around TSS, SCSs are located preferentially at –500/400 bp or at +600 bp from the TSS.

Next, we asked whether the three binding motifs showed a preferential order within SCSs and whether this order was conserved in mouse and bovine orthologous regions bound by SOX9. To this aim, we counted the occurrence of every possible multimer of each binding motif (from trimers to octamers) in both ChIP-seq datasets, taking in account their direct (D) or reverse orientation (R) relative to the direction of transcription of the neighboring gene. Analysis of the occurrence of motif tetramers (for detailed analysis see Supplementary Figure S6A and B) showed that among the 1296 possible tetramer combinations, 16 of the 20 most represented tetramers (top 20) were common between mouse and bovine SOX9 target regions (Figure 4H, black lines in left panels). This demonstrates the presence of a common, preferential organization of the motifs composing the SCS in both species. Of note, the two most represented tetramers were the same in both species, but in the reverse orientation. However, among the 3849 orthologous genes bound by SOX9 in both species (Figure 1B), only 670 (17.4%) displayed a strictly conserved organization of SCS tetramer motifs. Among these genes, we ranked the 20 most represented tetramers (Figure 4H, right panels and Supplementary Figure S6C) and found that 12 belonged to the previously identified top 20 tetramers (Figure 4H, red lines).

Surprisingly, in both mammals, the top 20 tetramers included only SOX9 and GATA4 motifs in both orientations, and the first tetramers that included a DMRT1 motif were ranked at positions below 50. This suggests that in regions bound by SOX9, the position of DMRT1 motifs, even if strongly correlated with either SOX9 or GATA4 motifs (see Figure 4B), is less constrained than that of the two other motifs. In summary, this analysis highlighted a strong preferential SOX9/DMRT1/GATA4 motif organization in

mouse and bovine SCSs, although orthologous genes displayed only a relatively low conservation of the motif organization. Among the three motifs, SOX9 and GATA4 showed the strongest association within SCSs.

To test whether the predicted DNA motifs present in SCS were bound by SOX9, DMRT1 and GATA4, we performed *in-vitro* gel shift assays using *in-vitro* translated proteins and different probes with various combinations of motifs derived from SOX9 peaks harbouring SCS (Figure 4I) or with the SOX9, DMRT1 and GATA4 consensus binding motifs (controls; panels 'BS' in Figure 4I). SOX9 and DMRT1, but not GATA4, could bind to the *Lats2* probes (only DNA motifs for SOX9 and DMRT1). The *Lmo4* probe (SOX9 and GATA4 motifs) interacted only with SOX9 and GATA4, but not with DMRT1. Finally, the *Mrpl45* probe (all three motifs) bound to all three factors. In each case, we observed always two distinct complexes for SOX9, suggesting that SOX9 could binds either as monomeric (*) or dimeric (†) forms, in contrast with the BS probe that contains the *in vitro* defined SOX9 consensus motif (panel SOX9 BS on Figure 4I). However, we did not observe a clear preference for monomeric or dimeric SOX9, it depends of the probe used. Indeed, SOX9 bound preferentially as a homodimer to the *Lats2* probe, and as a monomer to the *Lmo4* and *Mrpl45* probes. Interestingly, SOX9 could bind as a homodimer also to a probe with a single predicted motif (probe *Lats2*). We also observed at least two protein-DNA complexes for DMRT1, as already published (41), and only one for GATA4. We conclude that the *in silico* predicted DNA motifs of the SCS are effectively bound, at least *in vitro*, by SOX9, DMRT1 and GATA4.

Genes bound by DMRT1 in foetal testis harbour SCSs only if they are also bound by SOX9

In foetal testis, *Dmrt1* is expressed in Sertoli and germ cells (85). As DMRT1 motifs were highly correlated with SOX9 motifs within SCSs, we hypothesized that these two transcription factors have common target genes in foetal Sertoli cells. We first confirmed that both SOX9 and DMRT1 were co-expressed in the nucleus of Sertoli cells at E13.5 (Figure 5A). Then, to determine whether SOX9 and DMRT1 had common target genes, we compared E13.5 mouse DMRT1

---

bars) were used as controls. (**B**) Pearson correlation coefficients (PCC; Y axis) for the indicated combinations of DNA binding motifs in the mouse and bovine ChIP-seq datasets and scrambled sequences. (**C**) PCC (Y axis) for the three combinations of DNA binding motifs (SOX9-GATA4; SOX9-DMRT1 and GATA4-DMRT1) in the mouse (red bars), bovine (orange bars) ChIP-seq datasets and in orthologous regions from twelve other mammals (blue bars). Genome builds are detailed in Supplementary Figure S3C. (**D**) SOX9, DMRT1 and GATA4 binding motif enrichment in ChIP-seq datasets for transcription factors (GATA1, GLI1, PPARg, MEF2, ZFP281, CUX2, NAC1, REX1, NANOG, GFI1b, ASCL1 and TBX5) expressed in various tissue and cell types. (**E**) SOX9, DMRT1 and GATA4 binding motif enrichment in ChIP-seq for other SOX factors (SOX2, SOX2, SOX3, SOX4, SOX6, SOX10, SOX11 and SOX17). ES, ES cells; NPC, neural progenitor cells; SchC, Schwann cells; ExEnd, extra-embryonic endoderm; Fet Test, foetal testis. (**F**) SOX9, DMRT1 and GATA4 binding motif enrichment in SOX9 ChIP-seq datasets from various tissues. For (D), (E) and (F), see description of tissue/cell types used to obtain the datasets in Supplementary Tables S4 to S6. For panels (A), (D), (E), (F): data are the mean ± SD; **** $P < 0.0001$; *** $P < 0.001$; ** $P < 0.01$; ns: not significant (ANOVA with the Geisser–Greenhouse correction for multiple comparisons). (**G**) Graph showing for peaks close to the TSS in the mouse and bovine SOX9 ChIP-seq datasets, the averaged curves of the localization of the SOX9, GATA4 and DMRT1 binding motifs relative to the TSS. X-axis: nucleotide distance from the TSS. Y-axis: count of the three motifs. (**H**) The 20 most represented tetramer motifs among peaks bound by SOX9 in the mouse (left) and bovine (middle) datasets. On the right: the top 20 conserved tetramers among orthologous genes bound by SOX9 in the mouse and bovine ChIP-seq datasets. Motifs are in the direct (D) or reverse (R) orientation relative to the transcription of the nearby gene (black arrow). Black and red lines show identical tetramers in the two mammalian species. (**I**) Electrophoretic mobility shift assays showing binding of *in vitro* translated SOX9, DMRT1 and GATA4 proteins to DNA probes derived from mouse ChIP-seq peaks assigned to the *Lats2*, *Lmo4* and *Mrpl45* genes and containing SCSs. +/ indicate programmed and un-programmed lysates. Arrows indicate protein/DNA complexes. †: SOX9 dimers; *: SOX9 monomers; BS, control probes with the consensus binding motifs for SOX9, DMRT1 and GATA4. Coloured bars indicate the direct (D) or reverse (R) orientation of motifs in each DNA probe.
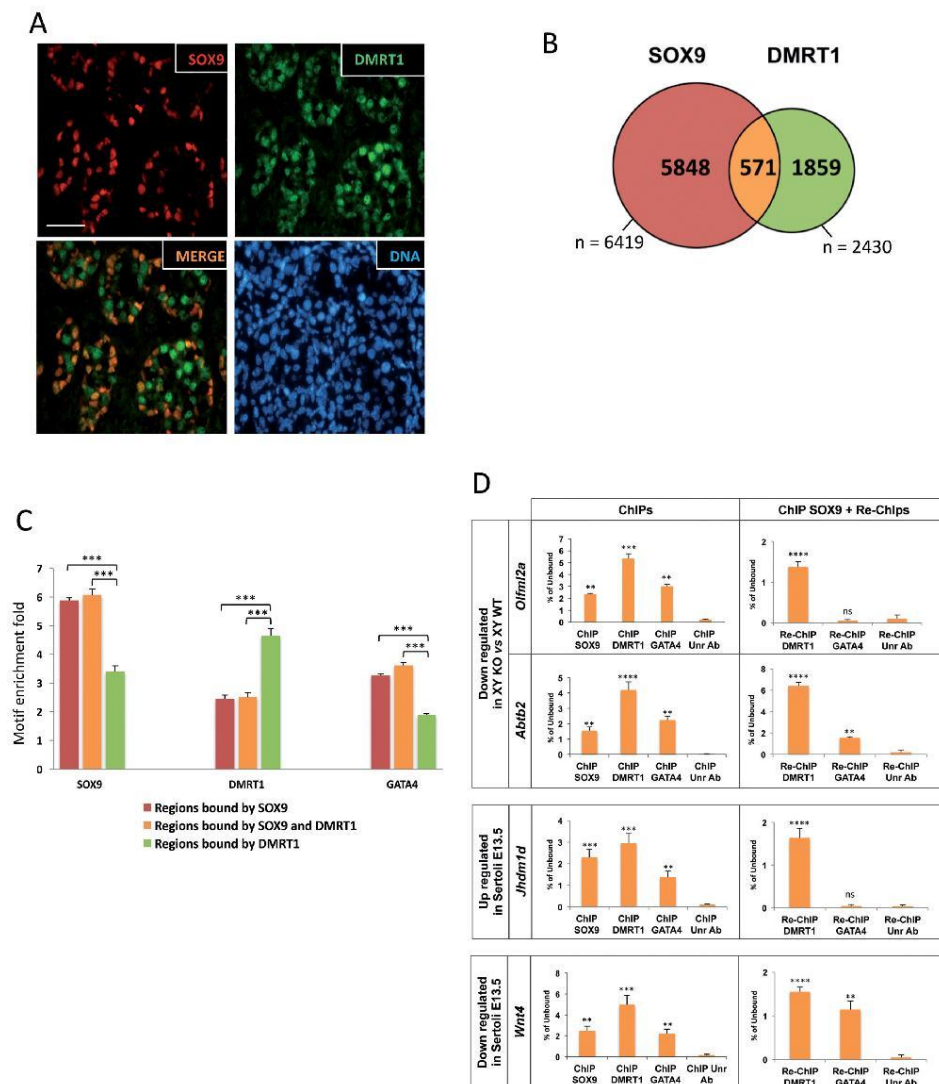
Figure 5. Genes bound by DMRT1 in foetal testis have SCSs only if they are bound also by SOX9. (**A**) Immunofluorescence experiments with antibodies against SOX9 (red) and DMRT1 (green) on sections of E13.5 wild type XY gonads. Merged view shows Sertoli cells that express both SOX9 and DMRT1 in the nucleus (orange). DNA was stained with DAPI (blue). Scale bar, 30 μm. (**B**) Venn diagram showing the genomic overlap between peaks bound both by SOX9 and DMRT1 from independent SOX9 and DMRT1 ChIP-seq datasets from E13.5 foetal testes. (**C**) SOX9, DMRT1 and GATA4 binding motif enrichment in regions bound by SOX9 only (red bars), SOX9 and DMRT1 (orange bars) and DMRT1 only (green bars). (**D**) ChIP-qPCR (left panels) and sequential ChIP-qPCR (right panels) assays of sheared chromatin from E13.5 foetal mouse testes. For ChIPs, chromatin samples were immunoprecipitated in parallel with anti-SOX9, -DMRT1 or -GATA4 antibodies. For sequential ChIPs, samples were first immunoprecipitated with an anti-SOX9 antibody and then with an anti-DMRT1 or anti-GATA4 antibody. The analysed genomic regions correspond to overlapping SOX9 and DMRT1 ChIP-seq peaks. *Olfml2a* and *Abtb2* are genes upregulated in E13.5 Sertoli cells versus granulosa cells and downregulated in XY KO gonads. *Jhdm1d* and *Wnt4* are genes up- and down-regulated, respectively, in E13.5 Sertoli cells versus granulosa cells. Data are the mean ± SD ($n = 3$); ****$P < 0.0001$; ***$P < 0.001$; **$P < 0.01$ (ANOVA with the Geisser–Greenhouse correction for multiple comparisons).

197

(25) and SOX9 ChIP-seq datasets and found that among the 2430 and 6419 respective peaks, 671 overlapped (Figure 5B). As a control, 30 sets of 2430 regions of equivalent size and randomly selected in the mouse genome displayed very little overlap (<10 regions) with the 6419 peaks of the SOX9 ChIP-seq dataset (not shown). From these 571 common regions, we also identified 411 (71%) orthologous regions in the bovine SOX9 ChIP-seq dataset (not shown).

We then analyzed separately the SCS content of the two populations of peaks in the DMRT1 ChIP-seq dataset (i.e. regions bound or not by SOX9). Overall, regions bound by DMRT1 displayed the same global enrichment for SOX9, DMRT1 and GATA4 binding sites as observed in the SOX9 ChIP-seq dataset. However, in peaks bound only by DMRT1, SOX9 and GATA4 sites were not as enriched as DMRT1 binding sites (Figure 5C). Similar results were obtained by calculating the PCCs (Supplementary Figure S7). From these analyses, we conclude that regions bound by DMRT1 in foetal testis display SCSs only when they are also bound by SOX9.

On the basis of these results, we hypothesized that on Sertoli cells chromatin, DMRT1 and GATA4 could co-habit in proximity of SOX9 on it target genes. To verify this hypothesis, we performed ChIP and sequential ChIP-qPCR assays using E13.5 foetal testis chromatin extracts. For sequential ChIP (also known as ChIp re-ChIP), we took advantage of the fact that in foetal testis, SOX9 is expressed only in Sertoli cells, while DMRT1 and GATA4 are expressed in Sertoli cells and also in germinal (Figure 5A) and interstitial compartment cells, respectively (Supplementary Figure S7B). Therefore, we first immunoprecipitated chromatin with an anti-SOX9 antibody to retain only chromatin from Sertoli cells, and after immune complex dissociation, we performed the second immunoprecipitation with an anti-DMRT1 or GATA4 antibody. For qPCR analysis, we chose probes that amplify the following four regions (among the 571 overlapping peaks in SOX9 and DMRT1 ChIP-seqs; orange area and bars in Figure 5B and C): the *Olfml2a* and *Abtb2* genes that are downregulated in $Sox9^{\Delta/\Delta}$ XY testes, and the *Jhdm1d* and *Wnt4* genes that are up- and down-regulated, respectively, in E13.5 Sertoli cells compared with granulosa cells (64). Single ChIP assay showed that the four genes were bound by SOX9, DMRT1 and GATA4 in E13.5 whole testis extracts (Figure 5D, left panels). Sequential ChIPs (Figure 5D, right panels) showed that in Sertoli cells, *Olfml2a, Abtb2, Jhdm1d* and *Wnt4* were bound by SOX9 and DMRT1, while only *Abtb2* and *Wnt4* were bound by SOX9, DMRT1 and GATA4. The fact that the genes *Olfml2a* and *Jhdm1d* were immunoprecipitated in the GATA4-ChIP, but not by SOX9-ChIP with GATA4-re-ChIP is explained by the expression of GATA4 by non-Sertoli cells (i.e. SOX9-negative cells) (Supplementary Figure S7B). As control, ChIP-seq peaks from genes that are strongly expressed in germ cells and bound only by DMRT1 (green circle and bars in Figure 5B and C), like *Cdk12* and *Nek3*, were not bound by SOX9 (not shown).

Our results show that, in SOX9 target genomic regions, DMRT1 and GATA4 bind near SOX9 in foetal Sertoli cells.

SCS scanning identified TRIM28 as a new SOX9 partner in foetal testis

As regions bound by DMRT1 with a SCS were also bound by SOX9 in foetal testes, we hypothesized that by searching for SCSs in ChIP-seq datasets of various unrelated transcription factors we might identify new proteins that contribute to SOX9-mediated transcriptional regulation in Sertoli cells. By analyzing ChIP-seq datasets for 50 different transcription factors obtained from GEO, we identified a SCS in the dataset for the nuclear factor TRIM28 in mouse embryonic stem (ES) cells (TRIM28 ChIP-seq dataset) (86) (Figure 6A) where 1501 peaks (44.5% of 3370) overlapped with those of the mouse SOX9 ChIP-seq dataset (Figure 6B). As this finding indicates that TRIM28 can bind to the same genomic regions as SOX9, the two might physically interact. Co-immunofluorescence experiments showed that TRIM28 and SOX9 were both expressed in the nucleus of foetal Sertoli cells (Supplementary Figure S8A) where they co-localize, as indicated by super-resolution three-dimensional structured-illumination (3D-SIM) microscopy with z-sections of 0.12 µm (87) (Figure 6C, white arrows). Moreover, two different antibodies against the N- or C-terminal moieties of SOX9 could co-immunoprecipitate TRIM28 with SOX9 in NT$_2$D$_1$ cells (Supplementary Figure S8B). Pull-down assays with purified recombinant proteins showed that GST-TRIM28 interacted directly with SOX9 (Figure 6D). SOX9 and TRIM28 were also co-immunoprecipitated in nuclear extracts from E13.5 mouse foetal testes, but not from foetal ovaries that do not express SOX9 (Figure 6E). This confirms that this interaction also occurs in foetal Sertoli cells. To test whether SOX9 and TRIM28 co-localized on foetal Sertoli cell chromatin, we then performed sequential ChIP-qPCR experiments. Among the 1501 genes that are bound by SOX9 and TRIM28 (orange in Figure 6B), we chose *Sox13* and *Sox10*, two genes that are downregulated in $Sox9^{\Delta/\Delta}$ XY gonads, and *Fgf18* and *Wnt4* that are up- and down-regulated, respectively, in E13.5 Sertoli cells compared with granulosa cells (64). Single ChIP-qPCR (Figure 6F, left panels) showed that both SOX9 and TRIM28 bound to these genes in E13.5 testes, and sequential ChIP (ChIP with anti-SOX9 antibody followed by re-ChIP with an anti-TRIM28 antibody) gave similar results. This demonstrates that, in Sertoli cells, for these SOX9 target genes TRIM28 binds to chromatin near SOX9.

To investigate whether SOX9 and TRIM28 could collaborate on transcriptional regulation, we transduced HEK293 human embryonic kidney cells with a tet-SOX9 lentiviral vector (tet-SOX9-HEK293 cells), as previously done in NT$_2$D$_1$ cells. We chose HEK293 cells for this experiment, rather than NT$_2$D$_1$ cells, because of their low endogenous SOX9 and TRIM28 expression levels. Tetracycline-induced expression of the *SOX9* transgene strongly induced the expression of endogenous *SOX10* compared with cells without tetracycline. This effect was significantly increased in tet-SOX9-HEK293 cells that overexpressed also TRIM28 (Figure 6G, upper panel). In agreement, SOX9-mediated downregulation of *EMX2*, a gene that is strongly repressed in differentiating foetal Sertoli cells (Figure 6F), also was significantly increased by co-expression of TRIM28 (Figure
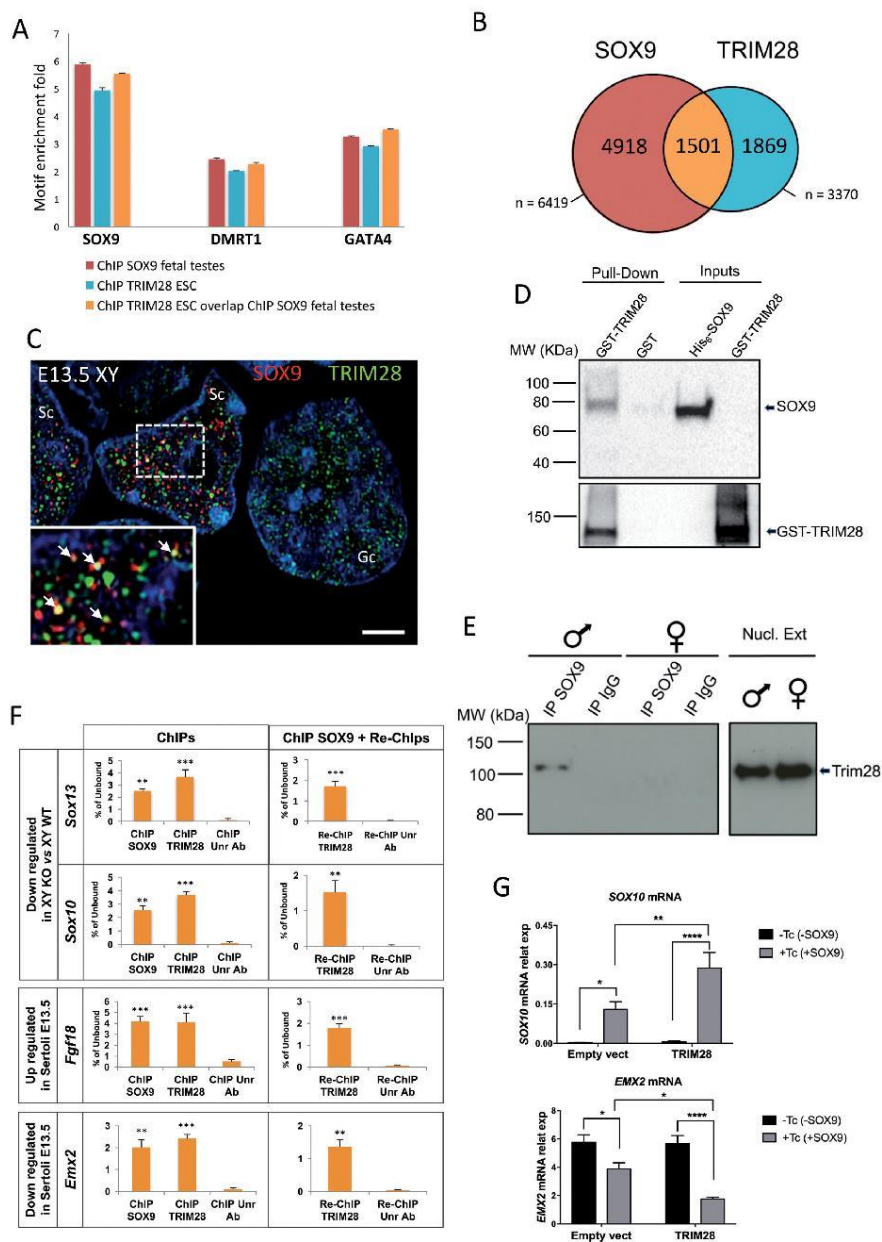
Figure 6. SCS screening allowed the identification of TRIM28 as a new SOX9 partner in foetal testis. (**A**) The three SOX9/DMRT1/GATA4 binding motifs are similarly enriched in the TRIM28 ChIP-seq dataset from mouse ES cells (blue bars) (Supplementary Table S7) as the SCSs observed in the

6G, lower panels). These results suggest that TRIM28 could contribute to SOX9-mediated activation or repression of its target genes.

These findings indicate that TRIM28 binds together with SOX9 to chromatin regions containing SCSs and may contribute to the transcriptional regulation SOX9 target genes in foetal Sertoli cells. This strongly supports a novel functional relationship between SOX9 and TRIM28 and suggests that TRIM28 might be a new factor of testis differentiation with a role that remains to be fully characterized.

DISCUSSION

In this study, we tried to elucidate how the transcription factor SOX9 controls Sertoli cell fate by regulating the expression/transcription of its target genes. First, we identified the set of genes bound by SOX9 in two distant mammals (mouse and cattle) at an equivalent stage of foetal testis development. The 4293 conserved SOX9-bound genes include many molecules with previously described roles in male and female somatic sex determination. Moreover, a considerable proportion of genes that are up- or down-regulated specifically in Sertoli cells at E13.5 (64) are bound by SOX9 (38% and 44% respectively), suggesting that SOX9 could simultaneously activate the male and repress the female differentiation pathway. Supporting this, we observed that in both mouse and bovine foetal testes, SOX9 also binds to typical female genes, such as *Wnt4* (61), *Fst, Bmp2* (62) and *FoxL2* (63).

To investigate the functional role of SOX9 in Sertoli cells, we then knocked-out the *Sox9* gene after primary sex determination specifically in Sertoli cells. This allowed creating a hypomorphic mutant of the SOX E group. Moreover, in this genetic background, *Sox8* remains active and plays a partial compensatory role (67). Therefore, the effects on the E13.5 gonad transcriptome should result from transcriptional mis-regulation only in Sertoli cells.

In $Sox9^{\Delta/\Delta}$ XY gonads, 240 genes were down- and 107 genes up-regulated compared with wild type XY gonads. SOX9-bound genes were more frequently found among the downregulated than the upregulated genes (40% versus 22%), suggesting that SOX9 acts mainly as a transcriptional activator. Alternatively, *Sox8* could replace *Sox9* for this function because in the double *Sox9* and *Sox8* knock-out, *FoxL2*, a female gene bound by SOX9 in the mouse and

bovine ChIP-seq datasets, shows ectopic testicular expression (88). Among the 95 SOX9-activated genes (*i.e.*, down-regulated in the absence of SOX9), 65 are also differentially expressed in male and female supporting cells and the expression of 37 of them in $Sox9^{\Delta/\Delta}$ XY gonads was intermediate between that observed in wild type XY and XX gonads. For example, *Sox10* displayed residual expression, probably the result of its activation by SOX8, as already reported (88). Also, our results identify *Sox10* as a direct target gene of SOX9 during sexual differentiation. The expression of other downregulated genes in $Sox9^{\Delta/\Delta}$ XY gonads was comparable or lower than in wild type XX gonads, showing that they are specifically regulated by SOX9 and not rescued by SOX8. Notably, the expression of 30 SOX9-bound genes that were downregulated in $Sox9^{\Delta/\Delta}$ XY gonads compared with wild type XY gonads was comparable in Sertoli cells of XY gonads and granulosa cells of XX gonads (64). This suggests that SOX9 contributes to the regulation of the expression of non-sex-specific genes involved in the fate of supporting cells. This role would depend on distinct transcription factors in female granulosa cells. Using an *in vitro* approach, we confirmed the activating role of SOX9 on genes that are downregulated in $Sox9^{\Delta/\Delta}$ XY gonads (such as *SOX10*). We also confirmed that genes (such as SOX6) upregulated in Sertoli cells and bound by SOX9 but not affected by in $Sox9^{\Delta/\Delta}$ XY gonads could be activated by SOX9. This observation is explained by SOX9 redundancy with SOX8 in mutant gonads.

We then took advantage of the RNA-seq technology to investigate whether SOX9 ablation could perturb RNA processing of its target genes. In $Sox9^{\Delta/\Delta}$ XY gonads, splicing of 154 transcripts (among which 70 of SOX9-bound genes) was significantly affected. In $Sox9^{\Delta/\Delta}$ XY gonads, splicing variations encompassed the five major splicing events. For example, incorporation of exon 2 in the *Atrx* transcript was more frequently observed in mutant testis and ovary than in wild type testis. *Fgfr2*, which is crucial for sex-determination (75), has two spliced isoforms that include either exon 8 (*Fgfr2b*) or exon 9 (*Fgfr2c* that encodes the high affinity FGF9 receptor) (89). Our results show that at E13.5, SOX9 inhibits the inclusion of exon 9 in the *Fgfr2* transcript and promotes the production of *Fgfr2b*, as already described in pancreas (90) and in agreement with our previous observation that the *Fgfr2c* isoform is more expressed in XY sex-reversed ovaries than in XY testes (91).

SOX9 ChIP-seq dataset from mouse foetal testes (red bars). Orange bars, TRIM28 ChIP-seq peaks that overlap with SOX9 ChIP-seq peaks as shown in the Venn diagram (**B**). (**C**) Super-resolution OMX fluorescence microscopy using 0.12 μm Z-sections showing the co-localization of SOX9 (red) and TRIM28 (green) in the nucleus of E13.5 Sertoli cells (orange/yellow spots indicated by white arrows in the insets). DNA was stained with DAPI (blue). Sc: Sertoli cells; Gc: germ cells. Bar: 2 μm. (**D**) In vitro pull-down experiments using purified mouse GST-TRIM28 or GST alone and 6xHis-tagged human recombinant SOX9. Proteins were analysed by western blotting using anti-SOX9 (upper panel) and anti-TRIM28 antibodies (lower panel). (**E**) Left panel: nuclear extracts from E13.5 male and female foetal gonads were immunoprecipitated using the anti-CT-SOX9 antibody or IgG (control) and analysed by western blotting with the anti-TRIM28 antibody. Right panel: detection of TRIM28 in nuclear extracts (Nucl. Ext) before immunoprecipitation (input). (**F**) ChIP-qPCR (left panels) and sequential ChIP-qPCR (right panels) of sheared chromatin from E13.5 foetal mouse testes with anti-SOX9 and –TRIM28 antibodies. The analysed genomic regions correspond to overlapping SOX9 and TRIM28 ChIP-seq peaks. *Sox13* and *Sox10* are genes upregulated in E13.5 Sertoli cells versus granulosa cells and downregulated in XY KO gonads. *Fgf18* and *Emx2* are genes up- and down-regulated, respectively, in E13.5 Sertoli cells versus granulosa cells. Data are the mean ± SD ($n = 3$); ***$P < 0.001$; **$P < 0.01$ compared to control unrelated antibody (Unr Ab) (ANOVA with the Geisser–Greenhouse correction for multiple comparisons for ChIP data; Student's t test for sequential ChIP data). (**G**) RT-qPCR analysis showing transcriptional activation or repression of the *SOX10* and *EMX2* genes, respectively) in tet-SOX9-HEK293T cells incubated (+Tc) or not (–Tc) with tetracycline to induce SOX9 expression and transfected or not (empty vector) with a TRIM28 expression plasmid. *SOX10* and *EMX2* expression data are relative to the *IPO8* control. Data are the mean ± SD ($n = 3$); ****$P < 0.0001$; **$P < 0.01$; *$P < 0.1$ (ANOVA with the Geisser–Greenhouse correction for multiple comparisons).

More generally, our results suggest that SOX9 could influence the proteome of a specific cell type by controlling its splicing programme. Beside the production of specific isoforms of proteins involved in the epithelial cell fate (*Ubfd1* and *Gadd45g*), intron retention could be a powerful mechanism to finely regulate the stoichiometry of active proteins without modifying transcription.

Concerning the molecular mechanisms whereby SOX9 might control RNA processing, recent studies showed that epigenetic regulation plays a direct role in the control of alternative splicing (for review see:(92)). For instance, alternative splicing of *Fgfr2* transcripts is regulated at the chromatin level (93), suggesting a possible link between SOX9 binding to its target genes and the splicing machinery. The finding that the SOX9 ChIP-seq peaks of 28% of SOX9-bound genes with perturbed mRNA splicing in *Sox9*$^{\Delta/\Delta}$ XY gonads overlapped with the exons/introns involved in the splicing events (Figure 3B) is strongly in favour of this hypothesis. As transcription and splicing are coupled, we could hypothesize that DNA-bound SOX9 might regulate the cross-talk between chromatin and the splicing machinery during transcription of its target genes. Alternatively, and as previously suggested for SOX proteins (71,94), direct binding of SOX9 to pre-mRNA cannot be excluded. Sex-specific RNA splicing is a key mechanism in *Drosophila* (95), but was not known in mammals. Although we showed that *in vitro* SOX9 can regulate splicing, this mechanism requires additional studies at the molecular level.

We then investigated whether SOX9-bound genes in mammalian testis shared genomic determinants that characterize the Sertoli cell fate developmental program. For this, we took advantage of the ChIP-seq analysis in two distant mammals that highlighted an important conservation of the SOX9 peak distribution in the two species. Therefore, instead of comparing the nucleotide conservation of putative binding sites for transcription factors among orthologous regions, we chose to analyse the distribution of pre-defined binding sites for five Sertoli cell differentiation/reprogramming factors (SOX9, GATA4, DMRT1, SF1 and WT1) (18) in the whole ChIP-seq datasets from both mammals. This led to the definition of a Sertoli cell signature (SCS) in which SOX9, GATA4 and DMRT1 motif enrichment characterizes the genomic regions bound by SOX9 in Sertoli cells. This genomic signature is conserved, as indicated by its presence in orthologous regions from twelve other mammals. We also observed this signature in other vertebrate genomes, for instance, in the chicken genome (not shown) where DMRT1 plays a crucial role in sex determination (96). The fact that SOX, GATA and DMRT motifs co-segregate in a set of genes involved in male gonad differentiation could explain why either DMRT domains (birds, some fish species) or SOX domains (mammals) are involved in testis determination in vertebrates.

We found that SCSs are not a common feature of regions bound by other transcription factors or other SOX factors. Moreover, SCSs are not present in SOX9 target regions in the other tissue/cell types we analyzed (80–83), but for mouse basal cell carcinoma and human colorectal cancer cells. This suggests that in these pathological conditions SOX9 genomic features show strong similarity with those observed in foetal Sertoli cells. As SOX9 overexpression has

an oncogenic role in basal cell carcinoma (83) and colorectal cancer (97), the presence of this genomic signature in other cancer types should now be investigated.

Analysis of SCS organization revealed a strong motif clustering, where motifs are separated by fewer than 50 nucleotides. Moreover, in peaks close to the gene body, motifs clustered at a precise distance upstream or downstream the TSS. This suggests that this genomic feature has functional significance in transcriptional regulation. Moreover, SOX9 and GATA4 binding motifs were preferentially associated, while the position of DMRT1 motifs was less constrained. Importantly using sequential ChIP-qPCR we showed that DMRT1 and GATA4 co-localize with SOX9 on chromatins of its target genes. Additional analyses are required to determine how these factors collaborate in gene regulation and how they bind to SCSs.

As DMRT1 is expressed in Sertoli and germ cells at E13.5, we searched for potential SCSs in DMRT1 ChIP-seq datasets (25). We found that peaks bound by both SOX9 and DMRT1 had SCSs, while those only bound by DMRT1 presented a different motif enrichment pattern. This suggests that a genomic region bound by DMRT1 will display a SCS only if it is also bound by SOX9.

As a proof of concept, we used our global motif-enrichment scanning method to identify new factors with SCSs in ChIP-seq datasets that could have functional relationship with SOX9. We found that in ES cells, TRIM28 interacts with many regions that are also bound by SOX9 in foetal testis and showed that the two proteins form a complex within the foetal testis. Moreover, as TRIM28 co-localizes on SOX9 target genes *in vivo* and cooperate with SOX9 *in vitro* to regulate gene expression, our results highlight an important role for TRIM28 in SOX9-dependent transcriptional regulation. Interestingly, our *in vitro* results suggest a bi-potential action for SOX9-TRIM28 complexes, either activating, either repressing the target genes. This observation fits well with the ChIP-seq results where SOX9 binds to male and also female genes.

Concerning the potential role of SCSs, they might facilitate the attraction of SOX9 or of other factors involved in male sexual differentiation, such as DMRT1 or GATA4, towards genes involved in the Sertoli cell programme, enhancing the probability of building multi-protein complexes on chromatin. This would make of SCSs important components of Sertoli cell fate. Additional studies with gain- or loss-of-function mouse models are required to validate this hypothesis. Moreover, it is not yet known whether in Sertoli cells SOX9 binds to all regions harbouring SCSs.

The motif-enrichment scanning method we developed for SCS identification uses matrices to characterize binding-motifs of a set of transcription factors defined by a reprogramming experiment, here the transcription factors required for the direct reprogramming of embryonic fibroblasts into Sertoli cells (18). This approach could be used also in other biological systems because many transcription factor combinations can directly reprogram the fate of different cell types (98).

In conclusion, our work shows that in mouse and bovine foetal testes, SOX9 binds to a core group of ∼4000 genes that includes all those with an already known role in somatic sex determination. Moreover, despite redundancy

with SOX8, SOX9 regulates specifically the transcription or splicing of a subset of target genes. However, we cannot rule out that SOX9 activity on splicing might be indirect. Finally, the presence of SOX9 on chromatin in foetal testes is correlated with a genomic signature (SCS) comprised of binding motifs for transcription factors involved in Sertoli cell programming, suggesting that this signature represents a Sertoli cell regulatory code. This genomic feature allowed us to discover TRIM28, a new SOX9 protein partner.

SUPPLEMENTARY DATA

Supplementary Data are available at NAR Online.

ACKNOWLEDGEMENTS

FUNDING

REFERENCES

1 Svingen,T. and Koopman,P. (2013) Building the mammalian testis: origins, differentiation, and assembly of the component cell populations. *Genes Dev.*, **27**, 2409–2426.
2 Sekido,R. and Lovell-Badge,R. (2008) Sex determination involves synergistic action of SRY and SF1 on a specific Sox9 enhancer. *Nature*, **453**, 930–934.
3 Qin,Y. and Bishop,C.E. (2005) Sox9 is sufficient for functional testis development producing fertile male mice in the absence of Sry. *Hum. Mol. Genet.*, **14**, 1221–1229.
4 Wagner,T., Wirth,J., Meyer,J., Zabel,B., Held,M., Zimmer,J., Pasantes,J., Bricarelli,F.D., Keutel,J., Hustert,E. *et al.* (1994) Autosomal sex reversal and campomelic dysplasia are caused by mutations in and around the SRY-related gene SOX9. *Cell*, **79**, 1111–1120.
5 Chaboissier,M.C., Kobayashi,A., Vidal,V.I., Lutzkendorf,S., van de Kant,H.J., Wegner,M., de Rooij,D.G., Behringer,R.R. and Schedl,A. (2004) Functional analysis of Sox8 and Sox9 during sex determination in the mouse. *Development*, **131**, 1891–1901.
6 Barrionuevo,F., Bagheri-Fam,S., Klattig,J., Kist,R., Taketo,M.M., Englert,C. and Scherer,G. (2006) Homozygous inactivation of Sox9 causes complete XY sex reversal in mice. *Biol. Reprod.*, **74**, 195–201.
7 Huang,B., Wang,S., Ning,Y., Lamb,A.N. and Bartley,J. (1999) Autosomal XX sex reversal caused by duplication of SOX9. *Am. J. Med. Genet.*, **87**, 349–353.
8 Bishop,C.E., Whitworth,D.J., Qin,Y., Agoulnik,A.I., Agoulnik,I.U., Harrison,W.R., Behringer,R.R. and Overbeek,P.A. (2000) A transgenic insertion upstream of sox9 is associated with dominant XX sex reversal in the mouse. *Nat. Genet.*, **26**, 490–494.

9 Vidal,V.P., Chaboissier,M.C., de Rooij,D.G. and Schedl,A. (2001) Sox9 induces testis development in XX transgenic mice. *Nat. Genet.*, **28**, 216–217.
10 Polanco,J.C., Wilhelm,D., Davidson,T.L., Knight,D. and Koopman,P. (2010) Sox10 gain-of-function causes XX sex reversal in mice: implications for human 22q-linked disorders of sex development. *Hum. Mol. Genet.*, **19**, 506–516.
11 Lavery,R., Chassot,A.A., Pauper,E., Gregoire,E.P., Klopfenstein,M., de Rooij,D.G., Mark,M., Schedl,A., Ghyselinck,N.B. and Chaboissier,M.C. (2012) Testicular differentiation occurs in absence of R-spondin1 and Sox9 in mouse sex reversals. *PLoS Genet.*, **8**, e1003170.
12 Murphy,M.W., Lee,J.K., Rojo,S., Gearhart,M.D., Kurahashi,K., Banerjee,S., Loeuille,G.A., Bashamboo,A., McElreavey,K., Zarkower,D. *et al.* (2015) An ancient protein-DNA interaction underlying metazoan sex determination. *Nat. Struct. Mol. Biol.*, **22**, 442–451.
13 Ono,M. and Harley,V.R. (2013) Disorders of sex development: new genes, new concepts. *Nat. Rev. Endocrinol.*, **9**, 79–91.
14 Raymond,C.S., Murphy,M.W., O'Sullivan,M.G., Bardwell,V.J. and Zarkower,D. (2000) Dmrt1, a gene related to worm and fly sexual regulators, is required for mammalian testis differentiation. *Genes Dev.*, **14**, 2587–2595.
15 Padua,M.B., Jiang,T., Morse,D.A., Fox,S.C., Hatch,H.M. and Tevosian,S.G. (2015) Combined loss of the GATA4 and GATA6 transcription factors in male mice disrupts testicular development and confers adrenal-like function in the testes. *Endocrinology*, **156**, 1873–1886.
16 Hammes,A., Guo,J.K., Lutsch,G., Leheste,J.R., Landrock,D., Ziegler,U., Gubler,M.C. and Schedl,A. (2001) Two splice variants of the Wilms' tumor 1 gene have distinct functions during sex determination and nephron formation. *Cell*, **106**, 319–329.
17 Luo,X., Ikeda,Y. and Parker,K.L. (1995) The cell-specific nuclear receptor steroidogenic factor 1 plays multiple roles in reproductive function. *Philos. Trans. R. Soc. Lond., B, Biol. Sci.*, **350**, 279–283.
18 Buganim,Y., Itskovich,E., Hu,Y.C., Cheng,A.W., Ganz,K., Sarkar,S., Fu,D., Welstead,G.G., Page,D.C. and Jaenisch,R. (2012) Direct reprogramming of fibroblasts into embryonic Sertoli-like cells by defined factors. *Cell Stem Cell*, **11**, 373–386.
19 Zhao,L., Svingen,T., Ng,E.T. and Koopman,P. (2015) Female-to-male sex reversal in mice caused by transgenic overexpression of Dmrt1. *Development*, **142**, 1083–1088.
20 Lindeman,R.E., Gearhart,M.D., Minkina,A., Krentz,A.D., Bardwell,V.J. and Zarkower,D. (2015) Sexual cell-fate reprogramming in the ovary by DMRT1. *Curr. Biol.*, **25**, 764–771.
21 Nowak,D.E., Tian,B. and Brasier,A.R. (2005) Two-step cross-linking method for identification of NF-kappaB gene network by chromatin immunoprecipitation. *Biotechniques*, **39**, 715–725.
22 Gasca,S., Canizares,J., De Santa Barbara,P., Mejean,C., Poulat,F., Berta,P. and Boizet-Bonhoure,B. (2002) A nuclear export signal within the high mobility group domain regulates the nucleocytoplasmic translocation of SOX9 during sexual determination. *Proc. Natl. Acad. Sci. U.S.A.*, **99**, 11199–11204.
23 Zhang,Y., Liu,T., Meyer,C.A., Eeckhoute,J., Johnson,D.S., Bernstein,B.E., Nusbaum,C., Myers,R.M., Brown,M., Li,W. *et al.* (2008) Model-based analysis of ChIP-Seq (MACS). *Genome Biol.*, **9**, R137.
24 Bardet,A.F., He,Q., Zeitlinger,J. and Stark,A. (2012) A computational pipeline for comparative ChIP-seq analyses. *Nat. Protoc.*, **7**, 45–61.
25 Krentz,A.D., Murphy,M.W., Zhang,T., Sarver,A.L., Jain,S., Griswold,M.D., Bardwell,V.J. and Zarkower,D. (2013) Interaction between DMRT1 function and genetic background modulates signaling and pluripotency to control tumor susceptibility in the fetal germ line. *Dev. Biol.*, **377**, 67–78.
26 Barrionuevo,F., Georg,I., Scherthan,H., Lecureuil,C., Guillou,F., Wegner,M. and Scherer,G. (2009) Testis cord differentiation after the sex determination stage is independent of Sox9 but fails in the combined absence of Sox9 and Sox8. *Dev. Biol.*, **327**, 301–312.
27 McFarlane,L., Truong,V., Palmer,J.S. and Wilhelm,D. (2013) Novel PCR assay for determining the genetic sex of mice. *Sex Dev.*, **7**, 207–211.
28 Bolger,A.M., Lohse,M. and Usadel,B. (2014) Trimmomatic: a flexible trimmer for Illumina sequence data. *Bioinformatics*, **30**, 2114–2120.

29 Kim,D., Pertea,G., Trapnell,C., Pimentel,H., Kelley,R. and Salzberg,S.L. (2013) TopHat2: accurate alignment of transcriptomes in the presence of insertions, deletions and gene fusions. *Genome Biol.*, **14**, R36.

30 Anders,S., Pyl,P.T. and Huber,W. (2015) HTSeq–a Python framework to work with high-throughput sequencing data. *Bioinformatics*, **31**, 166–169.

31 Law,C.W., Chen,Y., Shi,W. and Smyth,G.K. (2014) voom: Precision weights unlock linear model analysis tools for RNA-seq read counts. *Genome Biol.*, **15**, R29.

32 Ritchie,M.E., Phipson,B., Wu,D., Hu,Y., Law,C.W., Shi,W. and Smyth,G.K. (2015) limma powers differential expression analyses for RNA-sequencing and microarray studies. *Nucleic Acids Res.*, **43**, e47.

33 Robinson,M.D. and Oshlack,A. (2010) A scaling normalization method for differential expression analysis of RNA-seq data. *Genome Biol.*, **11**, R25.

34 Liu,R., Holik,A.Z., Su,S., Jansz,N., Chen,K., Leong,H.S., Blewitt,M.E., Asselin-Labat,M.L., Smyth,G.K. and Ritchie,M.E. (2015) Why weight? Modelling sample and observational level variability improves power in RNA-seq analyses. *Nucleic Acids Res.*, **43**, e97.

35 Ritchie,M.E., Diyagama,D., Neilson,J., van Laar,R., Dobrovic,A., Holloway,A. and Smyth,G.K. (2006) Empirical array quality weights in the analysis of microarray data. *BMC Bioinformatics*, **7**, 261.

36 Dobin,A., Davis,C.A., Schlesinger,F., Drenkow,J., Zaleski,C., Jha,S., Batut,P., Chaisson,M. and Gingeras,T.R. (2013) STAR: ultrafast universal RNA-seq aligner. *Bioinformatics*, **29**, 15–21.

37 Nnamani,M.C., Plaza,S., Romero,R. and Wagner,G.P. (2013) Evidence for independent evolution of functional progesterone withdrawal in primates and guinea pigs. *Evol. Med. Public Health*, **2013**, 273–288.

38 Katz,Y., Wang,E.T., Airoldi,E.M. and Burge,C.B. (2010) Analysis and design of RNA sequencing experiments for identifying isoform regulation. *Nat. Methods*, **7**, 1009–1015.

39 Thevenet,L., Mejean,C., Moniot,B., Bonneaud,N., Galeotti,N., Aldrian-Herrada,G., Poulat,F., Berta,P., Benkirane,M. and Boizet-Bonhoure,B. (2004) Regulation of human SRY subcellular distribution by its acetylation/deacetylation. *EMBO J.*, **23**, 3336–3345.

40 Thevenet,L., Albrecht,K.H., Malki,S., Berta,P., Boizet-Bonhoure,B. and Poulat,F. (2005) NHERF2/SIP-1 interacts with mouse SRY via a different mechanism than human SRY. *J. Biol. Chem.*, **280**, 38625–38630.

41 Murphy,M.W., Zarkower,D. and Bardwell,V.J. (2007) Vertebrate DM domain proteins bind similar DNA sequences and can heterodimerize on DNA. *BMC Mol. Biol.*, **8**, 58.

42 Rojas,A., Schachterle,W., Xu,S.M. and Black,B.L. (2009) An endoderm-specific transcriptional enhancer from the mouse Gata4 gene requires GATA and homeodomain protein-binding sites for function in vivo. *Dev. Dyn.*, **238**, 2588–2598.

43 Mertin,S., McDowall,S.G. and Harley,V.R. (1999) The DNA-binding specificity of SOX9 and other SOX proteins. *Nucleic Acids Res.*, **27**, 1359–1364.

44 Notarnicola,C., Malki,S., Berta,P., Poulat,F. and Boizet-Bonhoure,B. (2006) Transient expression of SOX9 protein during follicular development in the adult mouse ovary. *Gene Expr. Patterns*, **6**, 695–702.

45 Nielsen,A.L., Ortiz,J.A., You,J., Oulad-Abdelghani,M., Khechumian,R., Gansmuller,A., Chambon,P. and Losson,R. (1999) Interaction with members of the heterochromatin protein 1 (HP1) family and histone deacetylation are differentially involved in transcriptional silencing by members of the TIF1 family. *EMBO J.*, **18**, 6385–6395.

46 Cammas,F., Oulad-Abdelghani,M., Vonesch,J.L., Huss-Garcia,Y., Chambon,P. and Losson,R. (2002) Cell differentiation induces TIF1beta association with centromeric heterochromatin via an HP1 interaction. *J. Cell Sci.*, **115**, 3439–3448.

47 D'Astolfo,D.S., Pagliero,R.J., Pras,A., Karthaus,W.R., Clevers,H., Prasad,V., Lebbink,R.J., Rehmann,H. and Geijsen,N. (2015) Efficient intracellular delivery of native proteins. *Cell*, **161**, 674–690.

48 Munger,S.C. and Capel,B. (2012) Sex and the circuitry: progress toward a systems-level understanding of vertebrate sex determination. *Wiley Interdiscipl. Rev. Syst. Biol. Med.*, **4**, 401–412.

49 Colvin,J.S., Green,R.P., Schmahl,J., Capel,B. and Ornitz,D.M. (2001) Male-to-female sex reversal in mice lacking fibroblast growth factor 9. *Cell*, **104**, 875–889.

50 Munger,S.C., Natarajan,A., Looger,L.L., Ohler,U. and Capel,B. (2013) Fine time course expression analysis identifies cascades of activation and repression and maps a putative regulator of Mammalian sex determination. *PLoS Genet.*, **9**, e1003630.

51 Kuroki,S., Matoba,S., Akiyoshi,M., Matsumura,Y., Miyachi,H., Mise,N., Abe,K., Ogura,A., Wilhelm,D., Koopman,P. *et al.* (2013) Epigenetic regulation of mouse sex determination by the histone demethylase Jmjd1a. *Science*, **341**, 1106–1109.

52 Warr,N., Carre,G.A., Siggers,P., Faleato,J.V., Brixey,R., Pope,M., Bogani,D., Childers,M., Wells,S., Scudamore,C.L. *et al.* (2012) Gadd45gamma and Map3k4 interactions regulate mouse testis determination via p38 MAPK-mediated control of Sry expression. *Dev. Cell*, **23**, 1020–1031.

53 Tevosian,S.G., Albrecht,K.H., Crispino,J.D., Fujiwara,Y., Eicher,E.M. and Orkin,S.H. (2002) Gonadal differentiation, sex determination and normal Sry expression in mice require direct interaction between transcription partners GATA4 and FOG2. *Development*, **129**, 4627–4634.

54 Katoh-Fukui,Y., Miyabayashi,K., Komatsu,T., Owaki,A., Baba,T., Shima,Y., Kidokoro,T., Kanai,Y., Schedl,A., Wilhelm,D. *et al.* (2011) Cbx2, a polycomb group gene, is required for Sry gene expression in mice. *Endocrinology*, **153**, 913–924.

55 Cui,S., Ross,A., Stallings,N., Parker,K.L., Capel,B. and Quaggin,S.E. (2004) Disrupted gonadogenesis and male-to-female sex reversal in Pod1 knockout mice. *Development*, **131**, 4095–4105.

56 Kim,Y., Kobayashi,A., Sekido,R., DiNapoli,L., Brennan,J., Chaboissier,M.C., Poulat,F., Behringer,R.R., Lovell-Badge,R. and Capel,B. (2006) Fgf9 and Wnt4 act as antagonistic signals to regulate mammalian sex determination. *PLoS Biol.*, **4**, e187.

57 Yao,H.H. and Capel,B. (2002) Disruption of testis cords by cyclopamine or forskolin reveals independent cellular pathways in testis organogenesis. *Dev. Biol.*, **246**, 356–365.

58 Callier,P., Calvel,P., Matevossian,A., Makrythanasis,P., Bernard,P., Kurosaka,H., Vannier,A., Thauvin-Robinet,C., Borel,C., Mazaud-Guittot,S. *et al.* (2014) Loss of function mutation in the palmitoyl-transferase HHAT leads to syndromic 46,XY disorder of sex development by impeding hedgehog protein palmitoylation and signaling. *PLoS Genet.*, **10**, e1004340.

59 Morais da Silva,S., Hacker,H., Harley,V., Goodfellow,P.N., Swain,A. and Lovell-Badge,R. (1996) Sox9 expression during gonadal development implies a conserved role for the gene in testis differentiation in mammals and birds. *Nat. Genet.*, **13**, 62–68.

60 Schepers,G.E., Bullejos,M., Hosking,B.M. and Koopman,P. (2000) Cloning and characterisation of the Sry-related transcription factor gene Sox8. *Nucleic Acids Res.*, **28**, 1473–1480.

61 Vainio,S., Heikkila,M., Kispert,A., Chin,N. and McMahon,A.P. (1999) Female development in mammals is regulated by Wnt-4 signalling. *Nature*, **397**, 405–409.

62 Yao,H.H., Matzuk,M.M., Jorgez,C.J., Menke,D.B., Page,D.C., Swain,A. and Capel,B. (2004) Follistatin operates downstream of Wnt4 in mammalian ovary organogenesis. *Dev. Dyn.*, **230**, 210–215.

63 Boulanger,L., Pannetier,M., Gall,L., Allais-Bonnet,A., Elzaiat,M., Le Bourhis,D., Daniel,N., Richard,C., Cotinot,C., Ghyselinck,N.B. *et al.* (2014) FOXL2 is a female sex-determining gene in the goat. *Curr. Biol.*, **24**, 404–408.

64 Jameson,S.A., Natarajan,A., Cool,J., DeFalco,T., Maatouk,D.M., Mork,L., Munger,S.C. and Capel,B. (2012) Temporal transcriptional profiling of somatic and germ cells reveals biased lineage priming of sexual fate in the fetal mouse gonad. *PLoS Genet.*, **8**, e1002575.

65 Kist,R., Schrewe,H., Balling,R. and Scherer,G. (2002) Conditional inactivation of Sox9: a mouse model for campomelic dysplasia. *Genesis*, **32**, 121–123.

66 Lecureuil,C., Fontaine,I., Crepieux,P. and Guillou,F. (2002) Sertoli and granulosa cell-specific Cre recombinase activity in transgenic mice. *Genesis*, **33**, 114–118.

67 Barrionuevo,F., Georg,I., Scherthan,H., Lecureuil,C., Guillou,F., Wegner,M. and Scherer,G. (2008) Testis cord differentiation after the sex determination stage is independent of Sox9 but fails in the combined absence of Sox9 and Sox8. *Dev. Biol.*, **327**, 301–312.

68 Behringer,R.R., Finegold,M.J. and Cate,R.L. (1994) Mullerian-inhibiting substance function during mammalian sexual development. *Cell*, **79**, 415–425.

69 Bitgood,M.J., Shen,L. and McMahon,A.P. (1996) Sertoli cell signaling by Desert hedgehog regulates the male germline. *Curr. Biol.*, **6**, 298–304.

70 Knower,K.C., Sim,H., McClive,P.J., Bowles,J., Koopman,P., Sinclair,A.H. and Harley,V.R. (2007) Characterisation of urogenital ridge gene expression in the human embryonal carcinoma cell line NT2/D1. *Sex Dev.*, **1**, 114–126.

71 Ohe,K., Lalli,E. and Sassone-Corsi,P. (2002) A direct role of SRY and SOX proteins in pre-mRNA splicing. *Proc. Natl. Acad. Sci. U.S.A.*, **99**, 1146–1151.

72 Hata,K., Nishimura,R., Muramatsu,S., Matsuda,A., Matsubara,T., Amano,K., Ikeda,F., Harley,V.R. and Yoneda,T. (2008) Paraspeckle protein p54nrb links Sox9-mediated transcription with RNA processing during chondrogenesis in mice. *J. Clin. Invest.*, **118**, 3098–3108.

73 Li,Q., Lee,J.A. and Black,D.L. (2007) Neuronal regulation of alternative pre-mRNA splicing. *Nat. Rev. Neurosci.*, **8**, 819–831.

74 Bagheri-Fam,S., Argentaro,A., Svingen,T., Combes,A.N., Sinclair,A.H., Koopman,P. and Harley,V.R. (2011) Defective survival of proliferating Sertoli cells and androgen receptor function in a mouse model of the ATR-X syndrome. *Hum. Mol. Genet.*, **20**, 2213–2224.

75 Kim,Y., Bingham,N., Sekido,R., Parker,K.L., Lovell-Badge,R. and Capel,B. (2007) Fibroblast growth factor receptor 2 regulates proliferation and Sertoli differentiation during male sex determination. *Proc. Natl. Acad. Sci. U.S.A.*, **104**, 16558–16563.

76 Gierl,M.S., Gruhn,W.H., von Seggern,A., Maltry,N. and Niehrs,C. (2012) GADD45G functions in male sex determination by promoting p38 signaling and Sry expression. *Dev. Cell*, **23**, 1032–1042.

77 Yamagata,T., Nishida,J., Sakai,R., Tanaka,T., Honda,H., Hirano,N., Mano,H., Yazaki,Y. and Hirai,H. (1995) Of the GATA-binding proteins, only GATA-4 selectively regulates the human interleukin-5 gene promoter in interleukin-5-producing cells which express multiple GATA-binding proteins. *Mol. Cell. Biol.*, **15**, 3830–3839.

78 Hartwig,S., Ho,J., Pandey,P., Macisaac,K., Taglienti,M., Xiang,M., Alterovitz,G., Ramoni,M., Fraenkel,E. and Kreidberg,J.A. (2010) Genomic characterization of Wilms' tumor suppressor 1 targets in nephron progenitor cells during kidney development. *Development*, **137**, 1189–1203.

79 Ferraz-de-Souza,B., Lin,L., Shah,S., Jina,N., Hubank,M., Dattani,M.T. and Achermann,J.C. (2011) ChIP-on-chip analysis reveals angiopoietin 2 (Ang2, ANGPT2) as a novel target of steroidogenic factor-1 (SF-1, NR5A1) in the human adrenal gland. *FASEB J.*, **25**, 1166–1175.

80 Ohba,S., He,X., Hojo,H. and McMahon,A.P. (2015) Distinct transcriptional programs underlie Sox9 regulation of the mammalian chondrocyte. *Cell Rep.*, **12**, 229–243.

81 Garside,V.C., Cullum,R., Alder,O., Lu,D.Y., Vander Werff,R., Zhao,Y., Jones,S.J., Marra,M.A., Underhill,T.M. *et al.* (2015) SOX9 modulates the expression of key transcription factors required for heart valve development. *Development*, **142**, 4340–4350.

82 Kadaja,M., Keyes,B.E., Lin,M., Pasolli,H.A., Genander,M., Polak,L., Stokes,N., Zheng,D. and Fuchs,E. (2014) SOX9: a stem cell transcriptional regulator of secreted niche signaling factors. *Genes Dev.*, **28**, 328–341.

83 Larsimont,J.C., Youssef,K.K., Sanchez-Danes,A., Sukumaran,V., Defrance,M., Delatte,B., Liagre,M., Baatsen,P., Marine,J.C., Lippens,S. *et al.* (2015) Sox9 controls self-renewal of oncogene targeted cells and links tumor initiation and invasion. *Cell Stem Cell*, **17**, 60–73.

84 Shi,Z., Chiang,C.I., Labhart,P., Zhao,Y., Yang,J., Mistretta,T.A., Henning,S.J., Maity,S.N. and Mori-Akiyama,Y. (2015) Context-specific role of SOX9 in NF-Y mediated gene regulation in colorectal cancer cells. *Nucleic Acids Res.*, **43**, 6257–6269.

85 Raymond,C.S., Kettlewell,J.R., Hirsch,B., Bardwell,V.J. and Zarkower,D. (1999) Expression of Dmrt1 in the genital ridge of mouse and chicken embryos suggests a role in vertebrate sexual development. *Dev. Biol.*, **215**, 208–220.

86 Hu,G., Kim,J., Xu,Q., Leng,Y., Orkin,S.H. and Elledge,S.J. (2009) A genome-wide RNAi screen identifies a new transcriptional module required for self-renewal. *Genes Dev.*, **23**, 837–848.

87 Gustafsson,M.G., Shao,L., Carlton,P.M., Wang,C.J., Golubovskaya,I.N., Cande,W.Z., Agard,D.A. and Sedat,J.W. (2008) Three-dimensional resolution doubling in wide-field fluorescence microscopy by structured illumination. *Biophys. J.*, **94**, 4957–4970.

88 Georg,I., Barrionuevo,F., Wiech,T. and Scherer,G. (2012) Sox9 and Sox8 are required for basal lamina integrity of testis cords and for suppression of FOXL2 during embryonic testis development in mice. *Biol. Reprod.*, **87**, 1–11.

89 Santos-Ocampo,S., Colvin,J.S., Chellaiah,A. and Ornitz,D.M. (1996) Expression and biological activity of mouse fibroblast growth factor-9. *J. Biol. Chem.*, **271**, 1726–1731.

90 Seymour,P.A., Shih,H.P., Patel,N.A., Freude,K.K., Xie,R., Lim,C.J. and Sander,M. (2012) A Sox9/Fgf feed-forward loop maintains pancreatic organ identity. *Development*, **139**, 3363–3372.

91 Bagheri-Fam,S., Ono,M., Li,L., Zhao,L., Ryan,J., Lai,R., Katsura,Y., Rossello,F.J., Koopman,P., Scherer,G. *et al.* (2015) FGFR2 mutation in 46,XY sex reversal with craniosynostosis. *Hum. Mol. Genet.*, **24**, 6699–6710.

92 Luco,R.F., Allo,M., Schor,I.E., Kornblihtt,A.R. and Misteli,T. (2011) Epigenetics in alternative pre-mRNA splicing. *Cell*, **144**, 16–26.

93 Luco,R.F., Pan,Q., Tominaga,K., Blencowe,B.J., Pereira-Smith,O.M. and Misteli,T. (2010) Regulation of alternative splicing by histone modifications. *Science*, **327**, 996–1000.

94 Ohe,K., Tamai,K.T., Parvinen,M. and Sassone-Corsi,P. (2009) DAX-1 and SOX6 molecular interplay results in an antagonistic effect in pre-mRNA splicing. *Dev. Dyn.*, **238**, 1595–1604.

95 Salz,H.K. (2011) Sex determination in insects: a binary decision based on alternative splicing. *Curr. Opin. Genet. Dev.*, **21**, 395–400.

96 Smith,C.A., Roeszler,K.N., Ohnesorg,T., Cummins,D.M., Farlie,P.G., Doran,T.J. and Sinclair,A.H. (2009) The avian Z-linked gene DMRT1 is required for male sex determination in the chicken. *Nature*, **461**, 267–271.

97 Matheu,A., Collado,M., Wise,C., Manterola,L., Cekaite,L., Tye,A.J., Canamero,M., Bujanda,L., Schedl,A., Cheah,K.S. *et al.* (2012) Oncogenicity of the developmental transcription factor Sox9. *Cancer Res.*, **72**, 1301–1315.

98 Xu,J., Du,Y. and Deng,H. (2015) Direct lineage reprogramming: strategies, mechanisms, and applications. *Cell Stem Cell*, **16**, 119–134.